

Unique neural mechanisms of the migraine brain

Noemi Meylakh

A thesis submitted in fulfilment of the requirements for the degree of Doctor of
Philosophy

Laboratory of Neural Imaging
Faculty of Medicine and Health
The University of Sydney

May 2019

“The migraine headache represents a collapse of a way of dealing with life situations which are stressful to the individual.”

Harold Wolff (1898-1962)

Table of Contents

Preface	
Statement of Originality.....	v
Acknowledgements.....	vi
Authorship attribution statements.....	vii
Abstract.....	ix
Chapter 1: Introduction and Literature review	1
1.1 Migraine: an overview.....	2
1.2 Migraine mechanism: starting from the beginning.....	5
1.2.1 Neurovascular theory.....	7
1.2.2 The pons, midbrain and hypothalamus.....	8
1.2.3 The trigeminovascular system.....	11
1.2.3.1 Sensitization of the trigeminovascular pathway.....	15
1.2.4 Migraine as a central disorder?.....	19
1.2.5 Brainstem tone.....	21
1.3 Treating migraine.....	25
1.4 Neural imaging.....	28
1.5 Rationale and general aims of dissertation.....	30
1.6 References.....	33
Chapter 2: Deep in the brain: Changes in subcortical function immediately preceding a migraine attack	43
2.1 Abstract.....	44
2.2 Introduction.....	44
2.3 Methods.....	45
2.4 Results.....	48
2.5 Discussion.....	52
2.6 References.....	55
Chapter 3: Resting regional brain activity changes across the migraine cycle	57
3.1 Abstract.....	59
3.2 Introduction.....	60
3.3 Methods.....	61
3.4 Results.....	65
3.5 Discussion.....	71
3.6 References.....	77

Chapter 4: Brainstem functional oscillations across the migraine cycle: a longitudinal investigation	95
4.1 Abstract	97
4.2 Introduction	98
4.3 Methods	99
4.4 Results	104
4.5 Discussion	107
4.6 References	113
Chapter 5: General discussion, limitations, conclusions and future directions	124
5.1 General discussion	125
5.2 Limitations	132
5.3 Conclusions and future directions	133
5.4 References	137
Appendix	i
I. Altered brainstem anatomy in migraine	i
II. Changes in brainstem pain modulation circuitry function over the migraine cycle	xiii
III. Fluctuating brainstem anatomy across the migraine cycle	xlvii
IV. Dorsal raphe nucleus and harm avoidance: A resting-state investigation	lxxv

Statement of Originality

This is to certify that to the best of my knowledge, the intellectual content of this thesis is the product of my own work and that all sources and assistance received in preparing this thesis have been acknowledged. This thesis has not been submitted for any other degree or other purposes.

Noemi Meylakh

Department of Anatomy and Histology, Faculty of Medicine, The University of Sydney, Australia

Acknowledgements

This thesis would have been impossible without the people who supported me throughout. My supervisor, Prof Luke Henderson, adopted me in my Honours year and taught me the ways of neuroscience and imaging (with what often seemed like endless patience). He has given me opportunities I could only have dreamed of without his kindness, guidance, intelligence, sense of humor and “constant supervision.” Lab mates who have come and gone over the last five years, in particular my migraine buddy who shared in my insanity with me. My family, who gave me the freedom to take on such an impractical task of a PhD, encouraging me to stay curious and to remember, it’s not a means to an end that is important. My best friend, who kept me sane by listening to me and laughing with me on literally a daily basis and my partner, who gave me the strength to get to this moment. Thank you! We now have four degrees!

Authorship attribution statements

Selected peer-reviewed and/or submitted manuscripts have been used to compose the chapters of this thesis. Below are descriptions of co-authors' contributions to these manuscripts.

Chapter 2 of this thesis is published as:

Meylakh N, Marciszewski KK, Di Pietro F, Macefield VG, Macey PM, Henderson LA (2018)

Deep the brain: Changes in subcortical function immediately preceding a migraine attack. *Human Brain Mapping* 39:2651-2663.

I designed the study, analyzed the data and wrote/edited the manuscript drafts

Kasia Marciszewski: assistance with data collection, intellectual input, manuscript editing

Flavia Di Pietro: intellectual input, manuscript editing

Vaughan Macefield: intellectual input, manuscript editing

Paul Macey: assistance with data analysis

Luke Henderson: assistance with data analysis, intellectual input, manuscript editing

Chapter 3 of this thesis is under review as:

Meylakh N, Marciszewski KK, Di Pietro F, Macefield VG, Macey PM, Henderson LA (2018)

Resting regional brain activity changes across the migraine cycle. *Submitted to Neural Image: Clinical*.

I designed the study, analyzed the data and wrote/edited the manuscript drafts

Kasia Marciszewski: assistance with data collection, intellectual input, manuscript editing

Flavia Di Pietro: intellectual input, manuscript editing

Vaughan Macefield: intellectual input, manuscript editing

Paul Macey: assistance with data analysis

Luke Henderson: assistance with data analysis, intellectual input, manuscript editing

Chapter 4 of this thesis is submitted as:

Meylakh N, Marciszewski KK, Di Pietro F, Macefield VG, Macey PM, Henderson LA (2018)

Brainstem functional oscillations across the migraine cycle: a longitudinal study. *Submitted to Proceedings of the National Academy of Sciences of the United States of America.*

I designed the study, analyzed the data and wrote/edited the manuscript drafts

Kasia Marciszewski: assistance with data collection, intellectual input, manuscript editing

Flavia Di Pietro: intellectual input, manuscript editing

Vaughan Macefield: intellectual input, manuscript editing

Paul Macey: assistance with data analysis

Luke Henderson: assistance with data analysis, intellectual input, manuscript editing

Abstract

Whether migraine pathophysiology stems from vascular or centrally-driven origins has been debated for decades. However, facilitated by the development of modern neural imaging techniques and scientific technology, the last century has seen the largest advance in our understanding of migraine. It is now well accepted that sensitization of the trigeminovascular pathway plays a crucial role in the initiation and expression of a migraine. This is supported by experimental human studies that revealed abnormal activity of the trigeminovascular system. This abnormal activity was found particularly in areas of the brainstem, midbrain and hypothalamus during a migraine attack itself and during the interictal period, that is at least 72 hours following and not within 24 hours before a migraine. Research into the premonitory period, the critical 24-hour pain-free period preceding a migraine, is scarce and as a result, there is a gap in our understanding of how and why sensitization occurs. It may be that altered brain function, particularly in brainstem sites, may either trigger a migraine itself or facilitate a peripheral trigger that activates certain pain-processing brain regions, resulting in head pain. As it is impossible to predict when a migraine is imminent, few studies have investigated the premonitory period. Understanding the underlying mechanisms of the migraine cycle has potential to transform the way migraine disorder is treated. The aim of this thesis was to identify functional brain differences throughout the migraine cycle, in particular in the critical 24-hour pain-free period preceding a migraine.

The first investigation (Chapter 2) aimed to identify if neural activity within the brainstem and hypothalamus would alter over the migraine cycle. I employed high-resolution functional magnetic imaging (fMRI) to measure ongoing activity patterns reflected through infra-slow oscillations

(ISOs) and functional connectivity in the interictal, postdrome and premonitory periods of migraine compared with controls. A comparison between all groups provided evidence of unique activity in the 24-hour period immediately preceding a migraine. Increased ISO activity occurred exclusively in this period in areas of the trigeminovascular system including the spinal trigeminal nucleus (SpV), midbrain periaqueductal gray (PAG), dorsal pons, thalamus and hypothalamus. Remarkably, midbrain and hypothalamic sites were found to display increased functional connectivity and regional homogeneity immediately preceding a migraine suggesting a role for the PAG-hypothalamic interaction in migraine expression. Importantly, interictal and postdrome groups displayed similar activity as control groups, highlighting the unique nature of the premonitory period. It is possible that these increases in ISO power and regional homogeneity result from enhanced amplitude and synchrony of oscillatory gliotransmitter release immediately before a migraine attack, thus supporting the role of astrocytes and gliotransmission in migraine initiation and/or expression. These findings have never been reported in the premonitory period of migraine and reflect altered brainstem and hypothalamic function immediately preceding a migraine.

Along with the central nervous system, cerebral vasculature changes have been strongly implicated as critical for migraine initiation. The second investigation (Chapter 3) aimed to build on my previous study by determining whether changes in absolute activity levels, reflected through abnormal cerebral blood flow (CBF), could be identified throughout the migraine cycle. I used pseudocontinuous arterial spin labelling (pcASL) to measure CBF in the interictal, postdrome and premonitory periods of migraine compared with controls. In line with the findings of my first investigation, this analysis revealed distinctive activity in the 24-hour period immediately preceding a migraine with decreased CBF in the hypothalamus, PAG and SpV. In addition,

decreased CBF was revealed in higher brain structures such as the visual cortex, orbitofrontal cortex (OFC) and retrosplenial cortex. These findings also reflected alterations in the interictal group with decreases in CBF detected in higher brain structures including the nucleus accumbens, putamen, OFC and ventrolateral prefrontal cortex. Remarkably, decreased CBF in brainstem regions was found only in the period immediately preceding a migraine and these decreases occurred suddenly, as opposed to the decreased CBF found in the higher brain regions which tended to occur gradually throughout the interictal period as the migraine approached. The specialized activity of the brainstem in the period immediately preceding a migraine further emphasizes that brainstem abnormalities are involved in the initiation and/or expression of a migraine. Though many studies have explored CBF during other periods of migraine, this is the first study to measure resting CBF during the 24-hour period immediately preceding a migraine using ASL, and furthermore, to couple ongoing activity patterns (Chapter 2) with absolute brain activity.

The first two cross-sectional investigations (Chapters 2 and 3) revealed unique abnormal activity in the 24-hour period immediately preceding a migraine in areas of the brainstem, midbrain and hypothalamus. However, it remains unknown whether similar patterns would be revealed in a longitudinal study when comparing periods throughout an individual's migraine cycle. To complete this thesis, the third investigation (Chapter 4) aimed to follow the migraine cycle of three migraineurs by imaging them five days a week over four weeks. Due to the cyclic nature of migraine, I expected that when comparing the activity in the 24-hour period immediately preceding a migraine with other periods of migraine within these individuals, the findings would reflect similar patterns as our cross-sectional studies. Indeed, using fMRI I explored resting brainstem activity patterns and found that although resting activity variability was similar in controls and

migraineurs on most days, during the period immediately preceding a migraine, brainstem variability increased dramatically. These increases in resting variability were restricted to specific areas of the pain processing pathway including the SpV and dorsal pons. Remarkably, these changes were located in the same brainstem regions which have been shown to be activated during a migraine itself, but again they occurred whilst the individual was *not* in pain. These increases in brainstem variability were characterised by increased power at ISOs between 0.03-0.06 Hz and they were coupled to increases in resting regional homogeneity directly prior to a migraine. These oscillatory and regional homogeneity changes are consistent with the idea that changes in astrocyte function may precede a migraine and be responsible for its initiation and/or maintenance. These data provide the first evidence of altered brainstem function directly before a migraine throughout the migraine cycle of multiple individuals and provide compelling evidence for the hypothesis that brainstem function is altered immediately before a migraine.

Overall, these data reveal that the 24-hour period immediately preceding a migraine possesses unique qualities that may be crucial in the initiation and/or expression of the migraine. My findings reflect abnormal activity of the trigeminovascular system, in particular in areas of the brainstem, midbrain and hypothalamus. I found increases in ongoing activity patterns in the 24-hour period immediately preceding a migraine only, however abnormalities in absolute activity levels were also found in higher brain structures in the interictal period. Finally, when exploring the migraine cycle within three individuals, I found that the 24-hour period immediately preceding a migraine reflected very similar patterns to those revealed in my cross-sectional studies; relatively stable activity until the 24-hour period preceding a migraine, where a sudden over-exaggeration of activity occurred. It seems that migraine is indeed a cyclic disorder with brainstem function oscillating between altered states.

Chapter 1

Introduction and Literature review

1.1 Migraine: an overview

Migraine is a highly prevalent and disabling disorder, impacting approximately 6% of men and 15-18% of women in the general population (MacGregor, Brandes, & Eikermann, 2003). It has been labelled as the sixth most debilitating disorder by the World Health Organization, costing the United States and Europe \$19.6 billion and €27 billion a year respectively (Goadsby et al., 2017). Migraine prevalence has been found to be age-dependent, with onset usually in early teens and with peak of severity and frequency between the ages of 40 and 50 in both males and females (Breslau & Rasmussen, 2001). Therefore, the condition is most damaging in the years where the vast population is at their most productive. As a result, migraine has become one of the biggest medical burdens on society due to work absences, impaired productivity and billions of dollars spent globally on medical-related costs (Ferrari, 1998). Unfortunately, despite its high prevalence and debilitating nature, the neural and vascular mechanisms underlying the initiation, expression and treatment of migraine remain unclear (Nosedá & Burstein, 2013). This is due to the fact that migraine is a complex neurological disorder (Burstein, Nosedá, & Borsook, 2015) with a heritability factor estimated at 50% (Pietrobon & Moskowitz, 2013). The mechanisms explaining how migraine attacks are initiated in susceptible individuals has been a topic of hot debate for decades.

A migraine attack usually begins with warning signs and symptoms that occur within the 24 hours preceding the development of the headache; a period known as the prodrome or premonitory phase. The premonitory phase is the first stage of the migraine attack, and acts as a predictor that migraine pain is impending. Symptoms often consist of fatigue, dizziness, loss of concentration, heightened emotional state, sensory hypersensitivity (Giffin et al., 2003; Pietrobon & Moskowitz, 2013) and

sometimes transient focal neurological symptoms such as visual aura (Burstein et al., 2015). Visual aura occurs in approximately one-third of migraineurs and is linked to neurological deficits (Goadsby et al., 2017). According to a standardised diagnostic tool, the third edition International Classification of Headache Disorders (ICHD), the migraine headache must follow a particular set of criteria in order to distinguish it from other headache syndromes (Table 1).

The migraine headache commonly begins in a unilateral manner, and must possess at least one of the following: a pulsating and throbbing quality, moderate to severe pain intensity, or aggravation by physical activity (ICHD, 2013). Aggravation by physical activity is likely due to intensification caused by an increase in intracranial pressure (Burstein et al., 2015). The headache is typically accompanied by neurological symptoms such as photophobia and phonophobia, nausea and/or vomiting, as well as by an array of emotional, cognitive and autonomic disturbances (Noseda & Burstein, 2013). It is the presence of these accompanying symptoms that distinguishes migraine from other headache disorders, indicating that changes in neurological mechanisms including the nature of neural pathways and neuronal behaviour, is important in migraine pathophysiology. For 72-hours following the resolution of the migraine headache is the postdrome phase before which the individual enters the interictal phase, a pain-free state. The interictal phase ends as the premonitory phase begins, 24 hours preceding the development of migraine pain.

<p>Without aura</p> <ul style="list-style-type: none"> A. At least five attacks fulfilling criteria B-D B. Headache attacks lasting 4-72 h (untreated or unsuccessfully treated) C. Headache has at least two of the following four characteristics: <ul style="list-style-type: none"> 1. Unilateral location 2. Pulsating quality 3. Moderate or severe pain intensity 4. Aggravation by or causing avoidance of routine physical activity (e.g., walking or climbing stairs) D. During headache at least one of the following: <ul style="list-style-type: none"> 1. Nausea and/or vomiting 2. Photophobia and phonophobia E. Not better accounted for by another ICHD-3 diagnosis
<p>With aura</p> <ul style="list-style-type: none"> A. At least two attacks fulfilling criteria B and C B. One or more of the following fully reversible aura symptoms: <ul style="list-style-type: none"> 1. Visual 2. Sensory 3. Speech and/or language 4. Motor 5. Brainstem 6. Retinal C. At least two of the following four characteristics: <ul style="list-style-type: none"> 1. At least one aura symptom spreads gradually over ≥ 5 min, and/or two or more symptoms occur in succession 2. Each individual aura symptom lasts 5-60 min 3. At least one aura symptom is unilateral 4. The aura is accompanied, or followed within 60 min, by headache D. Not better accounted for by another ICHD-3 diagnosis, and transient ischemic attack has been excluded

Table 1: International Classification for Headache Disorders (ICHD)-3 β . List of criteria necessary for diagnosis of migraine, both with and without aura. Modified from Goadsby et al (2017) and ICHD (2013).

1.2 Migraine mechanism: starting from the beginning

The theory of migraine has evolved over thousands of years. As early as the year 936 AD, physicians studied how migraine headaches could be alleviated by applying pressure to the head, or by surgically ligating the superficial temporal artery (Shevel, 2007). In the 17th Century, Thomas Willis, who is widely considered one of the founders of modern neurology, supported these ideas by postulating that the source of pain in some headaches was enlarged blood vessels, laying the framework for what would become the vascular theory of migraine (Shevel, 2007). However, from the mid-1800s until now, the dichotomous debate between whether migraine originates from vasodilatation or from dysfunction of the central nervous system has been ongoing. In the late 1800s, Edward Liveing theorised that migraine results from a “*nerve storm*” or “*neurosal seizure*” (Liveing, 1874), whilst in the same time period Peter Wallwork Latham described migraine as originating from vasodilation triggered by aura (Goadsby et al., 2017).

With the development of medical and scientific technology, the last 70 years has yielded the largest advances in migraine theory (Goadsby et al., 2017). This new era was kicked off by Harold Wolff’s influential experiments in the 1940s. Wolff (1898-1962) and his colleagues were the first to subject the principles of vasodilatation to thorough experimental and scientific investigation by studying cranial blood vessels in conscious patients (Shevel, 2011). They observed that stimulation of the cerebral and meningeal blood vessels produced severe headaches (Parsons & Strijbos, 2003). Wolff’s vascular theory of migraine consisted of two statements: 1) intracranial vasospasm of the cerebral arteries causes the aura of migraine; 2) extracranial vasodilatation is instrumental in causing migraine pain (Shevel, 2011). The theory was supported by observations that migraine headache was usually accompanied by a pulsating quality, and by later experiments displaying the

effects of triptans on migraine pain and vasoconstriction, and the ability of calcitonin gene-related peptide (CGRP) to trigger migraine attacks (Goadsby et al., 2017). Wolff's vascular theory was widely accepted for over 40 years.

Wolff was described as "*a mixture of greatness and narrowness*"; his narrowness attributed to his extreme obsessiveness, and the general belief that his observations were too influenced by his own migraine experience (J. Blau, 2004). His observations were challenged and eventually his theory was invalidated by experimental findings.

The first statement of Wolff's theory was negated by the phenomenon of cortical spreading depression (CSD), which was originally proposed by Aristides Leao in 1944 (Parsons & Strijbos, 2003). CSD has been described as "*a slowly propagating wave of depolarisation/excitation followed by hyperpolarization/inhibition in cortical neurons and glia*" (Burstein et al., 2015; Hadjikhani et al., 2001; Sugaya, Takato, & Noda, 1975); "*a severe but transient disruption of neural activity in the brain, which spreads like waves in a pond in which a stone has been cast. It propagates to normal tissues...Its rate of spread correlates almost exactly with the observed spread of the aura of classical migraine*" (Pearce, 1985). CSD could not be accounted for by intracranial vasospasm of the cerebral arteries (Shevel, 2011). Subsequent experiments further challenged the statement. Olesen and colleagues showed that the pattern in the reduction of regional blood flow during migraine aura was inconsistent with the anatomical limitations of the major cerebral vessels (Jacobs & Dussor, 2016). Moreover, intracranial vessels were shown to only have minor dilation that was unaffected by sumatriptan (Humphrey & Goadsby, 1994) and meningeal vessels were not found to dilate during spontaneous migraines (Amin et al., 2013).

Wolff's second statement was also challenged when clinical studies were unable to prove that extracranial vasodilation could cause a headache, or support that significant extracranial vasodilation occurred during a migraine (Bernstein & Burstein, 2012). Clinical studies showed that the CGRP-evoked migraine aforementioned had modest arterial vasodilation, which was incapable of activating perivascular nociceptors (Goadsby et al., 2017).

Thus, the vascular theory was deemed an inadequate explanation of the pathophysiology of migraine. Migraine theory shifted from being considered solely a disorder of blood vessels to a *“highly choreographed interaction between major inputs from both the peripheral and central nervous systems, with the trigeminovascular system and the cerebral cortex among the main players”* (Pietrobon & Moskowitz, 2013), i.e. the neurovascular theory.

1.2.1 Neurovascular theory

Referred to as the *“prevailing view today”*, the neurovascular theory proposes that the migraine headache has intracranial origin, and that the headache phase is mediated by the activation of nociceptors that innervate meningeal blood vessels (Bernstein & Burstein, 2012). That is, migraine is a disorder of the brain with symptoms arising *“from a combination of dilation-independent vascular events and neurogenic mechanisms interacting throughout the brain and within the trigeminovascular system in the meninges”* (Jacobs & Dussor, 2016). In other words, vasculature does play a role in the neuronal mechanisms underlying migraine, simply not in the classical way that it was once considered. This theory is based on reports that stimulation of dural vasculature during craniotomy produced head pain in alert patients (Penfield & McNaughton, 1940). The dura is innervated by nociceptive A δ and C fiber afferents whose cell bodies are located in the

trigeminal ganglion and upper cervical dorsal root ganglia. These afferent fibers contain vasoactive neuropeptides such as substance P and CGRP (Bernstein & Burstein, 2012), a fact that will be relevant when discussing migraine treatments later on.

Although the neurovascular theory is the current prevailing theory explaining migraine initiation, some researchers suggest that this theory has similar inadequacies as the vascular theory, predominantly that there is not enough evidence to suggest that cerebral vasculature is instrumental in migraine pathophysiology (Schwedt & Dodick, 2009). Nevertheless, compelling evidence does suggest that the development of migraine-pain is dependent on the activation and sensitization of the trigeminal sensory afferents that innervate meninges and their large blood vessels (Pietrobon & Moskowitz, 2013), while dysfunction of central nervous system structures involved in pain modulation explains the symptoms of the premonitory phase (Noseda & Burstein, 2013).

1.2.2 The pons, midbrain and hypothalamus

The role of altered brain function, and in particular alterations in the brainstem, has begun to be investigated; predominantly the role of the dorsal pons, midbrain periaqueductal gray (PAG), and hypothalamus (S.K. Afridi et al., 2005; S. K. Afridi et al., 2005; A. Bahra, M. S. Matharu, C. Buchel, R. S. Frackowiak, & P. J. Goadsby, 2001b; Denuelle, Fabre, Payoux, Chollet, & Geraud, 2007; Karsan, Bose, & Goadsby, 2018; Weiller, May, Limmroth, Juptner, Kaube, Schayck, Coenen, & Diener, 1995). Indeed, migraine, potentially preceded by hypothalamic dysfunction, has been linked to episodic dysfunction of brainstem nuclei, which in turn activate cortical and subcortical structures that modulate nociceptive function and vascular control (Bartolini, Baruffaldi, Paolino, & Silvestrini, 2005; Denuelle et al., 2007). It is well known that the

hypothalamus is involved in autonomic and endocrine regulation including physiological functions such as the circadian rhythms, feeding, thirst and arousal, as well as homeostatic control (Burstein et al., 2015; Dampney, 2011; Nosedá & Burstein, 2013; Settle, 2000). Due to the sensitivity of the migraine brain to deviation from homeostasis, which commonly manifests in sleep disturbances, changes in mood, food cravings, thirst and urination in the premonitory phase, the hypothalamus dysfunction has been suggested to be important in the expression of early migraine symptoms (Denuelle et al., 2007; Goadsby et al., 2017; Nosedá & Burstein, 2013). Indeed, in a recent case study by Schulte and May, the hypothalamus was shown to have increased sensitivity to noxious stimuli and greater functional coupling with the dorsomedial pons and spinal trigeminal nucleus (SpV) during the premonitory phase (Schulte & May, 2016).

Whilst the role of the hypothalamus in the generation of migraine is gathering momentum, the role of the PAG remains controversial. It is well known that stimulation of the PAG can inhibit nociceptive transmission within the dorsal horn as well as correspondent pain reflexes causing an analgesic effect (H. L. Fields & Heinricher, 1985; Knight & Goadsby, 2001). Indeed, both pre-clinical (Goadsby et al., 2017) and clinical studies have also demonstrated analgesic effects during PAG stimulation (R. Levy, Deer, & Henderson, 2010). Tract tracing experiments have shown that the PAG does not directly project to the primary afferent synapse of the ascending pain pathways, but rather indirectly through descending projections to the rostral ventromedial medulla (RVM), which in turn projects to the dorsal horn and SpV (H. L. Fields & Heinricher, 1985; Floyd, Price, Ferry, Keay, & Bandler, 2001; Morgan, Whittier, Hegarty, & Aicher, 2008). The PAG-RVM pathway is considered part of the descending endogenous pain pathway (Goadsby et al., 2017) and human brain imaging studies have reported increased resting functional connectivity between the PAG and cortical and subcortical regions involved in nociceptive processing (C. Mainero, J.

Boshyan, & N. Hadjikhani, 2011a; Schwedt et al., 2013). Thus, projections from the PAG-RVM pathway to hypothalamic nuclei (Dampney, 2011) as well as to the SpV may be involved in the triggering of migraine symptoms associated with homeostatic changes (Goadsby et al., 2017). The dorsal pons has been more implicated in ictal (during a migraine attack) studies (S.K. Afridi et al., 2005; Bahra et al., 2001b; Denuelle et al., 2007; Weiller, May, Limmroth, Juptner, Kaube, Schayck, Coenen, & Diener, 1995), but due to its involvement in respiration, taste and sleep (Kandel, Schwartz, Jessell, Siegelbaum, & Hudspeth, 2012), it is likely to also be involved in the premonitory phase.

Though the exact role of the PAG in migraine has not been delineated, it has been shown to modulate trigeminovascular nociceptive responses (Goadsby et al., 2017). In an influential neural imaging study by Weiller and colleagues, it was suggested that migraine pathogenesis could be related to an imbalance in activity in the dorsal midbrain (Weiller, May, Limmroth, Juptner, Kaube, Schayck, Coenen, & Diener, 1995). They showed an increase in cerebral blood flow in the dorsal pons and PAG that persisted even after administration of sumatriptan (Weiller, May, Limmroth, Juptner, Kaube, Schayck, Coenen, & Diener, 1995).

Surprisingly, unlike the pons, midbrain and hypothalamus, SpV activation was not found in human ictal studies (S.K. Afridi et al., 2005; S. K. Afridi et al., 2005; Bahra et al., 2001b; Denuelle et al., 2007; Weiller, May, Limmroth, Juptner, Kaube, Schayck, Coenen, & Diener, 1995), though experimental animal studies have clearly shown SpV activation during dural stimulation (A. Strassman, Mason, Moskowitz, & Maciewicz, 1986). Interestingly, it was recently reported that noxious-evoked SpV activation is enhanced the closer the individual was to their next migraine (Stankewitz, Aderjan, Eippert, & May, 2011), suggesting that the SpV may play a role in the

initiation of a migraine attack. These findings support the idea that the hypothalamus, PAG, dorsal pons and SpV make up an interactive network that together are involved in the initiation and expression of a migraine attack.

1.2.3 The trigeminovascular system

Almost 80 years ago, Penfield and McNaughton reported that dura mater is innervated by three nerves, of which the cell somas of these nerves, are found in the trigeminal ganglion (Penfield & McNaughton, 1940). In the same year, Ray and Wolff demonstrated how electrical stimulation of dural and cerebral arteries could evoke nausea and headache-like pain in conscious human beings during brain surgery (Ray & Wolff, 1940). Due to the pain-sensitive quality they reported, the dura mater has been extensively studied with respect to its potential role in generating migraine pain (Olesen, Burstein, Ashina, & Tfelt-Hansen, 2009).

The trigeminovascular pathway comprises of neurons whose cell bodies are located in the trigeminal ganglion (Burstein et al., 2015). Their peripheral processes extend from the ganglion to the pial and dural meninges, in addition to the walls of large cerebral arteries (Uddman, Edvinsson, Ekman, Kingman, & McCulloch, 1985) (Figure 1). Their central processes extend through the pons to the medulla and terminate on the dorsal laminae of the SpV (Y. Liu, Broman, & Edvinsson, 2004). In addition, the trigeminal nerve relays sensory information from most extracranial (skin, muscles and blood vessels) and intracranial (dural and large cerebral arteries) structures to the SpV (Olesen et al., 2009). This convergent input may explain the observation that migraineurs often develop hypersensitivity in the periorbital skin, expressed as cutaneous allodynia (Bernstein & Burstein, 2012).

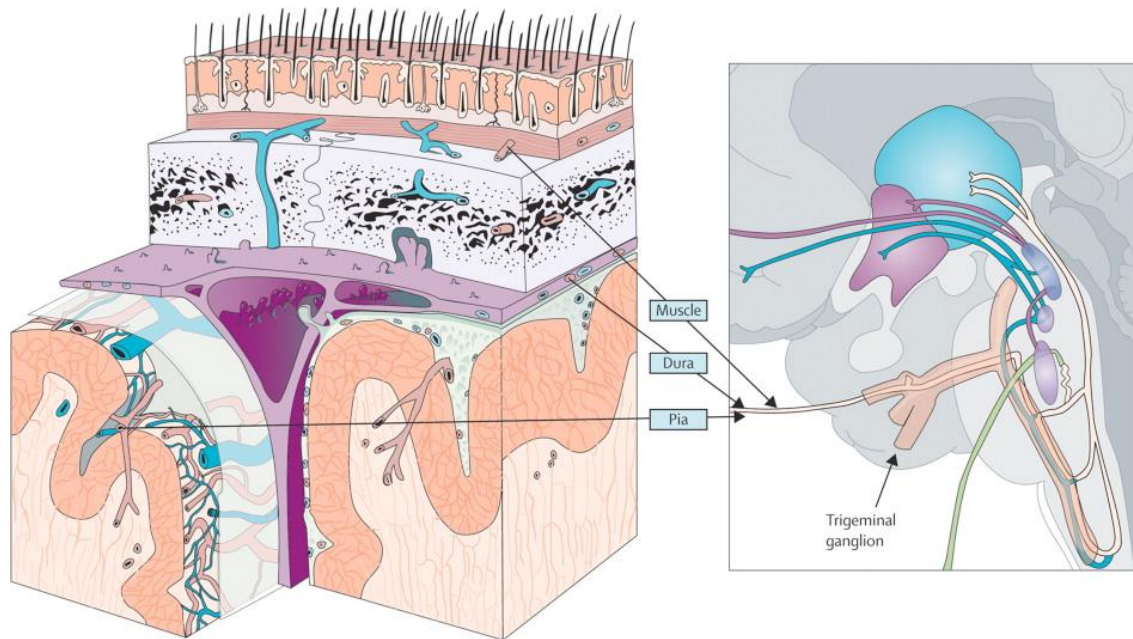


Figure 1: Extracranial and intracranial pain-sensitive structures. A schematic representing where the meninges (pia and dura mater) and extracranial structures/muscles are located in relation to the trigeminal nerve and brainstem. Input from the blood vessels of the pia, dura mater and extracranial structures/muscle carry on afferents that project mainly through the trigeminal nerve to reach the brainstem, before innervating the thalamus and cortex. Modified from Olesen et al (2009).

In the context of migraine, the trigeminovascular system refers to the afferents within the trigeminal nerve that transmit noxious information including those from the cerebral vascular system. Trigemino-vascular neurons terminate within the SpV onto second-order neurons that in turn send ascending projections to other brainstem nuclei including the ventrolateral PAG, brainstem reticular formation, superior salivatory, parabrachial and cuneiform nuclei, the nucleus of the solitary tract, as well as to hypothalamic and basal ganglia nuclei (Burstein et al., 2015; Nosedá & Burstein, 2013). These multiple ascending projections may be responsible for initiating the loss of appetite, yawning, nausea and vomiting and may send projections to higher cortical regions that in turn are responsible for the fatigue, anxiety, irritability and depression that accompanies the migraine headache itself (Burstein & Jakubowski, 2005; Burstein et al., 2015) (Figure 2).

In addition to projecting to regions of the brainstem, trigeminovascular-related SpV neurons project to the thalamic ventral posteromedial, posterior and parafascicular nuclei (Malick, Strassman, & Burstein, 2000). These thalamic neurons then project to the somatosensory, insular, motor, parietal association, retrosplenial, auditory, visual and olfactory cortices. These projections are likely crucial for expression of specific symptoms that are characteristic of migraine, such as difficulties focusing and motor control, amnesia, allodynia, phonophobia, photophobia and osmophobia (Nosedá, Jakubowski, Kainz, Borsook, & Burstein, 2011).

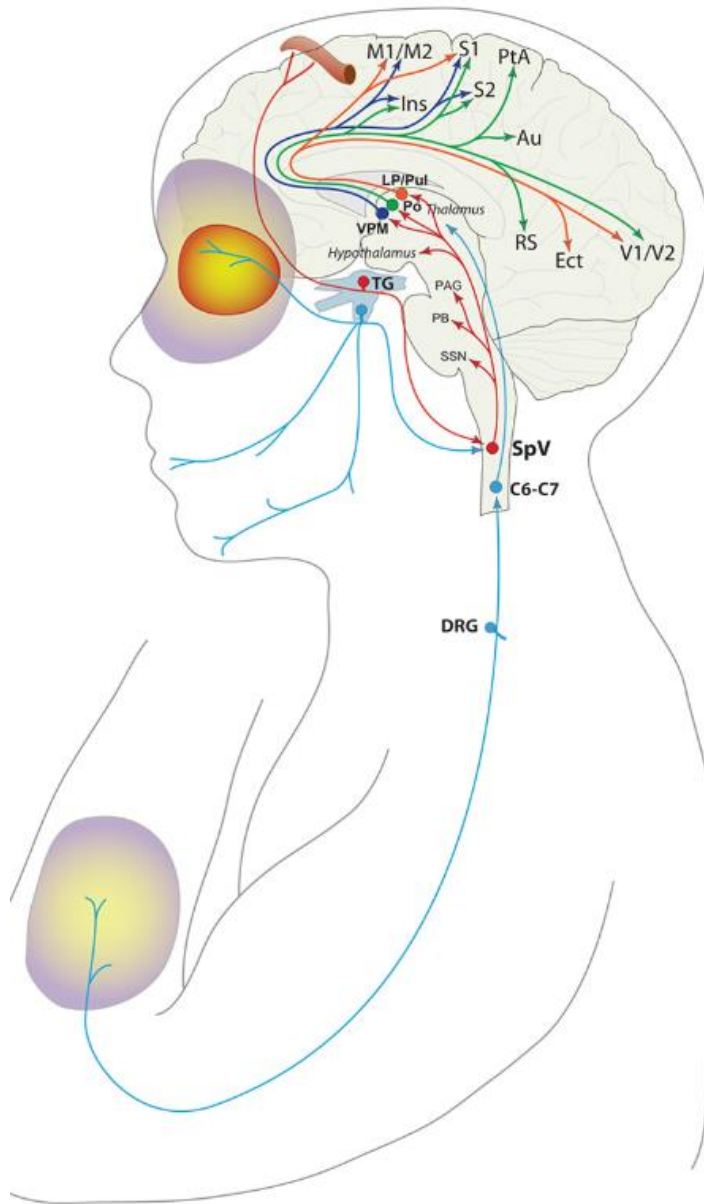


Figure 2: The ascending trigeminovascular pathway. A schematic representing the ascending trigeminovascular pathway. Au, Auditory cortex; C6–C7, sixth and seventh spinal cord segments; DRG, dorsal root ganglion; Ins, insular cortex; Ect, ectorhinal cortex; LP, lateral posterior thalamic nucleus; M1/M2, primary and secondary motor cortices; PAG, periaqueductal gray; PB, parabrachial nucleus; PO, posterior thalamus; PtA, parietal association cortex; Pul, pulvinar; RS, retrosplenial cortex; S1/S2, primary and secondary somatosensory cortices; SpV, spinal trigeminal nucleus; SSN, superior salivatory; TG, trigeminal ganglion; V1/V2, primary and secondary visual cortex; VPM, ventral posteromedial thalamus. Modified from Burstein et al (2015).

1.2.3.1 Sensitization of the trigeminovascular pathway

Over the past 50 years, a number of investigations have explored the underlying mechanism of migraine through the direct stimulation of the trigeminovascular pathway. For example, the 1980s animal models of neurovascular head pain involved electrical and mechanical stimulation of dural sinuses (Davis & Dostrovsky, 1986; A. Strassman et al., 1986) in an attempt to excite dura-sensitive neurons that project to the brain and spinal cord including to the SpV, thalamus, hypothalamus and PAG (Bernstein & Burstein, 2012; Burstein, Yamamura, Malick, & Strassman, 1998). Whilst these experimental animal investigations helped to identify the involvement of the trigeminovascular system in migraine head pain and accompanying symptoms, it has been reported that acute electrical or mechanical stimulation of the dura is not sufficient to trigger migraines in humans. Indeed it was shown that such electrical or mechanical stimuli had to induce central and/or peripheral sensitization in order for it to elicit migraine-like pain (Bernstein & Burstein, 2012).

Over the last 15 years, the theory of peripheral and central sensitization has come to be considered by many as critical in explaining some of the factors not considered or explored with respect to other migraine theories (Goadsby et al., 2017). It has been hypothesized that peripheral sensitization is critical for the initiation of a migraine through the activation of trigeminovascular neurons. This activation results in migraine-like symptoms such as throbbing head pain, nausea, vomiting, photophobia and phonophobia (Bernstein & Burstein, 2012; Borsook & Burstein, 2012) and the intensification of headache by activities that increase intracranial pressure (J. N. Blau & Dexter, 1981). In addition, it has been hypothesized that central sensitization of trigeminovascular neurons follows this peripheral sensitization and underlies the extracranial hypersensitivity associated with migraine (Bernstein & Burstein, 2012; Burstein et al., 1998) (Figure 3).

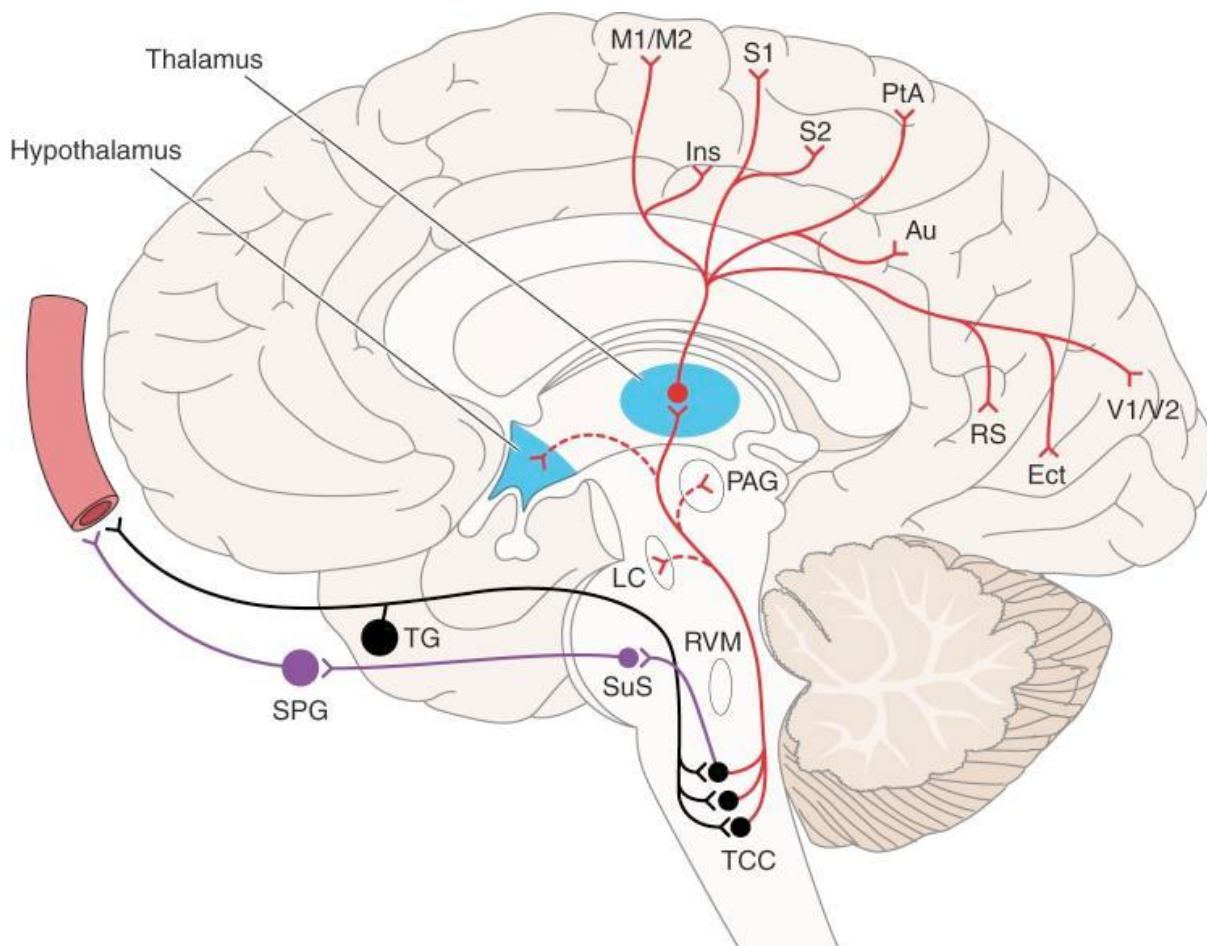


Figure 3: Sensitization of the trigeminovascular pathway. A schematic representing the sensitization and subsequent activation of the trigeminovascular pathway. The trigeminal ganglion (TG) carries trigeminal primary afferents which synapse on intracranial and extracranial structures. Sensitization of peripheral trigeminovascular neurons innervate meninges. Sensitization of neurons in the trigeminocervical complex (TCC) project along the ascending trigeminovascular pathway to innervate other brainstem areas including the rostral ventromedial medulla (RVM), locus coeruleus (LC) and periaqueductal gray (PAG) before reaching the hypothalamus, thalamus and cortical areas. (Au, Auditory cortex; Ect, ectothinal cortex; Ins, insular cortex; M1/M2, primary and secondary motor cortices; PtA, parietal association cortex; RS, retrosplenial; S1/S2, primary and secondary somatosensory cortices; SPG, sphenopalantine ganglion; SuS, superior salivatory nucleus; TG, trigeminal ganglion; V1/V2, primary and secondary visual cortex). Modified from Goadsby et al (2017).

In accordance with this theory, nociceptive input drives the attack whilst central sensitization modulates the headache pain (Olesen et al., 2009). However, this idea relies on the fact that the trigger for migraine begins in the periphery (Goadsby et al., 2017; Olesen et al., 2009; A. M. Strassman, Raymond, & Burstein, 1996). In other words, activation of the trigeminovascular system originates from primary sensory afferents responding to nociceptive input.

Whilst the trigeminovascular system itself is responsible for generating head pain through changes in sensitivity of both peripheral trigeminovascular afferents and central neural structures, descending projections from regions such as the PAG-RVM to the SpV can also play a critical role by either enhancing or suppressing incoming trigeminovascular inputs (Porreca, Ossipov, & Gebhart, 2002). Many modulatory supraspinal pathways converge on the PAG-RVM pathway, hence the threshold for incoming noxious inputs to trigger a migraine depends on the balance between incoming nociceptive signals and their modulation by spinal and supraspinal pathways (Bernstein & Burstein, 2012) (Figure 4).

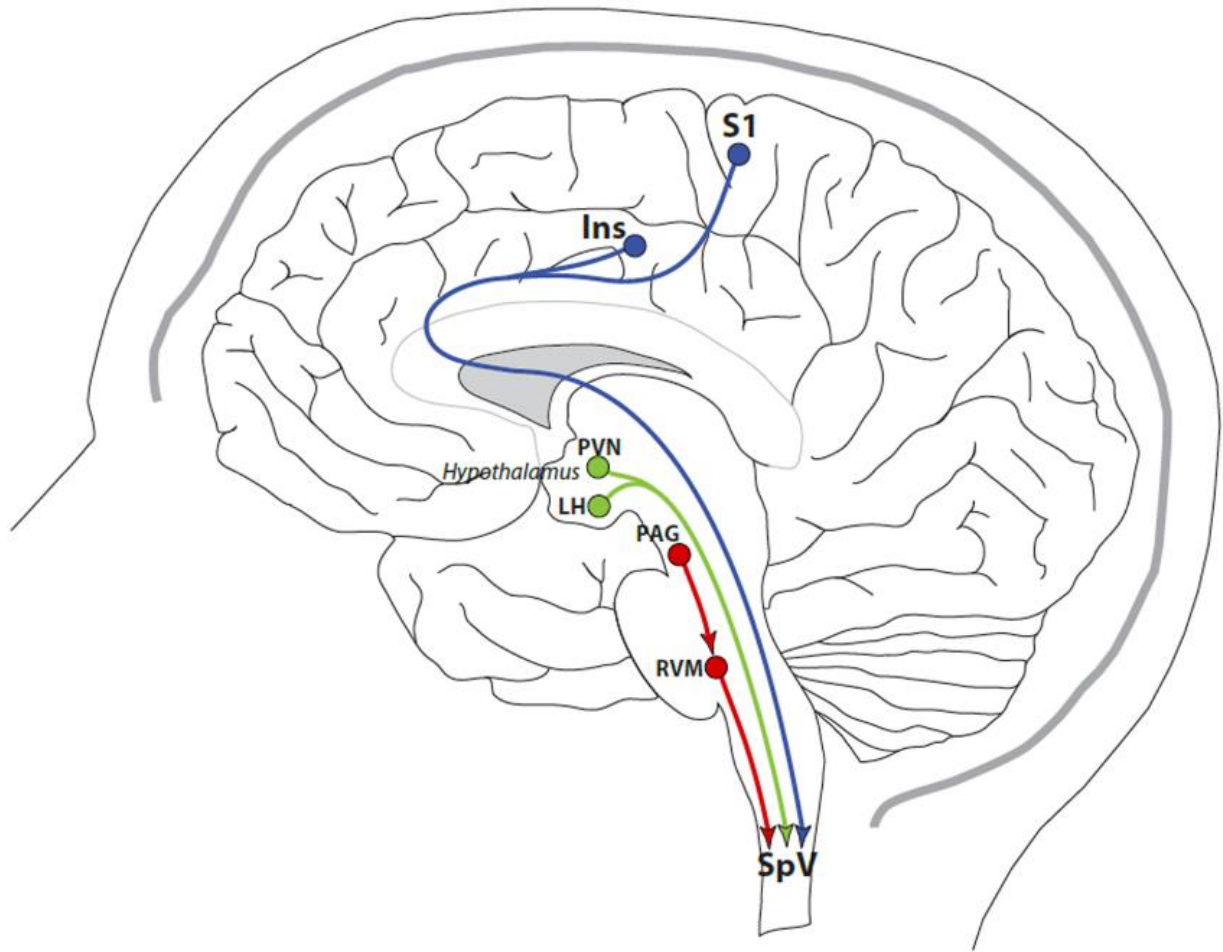


Figure 4: Descending modulation of the trigemino-vascular system. A schematic representation of the descending pathways that modulate trigemino-vascular nociceptive transmission in the SpV. Ins, Insula; LH, lateral hypothalamus; PAG, periaqueductal gray; PVN, paraventricular nucleus of hypothalamus; S1, primary somatosensory cortex; SpV, spinal trigeminal nucleus; RVM, rostral ventromedial medulla. Modified from Nosedá and Burstein (2013).

Therefore, if sensitization of trigeminovascular afferents and their central connections are thought to explain the headache phase of migraine; what about the premonitory phase of migraine? One could argue that the key to understanding how a migraine develops lies in the premonitory phase of the migraine attack since this period starts directly prior to pain onset and even in the absence of a trigger. Indeed, there is growing evidence that changes in the central nervous system may play a critical role in the generation of a migraine, regardless of the presence of a peripheral trigger and before headache onset (Akerman, Holland, & Goadsby, 2011; Goadsby, Charbit, Andreou, Akerman, & Holland, 2009). Furthermore, CSD was found to occur independently of peripheral input (Lambert, Truong, & Zagami, 2011).

Given these observations, it has been hypothesized that migraine is solely a disorder of the central nervous system (Schwedt & Dodick, 2009); that the migraine brain has a genetic predisposition to a generalised neuronal hyperexcitability (Ferrari, Klever, Terwindt, Ayata, & van den Maagdenberg, 2015; Pietrobon & Moskowitz, 2013), rendering it very sensitive to homeostatic changes (Burstein et al., 2015) and incapable of habituating itself (Coppola, Pierelli, & Schoenen, 2007).

1.2.4 Migraine as a central disorder?

Although there has been disparity amongst the migraine field about why, how and when a migraine is initiated (Goadsby et al., 2017), with the advance of neural imaging, migraine is now considered by many a neurological disorder; “*an inherited tendency for the brain to lose control of its inputs,*” namely by means of the trigeminovascular system (Goadsby et al., 2017). Evidence for this enabled the development of the controversial “central generator” theory, which has divided the

opinions of many researchers. It was a radical idea, introduced in a 1987 report by Raskin and colleagues, when 15 of 175 pain patients developed migraine-like headaches following the implantation of electrodes into the PAG (Raskin, Hosobuchi, & Lamb, 1987). These data were interpreted as the PAG being the source rather than consequence of migraine pain (Bahra et al., 2001b; Weiller, May, Limmroth, Juptner, Kaube, Schayck, Coenen, & Diener, 1995).

Whilst this central generator theory remains hotly debated, today there are a number of findings that call its validity into question. Firstly, it has been shown that persistent headaches lasting three months or longer can occur in up to 40% of subjects undergoing craniotomy regardless of the implantation of electrodes (Gee, Ishaq, & Vijayan, 2003; Kaur, Selwa, Fromes, & Ross, 2000; Olesen et al., 2009). Secondly, PAG activation was found to occur in other pain paradigms, rendering its activity nonspecific to migraine (Olesen et al., 2009). Thirdly, electrical stimulation of the PAG produced a general whole body pain relief, again nonspecific to migraine (Olesen et al., 2009). Finally, stimulation of the PAG or RVM can only increase or decrease firing in response to noxious stimulation of their peripheral receptive fields (Porreca et al., 2002). Therefore, it is activation in specific dorsal horn neurons by input that is received from peripheral nociceptors that determine where pain modulation is needed. In migraine, it is activation of the trigeminovascular neurons in SpV by inputs from meningeal nociceptors. As a result, after accounting for these factors, less than 1% of patients in Raskin and colleagues' report could have had headaches attributed to PAG stimulation, leading to the brainstem generator theory being labelled by many researchers as nonspecific to migraine and insufficient in explaining modulation of the trigeminovascular system (Olesen et al., 2009).

1.2.5 Brainstem tone

In an attempt to understand the pathophysiology of migraine, one needs to extend beyond a one-dimensional view of a “migraine generator” and understand that perhaps, after all, a peripheral cerebrovascular trigger is necessary to precipitate a migraine attack (Borsook & Burstein, 2012). However, timing of such a trigger is critical in determining whether it is successful in inducing a migraine. This is where we are in need of a compromise, an understanding that looks further than a dichotomy of central versus peripheral.

The idea of brainstem tone, also referred to as allostatic load, suggests that a peripheral cerebrovascular trigger may indeed be required to trigger a migraine attack, but cyclic sensitivity changes in brainstem regions that receive noxious orofacial inputs may be critical in allowing such triggers to successfully induce a migraine attack (Burstein et al., 2015). The allostatic load is defined as the level of brain activity required to appropriately manage levels of emotional or physiological stress (McEwen, 1998). Migraine is associated with a failure of intrinsic systems to evaluate errors and deviations from physiological signals about homeostatic levels (Borsook, Aasted, Burstein, & Becerra, 2014), i.e. the migraine brain is predisposed to having a higher allostatic load. Because of this, when allostatic load reaches high levels (diminished brainstem tone), the brain’s endogenous system is impaired. Therefore, when a trigger coincides with a compromised circadian cycle of brainstem, hypothalamic and thalamic neurons, it is successful in inducing a migraine (Burstein et al., 2015).

It has been hypothesized that brainstem function in migraineurs oscillates between enhanced, threshold and diminished neural “*tone*” states (Burstein et al., 2015). When the brainstem is in a

state of diminished tone, incoming noxious inputs can activate central pathways and evoke head pain. When in an enhanced tone state, endogenous analgesic mechanisms overcome incoming noxious inputs to activate higher brain centers and block the development of head pain (Figure 5).

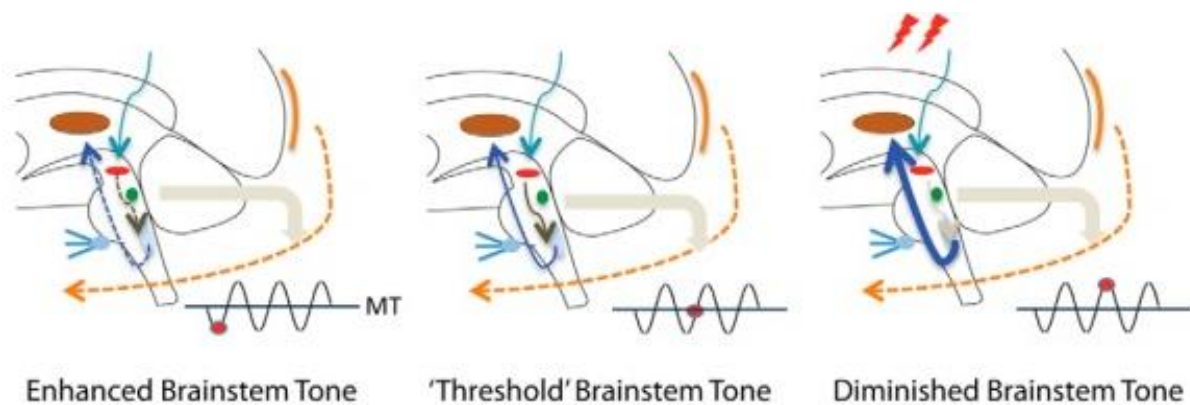


Figure 5: Brainstem tone. Conceptualization of how brainstem tone allows for a trigger to induce a migraine. The teal arrow in each diagram represents an identical noxious stimulus for each condition. When the brainstem tone is high (red dot below line of migraine threshold (MT)), nociceptive signals are repressed; and when the brainstem tone is low (red dot above MT), afferent signals are not effectively blocked. Therefore, in the ‘enhanced brainstem tone’ state, the endogenous analgesic mechanisms of the brainstem are strong enough to block a trigger from inducing a migraine. Therefore, the brainstem does not send afferent signals (via the blue arrow) to activate central trigeminovascular neurons and hence, induce migraine pain. In the ‘threshold brainstem tone’ the system is balanced but could tip into a state that could allow the dura to activate central trigeminovascular neurons. In the ‘diminished brainstem tone’ state, these mechanisms are compromised, thus allowing the signals to trigger a migraine. Modified from Burstein et al (2015).

By considering this concept, we are acknowledging that triggers are inconsistent in inducing a migraine, because a headache may or may not develop in response to identical environmental and/or endogenous condition changes based on the brainstem tone. The “*tone*” is driven by fluctuation of brainstem neuronal activity that modulates nociceptive signals from the meninges (Borsook & Burstein, 2012; Burstein et al., 2015). These nociceptive signals that drive central trigeminovascular neurons are controlled by a “*gate*.” The strength of the gate is determined by the threshold of the neural networks that modify the afferent signals (Borsook & Burstein, 2012; Burstein et al., 2015). Therefore, we may need to resign to the fact that natural fluctuations occur in neuronal excitability that are difficult to measure or quantify (Stankewitz & May, 2009), hence internal and/or external triggers will not elicit headache when the brain is protected, and will induce one when its excitability is at a peak (Goadsby et al., 2017).

The key in understanding this better would be to study the cyclic behaviour of the brainstem in migraineurs throughout their migraine cycle, in particular, in the hours leading up to a migraine. Very little is known about the mechanism by which triggers work to activate meningeal nociceptors and how premonitory symptoms initiate headache. However, it has been proposed that hypothalamic and brainstem neurons that respond to physiological and emotional deviation from homeostasis, can lower the threshold for trigeminovascular nociceptive transmission from the thalamus to the cortex, hence allowing for a headache to be triggered (Noseda, Kainz, Borsook, & Burstein, 2014). Understanding these processes could be influential in not only the study and treatment of migraine, but also to the study and treatment of other conditions that share similar genetic and pathophysiological backgrounds as migraine, such as epilepsy (Czapinska-Ciepiela, 2018). Indeed, migraine and epilepsy are often co-morbid conditions, with both diseases manifesting in patterns of neuronal hyperexcitation (Czapinska-Ciepiela, 2018; Liao, Tian, Wang,

& Xiao, 2018). Epilepsy, like migraine, remains a largely unknown and debilitating disease. Therefore, the translatability of migraine research to epilepsy enhances the importance of this body of work even more.

1.3 Treating migraine

Despite the debilitating effects of migraine both individually and globally, it is largely undertreated with sufferers often having no means of relieving their pain, let alone of preventing future attacks. This is not surprising, since the pathophysiology of migraine is still unclear. Nevertheless, given what we know of the trigeminovascular system and its involvement in migraine, treatments have been developed and have resulted in some success. The involvement of serotonin (5-HT) in migraine was proposed over 50 years ago, and with the identification of the receptors involved in aborting migraines, 5-HT_{1B/1D} receptor agonists were developed; commonly known as triptans (Goadsby et al., 2017). At first, triptans were designed to constrict intracranial blood vessels (D. Levy, Jakubowski, & Burstein, 2004), however it now appears that triptans act within the trigeminocervical complex to modulate trigeminovascular nociceptive neurons (Goadsby et al., 2017). Activation of the trigeminovascular system results in the release of neuropeptides such as CGRP. The main modulatory role of CGRP seems to be inflammation-induced vasodilation, and is commonly found in trigeminal sensory afferents, the SpV and other areas within the nervous system (Vikelis, Spingos, & Rapoport, 2018). Studies have shown that intravenous infusion of CGRP into the dura can induce migraine attacks whilst CGRP-antagonists and triptans can abort them (Goadsby et al., 2017; Olesen et al., 2009) (Figure 6).

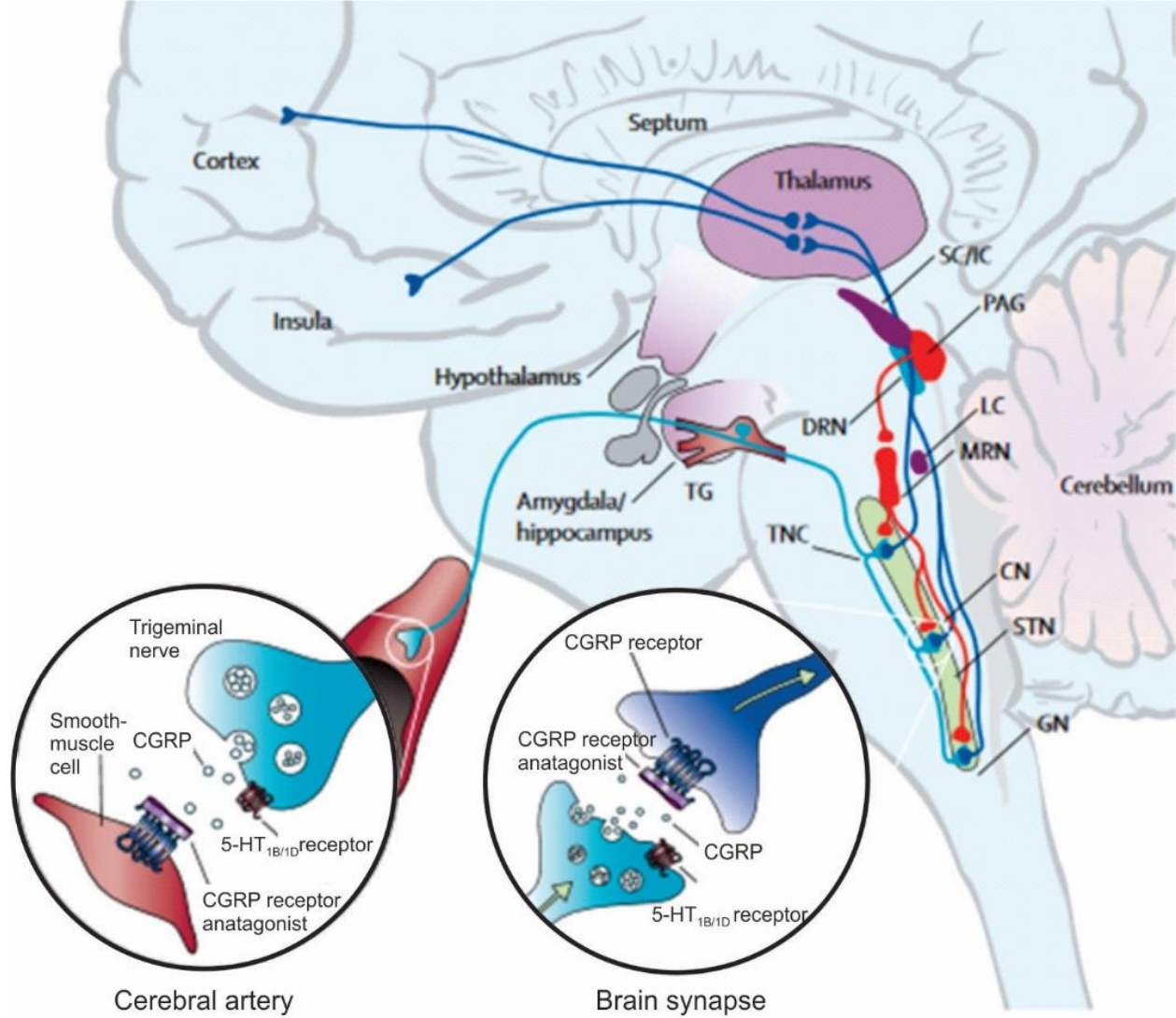


Figure 6: CGRP-blockers and triptans. A schematic representation of the brain areas expressing CGRP and 5-HT_{1B/1D} receptors that are possible sites of action of CGRP-blockers and triptans for treatment of migraine. CN, cochlear nucleus; DRN, dorsal raphe nucleus; GN, gracile nucleus; LC, locus coeruleus; MRN, median raphe nucleus; SC/IC, superior and inferior colliculus; STN, solitary tract nucleus; TG, trigeminal ganglion; TNC, trigeminal nucleus caudalis. CGRP = calcitonin gene-related peptide; 5-HT = serotonin. Modified from Edvinsson (2008).

Interestingly, efficacy of triptan administration based on time administered, has shed a light on migraine pathophysiology, supporting that meningeal nociceptors drive the initiation of a migraine (Burstein et al., 2015). In the rat, triptan administered simultaneously with chemical irritation of the dura prevents central sensitization from occurring (Bernstein & Burstein, 2012). Similarly, treating human patients early (within the first 60 minutes) effectively blocks the development of cutaneous allodynia. However, neither in the rat or human can central sensitization/allodynia be reversed by late triptan administration (two hours in animal model and four hours in human)(Burstein & Jakubowski, 2004) and thus, sensitized meningeal nociceptors are not inhibited by triptans (Bernstein & Burstein, 2012). Triptans abort migraine by a central action in the SpV that disrupts communication between peripheral (first-order) and central (second-order) trigeminovascular neurons (D. Levy et al., 2004).

Though triptans have been shown to be an effective treatment for alleviating migraine symptoms if administered in a timely fashion, many migraineurs continue to suffer the debilitating effects of migraine without relief by triptans. Further, for those who do experience pain relief many experience devastating side-effects, as triptans work to constrict blood vessels, therefore their use is limited (Vikelis et al., 2018). Prophylactic medications can also be taken on a daily basis for chronic migraine sufferers to reduce frequency of attacks and include Botox (Herd et al., 2018), CGRP-blockers (Burch & Rayhill, 2018; Edvinsson, 2008), calcium-channel blockers as well as serotonergic antidepressants (Kumar & Kadian, 2018). However patients often have to combine prophylactic with acute medication to manage their migraine pain (Kumar & Kadian, 2018), often leading to an overuse of medication (Vikelis et al., 2018). A new era in acute migraine prophylaxis has been focusing on CGRP-blockers, non-triptan serotonin receptor agonists, as well as different delivery systems for older medications such as triptans and nonsteroidal anti-inflammatory

medications (Vikelis et al., 2018).

1.4 Neural imaging

Earlier migraine studies have investigated neural activity during spontaneous/triggered migraine attacks (S.K. Afridi et al., 2005; S. K. Afridi et al., 2005; Bahra et al., 2001b; Denuelle et al., 2007; Weiller, May, Limmroth, Juptner, Kaube, Schayck, Coenen, & Diener, 1995), and interictal periods (Calandre, Bembibre, Arnedo, & Becerra, 2002; DaSilva et al., 2007; De Benedittis, Ferrari Da Passano, Granata, & Lorenzetti, 1999; Kassab, Bakhtar, Wack, & Bednarczyk, 2009; Kim et al., 2009; Kim et al., 2008). Unfortunately, findings throughout these studies are very inconsistent and this can be attributed to the limitations of earlier neural imaging techniques. Even the influential study by Weiller and colleagues in 1995 lacks the spatial acuity to specify the exact nuclei involved (Weiller, May, Limmroth, Juptner, Kaube, Schayck, Coenen, & Diener, 1995). Modern non-invasive magnetic resonance imaging (MRI) techniques with greater temporal and spatial resolution, such as functional magnetic resonance imaging (fMRI) and arterial spin labelling (ASL) have made it possible to identify specific nuclei associated with migraine-related dysfunction with more precision. As a result, data from earlier studies investigating changes during migraine attacks and in the interictal period, can be corroborated by newer imaging studies.

However, research into the critical 24-hour period preceding a migraine headache is lacking, leaving a huge gap in our understanding of the initiating quality of how, why and when a migraine occurs. This is likely due to the difficulty of acquiring data in this period, as well as limitations in patient reporting, as premonitory symptoms are often interpreted as either the migraine trigger itself or as nonspecific to the migraine (Karsan et al., 2018). Due to the insight that we can only

gain through investigation into this period, cross-sectional studies utilizing developed neural imaging techniques in this period should be our collective priority. If we can develop a more comprehensive understanding of these hours preceding a migraine headache, treatments could become more specialized and more effective at aborting attacks in the premonitory phase before pain onset (Karsan et al., 2018). Through analyzing resting fMRI data, it is possible to measure neural circuitry and local neural function using measures such as functional connectivity and regional homogeneity. Functional connectivity is suggested to reflect the level of functional communication between regions, by measuring the level of co-activation of spontaneous functional MRI time-series (Biswal, Kysten, & Hyde, 1997; van den Heuvel & Hulshoff Pol, 2010). Regional homogeneity is a marker of local signal coupling, and evaluates the synchronicity between the time series of a given voxel and its nearest neighbours (Zang, Jiang, Lu, He, & Tian, 2004). In addition, the magnitude of resting fluctuations in activity can be measured by assessing infra-slow oscillations (ISOs). During the resting state, the brain exhibits fluctuations at frequencies $<0.1\text{Hz}$, and increases in these fluctuations have been identified in chronic neuropathic conditions (Alshelh et al., 2016). These methods of studying resting-state fMRI have emerged as efficient approaches to the exploration of neural circuitry and function. In addition to measuring regional patterns of activity and basal connections through fMRI studies, subtler changes in absolute regional brain activity can also be identified through ASL data, measuring regional cerebral blood flow (rCBF). With the collaboration of both techniques, we are more likely to identify abnormalities of the migraine brain and draw insight into the intricacies of the premonitory phase of migraine.

Since migraine has been considered a cyclical disorder, longitudinal studies over individuals' migraine cycles are also of utmost importance in understanding the nature of migraine. As the

brainstem tone theory suggests, brainstem function oscillates between enhanced, threshold and diminished neural “*tone*” states (Burstein et al., 2015), with triggers only effective in inducing a migraine when they coincide with appropriate neural conditions. Therefore, investigation into these oscillating neural conditions can help to elucidate patterns in which migraines are triggered within an individual. Very little is known about the mechanism by which triggers work to activate meningeal nociceptors and how premonitory symptoms initiate headache. By collecting fMRI and ASL data in individuals on a daily basis over the cycle of a month as well as recording internal/external conditions, these oscillations in brainstem function can be identified, especially in the critical 24-hour period preceding a migraine. These longitudinal studies are necessary for development of treatments aimed at preventing attacks from occurring, as opposed to merely aborting attacks.

1.5 Rationale and general aims of dissertation

As discussed, the questions I ask in this dissertation are based on several key observations:

1. It is well established that sensitization of the trigeminovascular system is involved in the experience of migraine head pain. However, due to the lack of research into the critical 24-hour preceding a migraine, it is still unclear as to what drives the initial sensitization of the meningeal nociceptors.
2. Areas of the brainstem including the PAG, dorsal pons and SpV are involved in a network with the hypothalamus that are thought to modulate or drive the migraine experience. With the use of modern neural imaging techniques, elucidation of this network particularly in the 24-hour

period preceding a migraine would help the development of medications targeting brain regions involved in migraine pathophysiology.

3. The migraine brain has a generalised neuronal hyperexcitability, making it very sensitive to homeostatic changes. Therefore, when the allostatic load is high, changes in the external or internal environment can trigger a migraine headache. Understanding the cyclic behaviour of the brainstem can help to identify patterns throughout the migraine cycle.

The general aims of this thesis are as follows:

1. Experimental studies have explored neural alterations during a migraine headache and during the interictal period, but very few studies have examined the pattern of activity directly preceding the development of a migraine headache. This aim of this cross-sectional investigation was to determine if ongoing activity patterns, reflected through ISOs and functional connectivity, within the brainstem and hypothalamus would alter over the migraine cycle, particularly in the premonitory phase (Chapter 2, published in *Human Brain Mapping* 2018).
2. While fMRI measures assess regional activity pattern changes throughout the migraine cycle, ASL allows for the assessment of absolute regional brain activity levels. The aim of this cross-sectional investigation was to determine if rCBF differed over the migraine cycle, hence supporting the results from our previous investigation. Data from 21 of these migraine subjects were used in the previous investigation (Chapter 3, submitted to *Neural Image: Clinical* 2018).

3. In order to explore the concept of brainstem tone, regional activity patterns were measured within individuals every day over a four-week period as part of this longitudinal investigation. This aim of this longitudinal investigation was to determine if ongoing activity patterns, reflected through ISOs, regional homogeneity and functional connectivity, within the brainstem would alter over the individual migraine cycle. Data from one of these migraine subjects was also included in the previous two investigations (Chapter 4, submitted to *PNAS* 2018).

1.6 References

- Afridi, S. K., Giffin, N. J., Kaube, H., Friston, K. J., Ward, N. S., Frackowiak, R. S., & Goadsby, P. J. (2005). A positron emission tomographic study in spontaneous migraine. *Arch Neurol*, 62(8), 1270-1275. doi:10.1001/archneur.62.8.1270
- Afridi, S. K., Matharu, M. S., Lee, L., Kaube, H., Friston, K. J., Frackowiak, R. S., & Goadsby, P. J. (2005). A PET study exploring the laterality of brainstem activation in migraine using glyceryl trinitrate. *Brain*, 128(Pt 4), 932-939. doi:10.1093/brain/awh416
- Akerman, S., Holland, P. R., & Goadsby, P. J. (2011). Diencephalic and brainstem mechanisms in migraine. *Nat Rev Neurosci*, 12(10), 570-584. doi:10.1038/nrn3057
- Alshelh, Z., Di Pietro, F., Youssef, A. M., Reeves, J. M., Macey, P. M., Vickers, E. R., . . . Henderson, L. A. (2016). Chronic Neuropathic Pain: It's about the Rhythm. *J Neurosci*, 36(3), 1008-1018. doi:10.1523/JNEUROSCI.2768-15.2016
- Amin, F. M., Asghar, M. S., Hougaard, A., Hansen, A. E., Larsen, V. A., de Koning, P. J. H., . . . Ashina, M. (2013). Magnetic resonance angiography of intracranial and extracranial arteries in patients with spontaneous migraine without aura: a cross-sectional study. *The Lancet Neurology*, 12(5), 454-461. doi:[https://doi.org/10.1016/S1474-4422\(13\)70067-X](https://doi.org/10.1016/S1474-4422(13)70067-X)
- Bahra, A., Matharu, M. S., Buchel, C., Frackowiak, R. S., & Goadsby, P. J. (2001). Brainstem activation specific to migraine headache. *Lancet*, 357(9261), 1016-1017.
- Bartolini, M., Baruffaldi, R., Paolino, I., & Silvestrini, M. (2005). Cerebral blood flow changes in the different phases of migraine. *Funct Neurol*, 20(4), 209-211.
- Bernstein, C., & Burstein, R. (2012). Sensitization of the trigeminovascular pathway: perspective and implications to migraine pathophysiology. *J Clin Neurol*, 8(2), 89-99. doi:10.3988/jcn.2012.8.2.89

- Biswal, B. B., Kylen, J. V., & Hyde, J. S. (1997). Simultaneous assessment of flow and BOLD signals in resting-state functional connectivity maps. *NMR in Biomedicine*, *10*(4-5), 165-170. doi:10.1002/(SICI)1099-1492(199706/08)10:4/5<165::AID-NBM454>3.0.CO;2-7
- Blau, J. (2004). Harold G Wolff: the man and his migraine. *Cephalalgia*, *24*(3), 215-222. doi:10.1111/j.1468-2982.2003.00642.x
- Blau, J. N., & Dexter, S. L. (1981). The site of pain origin during migraine attacks. *Cephalalgia*, *1*(3), 143-147. doi:10.1046/j.1468-2982.1981.0103143.x
- Borsook, D., Aasted, C. M., Burstein, R., & Becerra, L. (2014). Migraine Mistakes: Error Awareness. *Neuroscientist*, *20*(3), 291-304. doi:10.1177/1073858413503711
- Borsook, D., & Burstein, R. (2012). The enigma of the dorsolateral pons as a migraine generator. *Cephalalgia*, *32*(11), 803-812. doi:10.1177/0333102412453952
- Breslau, N., & Rasmussen, B. K. (2001). The impact of migraine: Epidemiology, risk factors, and co-morbidities. *Neurology*, *56*(6 Suppl 1), S4-12.
- Burch, R., & Rayhill, M. (2018). New preventive treatments for migraine. *Bmj*, *361*, k2507. doi:10.1136/bmj.k2507
- Burstein, R., & Jakubowski, M. (2004). Analgesic triptan action in an animal model of intracranial pain: a race against the development of central sensitization. *Ann Neurol*, *55*(1), 27-36. doi:10.1002/ana.10785
- Burstein, R., & Jakubowski, M. (2005). Unitary hypothesis for multiple triggers of the pain and strain of migraine. *J Comp Neurol*, *493*(1), 9-14. doi:10.1002/cne.20688
- Burstein, R., Nosedà, R., & Borsook, D. (2015). Migraine: multiple processes, complex pathophysiology. *J Neurosci*, *35*(17), 6619-6629. doi:10.1523/JNEUROSCI.0373-15.2015

- Burstein, R., Yamamura, H., Malick, A., & Strassman, A. M. (1998). Chemical stimulation of the intracranial dura induces enhanced responses to facial stimulation in brain stem trigeminal neurons. *J Neurophysiol*, *79*(2), 964-982. doi:10.1152/jn.1998.79.2.964
- Calandre, E. P., Bembibre, J., Arnedo, M. L., & Becerra, D. (2002). Cognitive disturbances and regional cerebral blood flow abnormalities in migraine patients: their relationship with the clinical manifestations of the illness. *Cephalalgia*, *22*(4), 291-302. doi:10.1046/j.1468-2982.2002.00370.x
- Coppola, G., Pierelli, F., & Schoenen, J. (2007). Is the cerebral cortex hyperexcitable or hyperresponsive in migraine? *Cephalalgia*, *27*(12), 1427-1439. doi:10.1111/j.1468-2982.2007.01500.x
- Czapinska-Ciepiela, E. (2018). Treatment of migraine in a patient with epilepsy. *Wiad Lek*, *71*(9), 1793-1802.
- Dampney, R. (2011). The Hypothalamus and Autonomic Regulation: An Overview. In *Central Regulation of Autonomic Functions*: Oxford University Press.
- DaSilva, A. F. M., Granziera, C., Tuch, D. S., Snyder, J., Vincent, M., & Hadjikhani, N. (2007). Interictal alterations of the trigeminal somatosensory pathway and PAG in migraine. *Neuroreport*, *18*(4), 301-305. doi:10.1097/WNR.0b013e32801776bb
- Davis, K. D., & Dostrovsky, J. O. (1986). Activation of trigeminal brain-stem nociceptive neurons by dural artery stimulation. *Pain*, *25*(3), 395-401.
- De Benedittis, G., Ferrari Da Passano, C., Granata, G., & Lorenzetti, A. (1999). CBF changes during headache-free periods and spontaneous/induced attacks in migraine with and without aura: a TCD and SPECT comparison study. *J Neurosurg Sci*, *43*(2), 141-146; discussion 146-147.

- Denuelle, M., Fabre, N., Payoux, P., Chollet, F., & Geraud, G. (2007). Hypothalamic activation in spontaneous migraine attacks. *Headache*, *47*(10), 1418-1426. doi:10.1111/j.1526-4610.2007.00776.x
- Edvinsson, L. (2008). CGRP-receptor antagonism in migraine treatment. *The Lancet*, *372*(9656), 2089-2090. doi:10.1016/S0140-6736(08)61710-9
- Ferrari, M. D. (1998). The economic burden of migraine to society. *Pharmacoeconomics*, *13*(6), 667-676.
- Ferrari, M. D., Klever, R. R., Terwindt, G. M., Ayata, C., & van den Maagdenberg, A. M. (2015). Migraine pathophysiology: lessons from mouse models and human genetics. *Lancet Neurol*, *14*(1), 65-80. doi:10.1016/s1474-4422(14)70220-0
- Fields, H. L., & Heinricher, M. M. (1985). Anatomy and physiology of a nociceptive modulatory system. *Philos Trans R Soc Lond B Biol Sci*, *308*(1136), 361-374.
- Floyd, N. S., Price, J. L., Ferry, A. T., Keay, K. A., & Bandler, R. (2001). Orbitomedial prefrontal cortical projections to hypothalamus in the rat. *J Comp Neurol*, *432*(3), 307-328.
- Gee, J. R., Ishaq, Y., & Vijayan, N. (2003). Postcraniotomy headache. *Headache*, *43*(3), 276-278.
- Giffin, N. J., Ruggiero, L., Lipton, R. B., Silberstein, S. D., Tvedskov, J. F., Olesen, J., . . . Macrae, A. (2003). Premonitory symptoms in migraine: an electronic diary study. *Neurology*, *60*(6), 935-940.
- Goadsby, P. J., Charbit, A. R., Andreou, A. P., Akerman, S., & Holland, P. R. (2009). Neurobiology of migraine. *Neuroscience*, *161*(2), 327-341. doi:10.1016/j.neuroscience.2009.03.019

- Goadsby, P. J., Holland, P. R., Martins-Oliveira, M., Hoffmann, J., Schankin, C., & Akerman, S. (2017). Pathophysiology of Migraine: A Disorder of Sensory Processing. *Physiol Rev*, 97(2), 553-622. doi:10.1152/physrev.00034.2015
- Hadjikhani, N., Sanchez Del Rio, M., Wu, O., Schwartz, D., Bakker, D., Fischl, B., . . . Moskowitz, M. A. (2001). Mechanisms of migraine aura revealed by functional MRI in human visual cortex. *Proc Natl Acad Sci U S A*, 98(8), 4687-4692. doi:10.1073/pnas.071582498
- Herd, C. P., Tomlinson, C. L., Rick, C., Scotton, W. J., Edwards, J., Ives, N., . . . Sinclair, A. (2018). Botulinum toxins for the prevention of migraine in adults. *Cochrane Database Syst Rev*, 6, Cd011616. doi:10.1002/14651858.CD011616.pub2
- Humphrey, P. P., & Goadsby, P. J. (1994). The mode of action of sumatriptan is vascular? A debate. *Cephalalgia*, 14(6), 401-410; discussion 393. doi:10.1046/j.1468-2982.1994.1406401.x
- ICHD. (2013). The International Classification of Headache Disorders, 3rd edition (beta version). *Cephalalgia*, 33(9), 629-808. doi:10.1177/0333102413485658
- Jacobs, B., & Dussor, G. (2016). Neurovascular contributions to migraine: Moving beyond vasodilation. *Neuroscience*, 338, 130-144. doi:10.1016/j.neuroscience.2016.06.012
- Kandel, E. R., Schwartz, J. H., Jessell, T. M., Siegelbaum, S. A., & Hudspeth, A. J. (2012). *Principles of Neural Science* (Vol. 5). US: McGraw-Hill Education - Europe.
- Karsan, N., Bose, P., & Goadsby, P. J. (2018). The Migraine Premonitory Phase. *Continuum (Minneapolis)*, 24(4, Headache), 996-1008. doi:10.1212/con.0000000000000624
- Kassab, M., Bakhtar, O., Wack, D., & Bednarczyk, E. (2009). Resting brain glucose uptake in headache-free migraineurs. *Headache*, 49(1), 90-97. doi:10.1111/j.1526-4610.2008.01206.x

- Kaur, A., Selwa, L., Fromes, G., & Ross, D. A. (2000). Persistent headache after supratentorial craniotomy. *Neurosurgery*, *47*(3), 633-636.
- Kim, J. H., Kim, S., Suh, S. I., Koh, S. B., Park, K. W., & Oh, K. (2009). Interictal metabolic changes in episodic migraine: a voxel-based FDG-PET study. *Cephalalgia*, no-no. doi:10.1111/j.1468-2982.2009.01890.x
- Kim, J. H., Suh, S. I., Seol, H. Y., Oh, K., Seo, W. K., Yu, S. W., . . . Koh, S. B. (2008). Regional grey matter changes in patients with migraine: a voxel-based morphometry study. *Cephalalgia*, *28*(6), 598-604. doi:10.1111/j.1468-2982.2008.01550.x
- Knight, Y. E., & Goadsby, P. J. (2001). The periaqueductal grey matter modulates trigeminovascular input: a role in migraine? *Neuroscience*, *106*(4), 793-800.
- Kumar, A., & Kadian, R. (2018). Headache, Migraine Prophylaxis. In *StatPearls*. Treasure Island (FL): StatPearls Publishing
- StatPearls Publishing LLC.
- Lambert, G. A., Truong, L., & Zagami, A. S. (2011). Effect of cortical spreading depression on basal and evoked traffic in the trigeminovascular sensory system. *Cephalalgia*, *31*(14), 1439-1451. doi:10.1177/0333102411422383
- Levy, D., Jakubowski, M., & Burstein, R. (2004). Disruption of communication between peripheral and central trigeminovascular neurons mediates the antimigraine action of 5HT 1B/1D receptor agonists. *Proc Natl Acad Sci U S A*, *101*(12), 4274-4279. doi:10.1073/pnas.0306147101
- Levy, R., Deer, T. R., & Henderson, J. (2010). Intracranial neurostimulation for pain control: a review. *Pain Physician*, *13*(2), 157-165.
- Liao, J., Tian, X., Wang, H., & Xiao, Z. (2018). Epilepsy and migraine-Are they comorbidity? *Genes Dis*, *5*(2), 112-118. doi:10.1016/j.gendis.2018.04.007

- Liu, Y., Broman, J., & Edvinsson, L. (2004). Central projections of sensory innervation of the rat superior sagittal sinus. *Neuroscience*, *129*(2), 431-437.
doi:10.1016/j.neuroscience.2004.07.045
- Liveing, E. (1874). On Megrin, Sick-Headache, and some Allied Disorders. A Contribution to the Pathology of Nerve-Storms. by Edward Liveing, M.D. Cantab. London: J. and A. Churchill, 1873. *Journal of Mental Science*, *19*(88), 587-590. doi:10.1192/bjp.19.88.587
- MacGregor, E. A., Brandes, J., & Eikermann, A. (2003). Migraine prevalence and treatment patterns: the global Migraine and Zolmitriptan Evaluation survey. *Headache*, *43*(1), 19-26.
- Mainero, C., Boshyan, J., & Hadjikhani, N. (2011). Altered functional magnetic resonance imaging resting-state connectivity in periaqueductal gray networks in migraine. *Ann Neurol*, *70*(5), 838-845. doi:10.1002/ana.22537
- Malick, A., Strassman, R. M., & Burstein, R. (2000). Trigeminothalamic and reticulohypothalamic tract neurons in the upper cervical spinal cord and caudal medulla of the rat. *J Neurophysiol*, *84*(4), 2078-2112. doi:10.1152/jn.2000.84.4.2078
- McEwen, B. S. (1998). Stress, adaptation, and disease. Allostasis and allostatic load. *Ann NY Acad Sci*, *840*, 33-44.
- Morgan, M. M., Whittier, K. L., Hegarty, D. M., & Aicher, S. A. (2008). Periaqueductal gray neurons project to spinally projecting GABAergic neurons in the rostral ventromedial medulla. *Pain*, *140*(2), 376-386. doi:10.1016/j.pain.2008.09.009
- Nosedá, R., & Burstein, R. (2013). Migraine pathophysiology: anatomy of the trigeminovascular pathway and associated neurological symptoms, cortical spreading depression, sensitization, and modulation of pain. *Pain*, *154 Suppl 1*, S44-53.
doi:10.1016/j.pain.2013.07.021

- Nosedá, R., Jakubowski, M., Kainz, V., Borsook, D., & Burstein, R. (2011). Cortical projections of functionally identified thalamic trigeminovascular neurons: implications for migraine headache and its associated symptoms. *J Neurosci*, *31*(40), 14204-14217.
doi:10.1523/jneurosci.3285-11.2011
- Nosedá, R., Kainz, V., Borsook, D., & Burstein, R. (2014). Neurochemical pathways that converge on thalamic trigeminovascular neurons: potential substrate for modulation of migraine by sleep, food intake, stress and anxiety. *PLoS One*, *9*(8), e103929.
doi:10.1371/journal.pone.0103929
- Olesen, J., Burstein, R., Ashina, M., & Tfelt-Hansen, P. (2009). Origin of pain in migraine: evidence for peripheral sensitisation. *Lancet Neurol*, *8*(7), 679-690. doi:10.1016/S1474-4422(09)70090-0
- Parsons, A. A., & Strijbos, P. J. L. M. (2003). The neuronal versus vascular hypothesis of migraine and cortical spreading depression. *Current Opinion in Pharmacology*, *3*(1), 73-77. doi:[https://doi.org/10.1016/S1471-4892\(02\)00016-4](https://doi.org/10.1016/S1471-4892(02)00016-4)
- Pearce, J. M. (1985). Is migraine explained by Leao's spreading depression? *Lancet*, *2*(8458), 763-766.
- Penfield, W., & McNaughton, F. L. (1940). Dural headache and the innervation of the dura mater. *Arch Neurol Psychiatry*, *44*, 43/75.
- Pietrobon, D., & Moskowitz, M. A. (2013). Pathophysiology of migraine. *Annu Rev Physiol*, *75*, 365-391. doi:10.1146/annurev-physiol-030212-183717
- Porreca, F., Ossipov, M. H., & Gebhart, G. F. (2002). Chronic pain and medullary descending facilitation. *Trends Neurosci*, *25*(6), 319-325.
- Raskin, N. H., Hosobuchi, Y., & Lamb, S. (1987). Headache may arise from perturbation of brain. *Headache*, *27*(8), 416-420.



- Ray, B. S., & Wolff, H. G. (1940). Experimental studies on headache. Pain sensitive structures of the head and their significance in headache. *Arch Surg*, *41*, 813–856.
- Schwedt, T. J., & Dodick, D. W. (2009). Advanced neuroimaging of migraine. *Lancet Neurol*, *8*(6), 560-568. doi:10.1016/s1474-4422(09)70107-3
- Schwedt, T. J., Schlaggar, B. L., Mar, S., Nolan, T., Coalson, R. S., Nardos, B., . . . Larson-Prior, L. J. (2013). Atypical resting-state functional connectivity of affective pain regions in chronic migraine. *Headache*, *53*(5), 737-751. doi:10.1111/head.12081
- Settle, M. (2000). The hypothalamus. *Neonatal Netw*, *19*(6), 9-14. doi:10.1891/0730-0832.19.6.9
- Shevel, E. (2007). The role of the external carotid vasculature in migraine. *Migraine Disorders Research Trends. New York: Nova Science Publishers*, 165-182.
- Shevel, E. (2011). The extracranial vascular theory of migraine—a great story confirmed by the facts. *Headache: The Journal of Head and Face Pain*, *51*(3), 409-417.
- Stankewitz, A., Aderjan, D., Eippert, F., & May, A. (2011). Trigeminal nociceptive transmission in migraineurs predicts migraine attacks. *J Neurosci*, *31*(6), 1937-1943. doi:10.1523/JNEUROSCI.4496-10.2011
- Stankewitz, A., & May, A. (2009). The phenomenon of changes in cortical excitability in migraine is not migraine-specific--a unifying thesis. *Pain*, *145*(1-2), 14-17. doi:10.1016/j.pain.2009.03.010
- Strassman, A., Mason, P., Moskowitz, M., & Maciewicz, R. (1986). Response of brainstem trigeminal neurons to electrical stimulation of the dura. *Brain Res*, *379*(2), 242-250.
- Strassman, A. M., Raymond, S. A., & Burstein, R. (1996). Sensitization of meningeal sensory neurons and the origin of headaches. *Nature*, *384*(6609), 560-564. doi:10.1038/384560a0

- Sugaya, E., Takato, M., & Noda, Y. (1975). Neuronal and glial activity during spreading depression in cerebral cortex of cat. *J Neurophysiol*, *38*(4), 822-841.
doi:10.1152/jn.1975.38.4.822
- Uddman, R., Edvinsson, L., Ekman, R., Kingman, T., & McCulloch, J. (1985). Innervation of the feline cerebral vasculature by nerve fibers containing calcitonin gene-related peptide: trigeminal origin and co-existence with substance P. *Neurosci Lett*, *62*(1), 131-136.
- van den Heuvel, M. P., & Hulshoff Pol, H. E. (2010). Exploring the brain network: A review on resting-state fMRI functional connectivity. *European Neuropsychopharmacology*, *20*(8), 519-534. doi:<https://doi.org/10.1016/j.euroneuro.2010.03.008>
- Vikelis, M., Spingos, K. C., & Rapoport, A. M. (2018). A new era in headache treatment. *Neurol Sci*, *39*(Suppl 1), 47-58. doi:10.1007/s10072-018-3337-y
- Weiller, C., May, A., Limmroth, V., Juptner, M., Kaube, H., Schayck, R. V., . . . Diener, H. C. (1995). Brain stem activation in spontaneous human migraine attacks. *Nat Med*, *1*(7), 658-660.
- Zang, Y., Jiang, T., Lu, Y., He, Y., & Tian, L. (2004). Regional homogeneity approach to fMRI data analysis. *Neuroimage*, *22*(1), 394-400. doi:10.1016/j.neuroimage.2003.12.030

Chapter 2

**Deep in the brain: Changes in subcortical function
immediately preceding a migraine attack**

Deep in the brain: Changes in subcortical function immediately preceding a migraine attack

Noemi Meylakh¹ | Kasia K. Marciszewski¹ | Flavia Di Pietro¹ |
Vaughan G. Macefield² | Paul M. Macey³  | Luke A. Henderson¹ 

¹Department of Anatomy and Histology, University of Sydney, Sydney, New South Wales 2006, Australia

²School of Medicine, Western Sydney University, Sydney, New South Wales, Australia

³UCLA School of Nursing and Brain Research Institute, University of California, Los Angeles, California 90095

Correspondence

Luke A. Henderson, Department of Anatomy and Histology, F13, University of Sydney, Sydney, New South Wales 2006, Australia.
Email: lukeh@anatomy.usyd.edu.au

Funding information

National Health and Medical Research Council of Australia, Grant/Award Numbers: 1032072, 1059182

Abstract

The neural mechanism responsible for migraine remains unclear. While the role of an external trigger in migraine initiation remains vigorously debated, it is generally assumed that migraineurs display altered brain function between attacks. This idea stems from relatively few brain imaging studies with even fewer studies exploring changes in the 24 h period immediately prior to a migraine attack. Using functional magnetic resonance imaging, we measured infra-slow oscillatory activity, regional homogeneity, and connectivity strengths of resting activity in migraineurs directly before ($n = 8$), after ($n = 11$), and between migraine attacks ($n = 26$) and in healthy control subjects ($n = 78$). Comparisons between controls and each migraine group and between migraine groups were made for each of these measures. Directly prior to a migraine, increased infra-slow oscillatory activity occurred in brainstem and hypothalamic regions that also display altered activity during a migraine itself, that is, the spinal trigeminal nucleus, dorsal pons, and hypothalamus. Furthermore, these midbrain and hypothalamic sites displayed increased connectivity strengths and regional homogeneity directly prior to a migraine. Remarkably, these resting oscillatory and connectivity changes did not occur directly after or between migraine attacks and were significantly different to control subjects. These data provide evidence of altered brainstem and hypothalamic function in the period immediately before a migraine and raise the prospect that such changes contribute to the expression of a migraine attack.

KEYWORDS

hypothalamus, infra-slow oscillations, periaqueductal gray matter, spinal trigeminal nucleus

1 | INTRODUCTION

Migraine is an incapacitating pain disorder, which manifests in attacks of often unilateral headache accompanied by photophobia, phonophobia, and nausea. Cerebrovascular changes, particularly those associated with the large veins and sinuses, have been considered the foundation of migraine pathophysiology for some time. This peripheral sensitization theory is based on the notion that migraines are triggered by sensitization of meningeal nociceptors that evoke activation of trigemino-vascular neurons resulting in throbbing head pain and other migraine symptoms (Borsook & Burstein, 2012; Bernstein & Burstein, 2012). While the idea that a peripheral trigger is critical for the generation of migraine is well-accepted, there is growing evidence that changes in the central nervous system may also play a critical role (Akerman,

Holland, & Goadsby, 2011; Goadsby, 2009; Goadsby, Charbit, Andreou, Akerman, & Holland, 2009). Such evidence includes observations that symptoms such as fatigue, dizziness, and reduced concentration occur hours before the migraine onset (Giffin et al., 2003) and that activation of brainstem trigemino-vascular neurons by cortical spreading depression can occur independently of peripheral input (Lambert, Truong, & Zagami, 2011). Indeed, it was recently proposed that migraine results from dysfunction in subcortical sites which results in the perception of pain from "basal levels of primary traffic" (Goadsby & Akerman, 2012). This "central generator" theory is hotly debated with many researchers suggesting that a peripheral cerebrovascular trigger is necessary to precipitate a migraine attack (Borsook & Burstein, 2012).

However, even if a peripheral cerebrovascular trigger is required, sensitivity changes in brainstem regions that receive noxious orofacial

inputs may be critical in allowing such a trigger to evoke a migraine attack. Consistent with this idea, it has been hypothesized that in migraineurs, brainstem function oscillates between (a) enhanced, (b) threshold, and (c) diminished neural "tone" states (Burstein, Nosedá, & Borsook, 2015). When the brainstem is in a state of *diminished tone*, incoming noxious inputs can activate central pathways and evoke head pain. In contrast, when in an enhanced tone state, the effectiveness of endogenous analgesic mechanisms is too great to allow incoming noxious inputs to activate higher brain centers and head pain does not occur. Although *during* spontaneous or triggered migraine attacks, regional brainstem and hypothalamic activation occurs (Afridi et al., 2005a, 2005b; Bahra, Matharu, Buchel, Frackowiak, & Goadsby, 2001; Denuelle, Fabre, Payoux, Chollet, & Geraud, 2007; Weiller et al., 1995), there is currently little evidence to support the notion of cyclical changes in brainstem and/or hypothalamic function throughout the migraine cycle, particularly in the hours preceding a migraine headache. Some support comes from a recent case study which reported that the hypothalamus displayed increased sensitivity to noxious stimuli and greater functional coupling with the dorsomedial pons and spinal trigeminal nucleus (SpV) during the phase immediately prior to an attack (Schulte & May, 2016).

In individuals who experience migraine with aura, cortical spreading depression precedes the development of head pain. This phenomenon is characterized by a wave of electrophysiological hyperactivity followed by inhibition and there is evidence that this process is associated with astrocyte calcium waves (James, Smith, Boniface, Huang, & Leslie, 2001; Nedergaard, Cooper, & Goldman, 1995). These calcium waves are linked to gliotransmitter release and it has been proposed that in some pathological cases, greater numbers of astrocytes may display enhanced calcium wave synchrony and amplitude and this results in significantly altered synaptic function (Halassa, Fellin, & Haydon, 2007; Parri, Gould, & Crunelli, 2001). It is possible that altered brainstem *tone* during the migraine cycle results from synaptic activity modulated by changes in gliotransmission. Indeed, we recently reported that chronic neuropathic head pain is *not* associated with increased activity but rather with increased resting oscillations in the infra-slow range in the ascending trigeminal pathway, a frequency range remarkably similar to that of rhythmic gliotransmitter release (0.03–0.06 Hz) (Alshelh et al., 2016). Infra-slow oscillatory activity is a fundamental property of cerebral and thalamic function and is thought to be maintained by adenosine receptor-mediated signaling (Hughes, Lorincz, Parri, & Crunelli, 2011; Lorincz, Geall, Bao, Crunelli, & Hughes, 2009). This adenosine is likely released by astrocytes since they can display spontaneous intracellular infra-slow calcium oscillations and are responsive to glutamate and acetylcholine (Parri & Crunelli, 2001), and a link between adenosine and infra-slow oscillatory cortex activity has been demonstrated (Cunningham et al., 2006). Given this, we hypothesize that increased oscillatory gliotransmitter release in brainstem regions that regulate activity within the ascending trigeminal pathway could alter the propensity for an external noxious input to evoke a migraine attack.

The aim of this investigation is to determine if ongoing activity patterns, as reflected in infra-slow oscillations and functional connectivity

within the brainstem and hypothalamus, are altered over the migraine cycle and in particular directly prior to a migraine headache. We hypothesize that infra-slow oscillatory activity and functional connectivity within the brainstem and hypothalamus will increase significantly directly *prior* to a migraine headache and then return to control levels following the migraine headache. Furthermore, since in pathological conditions greater numbers of astrocytes may display enhanced calcium wave synchrony and amplitude, we speculate that immediately prior to a migraine attack, greater activity synchronization between adjacent voxels, that is greater regional homogeneity, will occur within brainstem and hypothalamic sites.

2 | METHODS

2.1 | Subjects

Twenty-six subjects with migraine (22 females; mean age 30.6 ± 2.1 years [\pm SEM]) and 78 pain-free controls (66 females; mean age 30.7 ± 1.3 years) were recruited for the study from the general population using an advertisement. There were no significant differences in age (*t* test; $p > .05$) or gender composition (chi-squared test, $p > .05$) between the two subject groups. Migraine subjects were diagnosed according to the IHC Classification ICHD-3 BETA criteria and five of the 26 migraine subjects reported an aura associated with their migraine attacks. Migraine subject characteristics, including medication use are shown in Table 1. All migraineurs were scanned during an interictal period, that is, at least 72 h after and 24 h prior to a migraine event. Eleven of these migraineurs were also scanned immediately (within 72 h) following an attack and eight immediately (within 24 h) prior to an attack. It is important to note that of the subjects scanned immediately prior to an attack, there was no predicting factor that they were within 24 h of a migraine. In five migraineurs, scans were collected during all three phases (interictal, immediately prior to and immediately following an attack). Exclusion criteria for controls were the presence of any pain condition including family history of migraines, current use of analgesics, or any neurological disorder. Exclusion criteria for migraineurs were any other pain condition or neurological disorder. No migraineur was excluded based on their medication use and no migraine or control subject had an incidental neurological finding that resulted in their exclusion from the study. All migraineurs indicated the intensity (6-point visual analogue scale; 0 = no pain, 5 = most intense imaginable pain) and drew the facial distribution of pain commonly experienced during a migraine attack. In addition, each subject described the qualities of their migraines and indicated any current treatments used to prevent or abort a migraine once started. Twenty-five of the 26 migraineurs had episodic migraine whereas the remaining migraineur had chronic migraine (> 15 migraines per month). Informed written consent was obtained for all procedures according to the Declaration of Helsinki and local Institutional Human Research Ethics Committees approved the study. Data from 25 of the 26 migraineurs and 30 of the control subjects were used in a previous investigation (Marciszewski et al., 2017).

TABLE 1 Migraine subject characteristics

Subject	Age	Sex	Years suffering	Pain side	Aura	Migraines, months	Intensity (0–5)	Medication taken during migraine	Daily medication
270	31	F	25	R	Y	5–8	3–4	Paracetamol	-
500	55	M	15	B	N	15 (chronic)	3	Paracetamol	-
548	24	F	20	B	N	4	4	Ibuprofen, paracetamol	OCP, budesonide/fomoterol
583	26	F	12	R	N	2	3–4	Ibuprofen	OCP
661	27	F	12	R	Y	1	4	Ibuprofen	OCP
664	23	F	4	R	N	4	4	Triptan	OCP, metformin hydrochloride
666	25	F	12	L	N	5	3	Aspirin, rizatriptan	Desvenlafaxine
668	21	F	1.5	L	N	4	3	Ibuprofen, paracetamol, codeine	OCP
670	26	F	1	L	N	3	5	Paracetamol	OCP
671	29	F	13	R	N	1	2.5	Ibuprofen	Zopiclone
672	26	F	5	R	N	1	2	Aspirin, codeine, ibuprofen	OCP
676	23	F	6	R	N	1	3–4	Ibuprofen	OCP
677	23	F	10	B	N	0.5–1	4	Ibuprofen, codeine	OCP
678	46	F	15–20	B	N	1	3	Sumatriptan	-
679	41	F	40	B	N	2	4	Sumatriptan	-
681	23	M	3–4	B	N	0.5–1	3.5	Paracetamol, codeine	-
688	23	M	4–5	B	N	0.5–1	4	Paracetamol	-
696	55	F	40	R	N	0.5–1	3–4	Sumatriptan	Telmisartan
800	26	M	20	R	N	0.5–1	4	Metamizole	Carbamazepine
814	49	F	30	B	N	0.5–1	5	Rizatriptan, paracetamol	-
815	54	F	30	B	N	0.5–1	5	Paracetamol, codeine, eletriptan,	Candesartan
818	34	F	15	L	Y	2	3	Paracetamol, ibuprofen	-
819	26	F	5	B	Y	1	3	Paracetamol	OCP
820	25	F	7–8	L	N	5–8	3	Rizatriptan benzoate	OCP
822	27	M	4	B	N	0.5–1	4	Ibuprofen	SSRI
825	28	F	25	R	Y	0.25	5	Ibuprofen	Methylphenidate

Note. Abbreviations: B = bilateral; L = left; OCP = oral contraceptive pill; R = right; SSRI = selective serotonin reuptake inhibitor.

2.2 | MRI acquisition

All subjects lay supine on the bed of a 3 T MRI scanner (Philips, Achieva) with their head immobilized in a tight-fitting head coil. With each subject relaxed and at rest, a high-resolution 3D T1-weighted anatomical image set, covering the entire brain, was collected (turbo field echo; field of view = 250 × 250 mm, matrix size = 288 × 288, slice thickness = 0.87 mm, repetition time = 5,600 ms; echo time = 2.5 ms, flip angle = 8°). Following this, a series of 180 gradient echo echo-planar functional MRI image volumes using blood oxygen level dependent (BOLD) contrast were collected. Each image volume contained 35 axial slices covering the entire brain (field of view = 240 × 240 mm, matrix size = 80 × 78,

slice thickness = 4 mm, repetition time = 2,000 ms; echo time = 30 ms, flip angle = 90°).

2.3 | MRI processing and statistical analysis

2.3.1 | Image preprocessing

Using SPM12 and Matlab software, all fMRI images were motion corrected and detrended to remove global signal drifts (Macey, Macey, Kumar, & Harper, 2004). In no subject was there significant movement (>0.5 mm in any direction) and all subjects were used for the subsequent analysis. In five migraineurs who experienced migraines most often on the left side, their images were reflected in the X plane ("flipped") so that fMRI signals could be assessed ipsilateral and

contralateral to the most common side of migraine. Each subject's fMRI image set was coregistered to their own T1-weighted anatomical image set. The T1 images were then spatially normalized to the Montreal Neurological Institute (MNI) template and the parameters applied to the fMRI image sets so that both the T1-weighted and fMRI images were in the same locations in three-dimensional space. To remove the potential influence of signal intensity changes within the cerebrospinal fluid, cerebrospinal fluid brain maps were created by segmenting the spatially normalized T1 anatomical images. This map was used to mask the fMRI images so that only grey and white matter remained. In all subsequent analyses, the anatomical locations of significant clusters were confirmed using the Atlas of the Human Brain by Mai, Paxinos, and Voss (2007) and the Atlas of the Human Brainstem by Paxinos and Huang (1995).

2.3.2 | Infra-slow oscillation power

Using the SPM DPARSF toolbox, raw power between 0.03 and 0.06 Hz was calculated for each voxel of the unsmoothed fMRI image sets in the control subjects, and in the migraine subjects during the interictal phase, and the phases immediately prior to and immediately following an attack. The resulting brain maps were then smoothed using a 3 mm full-width-half-maximum Gaussian filter. A small smoothing kernel was chosen to maintain spatial accuracy as we hypothesized that we would find differences in small brainstem and diencephalic structures. Three whole brain voxel-by-voxel comparisons were then performed: (a) controls ($n = 78$) compared with migraineurs during their interictal phase ($n = 26$), (b) controls ($n = 78$) compared with migraineurs during the phase immediately prior to a migraine ($n = 8$), and (c) controls ($n = 78$) compared with migraineurs during the phase immediately following an attack ($n = 11$). Significant differences were determined using two-sample random effects procedures with age and gender as nuisance variables ($p < .05$, false discovery rate corrected, minimum cluster size 5 voxels). Significant power differences compared with controls, occurred in migraineurs immediately prior to an attack only and the power values from these significant clusters were determined for controls and migraineurs during all three phases. For one large cluster that encompassed the hypothalamus, periaqueductal gray (PAG), and dorsomedial medulla, secondary peaks within the cluster were selected and the power values of these regions (10 most significant voxels around the peak) were extracted. Significant differences in these extracted power values between subjects scanned in interictal, immediately prior to and immediately following an attack were determined ($p < .05$, two-tailed, two-sample t test, Bonferroni corrected for multiple comparisons). Differences between controls and migraineurs were not assessed in the cluster analysis as these comparisons were performed in the initial voxel-by-voxel whole-brain analyses. To explore individual subject changes, raw power values from significant clusters were plotted in the five migraineurs in whom we collected fMRI scans during all three phases.

We also divided these raw power values by the total power over the entire frequency range to obtain fractional power value for each voxel. The mean fractional powers were also calculated for each significant cluster and significant differences between controls and subjects scanned in interictal, immediately prior to and immediately following an

attack were determined ($p < .05$, two-tailed, two-sample t test, Bonferroni corrected for multiple comparisons). For each significant cluster, we also calculated ALFF power for the four most commonly used infra-slow oscillatory frequency bands, slow 2: 0.198–0.25 Hz, slow 3: 0.073–0.198 Hz, slow 4: 0.027–0.073 Hz, and slow 5: 0.01–0.027 Hz). Significant differences between controls and subjects scanned in interictal, immediately prior to and immediately following an attack were then determined for each of these infra-slow oscillatory frequency bands ($p < .05$, two-tailed, two-sample t test, Bonferroni corrected for multiple comparisons).

2.3.3 | Regional homogeneity

To assess regional homogeneity, the similarity of the time series within each voxel and its 7 nearest neighbors were measured by calculating Kendall's coefficient of concordance. Using the unsmoothed fMRI image sets, subject-level Z-score maps were created by subtracting the mean Kendall's coefficient of concordance for the entire brain from each voxel and dividing by the mean standard deviation. The resulting brain maps were then smoothed using a 3 mm full-width-half-maximum Gaussian filter. Significant differences in regional homogeneity between controls and migraineurs immediately prior to an attack were then determined using a two-sample random effects procedure with age and gender as nuisance variables ($p < .05$, false discovery rate corrected, minimum cluster size 5 voxels). In addition, regional homogeneity values were extracted for each significant cluster and plotted for controls and migraineurs during all three phases and significant differences between controls, and subjects scanned in interictal, immediately prior to and immediately following an attack were determined ($p < .05$, two-tailed, two-sample t test, Bonferroni corrected for multiple comparisons). Differences between controls and migraineurs scanned immediately prior to an attack were not assessed as these comparisons were performed in the voxel-by-voxel whole-brain analysis. Regional homogeneity values from the significant clusters were also plotted in the five migraineurs in which we collected fMRI scans during all three phases.

2.3.4 | Functional connectivity

Finally, resting functional connectivity was assessed in controls and migraineurs using a seed located in the midbrain PAG. This seed was derived from the overlap between increased infra-slow oscillation power and regional homogeneity in migraineurs immediately prior to an attack. Mean resting signal intensity changes within this seed were calculated and a voxel-by-voxel analysis was performed to determine areas that displayed significant signal intensity covariations with the seed signal. In each subject, the 6 direction movement parameters calculated during the realignment step were included as nuisance variables. The resulting brain maps were then smoothed using a 3 mm full-width-half-maximum Gaussian filter. Significant differences in functional connectivity strengths between controls and migraineurs immediately prior to an attack were then determined using a two-sample random effects procedure with age and gender as nuisance variables ($p < .05$, false discovery rate corrected, minimum cluster size 5 voxels). In addition, connectivity strength values were extracted for each significant cluster and plotted for controls and

migraineurs during all three phases and significant differences between controls, and subjects scanned in interictal, immediately prior to and immediately following an attack were determined ($p < .05$, two-tailed, two-sample t test, Bonferroni corrected for multiple comparisons). Differences between controls and migraineurs scanned immediately prior to an attack were not assessed as these comparisons were performed in the voxel-by-voxel whole-brain analysis. Connectivity values from the significant clusters were also plotted in the five migraineurs in whom we collected fMRI scans during all three phases.

3 | RESULTS

3.1 | Infra-slow oscillations

Infra-slow oscillations were measured at rest using fMRI in 78 healthy controls and 26 migraineurs. Eight of the migraineurs were scanned immediately prior to an attack (within 24 h), 11 were scanned immediately following an attack (within 72 h) and all 26 migraineurs were scanned during the interictal phase (more than 24 h before the next migraine, and more than 72 h after a migraine).

We first compared resting fMRI signals throughout the entire brain in migraineurs during all three phases (interictal, immediately prior to and immediately following an attack) with resting fMRI signals in controls. Fast Fourier Transforms of resting fMRI signal intensity fluctuations were performed and the mean power between 0.03 and 0.06 Hz determined for each voxel in each subject. Comparison of power between controls and migraineurs in each voxel revealed a striking pattern of increased infra-slow oscillatory power in migraineurs *only* in the phase immediately prior to an attack (Figure 1a and Table 2). This increased infra-slow oscillatory power during the phase immediately prior to an attack was almost entirely restricted to the brainstem, hypothalamus, and thalamus. During the phase immediately prior to an attack, increased oscillatory power occurred in the region of the right (ipsilateral to side of most frequent migraine) spinal trigeminal nucleus (SpV) extending into the rostral ventromedial medulla (RVM), dorsomedial pons, midbrain in the region of the PAG, posterior hypothalamus, and in the thalamus in the region of the somatosensory nucleus (Figure 1b). In no brain region was infra-slow oscillatory power reduced in migraineurs compared with controls.

Plots of raw power extracted from these regions in controls and migraineurs during all three phases confirmed the specificity of power increases during the phase immediately prior to an attack only in the SpV/RVM (mean \pm SEM 0.03–0.06 Hz power: controls: 1.04 ± 0.03 , interictal: 1.19 ± 0.06 , immediately prior to an attack: 1.54 ± 0.13 , immediately following an attack: 1.02 ± 0.02), dorsomedial pons (controls: 1.01 ± 0.03 , interictal: 1.06 ± 0.04 , immediately prior to an attack: 1.55 ± 0.19 , immediately following an attack: 1.03 ± 0.01), PAG (controls: 1.05 ± 0.03 , interictal: 1.08 ± 0.05 , immediately prior to an attack: 1.59 ± 0.19 , immediately following an attack: 1.03 ± 0.02) hypothalamus (controls: 1.17 ± 0.03 , interictal: 1.24 ± 0.05 , immediately prior to an attack: 1.68 ± 0.17 , immediately following an attack: 1.17 ± 0.03) and somatosensory thalamus (controls: 0.99 ± 0.02 , interictal: 1.04 ± 0.05 , immediately prior to an attack: 1.32 ± 0.12 ,

immediately following an attack: 1.02 ± 0.02) (Figure 1c). In addition to the significant power increases in migraineurs in the phase immediately prior to an attack compared with controls, comparison of power values within the migraineurs group revealed significant differences between the phase immediately prior to an attack and the interictal phase in the dorsomedial pons, PAG, and hypothalamus and a significant difference between the phases immediately prior to and following an attack in the SpV/RVM, dorsomedial pons, and PAG.

As raw power can be influenced by an individual's global infra-slow oscillatory power, we also calculated fractional power by dividing the raw 0.03–0.06 Hz power at each voxel by the total power over the entire frequency range (0–0.25 Hz). For each of the significant clusters derived from the raw power analysis, we found significantly increased fractional power during only the phase immediately prior to an attack compared with controls. These fractional power increases occurred in the SpV (mean \pm SEM: controls: 0.76 ± 0.01 , interictal: 0.81 ± 0.02 , immediately prior to an attack: 0.87 ± 0.04 , immediately following an attack: 0.78 ± 0.01), dorsomedial pons (controls: 0.91 ± 0.01 , interictal: 0.93 ± 0.01 , immediately prior to an attack: 1.00 ± 0.02 , immediately following an attack: 0.91 ± 0.01), PAG (controls: 0.78 ± 0.01 , interictal: 0.83 ± 0.03 , immediately prior to an attack: 0.89 ± 0.05 , immediately following an attack: 0.80 ± 0.01) and hypothalamus (controls: 0.84 ± 0.01 , interictal: 0.87 ± 0.02 , immediately prior to an attack: 0.93 ± 0.04 , immediately following an attack: 0.83 ± 0.01). No significant differences in fractional power occurred in the somatosensory thalamus (controls: 0.95 ± 0.01 , interictal: 0.96 ± 0.03 , immediately prior to an attack: 0.98 ± 0.04 , immediately following an attack: 0.94 ± 0.01).

Assessments of four infra-slow oscillatory bands revealed an interesting frequency specificity (Figure 1d). While there were no significant differences in infra-slow oscillatory power during any migraine phase and controls for the SpV, in contrast the PAG and hypothalamus displayed greater power for band 4 (0.27–0.71 Hz) only in the phase immediately prior to the migraine compared with controls. This band includes the infra-slow oscillatory band specifically investigated in this study (0.03–0.06 Hz). Furthermore, for the dorsomedial pons and thalamus, power was significantly greater during the phase immediately prior to the migraine attack compared with controls for all four infra-slow oscillatory bands, suggestive of a more widespread increase in infra-slow oscillatory power.

3.2 | Regional homogeneity

If increased infra-slow oscillation power during the phase immediately prior to an attack is associated with increased synchronicity of astrocyte activation and the subsequent recruitment of surrounding astrocytes and neurons, neighboring voxels should display increased signal intensity synchronization. To determine if there was such an increase in regional homogeneity, we measured Kendall's coefficient of concordance (KCC) to evaluate the similarity of the time series within each voxel to its seven nearest neighbors, in controls and migraineurs. Comparison of regional homogeneity between migraineurs and controls at each voxel in the brain revealed a significant increase during the phase immediately prior to an attack but no significant differences between

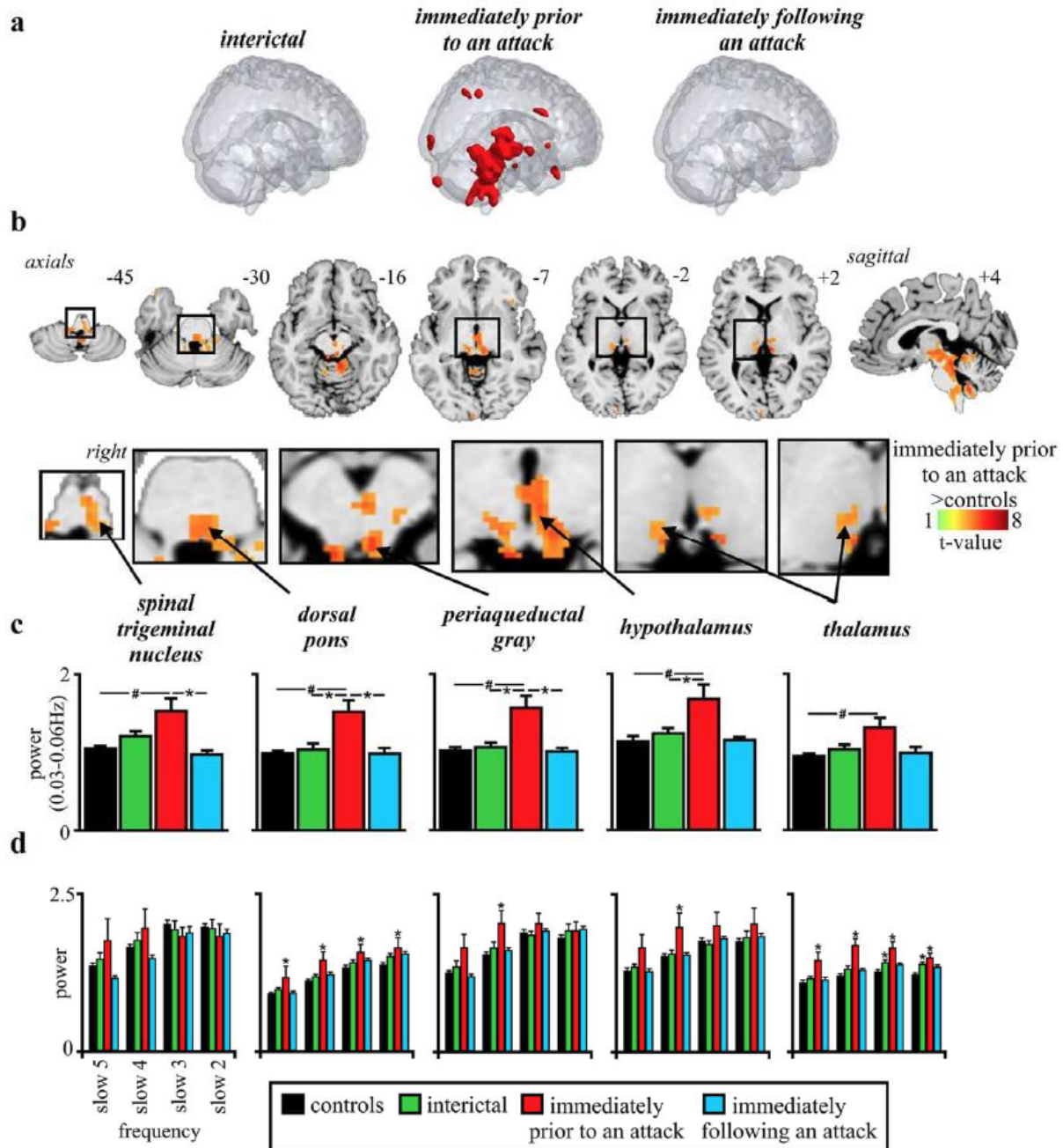


FIGURE 1 (a) Significant differences in infra-slow oscillation power between controls ($n = 78$) and migraineurs during interictal phase ($n = 26$), immediately prior to an attack ($n = 8$) and immediately following an attack ($n = 11$). Note that only during the phase immediately prior to an attack was power significantly different to controls and this difference occurred primarily in the brainstem and hypothalamus. (b) Brain regions in which infra-slow oscillation power was greater in migraineurs immediately prior to a migraine compared with controls (random effects, $p < .05$, false discovery rate corrected). Location of each axial slice in Montreal Neurological Institute space is indicated at the top right. (c) Plots of mean (\pm SEM) power between 0.03 and 0.06 Hz in significant clusters extracted from controls and migraineurs during all three phases. In addition to significant power increases in all clusters during the phase immediately prior to an attack compared with controls ($\#p < .05$ derived from random effects whole-brain analysis), there were significant differences between the phase immediately prior to an attack and the interictal phase in all clusters except for the thalamus ($*p < .05$ derived from post-hoc two-sample t test). (d) Plots of mean (\pm SEM) power over four standard infra-slow frequency bands: slow 2: 0.198–0.25 Hz, slow 3: 0.073–0.198 Hz, slow 4: 0.027–0.073 Hz, and slow 5: 0.01–0.027 Hz ($*p < .05$ significantly different to controls derived from post-hoc two-sample t test)

TABLE 2 Montreal Neurological Institute (MNI) coordinates, cluster size, and *t* score for regions of significant difference between control and migraineurs during the phase immediately prior to an attack

(a) Brain region	(b) MNI co-ordinate			Cluster size	<i>t</i> score
	<i>x</i>	<i>y</i>	<i>z</i>		
<i>Infra-slow oscillation power (0.03–0.06 Hz)</i>					
Immediately prior to an attack > controls					
Dorsal pons	8	–40	–24	817	5.47
Hypothalamus	0	–16	–10	59	5.31
Midbrain periaqueductal gray	4	–32	–18	228	5.29
Dorsomedial pons	–4	–38	–36		4.34
Spinal trigeminal nucleus/rostral ventromedial medulla	4	–34	–46		4.03
Thalamus	–6	–26	10		5.51
<i>Regional homogeneity</i>					
Immediately prior to an attack > controls					
midbrain periaqueductal gray	–4	–28	–8	42	4.36
Hypothalamus	2	–12	–12	6	4.64
Thalamus	–12	–24	2	10	4.18
<i>Resting functional connectivity</i>					
Immediately prior to an attack > controls					
Midbrain periaqueductal gray	4	–34	–18	7	4.82
Hypothalamus	0	–16	–10	23	4.86
Thalamus	–10	–24	–2	8	4.32

migraineurs and controls during either the interictal phase or the phase immediately following an attack. During the phase immediately prior to an attack, migraineurs had significantly increased regional homogeneity restricted almost entirely to regions of the PAG, hypothalamus, and somatosensory thalamus (Figure 2a and Table 2). In no brain region was regional homogeneity significantly lower in migraineurs than in controls.

Plots of regional homogeneity extracted from these regions in controls and migraineurs during all three phases revealed regional homogeneity increases during only the phase directly prior to an attack in the PAG (mean \pm SEM KCC: controls: 0.44 ± 0.01 , interictal: 0.46 ± 0.01 , immediately prior to an attack: 0.54 ± 0.03 , immediately following an attack: 0.44 ± 0.05) and thalamus (controls: 0.92 ± 0.01 , interictal: 0.97 ± 0.02 , immediately prior to an attack: 1.09 ± 0.03 , immediately following an attack: 0.94 ± 0.01) and increases during both the interictal phase and the phase immediately prior to an attack compared with controls in the hypothalamus (controls: 0.97 ± 0.01 , interictal: 1.03 ± 0.02 , immediately prior to an attack: 1.11 ± 0.04 , immediately following an attack: 0.99 ± 0.01). The PAG, hypothalamus, and thalamus all showed increases in both infra-slow oscillatory power and regional homogeneity in migraineurs during the phase immediately prior to an attack, compared with controls (Figure 2b). We also extracted these values from clusters derived from the infra-slow oscillation analysis, to confirm that there were no changes in regional homogeneity in the SpV/RVM (controls: 0.94 ± 0.01 , interictal: 0.98 ± 0.02 , immediately

prior to an attack: 0.99 ± 0.03 , immediately following an attack: 0.99 ± 0.02 , all $p > .05$) or dorsomedial pons (controls: 0.93 ± 0.01 , interictal: 0.94 ± 0.01 , immediately prior to an attack: 0.97 ± 0.03 , immediately following an attack: 0.95 ± 0.02 , all $p > .05$).

3.3 | Periaqueductal gray matter connectivity

Given previous reports of altered connectivity between the diencephalon and brainstem in migraineurs, we assessed resting functional connectivity changes using the PAG as a seed. Comparison of PAG connectivity in the phase immediately prior to an attack in migraineurs with that of controls revealed significant increases in functional connectivity strength between the PAG and the hypothalamus, thalamus and between the rostral and caudal regions of the PAG matter (Figure 3 and Table 2). In no region was connectivity strength significantly lower in migraineurs compared with controls. Plots of connectivity strengths extracted from these regions in controls and migraineurs during all three phases revealed a consistent pattern of difference; all three regions showed significantly greater connectivity strengths during the phase immediately prior to an attack than in the interictal phase and in the phase immediately following an attack in migraineurs, and compared with controls: PAG (mean \pm SEM connectivity strength: controls: 0.34 ± 0.03 , interictal: 0.23 ± 0.07 , immediately prior to an attack: 0.76 ± 0.13 , immediately following an attack: 0.36 ± 0.02), hypothalamus (controls: 0.34 ± 0.05 ,

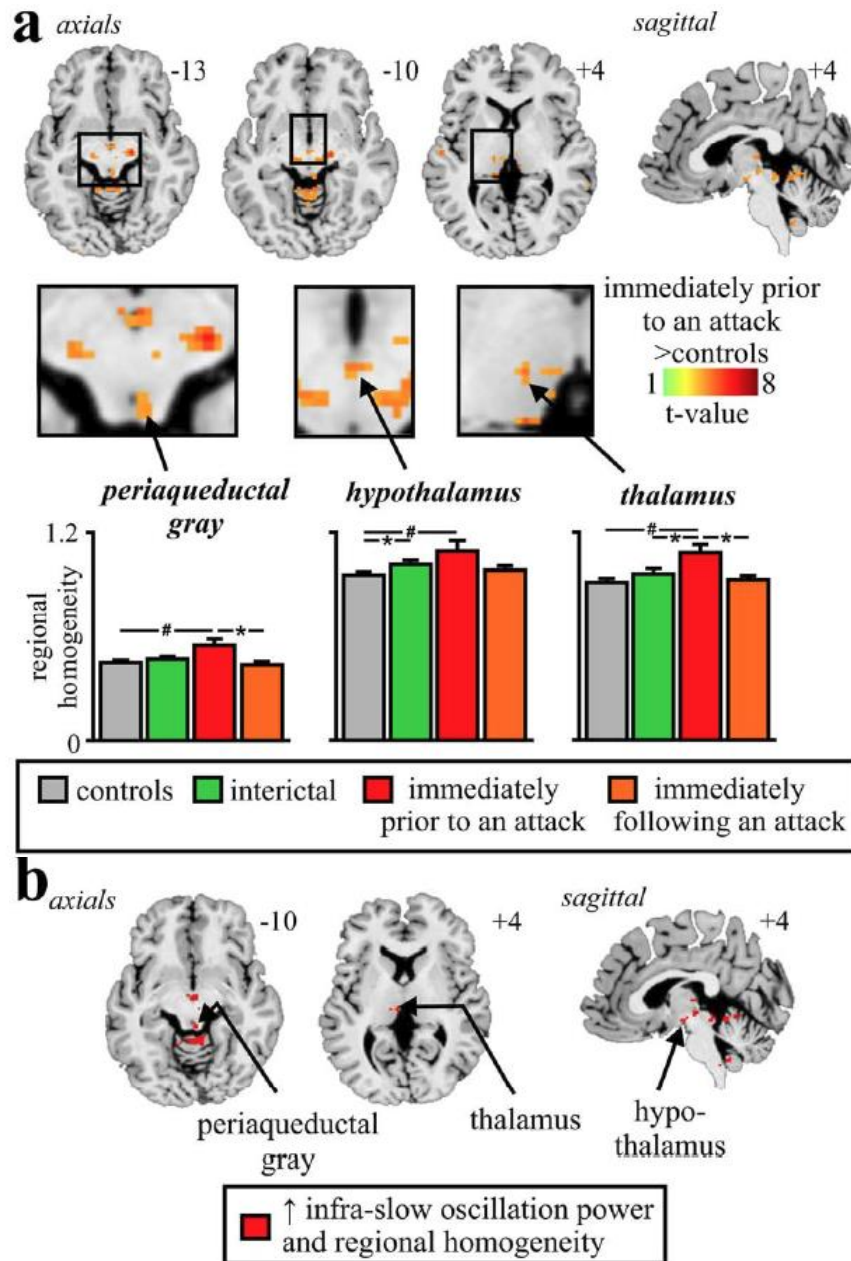


FIGURE 2 (a) Brain regions in which regional homogeneity was significantly different between controls ($n = 78$) and migraineurs during the phase immediately prior to an attack ($n = 8$). Location of each axial slice in Montreal Neurological Institute space is indicated at the top right. Significant increases in regional homogeneity occurred in the rostral brainstem, hypothalamus, and thalamus. Below are plots of mean (\pm SEM) regional homogeneity in significant clusters extracted from controls and migraineurs during all three phases. In addition to significant power increases in all clusters during the phase immediately prior to an attack compared with controls ($^{\#}p < .05$ derived from random effects whole-brain analysis), there were significant differences between the phases immediately prior to, and following an attack ($n = 11$) in the PAG and between controls and interictal phase in migraineurs ($n = 26$), in the hypothalamus ($^*p < .05$ derived from post-hoc two-sample t test). (b) Brain regions in which during the phase immediately prior to an attack, migraineurs displayed greater infra-slow oscillation power and regional homogeneity compared with controls

interictal: 0.36 ± 0.09 , immediately prior to an attack: 1.01 ± 0.12 , immediately following an attack: 0.58 ± 0.05 and thalamus (controls: 0.19 ± 0.03 , interictal: 0.24 ± 0.04 , immediately prior to an attack:

0.57 ± 0.08 , immediately following an attack: 0.24 ± 0.02). To ensure that there was indeed no change in resting functional connectivity between the PAG and/or dorsomedial pons SpV/RVM we extracted

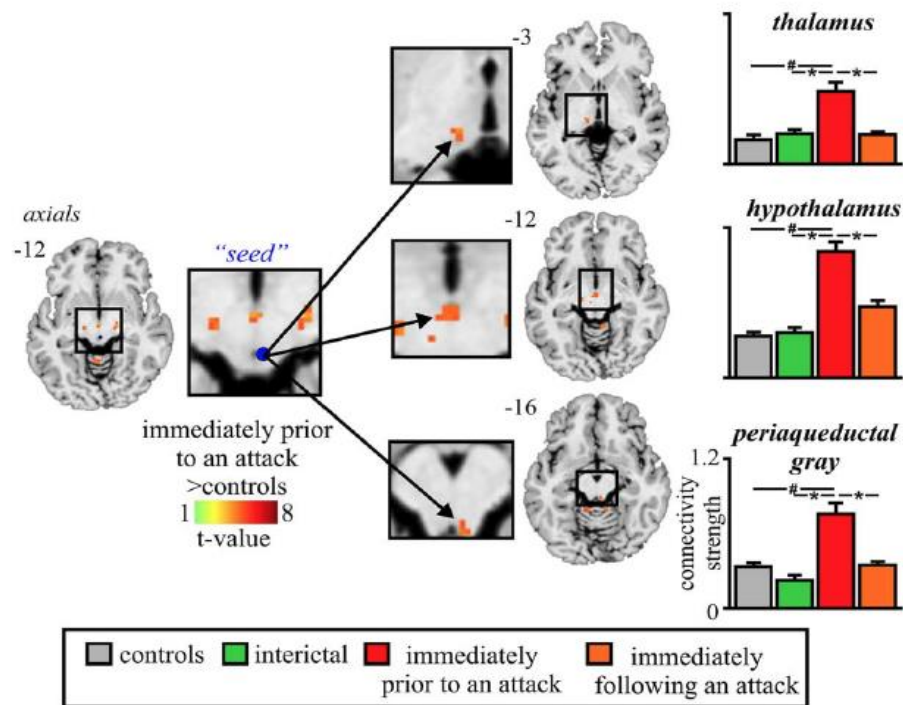


FIGURE 3 Brain regions in which resting functional connectivity was significantly different between controls ($n = 78$) and migraineurs during the phase immediately prior to an attack ($n = 8$). Location of each axial slice in Montreal Neurological Institute space is indicated at the top right. Significant increases in resting connectivity occurred in migraineurs between the PAG and the thalamus, hypothalamus, and between the rostral and caudal PAG. To the right are plots of mean (\pm SEM) connectivity strength in significant clusters extracted from connectivity strength in controls and migraineurs during all three phases. In addition to significant increases in connectivity strength in all clusters during the phases immediately prior to, and following an attack ($n = 11$) in migraineurs compared with controls ($*p < .05$ derived from random effects whole-brain analysis), there were significant differences between the phases immediately prior to and following an attack in the PAG and between controls and interictal phase in the hypothalamus. # $p < .05$ derived from random effects whole-brain analysis ($*p < .05$ derived from post-hoc two-sample t test)

values from these regions and found no significant PAG connectivity with the SpV/RVM (controls: -0.02 ± 0.02 , interictal: -0.13 ± 0.11 , immediately prior to an attack: -0.08 ± 0.08 , immediately following an attack: 0.01 ± 0.08 , all $p > .05$) or dorsomedial pons (controls: 0.15 ± 0.02 , interictal: 0.19 ± 0.07 , immediately prior to an attack: 0.33 ± 0.12 , immediately following an attack: 0.09 ± 0.07 , all $p > .05$).

3.4 | Individual subject changes

In five migraineurs, resting fMRI scans were collected during all three phases, that is, interictal, the phases immediately prior to and following an attack. To explore individual variations, we plotted infra-slow oscillatory power, regional homogeneity, and connectivity for each subject during each migraine phase. These plots reveal a remarkably consistent pattern of changes with greater infra-slow oscillatory power (Figure 4a), increased regional homogeneity (Figure 4b), and greater functional connectivity strength (Figure 4c) during the phase immediately prior to an attack compared with the interictal and the phase immediately following an attack.

4 | DISCUSSION

We describe here a series of experimental findings revealing altered brainstem and hypothalamic function in the period immediately prior to a migraine headache. These changes include increases in infra-slow oscillatory activity, hypothalamic-brainstem functional connectivity, and regional homogeneity. Importantly, these oscillatory and network alterations only occur directly prior to a migraine headache, while the individual is not in pain, and do not occur during other migraine phases. While these results do not provide direct evidence that changes in these brain regions are subsequently responsible for the initiation of a migraine attack, they clearly show that brain activity pattern changes occur immediately prior to a migraine attack while the individual is not in pain. These data are consistent with the idea that changes within the central nervous system are potentially involved in the expression of migraine.

Remarkably, even though we investigated every voxel in the brain during different phases of migraine, only brainstem, hypothalamic, and thalamic regions displayed altered oscillatory activity directly prior to a migraine headache. It is important to emphasize that these alterations

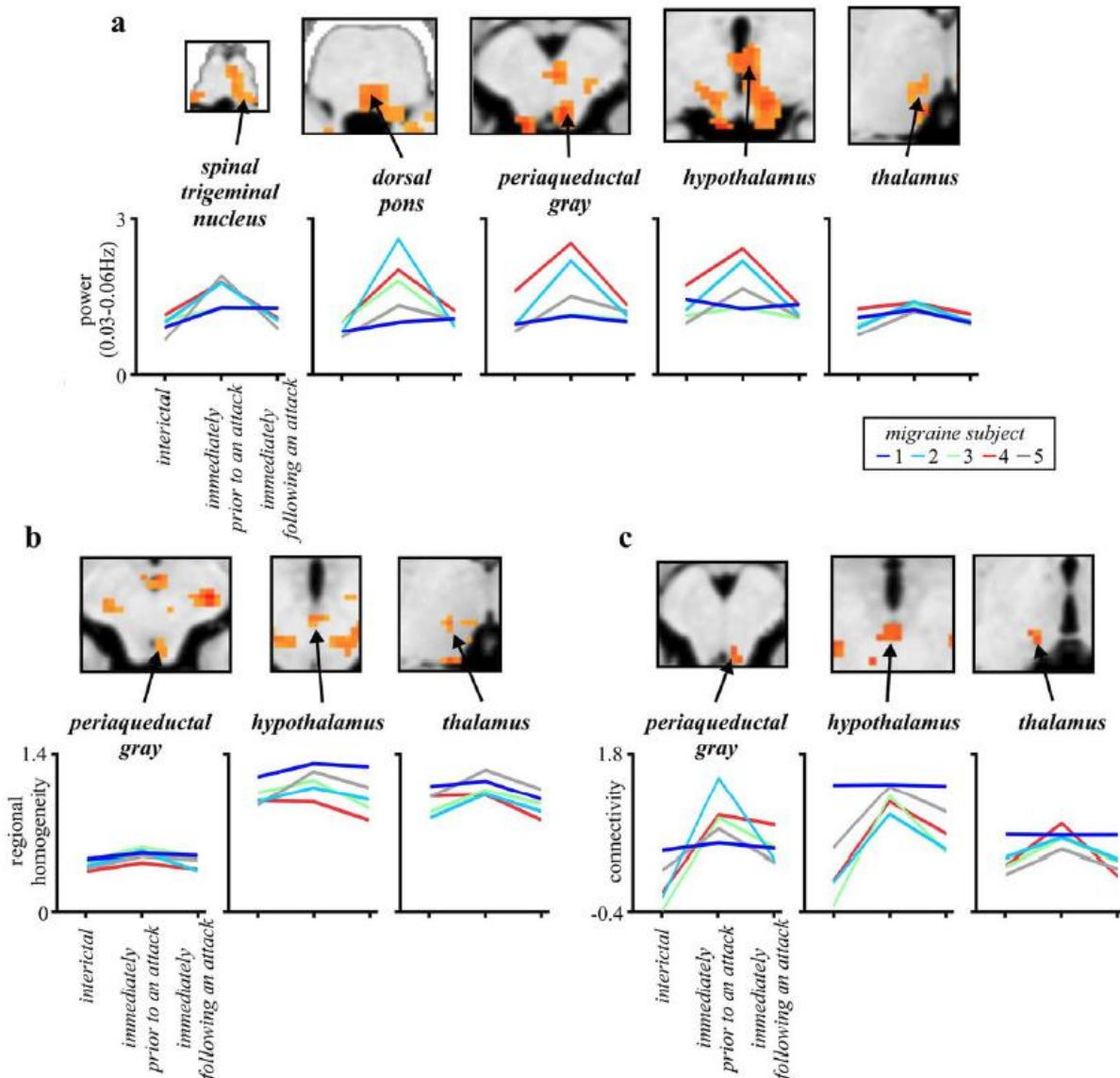


FIGURE 4 (a) Infra-slow oscillation power, (b) regional homogeneity, and (c) resting functional connectivity in migraineurs ($n = 5$) during the interictal phase, and the phases immediately prior to and following an attack. Values were extracted from clusters derived from whole group analyses. The results indicate that at the individual subject level, the phase immediately prior to an attack is consistently associated with increased infra-slow power, regional homogeneity, and resting connectivity in the brainstem, hypothalamus, and thalamus

were observed while the individual was not in pain, that is, was not experiencing a migraine headache. Interestingly, the spatial pattern of this increase in oscillatory power directly prior to a migraine is remarkably similar to that which occurs during a migraine headache itself (Afridi et al., 2005a, 2005b; Bahra et al., 2001; Denuelle et al., 2007; Weiller et al., 1995); that is, the dorsal pons, hypothalamus, and possibly PAG. Recent evidence suggests that infra-slow oscillations are maintained by adenosine receptor-mediated signaling which is itself associated with cyclic gliotransmitter release (Halassa et al., 2007; Parri & Crunelli, 2001). It has been proposed that astrocytes can exhibit pacemaker oscillations at frequencies between 0.03 and 0.06 Hz and

that astrocyte calcium waves can propagate among surrounding astrocytes through gap junction-mediated coupling and/or gliotransmitter release (Cunningham et al., 2006; Lorincz et al., 2009; Parri & Crunelli, 2001). It has been suggested that in pathological cases greater numbers of astrocytes display enhanced calcium-wave synchrony and amplitude and enhanced *N*-methyl-D-aspartate receptor function (Crunelli et al., 2002; Halassa et al., 2007; Parri & Crunelli, 2001). It is possible that the increases in infra-slow oscillatory power and in regional homogeneity within the brainstem and hypothalamus during the phase immediately prior to an attack results from enhanced amplitude and synchrony of oscillatory gliotransmitter release. These infra-slow oscillations are

coupled to high frequency cortical power fluctuations and to the development of paroxysmal events (Hughes et al., 2011; Mantini, Perrucci, Del Gratta, Romani, & Corbetta, 2007; Vanhatalo et al., 2004).

Over the past two decades, numerous studies have focused on the role of the PAG and its output projections in the pathogenesis of migraine. The PAG can alter incoming noxious inputs, and migraine-like episodes can develop following stereotactic placement of electrodes into the PAG (Veloso, Kumar, & Toth, 1998). The PAG is reciprocally connected to the hypothalamus and sends descending projections to the SpV via the RVM (Floyd, Price, Ferry, Keay, & Bandler, 2001; Holstege & Kuypers, 1982; Morgan, Whittier, Hegarty, & Aicher, 2008). Stimulation of the PAG inhibits incoming neural traffic evoked by dural stimulation (Knight & Goadsby, 2001) and it is possible that modulation of the SpV by the PAG results from activation of "on" cells and inhibition of "off" cells within the RVM (Akerman et al., 2011). Although significant activation of the pons, midbrain, and hypothalamus has been shown to occur during migraine headaches, no activation has been shown to occur within the SpV (Afridi et al., 2005a, 2005b; Bahra et al., 2001; Denuelle et al., 2007; Weiller et al., 1995). This lack of activation might be due to the limited spatial resolution of early brain imaging techniques as experimental animal studies clearly show SpV activation during dural stimulation (Strassman, Mason, Moskowitz, & Maciewicz, 1986; Strassman, Mineta, & Vos, 1994). Additionally, consistent with the idea of oscillating brainstem tone, it was recently shown that SpV activity during nociceptive stimulation was enhanced the closer the individual was to their next migraine (Stankewitz, Aderjan, Eippert, & May, 2011). The results are consistent with our findings of altered brainstem activity patterns, specifically in areas regulating noxious trigeminal inputs. The authors also found increased dorsomedial pontine activation to noxious trigeminal stimulation during migraine headaches, further supporting the role of this region in migraine pain.

In support of the theory that infra-slow frequency calcium waves can propagate among neighboring astrocytes, we found that increased regional homogeneity, a measure of neighboring synchronization, occurred in the same regions of the PAG, hypothalamus, and thalamus during *only* the phase immediately prior to an attack. Increases in regional homogeneity did *not* occur in the dorsal pons or medulla, suggesting that the PAG and hypothalamus are critical for the expression of migraine. While there is no direct evidence that migraine is associated with cyclic astrocyte activation, the idea that in some conditions altered astrocyte function can result in altered neural firing has some foundation. Persistent neuropathic pain has been found to be associated with astrocyte activation in the dorsal horn/SpV (Garrison, Dougherty, Kajander, & Carlton, 1991; Okada-Ogawa et al., 2009; Shi, Gelman, Lisinicchia, & Tang, 2012), and with increased infra-slow oscillation power specifically within the trigeminal pathway including the SpV (Alshelh et al., 2016). Furthermore, inhibiting astrocyte activation attenuates and even reverses neuropathic pain markers in experimental animal models (Chui, Abdel-Aleem, Tumber, Scuderio-Porter, & Taylor, 2008; Ji et al., 2013; Morgenweck, Griggs, Donahue, Zadina, & Taylor, 2013). Additionally, there is a large body of evidence, including from postmortem studies, showing that dysfunctional astrocytes are crucial players in epilepsy pathogenesis (Hubbard & Binder, 2016). One of the

more effective migraine prophylactic medications is the anti-convulsant valproic acid (Linde, Mulleners, Chronicle, & McCrory, 2013), whose anti-epileptic action likely occurs through its ability to reduce the capability of astrocytes to transmit calcium signaling (Tian et al., 2005; Wang et al., 2012). Given the episodic nature of both migraine and epilepsy, it might be the case that cyclical regulation of synaptic transmission by astrocytes results in periods of heightened sensitivity that results in increased firing in both conditions. Furthermore, a form of familial hemiplegic migraine (FHM2) is linked to mutations in a gene that encodes part of the sodium-potassium pump; this gene is expressed primarily in neurons in infants and in astrocytes in adulthood. Curiously, in infancy this mutation manifests as epilepsy, presumably due to neuronal hyperexcitability, but in adults it manifests as migraine, likely due to impaired astrocyte functioning (Benarroch, 2005). That migraineurs display increased infra-slow oscillations directly prior to a migraine headache whilst the individual is pain-free, but in some of the same regions that are subsequently activated during a painful migraine headache, is consistent with the idea that *altered sensitivity in these regions may trigger the migraine itself* or alternatively may reflect altered brainstem "tone" which allows cerebrovascular triggers to evoke an attack.

The restricted nature of regional homogeneity increases during the phase immediately prior to an attack, their overlap with increased infra-slow oscillation power and the increased functional connectivity provide support for a critical role of a PAG-hypothalamic interaction in migraine. The PAG and the posterior hypothalamus have direct neural connections with each other, (Bernard & Bandler, 1998; Floyd et al., 2001) and the increased functional covariation between these regions directly prior to a migraine likely occurs via this direct anatomical connection. A recent case study reported that the hypothalamus showed increased sensitivity to noxious stimuli and greater functional coupling with the dorsomedial pons and SpV during the phase immediately prior to an attack (Schulte & May, 2016). In contrast, we found that functional connectivity changes were restricted to the PAG, hypothalamus, and thalamus during the phase immediately prior to an attack. However, we did not find connectivity changes within lower brainstem regions, despite increased oscillatory changes in the dorsomedial pons and SpV/RVM. A lack of robust signal covariation within the PAG-RVM-SpV circuitry is surprising given its role in modulating incoming noxious information but may stem from the complex interaction between the PAG and the "on" and "off" cells within the RVM. Alternatively, it may be that changes in interactions between the PAG, hypothalamus, and thalamus—in addition to increased regional homogeneity—reflect different roles for these regions in the expression of migraine compared with the lower brainstem.

Finally, there are a number of limitations that need to be acknowledged. First, given the relatively low spatial resolution of resting-state fMRI, it is difficult to accurately localize each cluster to a particular brain nucleus or region. Given that we compared indices across every voxel in the brain and remarkably, those regions previously implicated in migraine were almost exclusively different, we are confident that the locations of the described changes are accurate. However, while we are confident that the cluster locations described in this study include

the regions labeled, most clusters encompassed other adjacent regions and caution must be taken when attributing changes to a single brain region. A second limitation is the modest group sample size and the absence of scans during the headache phase of the migraine cycle. While the results reported here were generated with random-effects, population-based statistics that were corrected for multiple comparisons, future studies with greater sample sizes, particularly in the phase immediately prior to a migraine and during a migraine attack would be extremely valuable.

Our findings provide evidence that brainstem and hypothalamic functions are altered prior to the initiation of the headache, with the temporal and spatial distributions consistent with altered astrocyte function. Whether these central changes are enough in themselves to initiate a migraine attack remains to be determined, although they are consistent with the idea that altered brainstem and hypothalamic activity are potentially involved in the expression of a migraine attack. Understanding how these functional changes precipitate a migraine attack may lead to the development of treatment strategies aimed at the astrocytes, rather than neurons. Indeed, as we learn more about the complexities of glial ion channels and gliotransmission, we may well find means of targeting other forms of pain.

ACKNOWLEDGMENTS

The authors wish to thank the many volunteers involved in this study. The authors declare that there are no conflicts of interest.

ORCID

Paul M. Macey  <http://orcid.org/0000-0003-4093-7458>

Luke A. Henderson  <http://orcid.org/0000-0002-1026-0151>

REFERENCES

- Afridi, S. K., Giffin, N. J., Kaube, H., Friston, K. J., Ward, N. S., Frackowiak, R. S., & Goadsby, P. J. (2005). A positron emission tomographic study in spontaneous migraine. *Archives of Neurology*, *62*(8), 1270–1275.
- Afridi, S. K., Matharu, M. S., Lee, L., Kaube, H., Friston, K. J., Frackowiak, R. S., & Goadsby, P. J. (2005b). A PET study exploring the laterality of brainstem activation in migraine using glyceryl trinitrate. *Brain*, *128*, 932–939.
- Akerman, S., Holland, P. R., & Goadsby, P. J. (2011). Diencephalic and brainstem mechanisms in migraine. *Nature Reviews. Neuroscience*, *12*(10), 570–584.
- Alshelh, Z., Di Pietro, F., Youssef, A. M., Reeves, J. M., Macey, P. M., Vickers, E. R., ... Henderson, L. A. (2016). Chronic neuropathic pain: It's about the rhythm. *Journal of Neuroscience*, *36*(3), 1008–1018.
- Batra, A., Matharu, M. S., Buchel, C., Frackowiak, R. S., & Goadsby, P. J. (2001). Brainstem activation specific to migraine headache. *Lancet*, *357*(9261), 1016–1017.
- Benarroch, E. E. (2005). Neuron-astrocyte interactions: Partnership for normal function and disease in the central nervous system. *Mayo Clinic Proceedings*, *80*(10), 1326–1338.
- Bernard, J. F., & Bandler, R. (1998). Parallel circuits for emotional coping behaviour: New pieces in the puzzle. *Journal of Comparative Neurology*, *401*(4), 429–436.
- Bernstein, C., & Burstein, R. (2012). Sensitization of the trigeminovascular pathway: Perspective and implications to migraine pathophysiology. *Journal of Clinical Neurology*, *8*(2), 89–99.
- Borsook, D., & Burstein, R. (2012). The enigma of the dorsolateral pons as a migraine generator. *Cephalgia*, *32*(11), 803–812.
- Burstein, R., Nosedà, R., & Borsook, D. (2015). Migraine: Multiple processes, complex pathophysiology. *Journal of Neuroscience*, *35*(17), 6619–6629.
- Churi, S. B., Abdel-Aleem, O. S., Tumber, K. K., Scuderi-Porter, H., & Taylor, B. K. (2008). Intrathecal rosiglitazone acts at peroxisome proliferator-activated receptor-gamma to rapidly inhibit neuropathic pain in rats. *Journal of Pain*, *9*(7), 639–649.
- Crunelli, V., Blethyn, K. L., Cope, D. W., Hughes, S. W., Parri, H. R., Tumer, J. P., ... Williams, S. R. (2002). Novel neuronal and astrocytic mechanisms in thalamocortical loop dynamics. *Philosophical Transactions of the Royal Society B: Biological Sciences*, *357*(1428), 1675–1693.
- Cunningham, M. O., Pervouchine, D. D., Racca, C., Kopell, N. J., Davies, C. H., Jones, R. S., ... Whittington, M. A. (2006). Neuronal metabolism governs cortical network response state. *Proceedings of the National Academy of Sciences of the United States of America*, *103*(14), 5597–5601.
- Denuelle, M., Fabre, N., Payoux, P., Chollet, F., & Geraud, G. (2007). Hypothalamic activation in spontaneous migraine attacks. *Headache: The Journal of Head and Face Pain*, *0*(0), 070503104159006.
- Floyd, N. S., Price, J. L., Ferry, A. T., Keay, K. A., & Bandler, R. (2001). Orbitomedial prefrontal cortical projections to hypothalamus in the rat. *Journal of Comparative Neurology*, *432*(3), 307–328.
- Garrison, C. J., Dougherty, P. M., Kajander, K. C., & Carlton, S. M. (1991). Staining of glial fibrillary acidic protein (GFAP) in lumbar spinal cord increases following a sciatic nerve constriction injury. *Brain Research*, *565*(1), 1–7.
- Giffin, N. J., Ruggiero, L., Lipton, R. B., Silberstein, S. D., Tvedskov, J. F., Olesen, J., ... Macrae, A. (2003). Premonitory symptoms in migraine: An electronic diary study. *Neurology*, *60*(6), 935–940.
- Goadsby, P. J., & Akerman, S. (2012). The trigeminovascular system does not require a peripheral sensory input to be activated—migraine is a central disorder. Focus on 'Effect of cortical spreading depression on basal and evoked traffic in the trigeminovascular sensory system'. *Cephalgia*, *32*(1), 3–5.
- Goadsby, P. J., Charbit, A. R., Andreou, A. P., Akerman, S., & Holland, P. R. (2009). Neurobiology of migraine. *Neuroscience*, *161*(2), 327–341.
- Halassa, M. M., Fellin, T., & Haydon, P. G. (2007). The tripartite synapse: Roles for gliotransmission in health and disease. *Trends in Molecular Medicine*, *13*(2), 54–63.
- Holstege, G., & Kuypers, H. G. (1982). The anatomy of brain stem pathways to the spinal cord in cat. A labeled amino acid tracing study. *Progress in Brain Research*, *57*, 145–175.
- Hubbard, J. A., & Binder, D. K. (2016). *Astrocytes and epilepsy*. Academic Press.
- Hughes, S. W., Lorincz, M. L., Parri, H. R., & Crunelli, V. (2011). Infralow (<0.1 Hz) oscillations in thalamic relay nuclei: basic mechanisms and significance to health and disease states. *Progress in Brain Research*, *193*, 145–162.
- James, M. F., Smith, J. M., Boniface, S. J., Huang, C. L., & Leslie, R. A. (2001). Cortical spreading depression and migraine: New insights from imaging? *Trends in Neuroscience*, *24*(5), 266–271.
- Ji, X. T., Qian, N. S., Zhang, T., Li, J. M., Li, X. K., Wang, P., ... Niu, L. (2013). Spinal astrocytic activation contributes to mechanical

- allodynia in a rat chemotherapy-induced neuropathic pain model. *PLoS One*, 8(4), e60733.
- Knight, Y. E., & Goadsby, P. J. (2001). The periaqueductal grey matter modulates trigeminovascular input: A role in migraine? *Neuroscience*, 106(4), 793–800.
- Lambert, G. A., Truong, L., & Zagami, A. S. (2011). Effect of cortical spreading depression on basal and evoked traffic in the trigeminovascular sensory system. *Cephalalgia*, 31(14), 1439–1451.
- Linde, M., Mulleners, W. M., Chronicle, E. P., & McCrory, D. C. (2013). Valproate (valproic acid or sodium valproate or a combination of the two) for the prophylaxis of episodic migraine in adults. *Cochrane Database of Systematic Reviews*, CD010611.
- Lorincz, M. L., Geall, F., Bao, Y., Crunelli, V., & Hughes, S. W. (2009). ATP-dependent infra-slow (<0.1 Hz) oscillations in thalamic networks. *PLoS One*, 4(2), e4447.
- Macey, P. M., Macey, K. E., Kumar, R., & Harper, R. M. (2004). A method for removal of global effects from fMRI time series. *NeuroImage*, 22(1), 360–366.
- Mai, J. K., Paxinos, G., & Voss, T. (2007). *Atlas of the human brain*. Academic Press.
- Mantini, D., Perrucci, M. G., Del Gratta, C., Romani, G. L., & Corbetta, M. (2007). Electrophysiological signatures of resting state networks in the human brain. *Proceedings of the National Academy of Sciences of the United States of America*, 104(32), 13170–13175.
- Marciszewski, K. K., Meylakh, N., Di Pietro, F., Macefield, V. G., Macey, P. M., & Henderson, L. A. (2017). Altered brainstem anatomy in migraine. *Cephalalgia*, 33(10), 2417694884.
- Morgan, M. M., Whittier, K. L., Hegarty, D. M., & Aicher, S. A. (2008). Periaqueductal gray neurons project to spinally projecting GABAergic neurons in the rostral ventromedial medulla. *Pain*, 140(2), 376–386.
- Morgenweck, J., Griggs, R. B., Donahue, R. R., Zadina, J. E., & Taylor, B. K. (2013). PPARgamma activation blocks development and reduces established neuropathic pain in rats. *Neuropharmacology*, 70, 236–246.
- Nedergaard, M., Cooper, A. J., & Goldman, S. A. (1995). Gap junctions are required for the propagation of spreading depression. *Journal of Neurobiology*, 28(4), 433–444.
- Okada-Ogawa, A., Suzuki, I., Sessle, B. J., Chiang, C. Y., Salter, M. W., Dostrovsky, J. O., ... Iwata, K. (2009). Astroglia in medullary dorsal horn (trigeminal spinal subnucleus caudalis) are involved in trigeminal neuropathic pain mechanisms. *Journal of Neuroscience*, 29(36), 11161–11171.
- Parri, H. R., & Crunelli, V. (2001). Pacemaker calcium oscillations in thalamic astrocytes in situ. *NeuroReport*, 12(18), 3897–3900.
- Parri, H. R., Gould, T. M., & Crunelli, V. (2001). Spontaneous astrocytic Ca²⁺ oscillations in situ drive NMDAR-mediated neuronal excitation. *Nature Neuroscience*, 4(8), 803–812.
- Paxinos, G., & Huang, X. (1995). *Atlas of the human brainstem*. San Diego, CA: Academic Press.
- Schulte, L. H., & May, A. (2016). The migraine generator revisited: Continuous scanning of the migraine cycle over 30 days and three spontaneous attacks. *Brain*, 139(7), 1987–1993.
- Shi, Y., Gelman, B. B., Lisinicchia, J. G., & Tang, S. J. (2012). Chronic-pain-associated astrocytic reaction in the spinal cord dorsal horn of human immunodeficiency virus-infected patients. *Journal of Neuroscience*, 32(32), 10833–10840.
- Stankewitz, A., Aderjan, D., Eippert, F., & May, A. (2011). Trigeminal nociceptive transmission in migraines predicts migraine attacks. *Journal of Neuroscience*, 31(6), 1937–1943.
- Strassman, A., Mason, P., Moskowitz, M., & Maciewicz, R. (1986). Response of brainstem trigeminal neurons to electrical stimulation of the dura. *Brain Research*, 379(2), 242–250.
- Strassman, A. M., Mineta, Y., & Vos, B. P. (1994). Distribution of FOS-like immunoreactivity in the medullary and upper cervical dorsal horn produced by stimulation of dural blood vessels in the rat. *Journal of Neuroscience*, 14, 3725–3735.
- Tian, G. F., Azmi, H., Takano, T., Xu, Q., Peng, W., Lin, J., ... Nedergaard, M. (2005). An astrocytic basis of epilepsy. *Nature Medicine*, 11(9), 973–981.
- Vanhatalo, S., Palva, J. M., Holmes, M. D., Miller, J. W., Voipio, J., & Kaila, K. (2004). Infraslow oscillations modulate excitability and interictal epileptic activity in the human cortex during sleep. *Proceedings of the National Academy of Sciences of the United States of America*, 101(14), 5053–5057.
- Veloso, F., Kumar, K., & Toth, C. (1998). Headache secondary to deep brain implantation. *Headache: The Journal of Head and Face Pain*, 38(7), 507–515.
- Wang, C. C., Chen, P. S., Hsu, C. W., Wu, S. J., Lin, C. T., & Gean, P. W. (2012). Valproic acid mediates the synaptic excitatory/inhibitory balance through astrocytes—a preliminary study. *Progress in Neuro-Psychopharmacology & Biological Psychiatry*, 37(1), 111–120.
- Weiller, C., May, A., Limmroth, V., Juptner, M., Kaube, H., Schayck, R. V., ... Diener, H. C. (1995). Brain stem activation in spontaneous human migraine attacks. *Nature Medicine*, 1(7), 658–660.

How to cite this article: Meylakh N, Marciszewski KK, Di Pietro F, Macefield VG, Macey PM, Henderson LA. Deep in the brain: Changes in subcortical function immediately preceding a migraine attack. *Hum Brain Mapp*. 2018;39:2651–2663. <https://doi.org/10.1002/hbm.24030>

Chapter 3

Resting regional brain activity changes across the migraine cycle

Resting regional brain activity changes across the migraine cycle

N. Meylakh¹, K.K. Marciszewski¹, F. Di Pietro¹, V.G. Macefield², P.M. Macey³ and L.A.

Henderson¹

¹Department of Anatomy and Histology, University of Sydney, Australia, 2006; ²School of Medicine, Western Sydney University, Sydney, Australia; ³UCLA School of Nursing and Brain Research Institute, University of California 90095, Los Angeles, United States.

Corresponding author: Luke A. Henderson, Department of Anatomy and Histology, F13, University of Sydney, Australia. lukeh@anatomy.usyd.edu.au (email); +612 9351 7063 (Tel) +612 9351 6556 (Fax)¹

Abstract

Whilst the pathophysiology of migraine remains unresolved, it is likely that both the central nervous system and cerebral vasculature changes are critical for migraine initiation. Since it is impossible to predict when a migraine will occur, very few studies have explored brain activity changes in the critical 24-hour period preceding a migraine. Nevertheless, we recently reported changes in the pattern of resting activity in brainstem, hypothalamus and thalamus sites immediately prior to a migraine attack, findings consistent with the idea that changes in brain function are required to trigger a migraine. It remains unknown however, if these regional activity pattern changes are coupled to alterations in absolute regional brain activity levels. To address this question, we used pseudocontinuous arterial spin labelling, to measure regional blood flow in migraineurs immediately prior to (n=6), immediately following (n=10) and between migraine attacks (n=20) and in healthy control subjects (n=50). We found that immediately prior to a migraine, blood flow decreases occurred in the brainstem in the region of the midbrain periaqueductal gray matter, spinal trigeminal nucleus and hypothalamus, as well as in higher brain regions such as the orbitofrontal, visual and retrosplenial cortices. In addition, significantly reduced regional blood flow occurred during the interictal phase in the nucleus accumbens, anterior insula, ventrolateral prefrontal cortex, orbitofrontal cortex and putamen. These changes support the suggestion that abnormal regional brain activity occurs before a migraine attack and is involved in underlying migraine pathogenesis.

Keywords: cerebral blood flow, spinal trigeminal nucleus, periaqueductal gray matter, migraine, arterial spin labelling

3.2 Introduction

Migraine is a highly complex disorder, with headaches accompanied by an array of neurological symptoms such as nausea, photophobia, phonophobia, as well as emotional, cognitive and autonomic disturbances (Nosedá & Burstein, 2013). The presence of these accompanying neurological symptoms supports that migraine is more than just a headache and that it likely involves changes in multiple brain systems (Burstein et al., 2015). For years, vascular changes have been considered the main factor in migraine pathogenesis (Nosedá & Burstein, 2013), although many now consider migraine as a disorder of the central nervous system (Schwedt & Dodick, 2009). Even if the central nervous system is involved in the generation of a migraine attack, the significance of cerebral vasculature in migraine cannot be dismissed. Indeed, a large body of evidence exists suggesting that the development of migraine-pain is dependent on the activation and sensitization of the trigeminal sensory afferents that innervate meninges and their large blood vessels (Pietrobon & Moskowitz, 2013).

Irrespective of the precise mechanism responsible for the initiation of migraine, there is evidence of changes in brain function immediately prior to a migraine attack. Indeed, we have recently shown an altered pattern of brain activity in the 24-hour period *preceding* a migraine attack (Noemi Meylakh et al., 2018). These changes are characterized by increases in resting infra-slow oscillations in regions including the hypothalamus, midbrain periaqueductal gray matter (PAG), dorsal pons and spinal trigeminal nucleus (SpV); regions that have also been shown to exhibit an increase in activity during a migraine attack itself (S.K. Afridi et al., 2005; Bahra et al., 2001b; Denuelle et al., 2007; Matharu et al., 2004).

Whilst we have shown changes in the *pattern* and *functional connectivity* of resting activity immediately prior to a migraine attack, it remains unknown if these changes are coupled to alterations in absolute activity levels. Whilst traditional human brain imaging methods such as positron emission tomography (PET) can measure resting blood flow as an index of on-going neural activity levels, this technique does not have the spatial acuity to explore changes within the brainstem. Pseudocontinuous arterial spin labelling is a relatively new magnetic resonance imaging technique that allows for non-invasive regional blood flow assessment that is based on the direct magnetic labelling of blood water protons as an endogenous tracer (Hendrikse, Petersen, & Golay, 2012). Whilst, some studies have measured cerebral blood flow (CBF) during the interictal phase (i.e. between attacks but not immediately prior or following a migraine) and even during a migraine aura, no study has explored regional CBF, particularly within the brainstem, in the period immediately *preceding* a migraine attack. If changes in regional brain activity occur in brainstem and hypothalamic regions immediately prior to a migraine attack, it would provide additional evidence that changes in brain activity precede the head pain that characterizes most migraine attacks.

The aim of this investigation is to determine whether regional brain activity is altered during different phases of migraine, i.e. interictal, immediately prior to and immediately following a migraine attack. We hypothesise that the same areas displaying changes in resting activating patterns immediately prior to a migraine attack, that is in the SpV, PAG, hypothalamus and thalamus, will show significant CBF alterations immediately prior to a migraine.

3.3 Methods

3.3.1 Subjects

Thirty-one subjects with migraine (23 females; mean age 31 ± 2.0 years [\pm SEM]) and 50 pain-free controls (36 females; mean age 28.8 ± 1.5 years [\pm SEM]) were recruited for the study from the general population using an advertisement. There were no significant differences in age (t-test, $p > 0.05$) or gender composition (*chi-squared* test, $p > 0.05$) between the two subject groups. Migraine subjects were diagnosed according to the IHC Classification ICHD-3 BETA criteria and 5 of the 31 migraine subjects reported an aura associated with their migraine attacks. Migraine subject characteristics, including medication use are shown in Table 1. 22 migraineurs were scanned during an interictal period, that is, at least 72 hours after and 24 hours prior to a migraine event. Ten migraineurs were scanned immediately (within 72 hours) following an attack, and of these ten, four were also scanned during the interictal period. Six migraineurs were scanned immediately (within 24 hours) prior to an attack, and of these four were also scanned during the interictal period. In one migraineur scans were collected in all three phases.

Exclusion criteria for controls were the presence of any pain condition including family history of migraines, current use of analgesics, or any neurological disorder. Exclusion criteria for migraineurs were any other pain condition or neurological disorder. No migraineur was excluded based on their medication use and no migraine or control subject had an incidental neurological finding that resulted in their exclusion from the study. All migraineurs indicated the intensity (6-point visual analogue scale; 0=no pain, 5=most intense imaginable pain) and drew the facial distribution of pain commonly experienced during a migraine attack. In addition, each subject described the qualities of their migraines and indicated any current treatments used to prevent or abort a migraine once started. Twenty nine of the 31 migraineurs had episodic migraine whereas the remaining two migraineurs had chronic migraine (>15 migraines per month). Informed written consent was obtained for all procedures according to the Declaration of Helsinki and local

Institutional Human Research Ethics Committees approved the study. Data from 21 of the 31 migraineurs and 14 of the control subjects were used in a previous investigation (Marciszewski et al., 2017), as well as data from 26 of the 31 migraineurs, and 14 of the control subjects in our previous investigation (Noemi Meylakh et al., 2018).

3.3.2 MRI Acquisition

All subjects lay supine on the bed of a 3 Tesla MRI scanner (Philips, Achieva) with their head immobilized in a tight-fitting head coil. With each subject relaxed and at rest, a high-resolution 3D T1-weighted anatomical image set, covering the entire brain, was collected (turbo field echo; field of view=250x250mm, matrix size=288x288, slice thickness=0.87mm, repetition time=5600ms; echo time=2.5ms, flip angle=8°). Following this, a series of 108 pseudocontinuous arterial spin labelling images (50 axial slices, 54 label/control image pairs, [TE]=12.7ms, [TR]=5310ms, raw voxel size=2.4x2.4x3.0mm, labelling time=1650ms, slice time=36.6ms, post label delay time=1600ms, background suppression).

3.3.3 MRI processing and statistical analysis

3.3.3.1 Image preprocessing

Using SPM12 and Matlab software, Statistical Parametric Mapping, all pseudocontinuous arterial spin labelling images were realigned, co-registered to each individual's T1-weighted image set, the label and control images averaged and a mean cerebral blood flow (CBF) image created using the subtraction method using the ASL toolbox (Wang et al., 2008). Each subject's T1-weighted

anatomical image was then spatially normalized to a template in Montreal Neurological Institute (MNI) space and the parameters applied to the CBF maps. The wholebrain CBF maps were then smoothed using a 5mm full-width at half-maximum (FWHM) Gaussian filter. We also performed a brainstem specific analysis in each subject. Using the Spatially Unbiased Infratentorial Template (SUIT) toolbox (Diedrichsen et al., 2011), the brainstem was isolated from the T1-weighted anatomical image and normalized into MNI space and the parameters applied to the CBF maps resulting in a blood flow map of the brainstem only in MNI space. These brainstem maps were then spatially smoothed using a 3mm FWHM Gaussian filter. A grey matter mask derived from the T1-weighted anatomical image segmentation was used to restrict the wholebrain analysis to grey matter, and a brainstem-specific mask was used for the brainstem analyses.

We performed three separate voxel-by-voxel analyses to determine if there were any significant differences in regional CBF between i) controls versus migraineurs during the interictal phase, ii) controls versus migraineurs during the 24-hour period immediately prior to a migraine attack, and iii) controls versus migraineurs during the 72-hour period immediately after a migraine attack. Significant differences in CBF between groups were determined using a two-sample random effects analysis ($p < 0.05$ false discovery rate corrected). Significant clusters were overlaid onto an individual T1-weighted anatomical image and also rendered onto a glass three-dimensional view of the brainstem and wholebrain. We also measured global CBF to determine if there were any significant differences in global CBF values between each group. These values were then used as a confound variable when testing regional differences, to ensure that global CBF was not a factor in the context of regional CBF. In all analyses, the anatomical locations of significant clusters were confirmed using the Atlas of the Human Brain (Mai, Paxinos, & Voss, 2007) and the Atlas of the Human Brainstem (G. Paxinos & X. Huang, 1995).

For each significant cluster derived from each of the three wholebrain and three brainstem analyses, the CBF values were extracted from each subject in each of the four subject groups and the mean and SEM plotted. Significant differences between controls and each of the other two migraine groups were determined ($p < 0.05$, two-tailed, two-sample t-test, Bonferroni corrected for multiple comparisons). Differences in CBF values between the groups in the original voxel-by-voxel analysis from which the cluster was derived were not compared to avoid “double-dipping.”

In addition to exploring differences between controls and migraineurs during three phases, for each significant cluster derived from the controls versus migraineurs during the phase immediately prior to a migraine, we plotted CBF values against each individual’s time to their next migraine attack. That is, from the day of scanning, how many days until the next migraine to an upper limit of 30 days. Furthermore, for visualization purposes, mean CBF values for migraineurs with greater than 30 days prior, 30-12 days prior, 11-2 days prior and 1 day prior to a migraine attack were averaged and plotted. Finally, since others have reported increases in CBF specifically within the primary somatosensory cortex (Hodkinson et al., 2015; Youssef et al., 2017), we performed a targeted analysis of this region by restricting our analysis to the right and left primary somatosensory cortices for each of the three voxel-by-voxel analyses ($p < 0.05$ family discovery rate 5 corrected).

3.4 Results

Comparisons of resting CBF within the brainstem revealed no significant differences between controls and migraineurs during either the interictal phase or immediately following a migraine attack (Figure 1A). However, in striking contrast, during the phase immediately prior to a migraine, CBF was significantly lower in migraineurs compared with controls in two regions: the

region encompassing the right PAG and the area encompassing the left SpV (Figure 1B, Table 2). Extraction of CBF values from these two clusters in controls and the three migraine groups confirmed the specificity of the CBF decreases; that is, CBF decreased in the PAG and SpV regions only during the phase immediately prior to a migraine attack (CBF mean \pm SEM ml/100g/min: PAG: controls: 78.3 \pm 3.8, interictal: 67.8 \pm 4.3, immediately prior to an attack: 38.7 \pm 9.0, immediately following an attack: 56.1 \pm 10.0; SpV: controls: 113.2 \pm 2.7, interictal: 106.3 \pm 5.4, immediately prior to an attack: 73.3 \pm 10.6, immediately following an attack: 92.6 \pm 8.9).

In addition to rCBF, we also measured global CBF to ensure that the patterns of rCBF were not influenced by global CBF. Extraction of global CBF values confirmed a similar pattern in the brainstem as seen in the rCBF (CBF mean \pm SEM ml/100g/min: controls: 60.0 \pm 1.6, interictal: 60.3 \pm 3.2, immediately prior to an attack: 47.2 \pm 3.5, immediately following an attack: 52.8 \pm 5.9). Furthermore, the global CBF values were added as a confound variable in the testing of regional differences. These findings did not change the nature of the results aforementioned, however the threshold was affected. For these results, significant differences in CBF between groups were determined using a two-sample random effects analysis ($p < 0.005$). Comparisons of resting CBF with global CBF as a confound variable within the brainstem revealed that during the phase immediately prior to a migraine, CBF was significantly lower in migraineurs compared with controls in two regions: the region encompassing the right PAG and the area encompassing the left SpV (Figure 1D). (CBF mean \pm SEM ml/100g/min: PAG: controls: 80.7 \pm 3.8, interictal: 69.9 \pm 4.4, immediately prior to an attack: 39.0 \pm 9.1, immediately following an attack: 57.5 \pm 10.2; SpV: controls: 115.2 \pm 2.8, interictal: 108.1 \pm 5.3, immediately prior to an attack: 73.2 \pm 11.2, immediately following an attack: 96.1 \pm 8.5).

Wholebrain analysis also revealed significant reductions in CBF in migraineurs compared with controls during the phase immediately prior to an attack (Figure 2A and B, Table 2). Migraineurs displayed significantly reduced CBF in a number of discrete brain regions including the region encompassing the right hypothalamus, right orbitofrontal cortex (OFC), left visual cortex and the retrosplenial cortex (RSC) bilaterally. Consistent with the brainstem changes, extraction of CBF values confirmed the specificity of the CBF decreases during the immediately prior to migraine phase only (right hypothalamus: controls: 45.9 ± 1.6 , interictal: 40.3 ± 2.4 , immediately prior to an attack: 27.7 ± 4.6 , immediately following an attack: 36.9 ± 3.3 ; right OFC: controls: 53.1 ± 1.4 , interictal: 48.1 ± 2.2 , immediately prior to an attack: 38.8 ± 1.8 , immediately following an attack: 44.1 ± 4.1 ; left visual cortex: controls: 70.3 ± 3.3 , interictal: 61.8 ± 5.8 , immediately prior to an attack: 34.1 ± 5.3 , immediately following an attack: 67.9 ± 8.5 ; RSC: controls: 66.7 ± 2.7 , interictal: 61.2 ± 4.2 , immediately prior to an attack: 37.5 ± 7.7 , immediately following an attack: 51.0 ± 4.4). Plots of CBF values for each cluster in individual migraineurs also confirmed the specificity of these decreases during the period immediately prior to a migraine attack (Figure 3). They also reveal that in the SpV, PAG and hypothalamus, CBF was relatively stable during the interictal period, i.e., CBF was stable until the day before the migraine attack during which time they decreased abruptly. In contrast, CBF in cortical regions such as the OFC, RSC and visual cortex appeared to decrease from approximately 1 week prior to the migraine attack.

In addition to changes in resting CBF in the brainstem and higher brain regions during the phase immediately prior to a migraine, we found changes in higher brain centres in the interictal phase (Figures 4A and 4B, Table 2). Significantly reduced CBF occurred in migraineurs during the interictal phase in areas including in the region of the left nucleus accumbens (NAc), left anterior insula, left and right ventrolateral prefrontal cortex (vlPFC), right OFC, as well as in the region of

the left putamen. Extraction of CBF values from these clusters during all migraine phases revealed that in no cluster was CBF significantly different between controls and migraineurs during the phase immediately prior to a migraine, although all apart from the NAc displayed significantly reduced CBF during the phase immediately following a migraine (left NAc: *controls*: 68.0±2.4, *interictal*: 52.4±2.5, *immediately prior to an attack*: 55.7±4.4, *immediately following an attack*: 53.8±5.7; left anterior insula: *controls*: 43.1±1.3, *interictal*: 34.3±1.7, *immediately prior to an attack*: 34.9±3.1, *immediately following an attack*: 31.8±4.9; left vIPFC: *controls*: 74.9±2.2, *interictal*: 61.1±2.5, *immediately prior to an attack*: 61.3±3.9, *immediately following an attack*: 59.2±5.6; right vIPFC: *controls*: 93.4±2.6, *interictal*: 76.6±2.9, *immediately prior to an attack*: 74.4±3.7, *immediately following an attack*: 71.5±6.8; right OFC: *controls*: 84.5±2.5, *interictal*: 66.4±2.4, *immediately prior to an attack*: 69.7±4.7, *immediately following an attack*: 62.2±5.7; left putamen: *controls*: 48.2±1.5, *interictal*: 36.7±1.6, *immediately prior to an attack*: 37.9±2.7, *immediately following an attack*: 37.6±3.5).

Again, in addition to rCBF, we also measured global CBF flow to ensure that the patterns of rCBF were not influenced by global CBF. Extraction of global CBF values confirmed a similar pattern in the wholebrain as seen in the rCBF (*controls*: 60.5±1.9, *interictal*: 57.2±3.0, *immediately prior to an attack*: 48.2±3.7, *immediately following an attack*: 55.1±4.4). When adding the global CBF values as a confound variable, the regions displayed in the rCBF analysis did not change, however the threshold was affected. For these results, significant differences in CBF between groups were determined using a two-sample random effects analysis ($p < 0.005$). Wholebrain analysis of resting CBF with global CBF as a confound variable confirmed that migraineurs displayed significantly reduced rCBF in a number of brain regions including the region encompassing the right hypothalamus, right orbitofrontal cortex (OFC), left visual cortex and the retrosplenial cortex

(RSC) bilaterally during the phase immediately prior to a migraine (Figure 2D) (right hypothalamus: *controls*: 46.2±1.6, *interictal*: 40.5±2.5, *immediately prior to an attack*: 27.1±4.8, *immediately following an attack*: 37.3±3.3; right OFC: *controls*: 48.6±1.3, *interictal*: 44.8±2.2, *immediately prior to an attack*: 35.7±1.9, *immediately following an attack*: 41.5±3.9; left visual cortex: *controls*: 70.2±3.3, *interictal*: 61.7±5.6, *immediately prior to an attack*: 34.8±5.3, *immediately following an attack*: 67.1±8.5; RSC: *controls*: 68.8±2.3, *interictal*: 64.1±4.3, *immediately prior to an attack*: 35.7±7.5, *immediately following an attack*: 53.7±4.6).

Furthermore, wholebrain analysis of resting CBF with global CBF as a confound variable confirmed that migraineurs displayed significantly reduced CBF occurred in migraineurs during the interictal phase in areas including in the region of the left nucleus accumbens (NAc), left and right ventrolateral prefrontal cortex (vlPFC), right OFC, as well as in the region of the left putamen (Figure 4D) (left NAc: *controls*: 49.9±1.6, *interictal*: 38.7±1.8, *immediately prior to an attack*: 39.5±2.8, *immediately following an attack*: 39.3±3.6; left vlPFC: *controls*: 61.8±1.7, *interictal*: 50.5±2.3, *immediately prior to an attack*: 49.8±3.2, *immediately following an attack*: 47.9±5.1; right vlPFC: *controls*: 93.0±2.6, *interictal*: 77.0±3.4, *immediately prior to an attack*: 74.2±3.9, *immediately following an attack*: 71.5±6.7; right OFC: *controls*: 82.7±2.4, *interictal*: 65.7±2.5, *immediately prior to an attack*: 68.5±5.0, *immediately following an attack*: 61.2±5.6; left putamen: *controls*: 49.9±1.6, *interictal*: 38.7±1.8, *immediately prior to an attack*: 39.5±2.8, *immediately following an attack*: 39.3±3.6).

Analysis of medication use in migraineurs revealed that medication use had no significant effect on CBF in the regions that showed significant reductions during the phase immediately prior to an attack (CBF mean ± SEM ml/100g/min: PAG: *interictal*: *medication*: 61.1 ± 6.2, *no medication*:

71.8 ± 5.7, $p=0.22$; immediately prior to an attack: *medication*: 44.4 ± 20.0, *no medication*: 34.4 ± 8.2, $p=0.68$; SpV: interictal: *medication*: 97.5 ± 5.9, *no medication*: 111.4 ± 7.6, $p=0.17$; immediately prior to an attack: *medication*: 80.8 ± 21.3, *no medication*: 67.7 ± 12.0, $p=0.63$; right hypothalamus: interictal: *medication*: 36.1 ± 3.3, *no medication*: 43.0 ± 3.2, $p=0.17$; immediately following an attack: *medication*: 40.4 ± 3.6, *no medication*: 34.5 ± 4.9, $p=0.36$; OFC: interictal: *medication*: 49.0 ± 2.6, *no medication*: 47.5 ± 3.4, $p=0.75$; immediately following an attack: *medication*: 48.4 ± 6.8, *no medication*: 41.2 ± 5.2, $p=0.43$; left visual cortex: interictal: *medication*: 60.9 ± 8.6, *no medication*: 62.3 ± 8.0, $p=0.91$; immediately following an attack: *medication*: 73.6 ± 8.1, *no medication*: 64.0 ± 13.6, $p=0.56$; RSC: interictal: *medication*: 49.8 ± 3.6, *no medication*: 68.7 ± 5.7, $p=0.02$; immediately following an attack: *medication*: 52.5 ± 8.1, *no medication*: 49.9 ± 5.5, $p=0.80$). Furthermore, there was no effect of medication use on CBF in the regions that showed significant reductions during the interictal phase (NaC: interictal: *medication*: 46.8 ± 2.8, *no medication*: 56.2 ± 4.1, $p=0.11$; immediately following an attack: *medication*: 58.4 ± 7.7, *no medication*: 50.8 ± 8.3, $p=0.52$; left anterior insula: interictal: *medication*: 31.0 ± 2.9, *no medication*: 36.5 ± 2.4, $p=0.16$; immediately following an attack: *medication*: 28.5 ± 6.3, *no medication*: 33.9 ± 7.3, $p=0.59$; left vlPFC: interictal: *medication*: 58.3 ± 3.2, *no medication*: 63.0 ± 4.2, $p=0.44$; immediately following an attack: *medication*: 62.9 ± 11.4, *no medication*: 56.8 ± 6.3, $p=0.66$; right vlPFC: interictal: *medication*: 73.9 ± 4.0, *no medication*: 78.4 ± 4.8, $p=0.51$; immediately following an attack: *medication*: 71.1 ± 11.7, *no medication*: 71.8 ± 9.2, $p=0.96$; right OFC: interictal: *medication*: 63.2 ± 4.3, *no medication*: 68.5 ± 3.3, $p=0.34$; immediately following an attack: *medication*: 62.8 ± 11.4, *no medication*: 61.9 ± 6.8, $p=0.95$; and left putamen: interictal: *medication*: 33.2 ± 2.0, *no medication*: 39.0 ± 2.6, $p=0.12$; immediately following an attack: *medication*: 40.8 ± 5.7, *no medication*: 35.5 ± 4.7, $p=0.50$).

Finally, our restricted analysis of the primary somatosensory cortex revealed no significant differences in CBF between controls and any of the three migraine groups. This lack of difference was evident even at corrected thresholds and even at more liberal thresholds such as $p < 0.01$ uncorrected for multiple comparisons. A small cluster in the orofacial region of the right primary somatosensory cortex did appear at $p < 0.05$ uncorrected in the interictal greater than control comparison, however the extraction of CBF values revealed no significant difference between the groups.

3.5 Discussion

Our data provides strong evidence that in migraineurs, regional on-going activity in a discrete set of brainstem and higher brain structures decreases immediately prior to a migraine attack. Importantly, these regional activity decreases occurred in many of the same regions in which we have shown altered on-going activity patterns during the phase immediately prior to a migraine, in particular the hypothalamus, PAG and SpV, and in which others have shown activations and alterations during a migraine attack itself (S.K. Afridi et al., 2005; Bahra et al., 2001b; Bednarczyk, Remler, Weikart, Nelson, & Reed, 1998; Weiller, May, Limmroth, Juptner, Kaube, Schayck, Coenen, & Diener, 1995). Furthermore, CBF in these regions remained at controls levels during the interictal phase, decreasing exclusively during the 24-hour period before a migraine attack. These data support that CBF is altered in areas of the pain processing system prior to the development of migraine head pain and are consistent with the idea that changes in brain circuitry activity and/or responsivity may be involved in the initiation of migraine.

Whilst numerous investigations have explored resting regional CBF in migraineurs during the

interictal phase, very few have explored the period immediately prior to a migraine attack during the prodrome or premonitory phase. Consistent with our data, early investigations using intra-carotid injection of ^{133}Xe found that during the premonitory phase, CBF decreased in the carotid artery territory (Norris, Hachinski, & Cooper, 1975). Furthermore, these CBF decreases were replaced by CBF increases during the subsequent migraine attack. More recently, a PET study exploring regional CBF during triggered premonitory symptoms through the administration of nitroglycerin, reported increased blood flow in areas of the hypothalamus, PAG, dorsal pons and cortical regions such as occipital, temporal and prefrontal cortices (Maniyar, Sprenger, Monteith, Schankin, & Goadsby, 2014). Whilst this appears contradictory to our results, in the aforementioned study, individuals reported symptoms such as photophobia, nausea, tiredness and neck stiffness, whereas in our study individuals did not report any such premonitory symptoms. It is likely that our regional CBF decreases in many of the same brain regions, reflect neural activity changes immediately prior to the onset of premonitory symptoms, which may result in the expression of premonitory symptoms and head pain.

In the 24-hour period prior to a migraine, we found CBF decreases in the regions encompassing the hypothalamus, PAG and SpV, areas in which we previously reported increased infra-slow oscillation (0.03-0.06Hz) strength of resting fMRI signal fluctuations during the same period in migraineurs (Meylakh et al., 2018). The hypothalamus and PAG have long been hypothesised to be involved in the initiation of migraine, although the precise roles of these regions remain unknown (Denuelle et al., 2007). Tract tracing studies have shown that the PAG and hypothalamus are reciprocally connected and that the PAG sends projections to the SpV via the rostral ventromedial medulla (Floyd et al., 2001; Holstege & Kuypers, 1982; Morgan et al., 2008). This circuitry forms part of the descending pain modulating circuitry that can inhibit or enhance

incoming nociceptor inputs at the level of the primary afferent synapse, including at the SpV (H. L. Fields & Heinricher, 1985), and PAG stimulation that inhibits incoming dural afferent information (Knight & Goadsby, 2001).

Indeed, the role of the PAG in migraine generation has been the subject of much debate since Raskin and colleagues induced migraine-like headaches with the implantation of electrodes into the PAG of non-migraine chronic pain patients (Matharu et al., 2004). Decreases in PAG blood flow are however consistent with anatomical reports of decreased grey matter volumes and/or increased mean diffusivity in the SpV, rostral ventromedial medulla and PAG (Marciszewski et al., 2017), as well as lower fractional anisotropy in the PAG of migraineurs (DaSilva et al., 2007). It has been suggested that it is an imbalance between the regulation of antinociception by brainstem nuclei and vascular control that contributes to the development of a migraine (Bartolini et al., 2005). Given these reports and the data presented here, it is likely that the hypothalamus and PAG are involved in the transmission of incoming noxious inputs to higher brain centres directly or via their modulatory actions at the level of the SpV (Burstein et al., 2015).

Interestingly we found no perfusion changes in migraineurs in the region of the dorsomedial pons, although we have previously shown activity pattern changes in this region in the phase immediately prior to migraine. Whilst a recent case-study reported greater functional coupling between the hypothalamus and dorsomedial pons and SpV during the phase immediately prior to an attack (Schulte & May, 2016), in our previous study we found only increased coupling between the hypothalamus, PAG and thalamus during this same period. Whilst numerous studies have shown dorsomedial pons activation during a migraine attack (S.K. Afridi et al., 2005; S. K. Afridi et al., 2005; Bahra et al., 2001b; Denuelle et al., 2007; Weiller, May, Limmroth, Juptner, Kaube,

Schayck, Coenen, & Diener, 1995), our data suggests that unlike the hypothalamus, PAG and SpV, the precise nature and timing of changes in the dorsomedial pons is different which may result from an overall difference in the underlying role of this region in migraine.

In addition to decreased CBF in the brainstem and diencephalon, we found CBF decreases in the phase immediately prior to migraine in the OFC, RSC and visual cortex. In contrast to the brainstem and hypothalamus, these changes tended to occur gradually, decreasing over the interictal period as the 24-hour period before the migraine approached. Interestingly, reduced visual cortex CBF occurred in migraineurs, even though the vast majority did not experience migraine with visual aura. Whilst CBF changes in the visual cortex in migraineurs without aura has rarely been observed (Andersson et al., 1997), multiple CBF studies have reported visual cortex hypo-perfusion in migraineurs during an attack, in the interictal phase, and following migraine relief (Cheng et al., 2013; Denuelle, Fabre, Payoux, Chollet, & Geraud, 2008; Lauritzen, Olsen, Lassen, & Paulson, 1983; Levine, Welch, Ewing, Joseph, & D'Andrea, 1987; Mirza et al., 1998; Sanchez del Rio et al., 1999; Woods, Iacoboni, & Mazziotta, 1994).

Although the focus of our investigation was to determine regional blood flow changes in the phase immediately prior to a migraine, we also found significant regional CBF decreases in migraineurs during the interictal phase. These included decreases in the region of the NAc, OFC and vIPFC. Overall, studies using measures of on-going perfusion in interictal states have proven to be inconsistent. Single photon emission computed tomography and PET studies have displayed reduced CBF (Calandre et al., 2002; De Benedittis et al., 1999), increased CBF (Kassab et al., 2009), asymmetry (Levine et al., 1987; Mirza et al., 1998), or no CBF alterations (Bartolini et al., 2005) in various brain regions during the interictal state. More recently, selective CBF increases

in the primary somatosensory cortex have been reported in adult and adolescent migraineurs, findings that are contrary to that of this investigation (Youssef et al., 2017). Nevertheless, reported anterior cingulate cortex CBF decreases and our finding of CBF decreases in the OFC and NAc, appear consistent with reports of reduced grey matter volumes in these same regions in migraineurs (Jin et al., 2013; Kim et al., 2009; Kim et al., 2008; Schmidt-Wilcke, Ganssbauer, Neuner, Bogdahn, & May, 2008; Yuan et al., 2013).

In contrast to the decreases in regional CBF during the phase immediately prior to a migraine, the CBF decreases in the NAc, OFC and vIPFC appear to be relatively stable over the migraine cycle, being significantly reduced during the interictal and the phase immediately following a migraine. It is well known that the NAc is activated by noxious stimuli (Becerra & Borsook, 2008); morphine injections into the NAc increase pain thresholds (Zhou, Xuan, & Han, 1984), and NAc-prefrontal connectivity can predict an individual's chronic pain intensity (Baliki, Geha, Fields, & Apkarian, 2010). Furthermore, we have recently shown that an individual's analgesic propensity, measured by their condition pain modulation ability, is significantly correlated to changes in activity within the NAc and OFC (Youssef, Macefield, & Henderson, 2016a). Interestingly, this analgesic ability is associated with activity within the medullary subnucleus reticularis dorsalis and not the PAG-RVM-SpV pathway (Le Bars, Dickenson, & Besson, 1979; Youssef, Macefield, & Henderson, 2016b). Whilst we did not find on-going changes in the medulla during the interictal phase, it is possible that during this phase, the NAc and OFC limit the effectiveness of external triggers or the ability of resting basal firing levels within the trigeminal pathway to activate higher brain centres and to evoke head pain. Hence, only when CBF decreases in the hypothalamus, PAG and SpV immediately prior to a migraine can signals reach the cortex resulting in head pain. Of course this is speculation and further investigations exploring the role of the brain's endogenous pain

modulation circuitry over the migraine cycle is needed to confirm that such changes occur.

Whilst our results provide evidence of neural changes prior to the initiation of a migraine attack, there are a number of limitations that need to be considered. Firstly, although we utilised spatial normalization techniques that are designed specifically for the brainstem, the precise localization of clusters to specific brainstem nuclei is difficult. Indeed, whilst we are confident that the CBF changes we report encompass the areas described, they also extend to surrounding voxels which may be involving other functional nuclei. Secondly, as it is not possible to predict when an individual's next migraine will occur, it is difficult to collect MRI scans during the 24-hour period immediately prior to a migraine attack. Essentially this occurs by chance and as a consequence the group numbers for this phase are relatively low compared with other migraine phases. Although we did employ population based statistical tests that were corrected for multiple comparisons, increasing the sample size of the group immediately prior to a migraine would add veracity to the current data and our interpretation.

3.6 References

- Afridi, S. K., Giffin, N. J., Kaube, H., Friston, K. J., Ward, N. S., Frackowiak, R. S., & Goadsby, P. J. (2005). A positron emission tomographic study in spontaneous migraine. *Arch Neurol*, 62(8), 1270-1275. doi:10.1001/archneur.62.8.1270
- Afridi, S. K., Matharu, M. S., Lee, L., Kaube, H., Friston, K. J., Frackowiak, R. S., & Goadsby, P. J. (2005). A PET study exploring the laterality of brainstem activation in migraine using glyceryl trinitrate. *Brain*, 128(Pt 4), 932-939. doi:10.1093/brain/awh416
- Andersson, J. L. R., Muhr, C., Lilja, A., Valind, S., Lundberg, P. O., Långström, B., . . . Långström, B. (1997). Regional cerebral blood flow and oxygen metabolism during migraine with and without aura. *Cephalalgia*, 17(5), 570-579. doi:10.1046/j.1468-2982.1997.1705570.x
- Bahra, A., Matharu, M. S., Buchel, C., Frackowiak, R. S., & Goadsby, P. J. (2001). Brainstem activation specific to migraine headache. *Lancet*, 357(9261), 1016-1017.
- Baliki, M. N., Geha, P. Y., Fields, H. L., & Apkarian, A. V. (2010). Predicting Value of Pain and Analgesia: Nucleus Accumbens Response to Noxious Stimuli Changes in the Presence of Chronic Pain. *Neuron*, 66(1), 149-160. doi:<https://doi.org/10.1016/j.neuron.2010.03.002>
- Bartolini, M., Baruffaldi, R., Paolino, I., & Silvestrini, M. (2005). Cerebral blood flow changes in the different phases of migraine. *Funct Neurol*, 20(4), 209-211.
- Becerra, L., & Borsook, D. (2008). Signal valence in the nucleus accumbens to pain onset and offset. *Eur J Pain*, 12(7), 866-869. doi:10.1016/j.ejpain.2007.12.007
- Bednarczyk, E. M., Remler, B., Weikart, C., Nelson, A. D., & Reed, R. C. (1998). Global cerebral blood flow, blood volume, and oxygen metabolism in patients with migraine headache. *Neurology*, 50(6), 1736-1740.

- Burstein, R., Nosedá, R., & Borsook, D. (2015). Migraine: multiple processes, complex pathophysiology. *J Neurosci*, *35*(17), 6619-6629. doi:10.1523/JNEUROSCI.0373-15.2015
- Calandre, E. P., Bembibre, J., Arnedo, M. L., & Becerra, D. (2002). Cognitive disturbances and regional cerebral blood flow abnormalities in migraine patients: their relationship with the clinical manifestations of the illness. *Cephalalgia*, *22*(4), 291-302. doi:10.1046/j.1468-2982.2002.00370.x
- Cheng, M. H., Wen, S. L., Zhou, H. J., Lian-Fang, B., Li, J. F., & Xie, L. J. (2013). Evaluation of headache and regional cerebral blood flow in patients with migraine. *Clin Nucl Med*, *38*(11), 874-877. doi:10.1097/RLU.0b013e3182a75927
- DaSilva, A. F. M., Granziera, C., Tuch, D. S., Snyder, J., Vincent, M., & Hadjikhani, N. (2007). Interictal alterations of the trigeminal somatosensory pathway and PAG in migraine. *Neuroreport*, *18*(4), 301-305. doi:10.1097/WNR.0b013e32801776bb
- De Benedittis, G., Ferrari Da Passano, C., Granata, G., & Lorenzetti, A. (1999). CBF changes during headache-free periods and spontaneous/induced attacks in migraine with and without aura: a TCD and SPECT comparison study. *J Neurosurg Sci*, *43*(2), 141-146; discussion 146-147.
- Denuelle, M., Fabre, N., Payoux, P., Chollet, F., & Geraud, G. (2007). Hypothalamic activation in spontaneous migraine attacks. *Headache*, *47*(10), 1418-1426. doi:10.1111/j.1526-4610.2007.00776.x
- Denuelle, M., Fabre, N., Payoux, P., Chollet, F., & Geraud, G. (2008). Posterior Cerebral Hypoperfusion in Migraine Without Aura. *Cephalalgia*, *28*(8), 856-862. doi:10.1111/j.1468-2982.2008.01623.x

- Diedrichsen, J., Maderwald, S., Kuper, M., Thurling, M., Rabe, K., Gizewski, E. R., . . . Timmann, D. (2011). Imaging the deep cerebellar nuclei: a probabilistic atlas and normalization procedure. *Neuroimage*, *54*(3), 1786-1794.
doi:10.1016/j.neuroimage.2010.10.035
- Fields, H. L., & Heinricher, M. M. (1985). Anatomy and physiology of a nociceptive modulatory system. *Philos Trans R Soc Lond B Biol Sci*, *308*(1136), 361-374.
- Floyd, N. S., Price, J. L., Ferry, A. T., Keay, K. A., & Bandler, R. (2001). Orbitomedial prefrontal cortical projections to hypothalamus in the rat. *J Comp Neurol*, *432*(3), 307-328.
- Hendrikse, J., Petersen, E. T., & Golay, X. (2012). Vascular Disorders: Insights from Arterial Spin Labeling. *Neuroimaging Clinics of North America*, *22*(2), 259-269.
doi:<https://doi.org/10.1016/j.nic.2012.02.003>
- Hodkinson, D. J., Veggeberg, R., Wilcox, S. L., Scrivani, S., Burstein, R., Becerra, L., & Borsook, D. (2015). Primary Somatosensory Cortices Contain Altered Patterns of Regional Cerebral Blood Flow in the Interictal Phase of Migraine. *PLoS One*, *10*(9), e0137971. doi:10.1371/journal.pone.0137971
- Holstege, G., & Kuypers, H. G. (1982). The anatomy of brain stem pathways to the spinal cord in cat. A labeled amino acid tracing study. *Prog Brain Res*, *57*, 145-175.
doi:10.1016/S0079-6123(08)64128-X
- Jin, C., Yuan, K., Zhao, L., Zhao, L., Yu, D., von Deneen, K. M., . . . Tian, J. (2013). Structural and functional abnormalities in migraine patients without aura. *NMR Biomed*, *26*(1), 58-64. doi:10.1002/nbm.2819

- Kassab, M., Bakhtar, O., Wack, D., & Bednarczyk, E. (2009). Resting brain glucose uptake in headache-free migraineurs. *Headache*, *49*(1), 90-97. doi:10.1111/j.1526-4610.2008.01206.x
- Kim, J. H., Kim, S., Suh, S. I., Koh, S. B., Park, K. W., & Oh, K. (2009). Interictal metabolic changes in episodic migraine: a voxel-based FDG-PET study. *Cephalalgia*, no-no. doi:10.1111/j.1468-2982.2009.01890.x
- Kim, J. H., Suh, S. I., Seol, H. Y., Oh, K., Seo, W. K., Yu, S. W., . . . Koh, S. B. (2008). Regional grey matter changes in patients with migraine: a voxel-based morphometry study. *Cephalalgia*, *28*(6), 598-604. doi:10.1111/j.1468-2982.2008.01550.x
- Knight, Y. E., & Goadsby, P. J. (2001). The periaqueductal grey matter modulates trigeminovascular input: a role in migraine? *Neuroscience*, *106*(4), 793-800.
- Lauritzen, M., Olsen, T. S., Lassen, N. A., & Paulson, O. B. (1983). Changes in regional cerebral blood flow during the course of classic migraine attacks. *Ann Neurol*, *13*(6), 633-641. doi:10.1002/ana.410130609
- Le Bars, D., Dickenson, A. H., & Besson, J. M. (1979). Diffuse noxious inhibitory controls (DNIC). I. Effects on dorsal horn convergent neurones in the rat. *Pain*, *6*(3), 283-304.
- Levine, S. R., Welch, K. M., Ewing, J. R., Joseph, R., & D'Andrea, G. (1987). Cerebral blood flow asymmetries in headache-free migraineurs. *Stroke*, *18*(6), 1164-1165.
- Mai, J. K., Paxinos, G., & Voss, T. (2007). *Atlas of the Human Brain* (3rd ed.): Academic Press.
- Maniyar, F. H., Sprenger, T., Monteith, T., Schankin, C., & Goadsby, P. J. (2014). Brain activations in the premonitory phase of nitroglycerin-triggered migraine attacks. *Brain*, *137*(Pt 1), 232-241. doi:10.1093/brain/awt320

- Marciszewski, K. K., Meylakh, N., Di Pietro, F., Macefield, V. G., Macey, P. M., & Henderson, L. A. (2017). Altered brainstem anatomy in migraine. *Cephalalgia*, 333102417694884. doi:10.1177/0333102417694884
- Matharu, M. S., Bartsch, T., Ward, N., Frackowiak, R. S., Weiner, R., & Goadsby, P. J. (2004). Central neuromodulation in chronic migraine patients with suboccipital stimulators: a PET study. *Brain*, 127(Pt 1), 220-230. doi:10.1093/brain/awh022
- Meylakh, N., Marciszewski Kasia, K., Di Pietro, F., Macefield Vaughan, G., Macey Paul, M., & Henderson Luke, A. (2018). Deep in the brain: Changes in subcortical function immediately preceding a migraine attack. *Human Brain Mapping*, 0(0). doi:10.1002/hbm.24030
- Mirza, M., Tutus, A., Erdogan, F., Kula, M., Tomar, A., Silov, G., & Koseoglu, E. (1998). Interictal SPECT with Tc-99m HMPAO studies in migraine patients. *Acta Neurol Belg*, 98(2), 190-194.
- Morgan, M. M., Whittier, K. L., Hegarty, D. M., & Aicher, S. A. (2008). Periaqueductal gray neurons project to spinally projecting GABAergic neurons in the rostral ventromedial medulla. *Pain*, 140(2), 376-386. doi:10.1016/j.pain.2008.09.009
- Norris, J. W., Hachinski, V. C., & Cooper, P. W. (1975). Changes in cerebral blood flow during a migraine attack. *Br Med J*, 3(5985), 676-677.
- Nosedá, R., & Burstein, R. (2013). Migraine pathophysiology: anatomy of the trigeminovascular pathway and associated neurological symptoms, cortical spreading depression, sensitization, and modulation of pain. *Pain*, 154 Suppl 1, S44-53. doi:10.1016/j.pain.2013.07.021
- Paxinos, G., & Huang, X. (1995). *Atlas of the Human Brainstem* (1st ed.). San Diego: Academic Press.

- Pietrobon, D., & Moskowitz, M. A. (2013). Pathophysiology of migraine. *Annu Rev Physiol*, 75, 365-391. doi:10.1146/annurev-physiol-030212-183717
- Sanchez del Rio, M., Bakker, D., Wu, O., Agosti, R., Mitsikostas, D. D., Ostergaard, L., . . . Cutrer, F. M. (1999). Perfusion weighted imaging during migraine: spontaneous visual aura and headache. *Cephalalgia*, 19(8), 701-707. doi:10.1046/j.1468-2982.1999.019008701.x
- Schmidt-Wilcke, T., Ganssbauer, S., Neuner, T., Bogdahn, U., & May, A. (2008). Subtle grey matter changes between migraine patients and healthy controls. *Cephalalgia*, 28(1), 1-4. doi:10.1111/j.1468-2982.2007.01428.x
- Schulte, L. H., & May, A. (2016). The migraine generator revisited: continuous scanning of the migraine cycle over 30 days and three spontaneous attacks. *Brain*, 139(Pt 7), 1987-1993. doi:10.1093/brain/aww097
- Schwedt, T. J., & Dodick, D. W. (2009). Advanced neuroimaging of migraine. *Lancet Neurol*, 8(6), 560-568. doi:10.1016/s1474-4422(09)70107-3
- Wang, Z., Aguirre, G. K., Rao, H., Wang, J., Fernandez-Seara, M. A., Childress, A. R., & Detre, J. A. (2008). Empirical optimization of ASL data analysis using an ASL data processing toolbox: ASLtbx. *Magn Reson Imaging*, 26(2), 261-269. doi:10.1016/j.mri.2007.07.003
- Weiller, C., May, A., Limmroth, V., Juptner, M., Kaube, H., Schayck, R. V., . . . Diener, H. C. (1995). Brain stem activation in spontaneous human migraine attacks. *Nat Med*, 1(7), 658-660.
- Woods, R. P., Iacoboni, M., & Mazziotta, J. C. (1994). Bilateral Spreading Cerebral Hypoperfusion during Spontaneous Migraine Headache. *New England Journal of Medicine*, 331(25), 1689-1692. doi:10.1056/NEJM199412223312505

- Youssef, A. M., Ludwick, A., Wilcox, S. L., Lebel, A., Peng, K., Colon, E., . . . Borsook, D. (2017). In child and adult migraineurs the somatosensory cortex stands out ... again: An arterial spin labeling investigation. *Hum Brain Mapp*, *38*(8), 4078-4087.
doi:10.1002/hbm.23649
- Youssef, A. M., Macefield, V. G., & Henderson, L. A. (2016a). Cortical influences on brainstem circuitry responsible for conditioned pain modulation in humans. *Hum Brain Mapp*, *37*(7), 2630-2644. doi:10.1002/hbm.23199
- Youssef, A. M., Macefield, V. G., & Henderson, L. A. (2016b). Pain inhibits pain; human brainstem mechanisms. *Neuroimage*, *124*(Pt A), 54-62.
doi:10.1016/j.neuroimage.2015.08.060
- Yuan, K., Zhao, L., Cheng, P., Yu, D., Zhao, L., Dong, T., . . . Tian, J. (2013). Altered structure and resting-state functional connectivity of the basal ganglia in migraine patients without aura. *J Pain*, *14*(8), 836-844. doi:10.1016/j.jpain.2013.02.010
- Zhou, Z. F., Xuan, Y. T., & Han, J. S. (1984). [Analgesic effect of morphine injected into habenula, nucleus accumbens or amygdala of rabbits]. *Zhongguo Yao Li Xue Bao*, *5*(3), 150-153.

Figure Legends:

Figure 1: A: Significant differences in regional cerebral blood flow between controls (n=42) and migraineurs during interictal (n=17), the phase immediately prior to (n=5) and the phase immediately following a migraine attack (n=6) in a brainstem specific voxel-by-voxel analysis. Note that only during the phase immediately prior to a migraine was blood flow significantly different from controls. **B:** Brain regions in which regional cerebral blood flow was significantly decreased (cool colour scale) in migraineurs directly prior to a migraine compared with controls overlaid onto a T1-weighted brainstem template. Locations of each slice in Montreal Neurological Institute space are indicated at the top left. Note the significantly reduced blood flow in the region of the midbrain periaqueductal gray matter (PAG) and spinal trigeminal nucleus (SpV). **C:** Plots of mean (\pm SEM) blood flow in significant clusters extracted from controls and migraineurs during all three phases. There were only significant decreases in regional cerebral blood flow compared to controls in these clusters in the phase immediately prior to a migraine (* $p < 0.05$ derived from voxel-by-voxel analysis). **D:** Brain regions in which regional cerebral blood flow, with global CBF as a confound variable, was significantly decreased (cool colour scale) in migraineurs directly prior to a migraine compared with controls overlaid onto a T1-weighted brainstem template. Note the same regions as reported in B. **E:** Plots of mean (\pm SEM) blood flow in significant clusters extracted from the regional cerebral blood flow analysis with global CBF as a confound variable. There were only significant decreases in regional cerebral blood flow compared to controls in these clusters in the phase immediately prior to a migraine (* $p < 0.05$ derived from voxel-by-voxel analysis).

Figure 2A: Significant differences in regional cerebral blood flow between controls (n=50) and migraineurs during interictal (n=20), the phase immediately prior to (n=6) and the phase immediately following a migraine attack (n=10) in a wholebrain voxel-by-voxel analysis. Note

that the interictal and phase immediately prior to a migraine showed significant differences compared with controls. **B:** Brain regions in which regional cerebral blood flow was significantly decreased (cool colour scale) in migraineurs immediately prior to a migraine compared with controls overlaid onto a mean T1-weighted anatomical image set. Locations of each slice in Montreal Neurological Institute space are indicated at the top left. Note the significant blood flow reductions in the hypothalamus, orbitofrontal cortex (OFC), retrosplenial cortex (RSC) and visual cortex. **C:** Plots of mean (\pm SEM) blood flow in significant clusters extracted from controls and migraineurs during all three phases. There were only significant decreases in regional cerebral blood flow compared to controls in these clusters in the phase immediately prior to a migraine ($*p < 0.05$ derived from voxel-by-voxel analysis). **D:** Brain regions in which regional cerebral blood flow, with global CBF as a confound variable, was significantly decreased (cool colour scale) in migraineurs directly prior to a migraine compared with controls overlaid onto a T1-weighted brainstem template. Note the same regions as reported in B. **E:** Plots of mean (\pm SEM) blood flow in significant clusters extracted from the regional cerebral blood flow analysis with global CBF as a confound variable. There were only significant decreases in regional cerebral blood flow compared to controls in these clusters in the phase immediately prior to a migraine ($*p < 0.05$ derived from voxel-by-voxel analysis; $\#p < 0.05$ derived from two-sample t-test).

Figure 3: Plots of blood flow in individual migraineurs (grey circles) against days until their next migraine for six brain regions found to have decreased regional cerebral blood flow in the period immediately prior to a migraine attack. The black squares represent the mean blood flow values for the periods greater than 30 days prior, 30-12 days prior, 11-2 days prior and 1 day prior to a migraine attack. Note that in the region of the spinal trigeminal nucleus (SpV), midbrain periaqueductal gray (PAG) and hypothalamus, blood flow remained relative stable until the phase

immediately prior to a migraine attack. In contrast, blood flow in the orbitofrontal cortex (OFC), retrosplenial cortex (RSC) and visual cortex gradually decreased throughout the interictal period.

Figure 4: A: Significant differences in regional cerebral blood flow between controls (n=50) and migraineurs during interictal (n=20), the phase immediately prior to (n=6) and the phase immediately following a migraine attack (n=10) in a wholebrain voxel-by-voxel analysis. Note that the interictal and phase immediately prior to a migraine showed significant differences compared with controls. **B:** Brain regions in which regional cerebral blood flow was significantly decreased (cool colour scale) in migraineurs during the interictal phase compared with controls overlaid onto a mean T1-weighted anatomical image set. Locations of each slice in Montreal Neurological Institute space are indicated at the top left. Note the significant blood flow reductions in the orbitofrontal cortex (OFC), ventrolateral prefrontal cortex (vlPFC), putamen and nucleus accumbens (NAc). **C:** Plots of mean (\pm SEM) blood flow in significant clusters extracted from controls and migraineurs during all three phases. Note that blood flow remained relatively stable and below that of controls during all phase of migraine (* $p < 0.05$ derived from voxel-by-voxel analysis; # $p < 0.05$ derived from two-sample t-test). **D:** Brain regions in which regional cerebral blood flow, with global CBF as a confound variable, was significantly decreased (cool colour scale) in migraineurs during the interictal phase compared with controls overlaid onto a T1-weighted brainstem template. Note the same regions as reported in B. **E.** Plots of mean (\pm SEM) blood flow in significant clusters extracted from the regional cerebral blood flow analysis with global CBF as a confound variable. Note that blood flow remained relatively stable and below that of controls during all phases of migraine (* $p < 0.05$ derived from voxel-by-voxel analysis; # $p < 0.05$ derived from two-sample t-test).

Table 1. Migraine subject characteristics. B: bilateral, L: left, OCP: oral contraceptive pill; R: right; SSRI: selective serotonin reuptake inhibitor

<i>Subject</i>	<i>Age</i>	<i>Sex</i>	<i>Years suffering</i>	<i>Pain side</i>	<i>Aura</i>	<i>Migraine/month</i>	<i>Intensity (0-5)</i>	<i>Medication taken during migraine</i>	<i>Daily Medication</i>
1	53	M	15	B	N	15 (chronic)	3	ibuprofen, paracetamol	-
2	24	F	20	B	N	4	4	ibuprofen, paracetamol	OCP, budesonide /formoterol
3	26	F	12	R	N	2	3-4	ibuprofen	OCP
4	27	F	12	R	Y	1	4	ibuprofen	OCP
5	23	F	4	R	N	4	4	triptan	OCP, metformin hydrochloride
6	25	F	12	L	N	5	3	aspirin, rizatriptan	desvenlafaxine
7	21	F	1.5	L	N	4	3	ibuprofen, paracetamol, codeine	OCP
8	26	F	1	L	N	3	5	paracetamol	OCP
9	26	F	5	R	N	1	2	aspirin, codeine, ibuprofen	OCP
10	32	F	22	L	N	12	5	paracetamol	-
11	31	F	20	B	N	4	5	panadeine forte, mersyndol	-
12	23	F	6	R	N	1	3-4	ibuprofen	OCP
13	23	F	10	B	N	0.5-1	4	ibuprofen, codeine	OCP
14	46	F	15-20	B	N	1	3	sumatriptan	-
15	41	F	40	B	N	2	4	sumatriptan	-
16	26	M	15	B	N	8	3	TCE, panadeine	-
17	23	M	3-4	B	N	0.5-1	3.5	paracetamol, codeine	-
18	27	F	16	R	Y	1	3-4	SSRI, opiates, muscle-relaxants	SSRI, OCP
19	23	M	4-5	B	N	0.5 - 1	4	paracetamol	-
20	55	F	40	R	N	0.5 - 1	3-4	sumatriptan	telmisartan
21	26	M	20	R	N	0.5-1	4	metamizole	carbamazepine
22	49	F	30	B	N	0.5-1	5	rizatriptan, paracetamol	-
23	51	F	50	L	Y	2	3-4	panadeine	-
24	34	F	15	L	Y	2	3	paracetamol, ibuprofen	-
25	26	F	5	B	Y	1	3	paracetamol	OCP
26	25	F	7-8	L	N	5-8	3	<u>rizatriptan</u> <u>benzoate</u>	OCP
27	25	M	6	L	N	0.5-1	4	panadeine forte	-
28	19	F	4-5	B	N	3-4	3	lexapro	OCP
29	25	M	12	L	N	2	4	paracetamol	Ciprimal
30	27	M	7	B	N	1	3	paracetamol, codeine, maxalt/rizatriptan	-

Table 2. Montreal Neurological Institute (MNI) coordinates, cluster size and t-score for regions in which on-going blood flow were significantly different between controls and migraineurs.

Brain region	MNI Co-ordinate			cluster size	t-score
	x	y	z		
<i>Controls greater migraineurs during immediately prior to a migraine phase</i>					
<u>Brainstem analysis</u>					
left spinal trigeminal nucleus	6	-44	-53	28	4.36
right midbrain periaqueductal gray matter	-6	-32	-3	23	4.62
<u>Wholebrain analysis</u>					
right hypothalamus	12	-6	-10	105	3.91
retrosplenial cortex	8	-46	-4	52	4.11
right orbitofrontal cortex	28	36	-11	28	3.35
left visual cortex	-12	-98	-19	183	4.33
<i>Controls greater migraineurs during interictal phase</i>					
<u>Wholebrain analysis</u>					
left nucleus accumbens	-12	4	-16	30	4.11
left putamen	-22	-2	4	58	4.13
left anterior insula	-34	30	8	17	4.17
left ventrolateral prefrontal cortex	-42	32	-10	14	3.87
right ventrolateral prefrontal cortex	40	26	-10	54	4.43
right orbitofrontal cortex	24	14	-22	60	4.97

Figure 1:

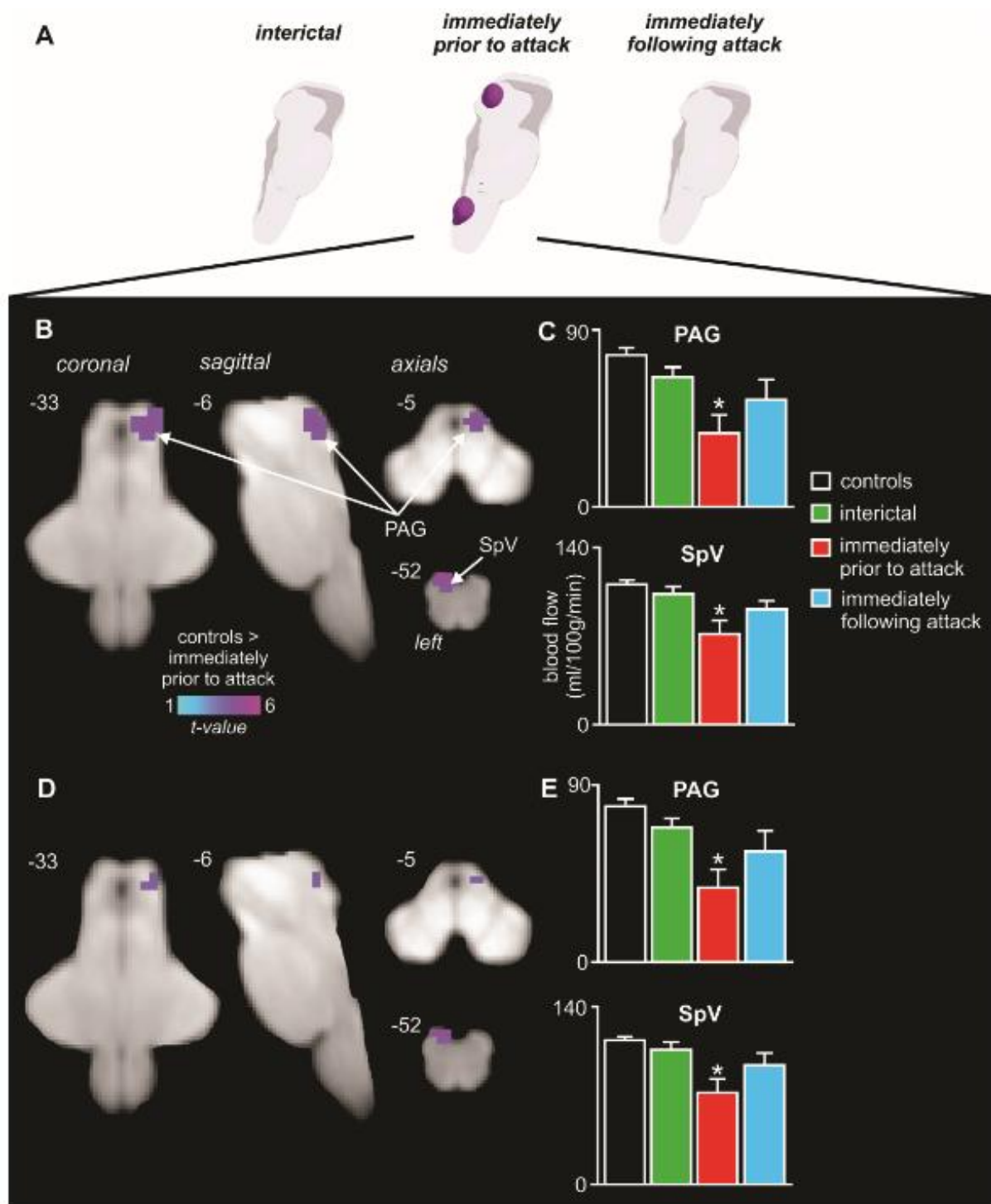
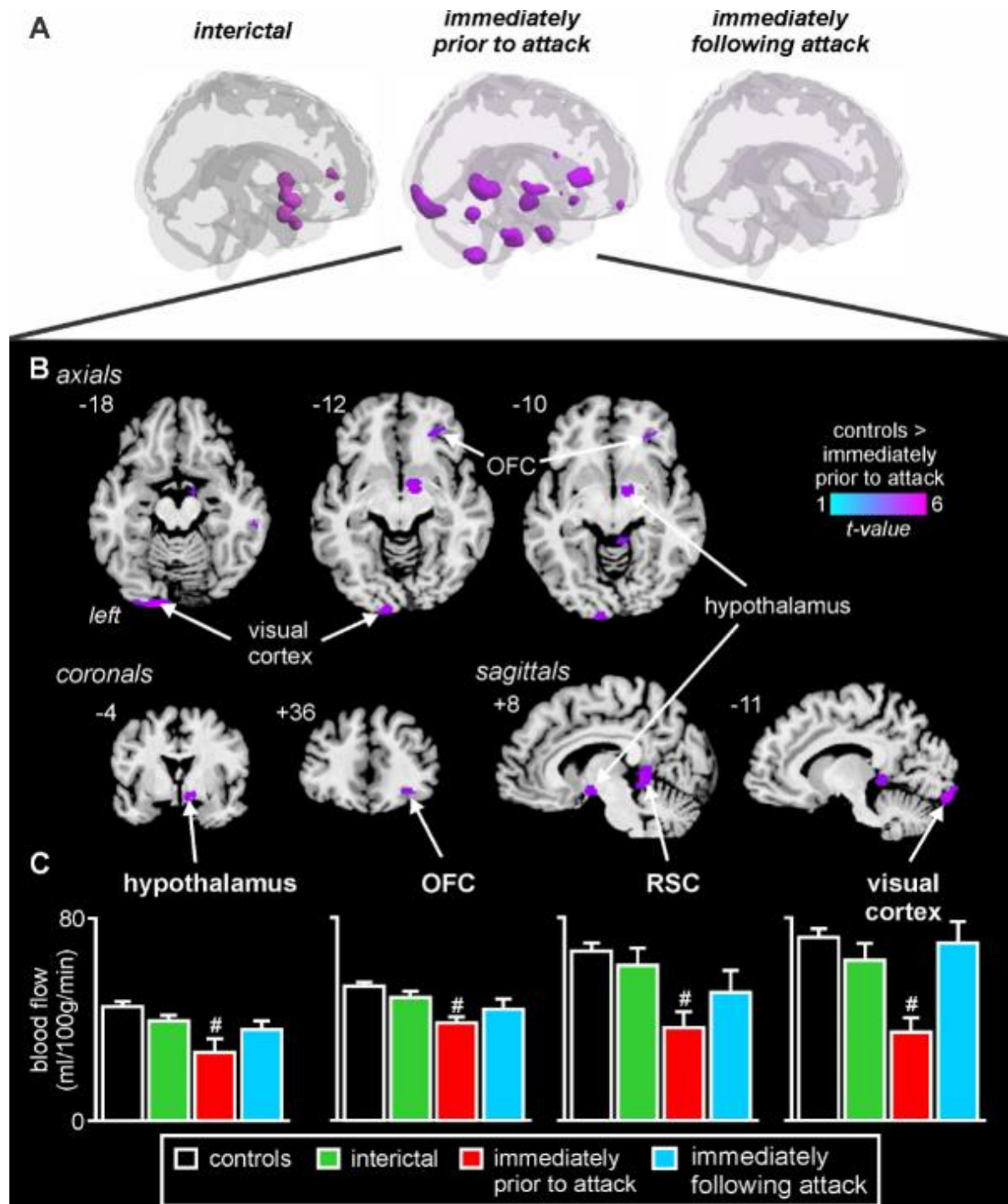


Figure 2:



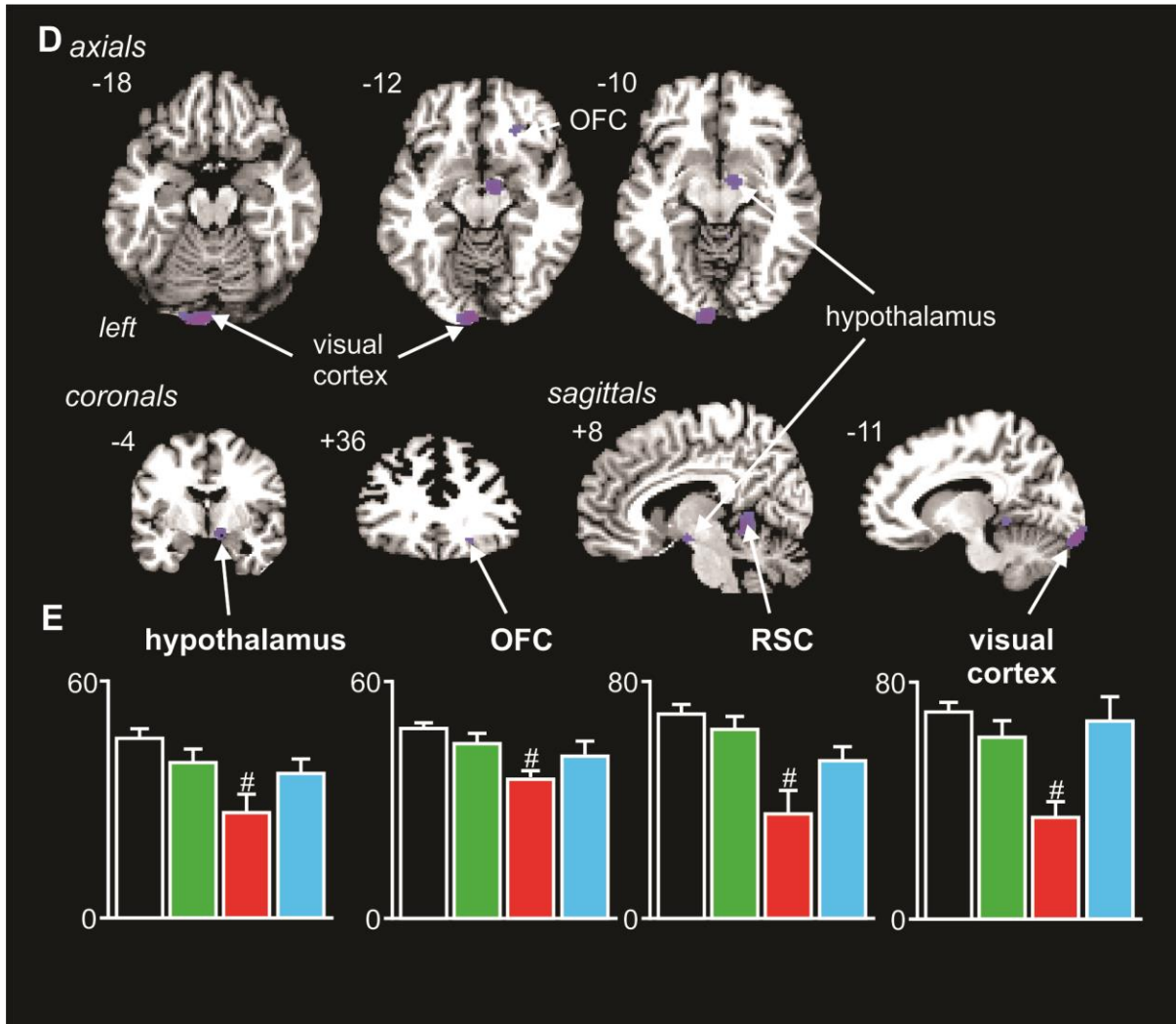


Figure 3:

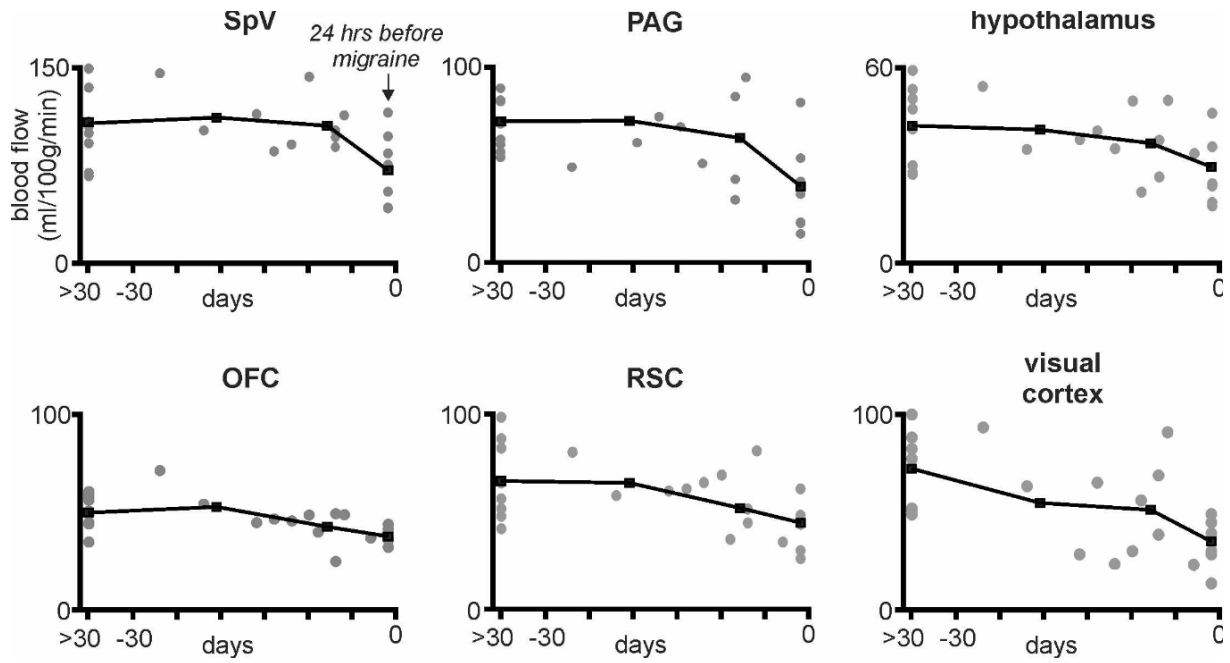
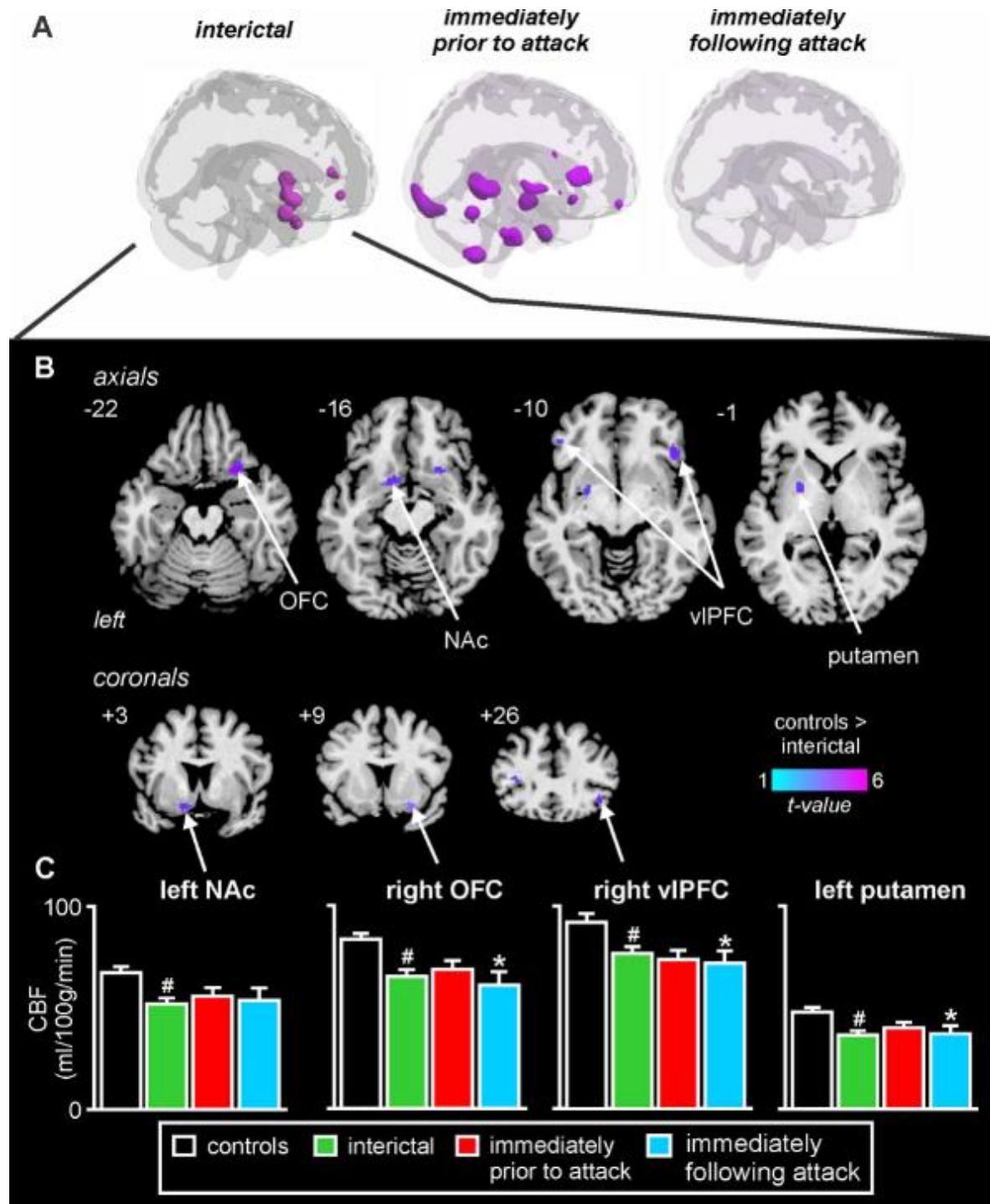
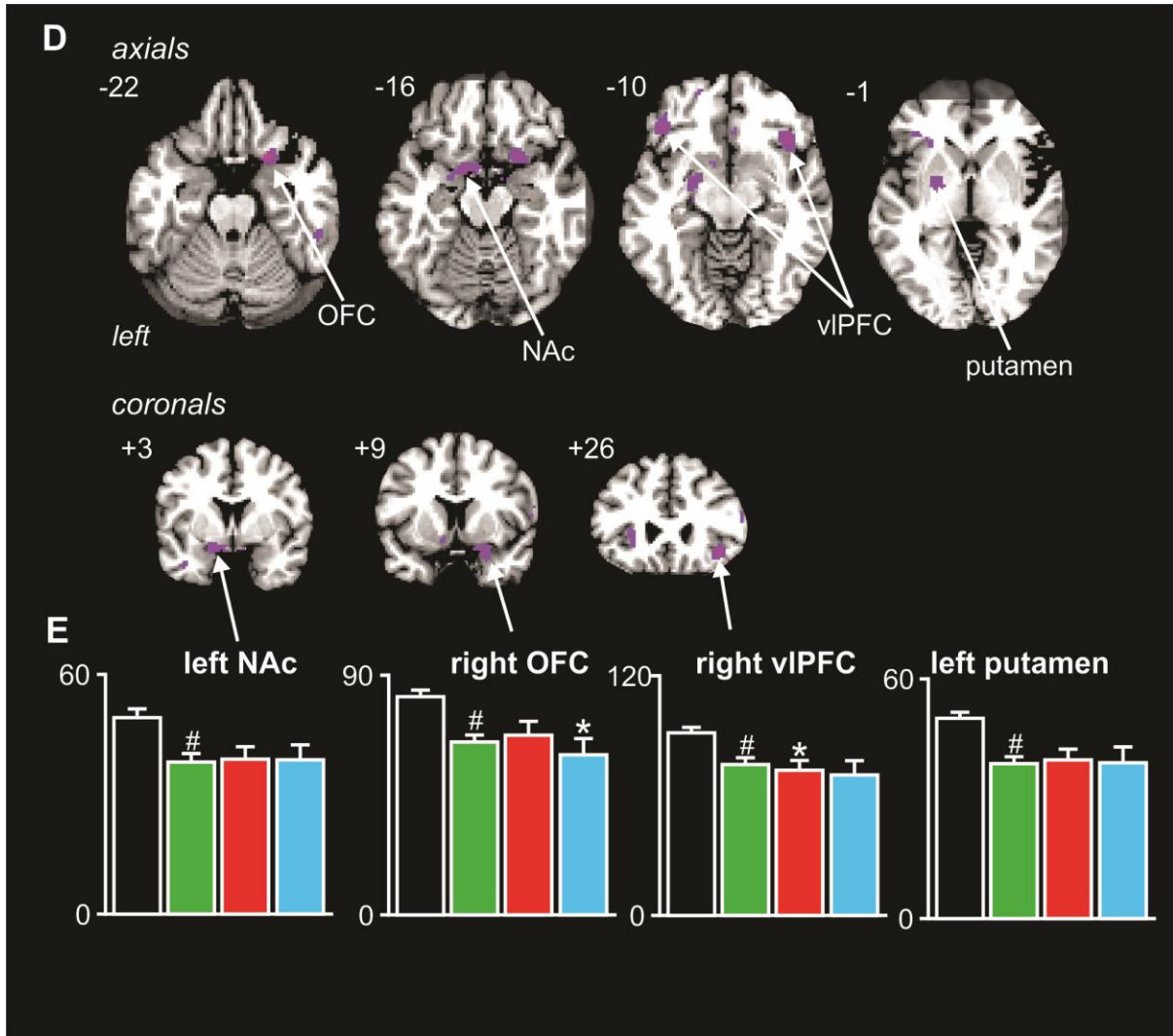


Figure 4:





Chapter 4

**Brainstem functional oscillations across the migraine cycle:
a longitudinal study**

Brainstem functional oscillations across the migraine cycle: a longitudinal investigation

Noemi Meylakh¹, Kasia K. Marciszewski¹, Flavia Di Pietro¹, Vaughan G. Macefield², Paul M. Macey³ and Luke A. Henderson¹

¹Department of Anatomy and Histology, University of Sydney, Sydney, NSW, Australia, 2006; ²School of Medicine, Western Sydney University, Sydney, Australia; ³UCLA School of Nursing and Brain Research Institute, University of California, Los Angeles, California 90095, United States.

Corresponding author: Luke A. Henderson, S513 Anderson Stuart Building F13, Department of Anatomy and Histology, University of Sydney, Australia. lukeh@anatomy.usyd.edu.au (email); +612 9351 7063 (Tel) +612 9351 6556 (Fax).

Abstract

Although the mechanisms responsible for the initiation of a migraine remain unknown, recent evidence from cross-sectional studies shows that brain function is different in people immediately prior to a migraine. This is consistent with the idea that altered brain function, particularly in brainstem sites, may either trigger a migraine itself or facilitate a peripheral trigger that activates the brain, resulting in head pain. It is impossible to predict when a migraine will occur, so few studies have explored brain activity changes in the critical 24-hour period preceding a migraine. To address this shortcoming, we performed resting state functional magnetic resonance imaging in three migraineurs and five controls each weekday for four weeks. Focussing on the brainstem, we found that although resting activity variability was similar in controls and migraineurs during the interictal period, brainstem variability increased dramatically during the 24-hour period immediately prior to a migraine. This increase in resting variability occurred in specific areas within the brainstem in which orofacial afferents terminate: the spinal trigeminal nucleus and dorsal pons. These increases in regional brainstem variability in this specific 24-hour period immediately prior to a migraine were characterized by increased power at infra-slow frequencies, principally between 0.03-0.06Hz. Furthermore, these power increases immediately before a migraine were associated with increased regional homogeneity, a measure of local signal coherence. These results show within-individual alterations in brain activity immediately prior to migraine onset, and support the hypothesis that altered regional brainstem function immediately before a migraine attack is involved in the underlying neurobiology of migraine.

Keywords: resting state fMRI, spinal trigeminal nucleus, dorsal pons, infra-slow oscillations, astrocytes.

4.2 Introduction

The pathophysiology of migraine has been hotly debated for years as either originating from vascular and/or centrally-driven mechanisms. The most prevalent hypothesis for the initiation of a migraine attack centres around the idea that sensitization of meningeal nociceptors leads to activation of trigeminovascular neurons that enter the central nervous system and evoke debilitating head pain (Bernstein & Burstein, 2012; Borsook & Burstein, 2012). More recently, an alternative idea of a “central generator” has been proposed, which posits that changes within the central nervous system initiate migraine attacks, even though the idea that a peripheral cerebrovascular trigger is not necessary for migraine initiation has been vigorously debated (Borsook & Burstein, 2012). Indeed, it has been suggested that cerebrovascular inputs may only trigger a migraine if the brain, in particular brainstem regions involved in mediating head pain, are in a sensitive state (Burstein et al., 2015). That is, the brainstem oscillates between a state where incoming cerebrovascular inputs can evoke head pain to a state where the same inputs are prevented from travelling to the cortex and evoking head pain.

Consistent with this brainstem oscillation theory, we recently explored the notion of cyclic changes throughout the migraine cycle in a series of cross-sectional studies. We found that during the 24-hour period immediately before a migraine attack, changes occur in both the pattern of resting activity (increased resting infra-slow oscillations) and the level of resting activity (decreased resting cerebral blood flow) in regions of the trigeminal pain pathway, including the spinal trigeminal nucleus (SpV), midbrain periaqueductal gray matter (PAG), dorsal pons and hypothalamus (Meylakh et al., 2018). Furthermore, during this 24-hour period there is an increased coupling strength between activity in the PAG and the hypothalamus. Interestingly, these same

brainstem regions have been shown to be activated during a migraine itself (S.K. Afridi et al., 2005; Bahra et al., 2001b; Denuelle et al., 2007; Matharu et al., 2004), raising the prospect that the changes in activity within the trigeminal pain pathway immediately prior to a migraine are precursors to subsequent activity increases and the development of migraine head pain.

Whilst we have shown functional changes in the brainstem in the period immediately prior to a migraine in cross-sectional studies, it remains unknown if these changes also occur in an individual subject over a full migraine cycle. Though there are obvious logistical difficulties in exploring brain function in an individual subject over weeks, given the individual variability in migraine attack occurrence, direct evidence of within-person alterations prior to migraine onset would strengthen the evidence of a precursor state. The aim of this longitudinal investigation is therefore to determine if brainstem function oscillates over a migraine cycle in individual subjects. We hypothesise that, consistent with our cross-sectional results, the pattern of resting signal intensity characterized by increased resting activity variability and infra-slow oscillations will occur in the ascending trigeminal pathway immediately prior to a migraine attack.

4.3 Methods

4.3.1 Subjects

Three subjects with migraine (2 females, ages 21 and 26; 1 male, age 25) and five pain-free controls (3 females; mean age 30.4 ± 4.2 years [\pm SEM]) were recruited for the study from the general population using an advertisement. There were no statistically significant differences in age (t-test, $p > 0.05$) or sex (*chi-squared* test, $p > 0.05$) between the two subject groups. Migraine subjects were diagnosed according to the IHS Classification ICHD-3 BETA criteria and none of

the migraine subjects reported an aura associated with their migraine attacks. Migraine subject characteristics, including medication use are shown in Table 1. All three migraineurs had episodic migraine. All subjects were scanned daily, from Monday to Friday over four weeks for a total of 20 scanning sessions each. The three migraineurs were scanned during three migraine periods: (i) interictal, at least 72 hours after and 24 hours prior to a migraine attack; (ii) immediately (within 24 hours) prior to an attack; (iii) immediately (within 72 hours) following an attack. Subject 1 was scanned a total of 20 times; 15 interictal periods, 1 immediately prior to an attack and 3 immediately following an attack. The last session was excluded due to image acquisition issues. Subject 2 was scanned during 12 interictal periods, 2 immediately prior to an attack and 4 immediately following an attack. The last session was also excluded due to image acquisition issues. Subject 3 was scanned during 14 interictal periods, 1 immediately prior to an attack and 2 immediately following an attack. Three sessions were excluded due to image acquisition difficulties.

Exclusion criteria for controls were the presence of any pain condition including family history of migraines, current use of analgesics, or any neurological disorder. Exclusion criteria for migraineurs were any other pain condition or neurological disorder. No migraineur was excluded based on their medication use and no migraine or control subject had an incidental neurological finding. All migraineurs indicated the intensity (6-point visual analogue scale; 0=no pain, 5=most intense imaginable pain) and drew the facial distribution of pain commonly experienced during a migraine attack. In addition, each subject described the qualities of their migraines and indicated any current treatments used to prevent or abort a migraine once started. Informed written consent was obtained for all procedures according to the Declaration of Helsinki and the local Institutional Human Research Ethics Committees approved the study.

4.3.2 MRI Acquisition

Subjects lay supine on the bed of a 3 Tesla magnetic resonance imaging (MRI) scanner (Philips, Achieva) with their head immobilized in a 32-channel transmit-receive head coil. Scans were acquired five days a week (Monday-Friday) for four weeks. For the first scan only, with each subject relaxed and at rest, a high-resolution 3D T1-weighted anatomical image set, covering the entire brain, was collected (turbo field echo; field of view=250x250mm, matrix size=288x288, slice thickness=0.87mm, repetition time=5600ms; echo time=2.5ms, flip angle=8°). Following this, during the first scanning session, and on every consecutive scan, a series of 180 gradient echo echo-planar functional MRI image volumes using blood oxygen level dependent (BOLD) contrast were collected. Each image volume contained 35 axial slices covering the entire brain (field of view = 240x240mm, matrix size = 80x78, slice thickness = 4mm, repetition time = 2,000ms; echo time = 30ms, flip angle = 90°).

4.3.3 MRI processing and statistical analysis

4.3.3.1 Image preprocessing

Using Statistical Parametric Mapping version 12 (SPM12) (Friston et al., 1995) and custom Matlab software, all functional MRI (fMRI) images were realigned and effects of movement modelled and removed from the resting signal intensity of each voxel. In no subject's scan was there significant movement (>0.5mm in any direction) and all sessions were used for the subsequent analysis. Images were then processed using the Dynamic Retrospective Filtering algorithm (Särkkä et al., 2012), a Bayesian method for physiological noise correction to reduce the potential effects of physiological noise on results. A cardiac frequency band of 60-120 beats per minute (+1

harmonic) and a respiratory frequency band of 8-25 breaths per minute (+1 harmonic) were removed. Global signal intensity changes were removed using the method described by Macey and colleagues (Macey, Macey, Kumar, & Harper, 2004), and the images were then co-registered to each individual's T1-weighted anatomical image set. Using brainstem-specific isolation software (SUIT toolbox) (Diedrichsen, 2006b), a mask of the brainstem was created on the T1-weighted anatomical image set and each of the subject's fMRI image sets. Using these masks, the brainstem of the T1 and each of the fMRI image sets were isolated and then spatially normalised to a brainstem-specific template in Montreal Neurological Institute (MNI) space. In all analyses, the anatomical locations of significant clusters were confirmed using the Atlas of the Human Brain (Mai et al., 2007) and the Atlas of the Human Brainstem (G. Paxinos & X. Huang, 1995).

4.3.3.2 Resting brainstem variability:

To assess resting variability of each fMRI scan, a brainstem map of resting signal variation as measured by the standard deviation was created for each daily fMRI scan in each migraineur and control subject. These signal variability maps were smoothed using a 3mm full-width-half-maximum (FWHM) Gaussian filter and the three migraineurs' image sets were then placed into a voxel-by-voxel fixed effects analysis. Using a boxcar model design where days immediately prior to a migraine were set to "1" and all other days "0", significant increases and decreases in variability were determined across all three migraineurs ($p < 0.05$, false discovery rate (FDR) corrected, minimum 5 contiguous voxels). For each significant cluster, the variability was extracted for each session in each control and migraineur, the average (\pm SEM) variability calculated and plotted for controls and migraineurs during the interictal, immediately prior to migraine and immediately following migraine days.

The signal variability of the entire brainstem was also determined and plotted for each session in each control and migraineur subject. In addition, for each significant cluster, power spectra were calculated from the resting state signals, and the interictal period was subtracted from power immediately prior to migraine in all three migraineurs. The resulting plot of power difference revealed, as we have previously shown, areas such as the SpV and dorsal pons displaying greater power in the 0.03-0.06Hz frequency band during the period immediately prior to a migraine compared with the interictal period. To ensure that any variability difference during the period immediately prior to a migraine was not due to differences in head movement, we measured the variability as standard deviation of each migraine and control subject, and 6 movement parameters were created during the realignment preprocessing step (x, y, z, yaw, roll, tilt). Significant differences between controls and each migraine period (2 sample t-tests, $p < 0.05$) and between migraine periods (paired t-tests, $p < 0.05$) were then determined.

4.3.3.3 Resting infra-slow (0.03-0.06Hz) oscillation power

Using the DPARSFA toolbox, raw infra-slow oscillation (ISO) power between 0.03 and 0.06Hz was calculated for each brainstem voxel for each session of each migraineur and control subject. The resulting ISO power maps were smoothed using a 3mm FWHM Gaussian filter and the three migraineurs' image sets were placed into a voxel-by-voxel fixed effects analysis. Using a boxcar model design identical to that described above, significant increases and decreases in power were determined across all three migraineurs ($p < 0.001$, minimum 5 contiguous voxels). For each significant cluster, power values were extracted for each session in each control and migraineur, and the average (\pm SEM) power was calculated and plotted for controls and migraineurs during the interictal, immediately prior to migraine and immediately following migraine days. In addition,

for each significant cluster, power spectra were calculated from the resting state signals during the interictal and immediately prior to migraine periods in all three migraineurs. The power spectra from these clusters were then plotted.

4.3.3.4 Regional homogeneity

To assess local signal covariation, we assessed regional homogeneity, i.e., the similarity of time series within each voxel and its 19 nearest neighbours were measured by calculating Kendall's coefficient of concordance. The resulting brainstem maps were smoothed using a 3mm FWHM Gaussian filter and the three migraineurs' image sets were placed into a voxel-by-voxel fixed effects analysis. Using a boxcar model design identical to that described above, significant increases and decreases in homogeneity were determined across all three migraineurs ($p < 0.001$, minimum 5 contiguous voxels). For each significant cluster, regional homogeneity values were extracted for each session in each control and migraineur, and the average (\pm SEM) homogeneity calculated and plotted for controls and migraineurs during the interictal, immediately prior to migraine and immediately following migraine days. The overlap between changes in ISO and regional homogeneity was also determined. Regional homogeneity and ISO values were extracted from each of these clusters in each migraineur and plotted and significant linear relationships determined (Pearson correlation $p < 0.05$).

4.4 Results

All three migraineurs had at least one migraine attack during the four week scanning period, although none were being scanned at the time of the migraine itself. Analysis of brainstem resting

activity variability revealed significantly increased standard deviation of the resting signal specifically during the 24-hour period immediately prior to a migraine in a number of brainstem pain processing regions (Figure 1A, Table 2). These regions included the left SpV (mean±SEM variability: controls: 30.6±4.6; interictal: 29.2±7.8; immediately prior to migraine 67.6±48.4; immediately following migraine 32.8±7.3), right SpV (controls: 21.1±1.0; interictal: 20.7±2.3; immediately prior to migraine 46.4±29.3; immediately following migraine 20.2±2.5), left dorsolateral pons (dlPons) (controls: 11.6±0.3; interictal: 13.8±1.6; immediately prior to migraine 23.4±7.2; immediately following migraine 12.8±1.3), right dlPons (controls: 16.5±0.6; interictal: 16.2±1.5; immediately prior to migraine 31.0±19.2; immediately following migraine 15.9±2.0) left substantia nigra (SN) (controls: 13.0±1.4; interictal: 8.3±1.8; immediately prior to migraine 15.5±11.4; immediately following migraine 7.8±1.6) and PAG (controls: 15.8±1.4; interictal: 15.0±0.9; immediately prior to migraine 24.8±12.1; immediately following migraine 16.6±1.5). In no region was variability significantly reduced during the period immediately prior to a migraine.

Plots of individual subjects' total brainstem variability revealed that the day-to-day variability of resting brainstem signal intensity was relatively consistent between controls and migraineurs (Figure 1B). However, in each migraineur there was a large increase in total brainstem variability on one or two days, which were, as evidenced by the results above, only on those days immediately prior to a migraine. In accordance with our previous cross-sectional studies, plots of the power differences in significantly different clusters between the immediately prior to migraine and interictal periods revealed a consistent increase in power between 0.03-0.06Hz in the left and right SpV and the left and right dlPons (Figure 1C). These variability differences were not related to head movement since we found no significant difference between the variability of x, y, z, yaw, roll or tilt movement parameters between controls and any migraine period, or between any of the

migraine periods (all $p > 0.05$).

A targeted voxel-by-voxel analysis of ISO power (0.03-0.06Hz) revealed a similar pattern of difference (Figure 2, Table 2). Increased ISO power occurred in numerous brainstem regions immediately prior to a migraine, including the right SpV (mean \pm SEM 0.03-0.06Hz power: controls: 3.72 ± 0.13 ; interictal: 3.71 ± 0.13 ; immediately prior to migraine 5.00 ± 0.81 ; immediately following migraine 3.89 ± 0.18) left dlPons (controls: 2.82 ± 0.03 ; interictal: 3.33 ± 0.37 ; immediately prior to migraine 4.43 ± 0.50 ; immediately following migraine 3.25 ± 0.33), right dlPons/dorsomedial pons (controls: 2.69 ± 0.04 ; interictal: 3.19 ± 0.51 ; immediately prior to migraine 4.15 ± 0.89 ; immediately following migraine 3.10 ± 0.42) and the left SN (controls: 2.76 ± 0.04 ; interictal: 2.51 ± 0.06 ; immediately prior to migraine 3.21 ± 0.64 ; immediately following migraine 2.41 ± 0.12). The PAG did not display any significant difference at this restricted frequency band. Notably, in no region was ISO power significantly reduced in the period immediately prior to a migraine. Plots of individual power spectra revealed a consistent power increase in low infra-slow frequencies immediately prior to a migraine compared with the interictal period (Figure 3). In particular, this power increase occurred at frequencies between 0.03-0.06Hz in the SpV and dlPons in all three migraineurs. In two of the migraineurs (subjects M1 and M3) these power increases appeared to peak at regular frequency intervals; for subject M3 these peaks occurred in the SpV with remarkable regularity at approximately 0.025Hz apart. In addition, plots of ISO power in each migraineur during the 20 day scanning period revealed that power consistently increased immediately prior to a migraine in the SpV and dlPons (Figure 4).

Finally, an analysis of regional homogeneity revealed that immediately prior to a migraine, significant increases occurred in most the same brainstem regions in which there were increases

in variability and infra-slow oscillations (Figure 5). That is, increases occurred in the region of the right SpV (mean \pm SEM regional homogeneity: controls: 1.78 \pm 0.03; interictal: 1.87 \pm 0.10; immediately prior to migraine 2.50 \pm 0.41; immediately following migraine 1.91 \pm 0.15), right dl/dmPons (controls: 2.64 \pm 0.03; interictal: 2.91 \pm 0.07; immediately prior to migraine 3.49 \pm 0.15; immediately following migraine 2.84 \pm 0.03) and the left SN (controls: 2.19 \pm 0.09; interictal: 2.32 \pm 0.16; immediately prior to migraine 2.71 \pm 0.06; immediately following migraine 2.34 \pm 0.20). In no region was regional homogeneity significantly reduced in the period immediately prior to a migraine. Finally, we assessed whether there were brainstem areas that displayed increases in both regional homogeneity and ISO and three regions emerged: the right SpV, right dl/dmPons and the left SN. Interestingly, in all three migraineurs, there were significant positive relationships between regional homogeneity and ISO in the right SpV (subject M1: $r=0.56$ $p=0.01$; subject M2: $r=0.80$ $p<0.001$; subject M3: $r=0.76$ $p<0.001$) and right dl/dmPons (subject M1: $r=0.60$ $p=0.006$; subject M2: $r=0.87$ $p<0.001$; subject M3: $r=0.66$ $p=0.003$) but not the left SN (subject M1: $r=-0.07$ $p=0.76$; subject M2: $r=-0.17$ $p=0.48$; subject M3: $r=0.10$ $p=0.71$).

4.5 Discussion

Our findings show that individual migraineurs' brainstem function alters through the migraine cycle. In particular, we found significantly greater variability in resting activity in the 24-hour period immediately prior to a migraine attack in brainstem regions that process head pain and that have been shown to be activated during a migraine itself. This increase in resting state variability is characterized by increased power at infra-slow frequency ranges and is associated with increased regional homogeneity, a marker of local signal coherence. This local signal coherence represents the synchronicity between the time series of a given voxel and its nearest neighbours (Zang, Jiang,

Lu, He, & Tian, 2004) and is representative of a neural circuitry. Since these changes occur immediately prior to a migraine and whilst the individual is *not* in pain, we suggest they are consistent with the idea that brainstem function alters over the migraine cycle. These brainstem functional changes can then lead to a migraine directly or by facilitating an incoming cerebrovascular trigger to activate higher brain centres resulting in head pain.

Whilst numerous studies have reported that activity increases in areas of the brainstem, including the dorsal pons, during migraine attacks (S.K. Afridi et al., 2005; S. K. Afridi et al., 2005; Denuelle et al., 2007; Weiller, May, Limmroth, Juptner, Kaube, Schayck, Coenen, & Diener, 1995), few studies have investigated whether functional changes occur in the brainstem immediately prior to a migraine. Of course exploring function prior to a migraine is extremely difficult since it is not possible to predict when a migraine will occur. Whilst the hypothesis that a cerebrovascular trigger is required to initiate a migraine attack has been circulating for many decades (Borsook & Burstein, 2012; Burstein et al., 2015; Burstein, Strassman, & Moskowitz, 2012), more recently it has been proposed that migraine results from dysfunction in subcortical sites which results in the perception of pain from “basal levels of primary traffic” (Goadsby & Akerman, 2012). Others have suggested that brainstem function oscillates and only when the brainstem is in a receptive state can an incoming trigger activate central pathways and evoke head pain (Borsook & Burstein, 2012).

Our findings show that brainstem function alters within a given individual throughout the migraine cycle, specifically in the SpV, the precise region where trigeminovascular afferents terminate, as well as in the dorsolateral/medial pons, an area shown to be activated during a migraine attack. Strikingly, in these two brainstem regions, the variability of resting signal fluctuations immediately prior to a migraine dramatically increased during the 24-hour period prior to a migraine before

returning to controls' levels during the interictal period. Indeed, overall brainstem variability in migraineurs is remarkably similar to that in controls with respect to day-to-day fluctuations; however only in migraineurs did dramatic increases occur, and they occurred just before a migraine. Importantly, during the period of increased variability, subjects were *not* experiencing head pain, and reported feeling no different from other interictal days. Whilst immediately before a migraine some individuals report fatigue, dizziness and reduced concentration (Giffin et al., 2003), our subjects did not report such changes and the changes in brainstem variability that occurred during this period were not associated with differences in head movements. This supports that the altered resting activity may be a centrally initiated phenomenon.

The increased variability during the 24-hour period immediately preceding a migraine is characterized by increased power at infra-slow frequency ranges and included the frequency band 0.03-0.06Hz. In addition to previously showing increases in 0.03-0.06Hz power in migraineurs immediately before a migraine in cross-sectional studies (N. Meylakh et al., 2018), we have also shown that individuals with chronic trigeminal neuropathic pain display increases in resting 0.03-0.06Hz oscillations in the trigeminal pain pathway including in the SpV (Alshelh et al., 2016). We have previously hypothesised that increased ISOs at frequencies between 0.03-0.06 Hz may reflect increased modulatory activity on local neurons by increased cyclic gliotransmitter release (Halassa, Fellin, & Haydon, 2007; Parri & Crunelli, 2001). Astrocytes display calcium wave oscillations at infra-slow frequency ranges similar to those seen here in migraineurs immediately prior to a migraine and these infra-slow astrocyte calcium waves can propagate among surrounding astrocytes (Crunelli et al., 2002). Indeed, it has been suggested that, in pathological situations, greater numbers of astrocytes may display enhanced calcium wave synchrony, amplitude and NMDA-receptor function (Halassa et al., 2007; Parri & Crunelli, 2001). Furthermore, increased

infra-slow oscillations are associated with paroxysmal events and coupled to high frequency power fluctuations in the cortex (Hughes, Lorincz, Parri, & Crunelli, 2011; Mantini, Perrucci, Del Gratta, Romani, & Corbetta, 2007; Vanhatalo et al., 2004).

Consistent with the idea that astrocytes may modulate neural activity immediately prior to a migraine is our finding of increased regional homogeneity in the same period of the migraine cycle. We found a significant positive relationship between regional homogeneity and infra-slow oscillation power in the SpV and dorsal pons assessed over the entire scanning period. Regional homogeneity evaluates the similarity or synchronization between the time series of a given voxel and its nearest neighbours (Zang et al., 2004). Whilst there is no evidence of a direct relationship between regional homogeneity and astrocytic gliotransmission, the idea that astrocyte activation results in greater and strong synchronicity between astrocytes and thus neighbouring synapses, is consistent with such a positive relationship. Indeed, it has been proposed that calcium oscillation in astrocytes contributes to the propagation of cortical spreading depression (Nedergaard, Cooper, & Goldman, 1995) and evidence from a genetic form of migraine, Familial Hemiplegic Migraine, also points to a critical role of astrocytes in migraine (Benarroch, 2005).

Importantly, we found that overall brainstem variability was similar in migraineurs during the interictal period as that of controls, suggesting that migraineurs do not simply have increased signal variability but rather that variability is *specifically altered immediately prior to a migraine attack*. One plausible theory is that altered astrocyte modulation of neural activity within the brainstem drastically changes function which then either triggers a migraine itself or provides a permissive brainstem state so that an external cerebrovascular trigger can activate higher brain centres and initiate a migraine attack. Interestingly, we recently found that in the 24-hour period before a

migraine, the perceived intensity of acute noxious orofacial stimuli are diminished, which appears contrary to the idea that immediately prior to a migraine the brainstem becomes more permissive to incoming orofacial stimuli (K. K. Marciszewski, N. Meylakh, F. Di Pietro, E. P. Mills, et al., 2018).

Whilst this is the first study to explore resting signal fluctuations in the brainstem over the migraine cycle in individual subjects, a previous study explored functional activity in one migraineur over the course of 30 days. Schulte and May (Schulte & May, 2016) reported that during the period immediately prior to a migraine, greater functional coupling occurred between the hypothalamus and SpV, whilst during a migraine attack, greater functional coupling occurred between the hypothalamus and dorsal rostral pons. While we did not explore hypothalamic function in the current study, these coupling changes are consistent with our data in that brainstem function changes in the period immediately prior to a migraine. If, for example, such functional changes are related to altered astrocyte modulation of local neural function, it may be possible to prevent a migraine from occurring by preventing such astrocyte changes.

Given the consistency between the results of this longitudinal study and our previous cross-sectional studies we are confident that our findings are robust. However, there are several important limitations to note. Firstly, since we focussed on the brainstem we have not provided any insight into diencephalic or higher cortical areas in this present study, though we are aware of the importance of these regions in migraine. Secondly, despite using spatial normalization techniques designed specifically for the brainstem, given the relatively low spatial resolution of resting state fMRI and the intricate parcellation of the brainstem, some clusters likely encompass multiple brainstem regions. Thirdly, due to the difficulty of recruiting patients with the availability

or willingness to perform multiple MRI sessions we were only able to recruit three migraineurs and five controls. Nevertheless, the large number of repeated measures per subject, together with the corroboration by our previous cross-sectional studies, helps ensure the findings are robust.

The findings of this study clearly show that resting brainstem function fluctuates over the migraine cycle in a given individual, with functional changes reflected particularly in the period immediately preceding a migraine. We suggest that this change in brainstem function could result from altered synaptic transmission evoked by increased gliotransmission, which could evoke a migraine by either an increase in basal firing or by creating a permissive state whereby an external trigger can activate trigeminal pain pathways. These data provide a target timeframe and biological process for prophylactic treatments for migraine. Whether this includes novel treatments targeting gliotransmission remains to be seen.

4.6 References

- Afridi SK, Giffin NJ, Kaube H, Friston KJ, Ward NS, Frackowiak RS, Goadsby PJ (2005a) A positron emission tomographic study in spontaneous migraine. *Arch Neurol* 62:1270-1275.
- Afridi SK, Matharu MS, Lee L, Kaube H, Friston KJ, Frackowiak RS, Goadsby PJ (2005b) A PET study exploring the laterality of brainstem activation in migraine using glyceryl trinitrate. *Brain* 128:932-939.
- Alshelh Z, Di Pietro F, Youssef AM, Reeves JM, Macey PM, Vickers ER, Peck CC, Murray GM, Henderson LA (2016) Chronic Neuropathic Pain: It's about the Rhythm. *J Neurosci* 36:1008-1018.
- Bahra A, Matharu MS, Buchel C, Frackowiak RS, Goadsby PJ (2001) Brainstem activation specific to migraine headache. *Lancet* 357:1016-1017.
- Benarroch EE (2005) Neuron-astrocyte interactions: partnership for normal function and disease in the central nervous system. *Mayo Clin Proc* 80:1326-1338.
- Burstein R, Bernstein R (2012) Sensitization of the trigeminovascular pathway: perspective and implications to migraine pathophysiology. *J Clin Neurol* 8:89-99.
- Borsook D, Burstein R (2012) The enigma of the dorsolateral pons as a migraine generator. *Cephalalgia* 32:803-812.
- Burstein R, Strassman A, Moskowitz M (2012) Can cortical spreading depression activate central trigeminovascular neurons without peripheral input? Pitfalls of a new concept. *Cephalalgia* 32:509-511.
- Burstein R, Nosedá R, Borsook D (2015) Migraine: multiple processes, complex pathophysiology. *J Neurosci* 35:6619-6629.

- Crunelli V, Blethyn KL, Cope DW, Hughes SW, Parri HR, Turner JP, Toth TI, Williams SR (2002) Novel neuronal and astrocytic mechanisms in thalamocortical loop dynamics. *Philos Trans R Soc Lond B Biol Sci* 357:1675-1693.
- Denuelle M, Fabre N, Payoux P, Chollet F, Geraud G (2007) Hypothalamic activation in spontaneous migraine attacks. *Headache* 47:1418-1426.
- Diedrichsen J (2006) A spatially unbiased atlas template of the human cerebellum. *Neuroimage* 33:127-138.
- Friston KJ, Holmes AP, Poline JB, Grasby PJ, Williams SC, Frackowiak RS, Turner R (1995) Analysis of fMRI time-series revisited. *Neuroimage* 2:45-53.
- Giffin NJ, Ruggiero L, Lipton RB, Silberstein SD, Tvedskov JF, Olesen J, Altman J, Goadsby PJ, Macrae A (2003) Premonitory symptoms in migraine: an electronic diary study. *Neurology* 60:935-940.
- Goadsby PJ, Akerman S (2012) The trigeminovascular system does not require a peripheral sensory input to be activated--migraine is a central disorder. Focus on 'Effect of cortical spreading depression on basal and evoked traffic in the trigeminovascular sensory system'. *Cephalalgia* 32:3-5.
- Halassa MM, Fellin T, Haydon PG (2007) The tripartite synapse: roles for gliotransmission in health and disease. *Trends Mol Med* 13:54-63.
- Hughes SW, Lorincz ML, Parri HR, Crunelli V (2011) Infralow (<0.1 Hz) oscillations in thalamic relay nuclei basic mechanisms and significance to health and disease states. *Prog Brain Res* 193:145-162.
- Macey PM, Macey KE, Kumar R, Harper RM (2004) A method for removal of global effects from fMRI time series. *Neuroimage* 22:360-366.
- Mai JK, Paxinos G, Voss T (2007) *Atlas of the Human Brain*, 3rd Edition: Academic Press.

- Mantini D, Perrucci MG, Del Gratta C, Romani GL, Corbetta M (2007) Electrophysiological signatures of resting state networks in the human brain. *Proc Natl Acad Sci U S A* 104:13170-13175.
- Marciszewski KK, Meylakh N, Di Pietro F, Mills EP, Macefield VG, Macey PM, Henderson LA (2018) Changes in brainstem pain modulation circuitry function over the migraine cycle. *J Neurosci*.
- Matharu MS, Bartsch T, Ward N, Frackowiak RS, Weiner R, Goadsby PJ (2004) Central neuromodulation in chronic migraine patients with suboccipital stimulators: a PET study. *Brain* 127:220-230.
- Meylakh N, Marciszewski KK, Di Pietro F, Macefield VG, Macey PM, Henderson LA (2018) Deep in the brain: Changes in subcortical function immediately preceding a migraine attack. *Hum Brain Mapp* 39:2651-2663.
- Nedergaard M, Cooper AJ, Goldman SA (1995) Gap junctions are required for the propagation of spreading depression. *J Neurobiol* 28:433-444.
- Parri HR, Crunelli V (2001) Pacemaker calcium oscillations in thalamic astrocytes in situ. *Neuroreport* 12:3897-3900.
- Paxinos G, Huang X (1995) *Atlas of the Human Brainstem*, 1st Edition. San Diego: Academic Press.
- Särkkä S, Solin A, Nummenmaa A, Vehtari A, Auranen T, Vanni S, Lin F-H (2012) Dynamic retrospective filtering of physiological noise in BOLD fMRI: DRIFTER. *NeuroImage* 60:1517-1527.
- Schulte LH, May A (2016) The migraine generator revisited: continuous scanning of the migraine cycle over 30 days and three spontaneous attacks. *Brain* 139:1987-1993.

- Vanhatalo S, Palva JM, Holmes MD, Miller JW, Voipio J, Kaila K (2004) Infralow oscillations modulate excitability and interictal epileptic activity in the human cortex during sleep. *Proc Natl Acad Sci U S A* 101:5053-5057.
- Weiller C, May A, Limmroth V, Juptner M, Kaube H, Schayck RV, Coenen HH, Diener HC (1995) Brain stem activation in spontaneous human migraine attacks. *Nat Med* 1:658-660.
- Zang Y, Jiang T, Lu Y, He Y, Tian L (2004) Regional homogeneity approach to fMRI data analysis. *Neuroimage* 22:394-400.

Figure Legends:

Figure 1: A: Significant increases (hot colour scale) in resting signal variability in migraineurs during the 24-hour period prior to the onset of a migraine. Increases are overlaid onto axial slices of a T1-weighted anatomical template of the brainstem. Below are plots of mean (\pm SEM) variability (standard deviation) in controls and migraineurs for the left spinal trigeminal nucleus (SpV), right SpV, right dorsomedial/dorsolateral pons (dm/dlPons), left substantia nigra (SN) and midbrain periaqueductal gray matter (PAG). The slice locations in Montreal Neurological Institute space are indicated at the top right of each slice. **B:** Plots of total brainstem variability in five controls (C1-5) and three migraine subjects (M1-3) for each scanning session. **C:** Plots of the power differences between the immediately prior to migraine and interictal periods for the left and right SpV and left and right dlPons. Positive values indicate greater power immediately prior to a migraine compared with the interictal period. The grey shading indicates the frequency band 0.03-0.06Hz. * $p < 0.05$ voxel-by-voxel analysis.

Figure 2: Significant increases (hot colour scale) in resting infra-slow oscillation (ISO) power (0.03-0.06Hz) in migraineurs during the 24-hour period prior to the onset of a migraine. Increases are overlaid onto axial slices of a T1-weighted anatomical template of the brainstem. Below are plots of mean (\pm SEM) ISO power in controls and migraineurs for the right spinal trigeminal nucleus (SpV), left dorsolateral pons (dlPons), right dorsomedial/dorsolateral pons (dm/dlPons) and left substantia nigra (SN). The slice locations in Montreal Neurological Institute space are indicated at the top right of each slice. * $p < 0.05$ voxel-by-voxel analysis.

Figure 3: Plots of power spectra of significant ISO clusters in the three migraineurs (M1, M2, M3). Mean power spectra during the interictal and immediately prior to migraine periods are

plotted for each subject for the right spinal trigeminal nucleus (SpV), left dorsolateral pons (dlPons), right dorsomedial/dorsolateral pons (dm/dlPons) and left substantia nigra (SN). Note that particularly for the SpV, dlPons and dm/dlPons, power is greater during the period immediately prior to migraine. These increases encompass the frequency band 0.03-0.06Hz as indicated by the grey shading.

Figure 4: Plots of daily ISO power (0.03-0.06Hz) in the three migraineurs (M1, M2, M3). Power is plotted for each subject for the right spinal trigeminal nucleus (SpV), left dorsolateral pons (dlPons), right dorsomedial/dorsolateral pons (dm/dlPons) and left substantia nigra (SN). Note that particularly for the SpV, dlPons and dm/dlPons, power is greater during the period immediately prior to migraine (black box) compared to other days, although there is also some variability in the interictal period.

Figure 5: A: Significant increases (hot colour scale) in resting regional homogeneity (ReHo) in migraineurs during the 24-hour period prior to the onset of a migraine. Increases are overlaid onto axial slices of a T1-weighted anatomical template of the brainstem. Below are plots of mean (\pm SEM) ReHo in controls and migraineurs for the right spinal trigeminal nucleus (SpV), right dorsomedial/dorsolateral pons (dm/dlPons) and left substantia nigra (SN). The slices locations in Montreal Neurological Institute space are indicated at the top right of each slice. * $p < 0.05$ voxel-by-voxel analysis. **B:** Areas in which ReHo and infra-slow oscillation (ISO) power were increased during the period immediately prior to a migraine (red colour shading). Below are plots of ReHo against ISO power for each cluster in each of the three migraineurs (M1, M2, M3). Note that for the right SpV and right dm/dlPons ReHo and ISO were significantly positively correlated in all three migraineurs. * $p < 0.05$ Pearsons correlation.

Table 1. Migraine subject characteristics.

<i>subject</i>	<i>age</i>	<i>sex</i>	<i>years suffering</i>	<i>pain side</i>	<i>aura</i>	<i>migraine/month</i>	<i>intensity (0-5)</i>	<i>medication taken during migraine</i>	<i>daily medication</i>
M1	21	F	1.5	left	no	2	3	ibuprofen, paracetamol, codeine	oral contraceptive pill
M2	25	M	12	left	no	2	4	paracetamol	Ciprimal
M3	26	F	9	right	no	1	3	ibuprofen	Levlen ED

Table 2. Montreal Neurological Institute (MNI) coordinates, cluster size and t-score for regions of significant increases in resting variability, amplitude of infra-slow oscillations and regional homogeneity immediately prior to a migraine.

Brain region	MNI Co-ordinate			cluster size	t-score
	x	y	z		
variability					
midbrain periaqueductal gray matter	0	-38	-19	12	5.73
left substantia nigra	-2	-14	-21	83	9.34
right dorsolateral pons	10	-18	-37	153	8.56
left dorsolateral pons	-8	-44	-35	17	6.31
right spinal trigeminal nucleus	4	-40	-61	118	12.22
left spinal trigeminal nucleus	-6	-40	-61	20	9.99
infra-slow oscillations (0.03-0.06Hz)					
left substantia nigra	-4	-16	-7	14	3.43
right dorsolateral pons	6	-34	-35	8	3.08
left dorsolateral pons	-8	-44	-35	16	4.23
right spinal trigeminal nucleus	4	-40	-60	19	4.14
regional homogeneity					
left substantia nigra	-4	-10	-7	112	7.72
right substantia nigra	12	-18	-5	34	3.96
right dorsolateral/medial pons	10	-32	-29	17	3.79
right spinal trigeminal nucleus	4	-46	-55	25	5.33
	8	-38	-47	16	3.74

Figure 1:

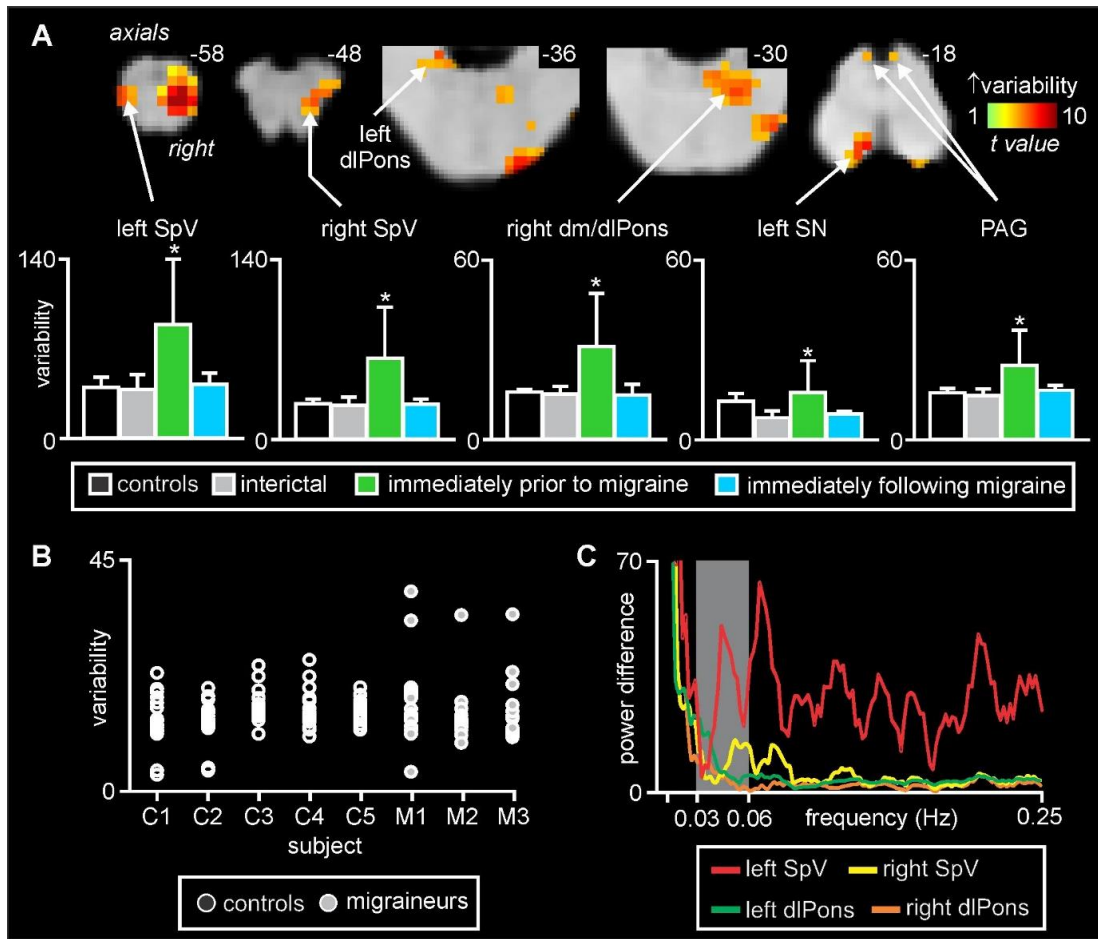


Figure 2:

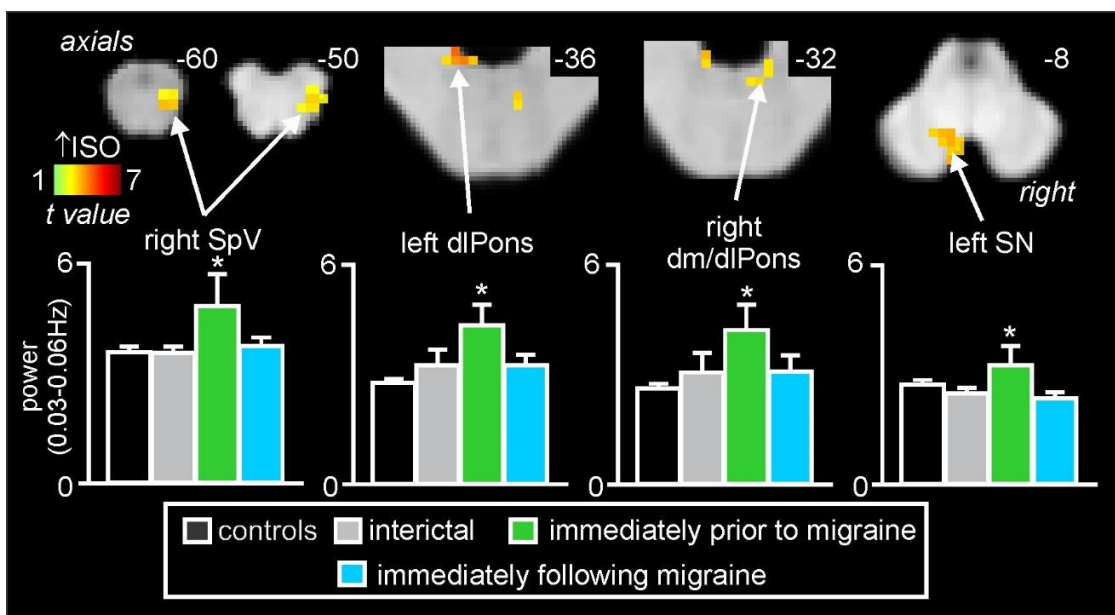


Figure 3:

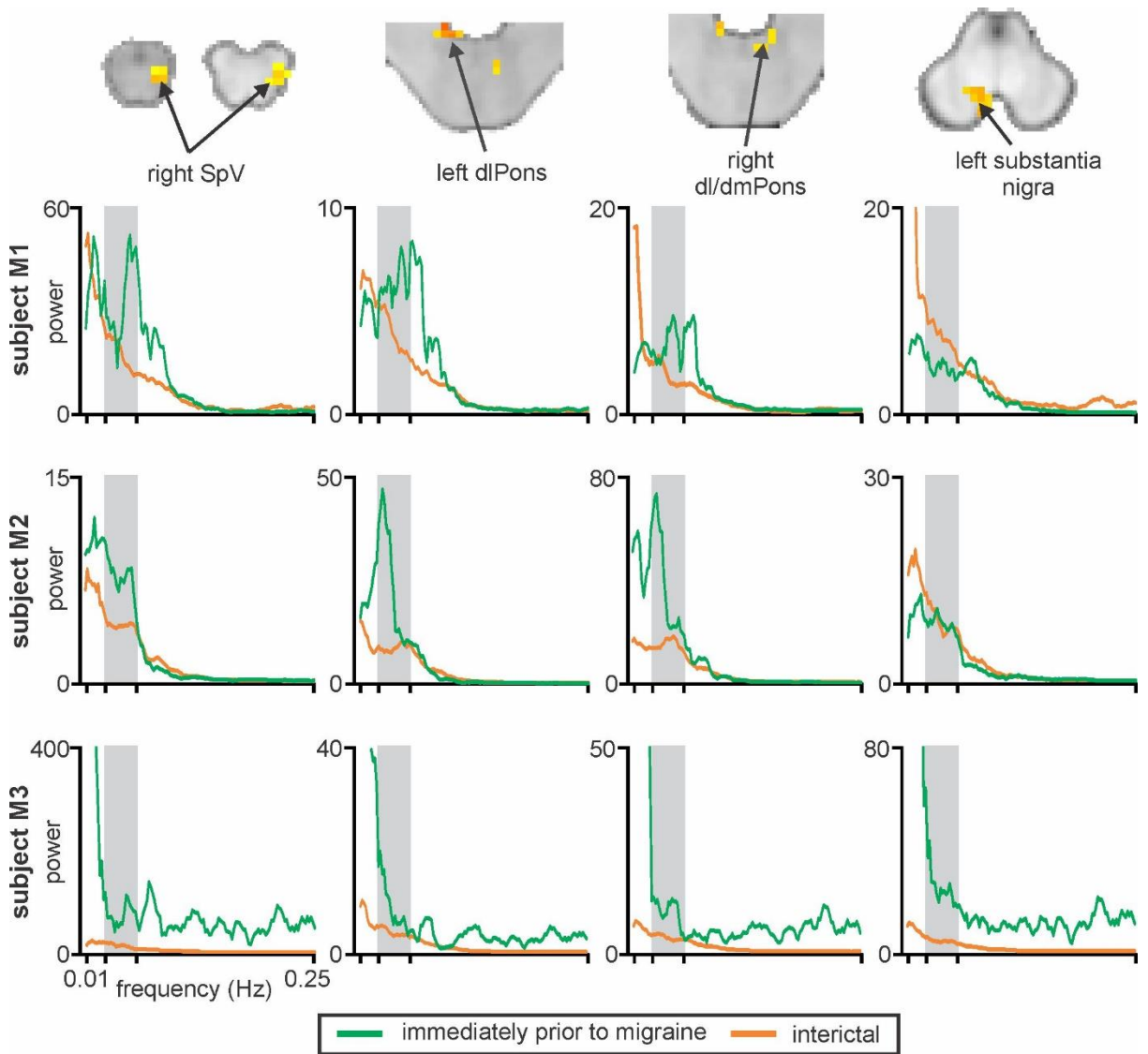


Figure 4:

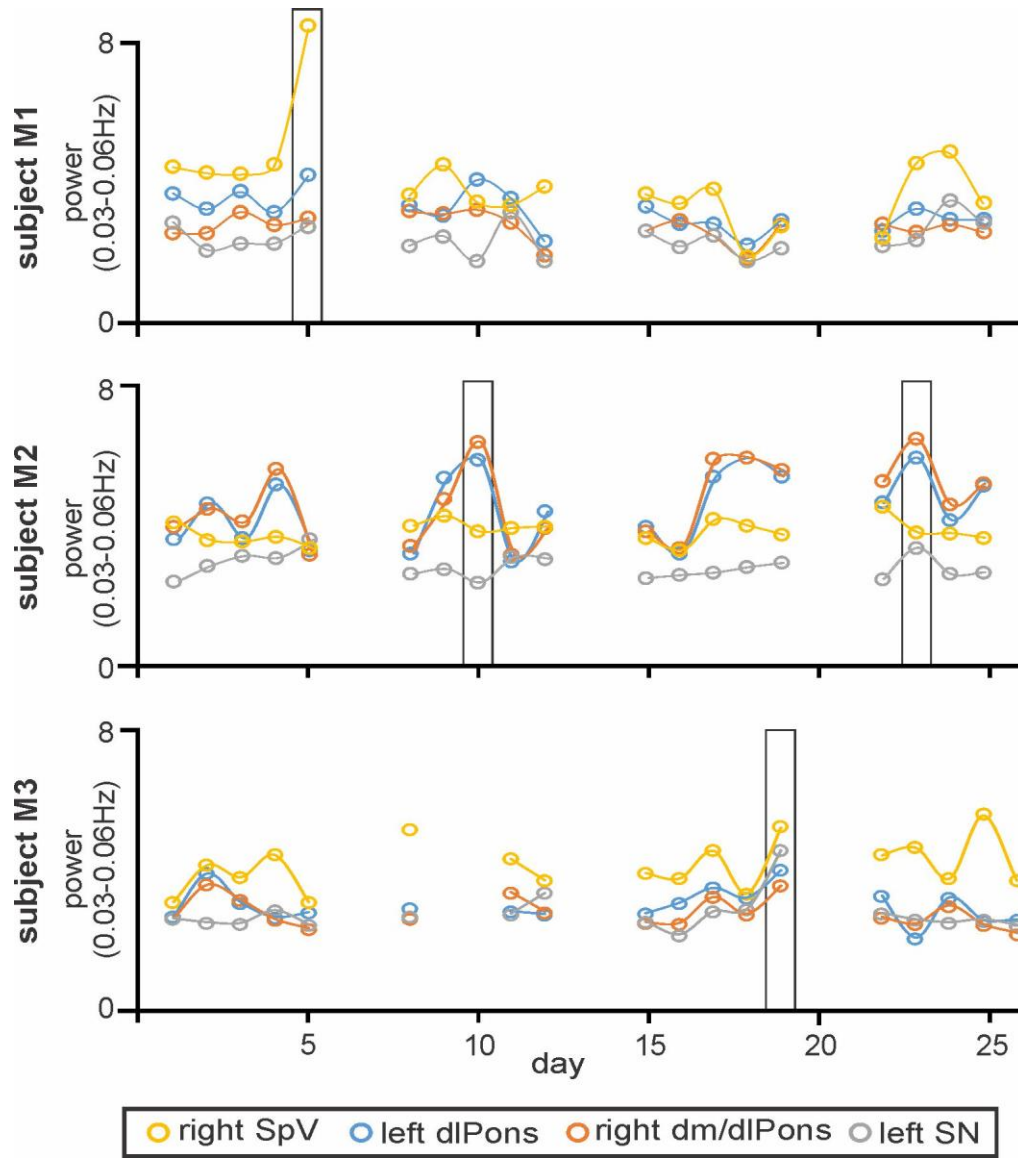
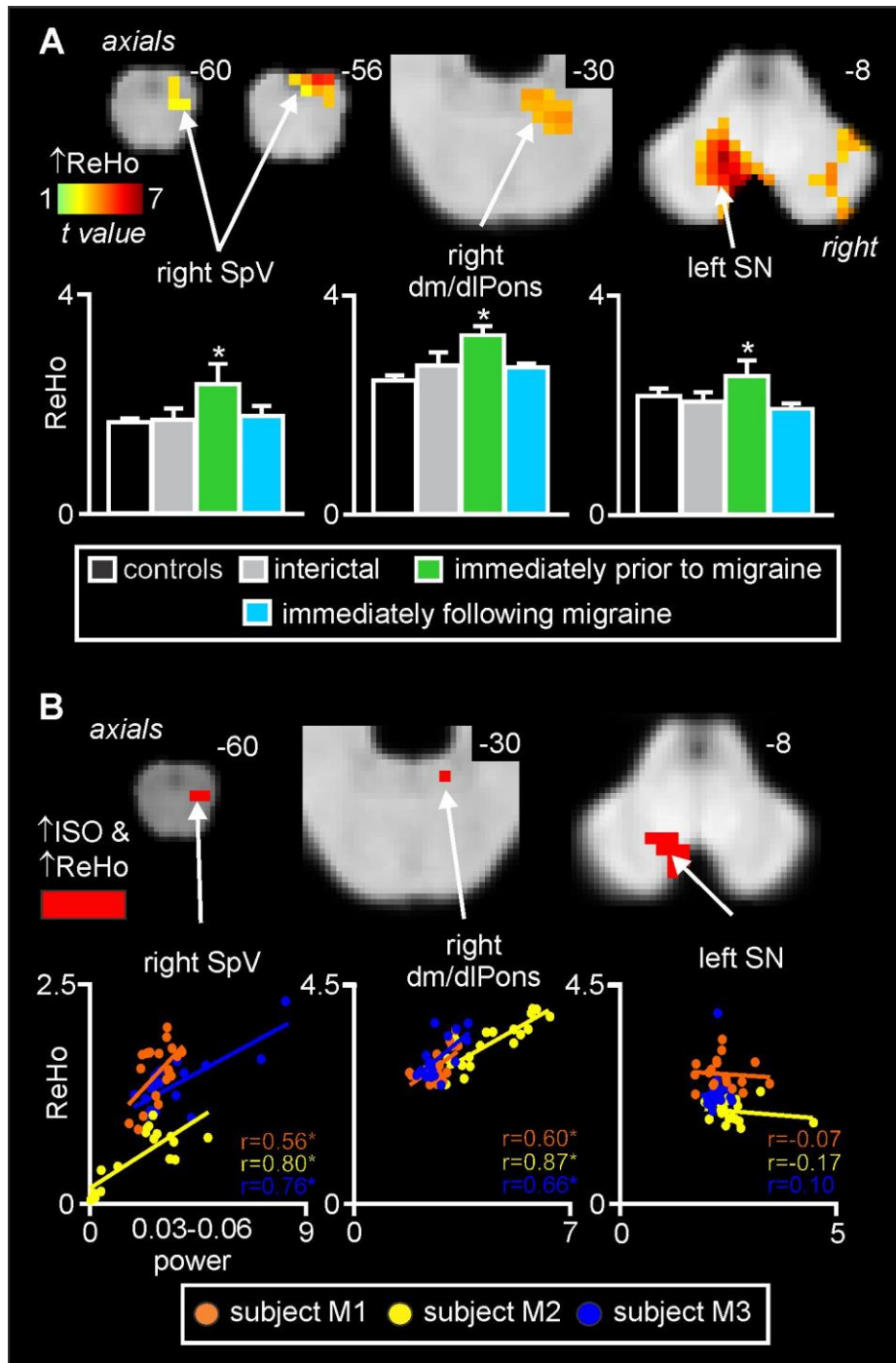


Figure 5:



Chapter 5

**General discussion, limitations, conclusions and future
directions**

5.1 General discussion

Our understanding of the neurobiology underlying migraine has evolved considerably over the past few decades, spurred on by the advent of modern human brain imaging techniques. Whilst very few studies have explored human brain function at different times of the migraine cycle, it has been proposed that migraine is not characterized by a static brain state but is instead a cyclic disorder fluctuating between altered states (Burstein et al., 2015). Whilst this may be the case, the lack of experimental data, particularly during the period immediately prior to a migraine (i.e. the premonitory period) means that we have a limited understanding of how and why such brain function fluctuations may occur and more specifically how these changes may trigger a migraine attack.

Although many researchers have suggested that increased sensitization of the trigeminovascular pathway is a key factor in migraine initiation (Bernstein & Burstein, 2012), without insight into changes during the premonitory period, it is difficult to determine if and why such sensitization occurs. Furthermore, it remains unknown if such sensitization changes need to be paired with external triggers for a migraine attack to occur. Indeed, it is entirely plausible that peripheral triggers are only capable of inducing a migraine when coinciding with high brainstem sensitivity levels (Burstein et al., 2015; Goadsby et al., 2017). Alternatively, it may be the case that changes in brain sensitivity alone result in a migraine due to ongoing basal levels of activity in the trigeminal pain pathway.

The overall aim of the experiments in this thesis was to determine if there are brain activity changes in the period immediately prior to a migraine and at other periods of the migraine cycle. The first

experimental chapter of this thesis focused on identifying functional differences in the premonitory period in an effort to understand the factors involved in the initial sensitization process (Chapter 2). This cross-sectional study was the first to use high-resolution functional magnetic resonance imaging (fMRI) to measure ongoing activity patterns reflected through increases in infra-slow oscillations (ISOs) and increases in functional connectivity strengths during the interictal, postdrome and premonitory periods of migraine compared with controls. A comparison between all migraine periods provided convincing evidence for unique brain activity changes specifically during the premonitory period. Increased ISO activity occurred exclusively during the premonitory period in areas of the trigeminovascular system including the spinal trigeminal nucleus (SpV), midbrain periaqueductal gray (PAG), dorsal pons, thalamus and hypothalamus. Importantly, these ISO increases were restricted to the premonitory period as during the interictal and postdrome periods, ISO power was similar to that of the control group.

Whilst the precise role of altered ISO activity patterns remains to be determined, ISO activity is recognized as an essential component of cerebral and thalamic function and is preserved by adenosine receptor-mediated signaling (Hughes et al., 2011; Lorincz, Geall, Bao, Crunelli, & Hughes, 2009). Because adenosine can display spontaneous intracellular infra-slow calcium oscillations (Parri & Crunelli, 2001), it is highly plausible that adenosine is released by astrocytes (Parri & Crunelli, 2001). ISOs have been associated with cyclic gliotransmitter release, with infra-slow astrocyte calcium waves proposed to propagate among surrounding astrocytes (Halassa et al., 2007; Parri & Crunelli, 2001). In pathological cases, great numbers of astrocytes have been found to show enhanced calcium wave synchrony and amplitude and enhanced NMDA receptor function (Parri & Crunelli, 2001). Thus, altered astrocyte function in the premonitory period of migraine may result in increased ISO power which in turn can potentially lead to the experience of pain.

Even though we cannot measure astrocyte calcium waves directly, given that it has been shown that they propagate to neighbouring astrocytes, we can measure an index of such regional propagation by calculating regional homogeneity. Regional homogeneity evaluates the synchronization between the signal fluctuations of a given voxel with its nearest neighbours and thus an increase in this measure is consistent with the idea of astrocyte ISO waves propagating to neighbouring astrocytes. In support of this idea, we found that regional homogeneity increased in the area of the PAG, thalamus and hypothalamus, again only during the premonitory period. Furthermore, the resting connectivity between these three regions also increased only during this period indicating greater communication between these brain regions. The results from these initial studies strongly suggest that the PAG-hypothalamic-thalamic interaction plays a critical role in migraine expression and this interaction may be modulated by astrocytic activity. This has never been shown before.

If ongoing activity patterns change dramatically immediately prior to a migraine, and normalize almost immediately after, the key to understanding the sensitization of the trigeminovascular pathway may indeed lie in this critical and short *pain-free* window preceding a migraine. Though our findings reflecting specific activity patterns in the premonitory period do not allow for direct deductions regarding the initiating processes of a migraine, they do support the argument that changes in the central nervous system are involved in migraine expression, especially since activity increases in these same brain regions have been previously reported to occur during a migraine itself (S.K. Afridi et al., 2005; S. K. Afridi et al., 2005; Bahra et al., 2001b; Denuelle et al., 2007; Weiller, May, Limmroth, Juptner, Kaube, Schayck, Coenen, & Diener, 1995). Therefore, altered sensitivity in these regions may either act as a migraine trigger by increasing the sensitivity of already ongoing basal activity levels, or alternatively they may reflect altered “*brainstem tone*”

allowing peripheral triggers to evoke a migraine.

The findings from this cross-sectional fMRI study show a unique resting activity pattern and functional connectivity in migraineurs during the premonitory period, but it remains unknown if these activity pattern changes are coupled to alterations in absolute activity levels. To address this question, the second experimental chapter in this thesis focused on identifying absolute activity level changes throughout the migraine cycle by using non-invasive arterial spin labelling (ASL) (Chapter 3). This was the first investigation to measure resting CBF during the premonitory period in migraineurs. Though many studies have explored CBF during other periods of migraine, particularly during migraine attacks themselves, most used positron emission tomography techniques with relatively poor spatial resolution and thus areas of the brainstem, for instance, were not specifically explored.

Consistent with our initial investigation, CBF was measured during the interictal, postdrome and premonitory periods and in controls. Our analysis revealed distinctive alterations in absolute activity levels occurring primarily during the premonitory period. These changes were characterized by decreased CBF in the hypothalamus, PAG and SpV, the same regions in which we showed altered ongoing activity patterns during the same migraine period. In addition, decreased CBF occurred in higher brain structures such as the visual, orbitofrontal (OFC) and retrosplenial cortices. Interestingly, the brainstem and hypothalamic CBF decreases occurred abruptly, remaining relatively stable throughout even as a migraine approached only to drop in the 24-hour period before the migraine. In contrast, CBF in higher brain structures appeared to gradually decline throughout the interictal period as the migraine approached, before seeing a greater decline in the 24-hour pain-free period preceding a migraine.

The identification of decreased CBF in brainstem, midbrain and hypothalamic regions in the premonitory period is consistent with the hypothesis that migraines are associated with altered trigeminal system activity in addition to an imbalance of the regulation of incoming noxious inputs by brainstem nuclei (Bartolini et al., 2005). Our data are consistent with the idea that only when CBF decreases in the PAG, SpV and hypothalamus immediately prior to a migraine can signals reach the cortex resulting in head pain. The findings of this study showing altered absolute activity levels, together with the initial study revealing altered ongoing activity levels (Chapter 2) in the premonitory period, support the hypothesis that the SpV, PAG and hypothalamus form a specialized set of brain structures critical for the initiation of a migraine attack (Floyd et al., 2001; Holstege & Kuypers, 1982; Morgan et al., 2008). Perhaps this interaction results in an altered endogenous analgesic state whereby an external trigger is able to activate the ascending trigeminal pain pathway and produce head pain.

Indeed, in another related investigation (see appendix II) we used fMRI to measure brain activation during acute noxious stimuli as well as resting connectivity in the brainstem pain modulation circuitry throughout the migraine cycle. We found that in individual migraineurs, pain sensitivity increased over the interictal period, but then dramatically decreased immediately prior to a migraine. Furthermore, despite overall similar pain intensity ratings between groups, in the premonitory period, compared to controls and other migraine periods, migraineurs displayed greater activation during noxious orofacial stimulation in the SpV and reduced functional connectivity of this region with a key area of the brainstem endogenous pain modulation system - the rostral ventromedial medulla. These data support the hypothesis that brainstem sensitivity fluctuates throughout the migraine cycle, although it suggests that immediately prior to a migraine attack, endogenous analgesic mechanisms are in fact enhanced and incoming noxious inputs are

less likely to reach higher brain centers. This result needs to be independently replicated and explored in more detail.

In addition to changes during the period immediately prior to a migraine, in this related investigation we also found that during the interictal period, migraineurs displayed reduced activation of the PAG during acute noxious stimulation and enhanced PAG connectivity with the rostral ventromedial medulla. Indeed, in chapter 3 of this thesis we found CBF decreases in higher brain structures including the nucleus accumbens, putamen, OFC and ventrolateral prefrontal cortex. Whilst we did not find changes in the pattern of resting brain activity during the interictal period of migraine, these two sets of data are consistent with previous studies showing changes in brain function during the interictal period of migraine. These include single photon emission computed tomography and positron emission tomography studies that have yielded contradictory results displaying both reduced CBF (Calandre et al., 2002; De Benedittis et al., 1999) and increased CBF (Kassab et al., 2009) during the interictal period. Furthermore, functional fMRI studies have shown abnormal activity in the brainstem, hypothalamus, thalamus, basal ganglia and cerebral cortex (Sprenger & Borsook, 2012), including increased resting-state connectivity between the PAG and cortical regions such as the thalamus in the interictal period (Caterina Mainero, Jasmine Boshyan, & Nouchine Hadjikhani, 2011).

Whilst the first two experimental chapters in the thesis outline results from cross-sectional investigations, it is important to determine if the changes in brain function that we found to occur across the migraine cycle also occur in individual migraineurs. Given this, the final experimental chapter in this thesis consists of a longitudinal investigation in which we explored brain function each weekday over a four-week period in three migraineurs and five control subjects (Chapter 4).

This aim of this study was to determine if brainstem function oscillates over a migraine cycle in individual subjects. Similar to our first investigation (Chapter 2), this study used fMRI to explore resting brainstem activity patterns.

We found that although resting activity variability was similar in controls and migraineurs on most of the 20 days that were investigated, during the premonitory period, brainstem variability increased dramatically. These increases were restricted to the same specific areas that we reported in our cross-sectional studies; the SpV and dorsal pons. Increased resting variability was characterized by increased ISO power and was furthermore associated with increased regional homogeneity. Remarkably, these changes were located in the same brainstem regions which have been shown to be activated during a migraine itself, and similar to our initial investigation, they occurred whilst the individual was *not* in pain.

These oscillatory and regional homogeneity changes immediately prior to a migraine in individual migraineurs are consistent with the idea that changes in astrocyte function in pathological situations can alter neural function (Crunelli et al., 2002; Halassa et al., 2007; Lorincz et al., 2009; Parri & Crunelli, 2001). Therefore, it is not unreasonable to suggest that these changes in astrocyte function may be involved in the initiation and/or maintenance of the migraine. Indeed, there is evidence directly linking migraine with altered glial function (Benarroch, 2005; Nedergaard et al., 1995). These data provide the first evidence of altered brainstem function directly before a migraine throughout the migraine cycle of multiple individuals and support that brainstem function alters over the migraine cycle with unique activity displayed in the 24-hour pain-free period immediately preceding a migraine. These changes cannot be attributed to individual differences as similar spatial patterns were identified in our cross-sectional studies.

Overall, the data presented in this thesis provide the first evidence of changes in brainstem function throughout the migraine cycle both in cross-sectional and longitudinal studies. The data support the hypothesis that migraine is characterized by fluctuations in brain function and is consistent with the idea that the brainstem oscillates between periods of increased and decreased sensitivity. Although contrary to the hypothesis that brainstem sensitivity increases immediately prior to a migraine, we found that it indeed appears to decrease. Whether this decrease in acute orofacial pain sensitivity reflects changes in the system that then evokes head pain remains to be determined. Nevertheless, there is little doubt that brain function alters dramatically immediately prior to the onset of a migraine when the individual is still in a pain-free state.

5.2 Limitations

In this series of investigations there are several important limitations in need of consideration. Firstly, due to the limited spatial resolution of resting-state fMRI and ASL, precise localization of clusters to specific nuclei, especially in brainstem regions, is difficult. As a result, most clusters described also extended to adjacent voxels involving other functional nuclei and brain regions. To minimize this effect, we utilized spatial normalization techniques designed specifically for brainstem analyses. We are confident that the regions in which we reported either fMRI and CBF changes encompass the areas described, especially due to the correspondence between our results and those reported in previous migraine investigations.

Secondly, several logistical limitations were associated with our experimental paradigm. Due to the inability to predict when an individual's next migraine will occur, collecting MRI data in the

24-hour period preceding a migraine is difficult. As a result, acquisition of this data was based on chance. Consequently, we had modest group sample sizes for the premonitory groups in comparison to other migraine groups, with an absence of scans during the headache period of the migraine cycle altogether. We were able to overcome these barriers in our longitudinal investigation (Chapter 4), however, the longitudinal study restricted those who could participate due to the time commitments necessary. Though we employed population-based statistical tests that were corrected for multiple comparisons, increasing the sample size, particularly in the longitudinal study, as well as acquiring data in the headache phase, would be extremely useful.

5.3 Conclusions and future directions

The findings presented in this thesis have shown for the first time that the trigeminovascular system, particularly the midbrain, brainstem and hypothalamic regions, exhibits abnormal behavior, reflected through changes in ongoing and absolute activity levels, in the 24 hours leading up to a migraine. The correlation between the findings of the cross-sectional and longitudinal studies has emphasized the importance of the premonitory period. Though no comment can be directly made regarding the initiating quality of migraine, this series of investigations has provided support for the idea that the central nervous system undergoes a change particularly in the 24-hour period preceding a migraine, and this change may be contributing to the initiation and/or expression of a migraine.

There is growing evidence to suggest that the mechanism underlying this change in migraine is altered glial function (Benarroch, 2005; Nedergaard et al., 1995). In this series of investigations, we reported increased ISOs at frequencies between 0.03-0.06 Hz. These infra-slow spontaneous

fluctuations in brain activity oscillate at similar ranges as infra-slow calcium waves. Astrocytes can exhibit infra-slow calcium oscillations that can propagate among surrounding astrocytes and it has been proposed that in pathological situations, enhanced calcium-wave synchrony and amplitude may occur which results in significantly altered synaptic function (Crunelli et al., 2002; Cunningham et al., 2006; Halassa et al., 2007; Lorincz et al., 2009; Parri & Crunelli, 2001). As we have hypothesized, increased ISOs at frequencies between 0.03-0.06 Hz may reflect increased modulatory activity on local neurons by cyclic gliotransmitter release (Halassa et al., 2007; Parri & Crunelli, 2001). Therefore, increased ISOs in brainstem regions that regulate activity of the ascending trigeminal pathway, could influence the susceptibility of an external noxious stimulus to act as a trigger, and may be reflective of altered astrocyte function.

Furthermore, in a recent series of investigations, we have shown that migraine is also associated with changes in regional anatomy in a number of brainstem regions that fluctuate over the migraine cycle (see Appendix III). This further supports the idea that the mechanisms underlying migraine are not permanent, but ever changing. These studies found that during the interictal period, migraineurs displayed increased free water movement in the PAG, raphe/SpV and dlPons. These anatomical data are consistent with the idea that astrocytes are activated and hence their processes expand immediately before a migraine leading to an increase in ISO activity and altered diffusivity and connectivity resulting in sensitivity within brainstem regions that receive and process orofacial noxious information. This change is very rapid and returns to normal levels following the resolution of the migraine headache. Therefore, altered brainstem function throughout the migraine cycle may result from abnormal neural-glia interactions.

In future studies, the nature of neural-glia interactions needs to be studied with much more

veracity. We are unable to comment on direct relationships at this point and hence are only speculating about the role of astrocytes in migraine. However, there is preliminary evidence showing that palmitoylethanolamide (PEA), a naturally occurring fatty acid amide that belongs to the N-acetyethanolamine family, can reduce astrocyte activation (Esposito et al., 2011; Skaper & Facci, 2012) and may reduce migraine severity. In a pilot study, 50 migraineurs were treated sublingually with ultra-micronized PEA for three months (Dalla Volta, 2016). PEA treatment resulted in a significant reduction in the mean number of days per month with migraine; pain intensity was significantly mitigated and the number of analgesics required significantly decreased. No serious adverse events were observed. Whilst this was a pilot study, it does lend support to the suggestion that migraine may indeed involve alterations in neural-glial interactions. Further studies using astrocyte inhibitors would be desirable to explore this interaction in more depth.

In addition to the potential of further exploring alterations of astrocyte function, the use of different MRI techniques particularly in the longitudinal investigation would allow for the extrapolation of patterns and changes otherwise undetected. Increasing sample sizes of the premonitory period would help to corroborate the findings and conclusions made, particularly due to the lack of research into this critical period of the migraine cycle. Insight into the headache period of the migraine cycle would provide us with a more accurate time frame of exactly when the alterations observed during the premonitory period reverse, and also the mechanisms associated with the headache. With the development of neural imaging technology, our understanding of migraine pathophysiology will continue to grow with the goal of advancing treatments in order to improve the quality of life of millions of migraine sufferers around the world. Our series of investigations have lent support to the idea that migraine is a cyclic disorder likely controlled by an interaction

between sensitization of the trigeminovascular pathway together with the presence of an appropriately timed peripheral trigger. These alterations in specific periods of the migraine cycle are potentially modulated by altered glial and astrocytic function.

5.4 References

- Afridi, S. K., Giffin, N. J., Kaube, H., Friston, K. J., Ward, N. S., Frackowiak, R. S., & Goadsby, P. J. (2005). A positron emission tomographic study in spontaneous migraine. *Arch Neurol*, 62(8), 1270-1275. doi:10.1001/archneur.62.8.1270
- Afridi, S. K., Matharu, M. S., Lee, L., Kaube, H., Friston, K. J., Frackowiak, R. S., & Goadsby, P. J. (2005). A PET study exploring the laterality of brainstem activation in migraine using glyceryl trinitrate. *Brain*, 128(Pt 4), 932-939. doi:10.1093/brain/awh416
- Bahra, A., Matharu, M. S., Buchel, C., Frackowiak, R. S., & Goadsby, P. J. (2001). Brainstem activation specific to migraine headache. *Lancet*, 357(9261), 1016-1017.
- Bartolini, M., Baruffaldi, R., Paolino, I., & Silvestrini, M. (2005). Cerebral blood flow changes in the different phases of migraine. *Funct Neurol*, 20(4), 209-211.
- Benarroch, E. E. (2005). Neuron-astrocyte interactions: partnership for normal function and disease in the central nervous system. *Mayo Clin Proc*, 80(10), 1326-1338. doi:10.4065/80.10.1326
- Bernstein, C., & Burstein, R. (2012). Sensitization of the trigeminovascular pathway: perspective and implications to migraine pathophysiology. *J Clin Neurol*, 8(2), 89-99. doi:10.3988/jcn.2012.8.2.89
- Burstein, R., Nosedà, R., & Borsook, D. (2015). Migraine: multiple processes, complex pathophysiology. *J Neurosci*, 35(17), 6619-6629. doi:10.1523/JNEUROSCI.0373-15.2015
- Calandre, E. P., Bembibre, J., Arnedo, M. L., & Bécerra, D. (2002). Cognitive disturbances and regional cerebral blood flow abnormalities in migraine patients: their relationship with

the clinical manifestations of the illness. *Cephalalgia*, 22(4), 291-302.

doi:10.1046/j.1468-2982.2002.00370.x

Crunelli, V., Blethyn, K. L., Cope, D. W., Hughes, S. W., Parri, H. R., Turner, J. P., . . .

Williams, S. R. (2002). Novel neuronal and astrocytic mechanisms in thalamocortical loop dynamics. *Philos Trans R Soc Lond B Biol Sci*, 357(1428), 1675-1693.

doi:10.1098/rstb.2002.1155

Cunningham, M. O., Pervouchine, D. D., Racca, C., Kopell, N. J., Davies, C. H., Jones, R. S., . . .

. Whittington, M. A. (2006). Neuronal metabolism governs cortical network response state. *Proc Natl Acad Sci U S A*, 103(14), 5597-5601. doi:0600604103 [pii]

10.1073/pnas.0600604103

Dalla Volta, G. (2016). *Ultramicronized palmitoylethanolamide reduces frequency and pain intensity in migraine. A pilot study* (Vol. 3).

De Benedittis, G., Ferrari Da Passano, C., Granata, G., & Lorenzetti, A. (1999). CBF changes during headache-free periods and spontaneous/induced attacks in migraine with and without aura: a TCD and SPECT comparison study. *J Neurosurg Sci*, 43(2), 141-146; discussion 146-147.

Denuelle, M., Fabre, N., Payoux, P., Chollet, F., & Geraud, G. (2007). Hypothalamic activation in spontaneous migraine attacks. *Headache*, 47(10), 1418-1426. doi:10.1111/j.1526-4610.2007.00776.x

Esposito, E., Paterniti, I., Mazzon, E., Genovese, T., Di Paola, R., Galuppo, M., & Cuzzocrea, S. (2011). Effects of palmitoylethanolamide on release of mast cell peptidases and neurotrophic factors after spinal cord injury. *Brain Behav Immun*, 25(6), 1099-1112. doi:10.1016/j.bbi.2011.02.006

- Floyd, N. S., Price, J. L., Ferry, A. T., Keay, K. A., & Bandler, R. (2001). Orbitomedial prefrontal cortical projections to hypothalamus in the rat. *J Comp Neurol*, *432*(3), 307-328.
- Goadsby, P. J., Holland, P. R., Martins-Oliveira, M., Hoffmann, J., Schankin, C., & Akerman, S. (2017). Pathophysiology of Migraine: A Disorder of Sensory Processing. *Physiol Rev*, *97*(2), 553-622. doi:10.1152/physrev.00034.2015
- Halassa, M. M., Fellin, T., & Haydon, P. G. (2007). The tripartite synapse: roles for gliotransmission in health and disease. *Trends Mol Med*, *13*(2), 54-63. doi:10.1016/j.molmed.2006.12.005
- Holstege, G., & Kuypers, H. G. (1982). The anatomy of brain stem pathways to the spinal cord in cat. A labeled amino acid tracing study. *Prog Brain Res*, *57*, 145-175. doi:10.1016/S0079-6123(08)64128-X
- Hughes, S. W., Lorincz, M. L., Parri, H. R., & Crunelli, V. (2011). Infralow (<0.1 Hz) oscillations in thalamic relay nuclei basic mechanisms and significance to health and disease states. *Prog Brain Res*, *193*, 145-162. doi:10.1016/B978-0-444-53839-0.00010-7
B978-0-444-53839-0.00010-7 [pii]
- Kassab, M., Bakhtar, O., Wack, D., & Bednarczyk, E. (2009). Resting brain glucose uptake in headache-free migraineurs. *Headache*, *49*(1), 90-97. doi:10.1111/j.1526-4610.2008.01206.x
- Lorincz, M. L., Geall, F., Bao, Y., Crunelli, V., & Hughes, S. W. (2009). ATP-dependent infralow (<0.1 Hz) oscillations in thalamic networks. *PLoS One*, *4*(2), e4447. doi:10.1371/journal.pone.0004447

- Mainero, C., Boshyan, J., & Hadjikhani, N. (2011). Altered functional magnetic resonance imaging resting-state connectivity in periaqueductal gray networks in migraine. *Annals of neurology*, 70(5), 838-845. doi:10.1002/ana.22537
- Morgan, M. M., Whittier, K. L., Hegarty, D. M., & Aicher, S. A. (2008). Periaqueductal gray neurons project to spinally projecting GABAergic neurons in the rostral ventromedial medulla. *Pain*, 140(2), 376-386. doi:10.1016/j.pain.2008.09.009
- Nedergaard, M., Cooper, A. J., & Goldman, S. A. (1995). Gap junctions are required for the propagation of spreading depression. *J Neurobiol*, 28(4), 433-444.
doi:10.1002/neu.480280404
- Parri, H. R., & Crunelli, V. (2001). Pacemaker calcium oscillations in thalamic astrocytes in situ. *Neuroreport*, 12(18), 3897-3900.
- Skaper, S. D., & Facci, L. (2012). Mast cell-glia axis in neuroinflammation and therapeutic potential of the anandamide congener palmitoylethanolamide. *Philos Trans R Soc Lond B Biol Sci*, 367(1607), 3312-3325. doi:10.1098/rstb.2011.0391
- Sprenger, T., & Borsook, D. (2012). Migraine changes the brain: neuroimaging makes its mark. *Curr Opin Neurol*, 25(3), 252-262. doi:10.1097/WCO.0b013e3283532ca3
- Weiller, C., May, A., Limmroth, V., Juptner, M., Kaube, H., Schayck, R. V., . . . Diener, H. C. (1995). Brain stem activation in spontaneous human migraine attacks. *Nat Med*, 1(7), 658-660.

Appendix I.

Altered brainstem anatomy in migraine

Altered brainstem anatomy in migraine

Kasia K Marciszewski¹, Noemi Meylakh¹, Flavia Di Pietro¹,
Vaughan G Macefield², Paul M Macey³ and
Luke A Henderson¹

Cephalalgia
2018, Vol. 38(3) 476–486
© International Headache Society 2017
Reprints and permissions:
sagepub.co.uk/journalsPermissions.nav
DOI: 10.1177/0333102417694884
journals.sagepub.com/home/cep



Abstract

Background: The exact mechanisms responsible for migraine remain unknown, although it has been proposed that changes in brainstem anatomy and function, even between attacks, may contribute to the initiation and maintenance of headache during migraine attacks. The aim of this investigation is to use brainstem-specific analyses of anatomical and diffusion weighted images to determine if the trigeminal system displays altered structure in individuals with migraine.

Methods: Voxel-based morphometry of T1-weighted anatomical images (57 controls, 24 migraineurs) and diffusion tensor images (22 controls, 24 migraineurs) were used to assess brainstem anatomy in individuals with migraine compared with controls.

Results: We found grey matter volume decreases in migraineurs in the spinal trigeminal nucleus and dorsomedial pons. In addition, reduced grey matter volume and increased free water diffusivity occurred in areas of the descending pain modulatory system, including midbrain periaqueductal gray matter, dorsolateral pons, and medullary raphe. These changes were not correlated to migraine frequency, duration, intensity or time to next migraine.

Conclusion: Brainstem anatomy changes may underlie changes in activity that result in activation of the ascending trigeminal pathway and the perception of head pain during a migraine attack.

Keywords

Spinal trigeminal nucleus, grey matter volume, periaqueductal gray matter, hypothalamus, diffusion tensor imaging

Date received: 12 December 2016; revised: 16 January 2017; accepted: 24 January 2017

Introduction

The exact neural mechanisms responsible for the initiation and maintenance of head pain associated with migraine remain unknown, although human brain imaging investigations have shown that during a migraine attack, activity increases in brainstem nuclei such as the spinal trigeminal nucleus, dorsal pons, midbrain periaqueductal gray matter, hypothalamus, and higher brain regions such as the thalamus, cingulate and insular cortices (1–3). In addition to activity changes during migraine attacks, a number of studies have also reported changes between migraines, such as altered sensitivity to somatosensory stimuli and indices of brain anatomy as well as changes in brainstem, thalamic and cortical oscillatory activity (4–6). The mechanisms behind how these functional and anatomical changes occur between migraines, the increases in regional brain activity during migraine and how the underlying factors that trigger a migraine attack all interact, remain hotly debated (7).

For some time, cerebrovascular changes that trigger changes in brain activity have been considered the foundation of migraine pathophysiology and critical

for the initiation of a migraine event. Although this might be true, an alternative proposal has emerged suggesting that migraine attacks are initiated by changes within one or more regions within the central nervous system, that is, a central “migraine generator” (8,9). It has been proposed that dysregulation of subcortical sites such as the hypothalamus and midbrain may enable brain activity changes that initiate and maintain a migraine attack, i.e. migraine could result from dysfunction of subcortical sites below the level of the diencephalon, leading to an “abnormal perception of basal level of primary traffic” (10). This idea is controversial, and has been the subject of fierce debate.

¹Department of Anatomy and Histology, University of Sydney, Sydney, NSW, Australia

²School of Medicine, Western Sydney University, Sydney, Australia

³UCLA School of Nursing and Brain Research Institute, University of California, Los Angeles, CA, USA

Corresponding author:

Luke A Henderson, Department of Anatomy and Histology, F13, University of Sydney, Australia.

Email: lukeh@anatomy.usyd.edu.au

A recent review focusing on the concept of a migraine generator suggested that in order to support this concept, evidence needs to be provided of "post-mortem histopathology showing potential anatomical and/or molecular abnormalities in candidate brainstem nuclei as compared between migraineurs and non-migraineurs" (11).

Whilst post-mortem studies are logistically difficult, it is possible to use anatomical brain imaging techniques to explore the anatomy of the brainstem in living individuals with and without migraine. Whilst several brain morphology studies have shown that migraine is associated with grey matter volume decreases in areas involved in pain processing including the prefrontal, cingulate and insular cortices as well as in the brainstem, none have focused specifically on the brainstem (5,12,13). This is critical, since the small size of the brainstem means that accurate spatial normalization is essential when exploring changes in regional anatomy. Using brainstem specific analysis techniques, we showed that individuals with painful trigeminal neuropathy, an orofacial neuropathic pain disorder, have reduced grey matter volume and free water movement ease (mean diffusivity) in the nucleus that receives direct nociceptor afferents from the orofacial region, the spinal trigeminal nucleus (14). Similar anatomical changes may also occur in individuals with migraine, as well as alterations in areas such as the midbrain periaqueductal grey matter. If such alterations exist, it would raise the possibility that such changes underlie functional changes that may aid in the generation of migraine or in the central transmission of peripherally initiated noxious information.

The aim of this investigation is to use voxel-based morphometry of T1-weighted anatomical and diffusion weighted images to determine if the trigeminal system displays altered anatomy in individuals with migraine. We hypothesize that, similar to painful trigeminal neuropathy, migraine is associated with reduced grey matter volume and mean diffusivity in the spinal trigeminal nucleus. Furthermore, given the mounting evidence of altered descending analgesic control in individuals with migraine, we also hypothesize that migraine is associated with altered anatomy in areas of the brainstem endogenous circuitry such as the midbrain periaqueductal gray matter.

Methods

Subjects

Twenty-five subjects with migraine (four males, mean [\pm SEM] age: 30.2 \pm 2.0) and 57 age and gender matched pain-free controls (14 males, age: 28.3 \pm 1.3) were studied. All control and migraine subjects were

recruited from the general population using an advertisement. There was no significant difference in age (t test; $p > 0.05$) or gender composition (χ^2 test, $p > 0.05$) between the two groups. Migraine subjects were diagnosed according to the criteria laid out by the International Classification of Headache Disorders (ICHD), 3rd edition, sections 1.1 and 1.2 (15). Five migraineurs reported aura associated with their migraines and the remaining 20 reported no aura. All migraineurs were scanned during an interictal period, that is, at least 72 hours after and 24 hours prior to a migraine event. Exclusion criteria for controls were the presence of any current pain or chronic pain condition, current use of analgesics or any neurological disorder. Exclusion criteria for migraineurs were any other pain condition other than migraine or any other neurological disorder. All migraine subjects indicated the intensity (6-point visual analogue scale; 0=no pain, 5=most intense imaginable pain) and drew the facial distribution of pain commonly experienced during a migraine attack. In addition, each subject described the qualities of their migraines and indicated any current treatments used to prevent or abort a migraine once started. Informed written consent was obtained for all procedures according to the Declaration of Helsinki seventh revision and local Institutional Human Research Ethics Committees approved the study.

MRI scanning

Subjects lay supine on the bed of a 3T MRI scanner (Philips Achieva, Neuroscience Research Australia, Sydney) with their head immobilized in a fitting 32-channel head coil. In all 25 migraine and 57 control subjects, a high-resolution T1-weighted anatomical image set covering the entire brain was collected (turbo field echo; echo time = 2.5 ms, repetition time = 5600 ms, flip angle = 8°, voxel size 0.8 \times 0.8 \times 0.8 mm). In addition, in 24 migraine and 22 of the 57 control subjects (no significant difference in age or gender), two high-resolution diffusion tensor imaging (DTI) image sets covering the entire brain were collected using a single-shot multisection spin-echo echo-planar pulse sequence (repetition time = 8788 ms; flip angle = 90°, matrix size = 112 \times 112, field of view = 224 \times 224 mm, slice thickness = 2.5 mm, 55 axial slices). For each slice, diffusion gradients were applied along 32 independent orientations with $b = 1000$ s/mm² after the acquisition of $b = 0$ s/mm² (b_0) images. Two DTI acquisitions were averaged to improve signal-to-noise ratios. One T1-weighted anatomical and one DTI image set from separate migraine subjects were later removed due to excessive head movement, resulting in 24 migraineurs in each of the brainstem analyses.

Image analysis

Brainstem VBM. Using Statistical Parametric Mapping version 12 software (Wellcome Trust Centre for Neuroimaging, University College London, UK), T1-weighted images were segmented and spatially normalized with a dedicated symmetrical brainstem template, using the SUIIT toolbox. Each image was cropped and the brainstem masked before spatial normalization. The subsequent spatial normalization and re-slicing was performed using the “preserve” option, which produced brainstem “maps” of grey matter probabilities modulated by the volume changes due to the normalization (probability \times volume), i.e. maps of regional grey matter volume. The maps were re-sliced into Montreal Neurological Institute (MNI) space, and spatially smoothed using a Gaussian filter (3 mm full-width-at-half-maximum). A small smoothing kernel was used to maintain spatial accuracy in small brainstem sites. Significant differences in grey matter between migraine and control subjects were determined using a voxel-by-voxel analysis ($p < 0.05$, false discovery rate corrected at a voxel level, minimum cluster size 5 contiguous voxels). Age and gender were included as nuisance variables. Clusters of significant difference were then overlaid onto the SUIIT brainstem template image for visualization. The location of these clusters was identified using the Atlas of the Human Brainstem by Paxinos and Huang (16).

Using SPM's Volumes toolbox, the values at each voxel in each significant cluster were extracted from the grey matter volume maps (probability \times volume) and averaged over the entire cluster. These values were plotted to illustrate possible correlations between local grey matter volumes and migraine characteristics, i.e. frequency, years suffering, intensity and days to next migraine (Pearson r , $p < 0.05$). To determine the potential influence of daily medication use, grey matter volumes in each cluster were compared between the migraineurs taking daily medication and those that were not (two-tailed t-test, $p < 0.05$, Bonferroni corrected for multiple comparisons). Differences in grey matter volumes in those with and without aura were also determined (two-tailed t-test, $p < 0.05$, Bonferroni corrected for multiple comparisons). In addition to extracting grey matter volumes, we extracted the mean, axial and radial diffusivity values from each significant cluster. We determined if any of these clusters showed significantly different diffusion values compared with controls, using a two-sample, two-tailed t-test ($p < 0.05$, Bonferroni corrected for multiple comparisons).

Brainstem DTI. The two diffusion tensor image sets from each subject were realigned based on the b_0 images, and the diffusion tensors were calculated from the images

using a linear model. Mean diffusivity (MD) whole-brain maps were then derived. These images were then coregistered to each individual subject's T1-weighted image and the brainstem was isolated, spatially normalized and re-sliced to the SUIIT template using the parameters derived from the aforementioned T1-weighted SUIIT analysis. This process resulted in brainstem maps of diffusion values, spatially normalized in MNI space with raw intensities preserved (non-modulated). The images were then smoothed (3 mm full-width-at-half-maximum) and significant differences in diffusion values between migraineurs and controls determined using a voxel-by-voxel analysis ($p < 0.05$, false discovery rate corrected at a voxel level, minimum cluster size 5 contiguous voxels). Age and gender were included as nuisance variables. No voxels survived this stringent threshold, so we reduced the stringency ($p < 0.001$, uncorrected) and performed cluster correction (Bonferroni correction by the number of voxels in each cluster) to assess if more subtle diffusion changes occurred. At this threshold, two clusters emerged and these were subsequently overlaid onto the SUIIT brainstem template image for visualization.

Using SPM's Volumes toolbox, the values at each voxel in each significant cluster were extracted from the mean, axial and radial diffusion maps and averaged over the entire cluster. These values were plotted, and correlations between these diffusion values and migraine characteristics were assessed (Pearson r , $p < 0.05$). To determine the potential influence of daily medication use, in migraineurs we compared diffusion values in each cluster in those taking daily medication with those that were not (two-tailed t-test, $p < 0.05$, Bonferroni corrected for multiple comparisons). Differences in diffusion values in those with and without aura were also determined (two-tailed t-test, $p < 0.05$, Bonferroni corrected for multiple comparisons). In addition, we extracted the grey matter volumes from each significant cluster and determined if these were significantly different to controls, using a two-sample, two-tailed t-test ($p < 0.05$, Bonferroni corrected for multiple comparisons).

Results

Migraine characteristics

Using a self-report questionnaire in which each migraine subject described the most common location of their migraines over the past 12 months, in 10 of the 25 migraineurs headaches were more common on the right side, in five they were more common on the left, and in the remaining 10 they were most often bilateral. A drawing showing the distribution of pain during migraine attacks is shown in Figure 1a. Migraine

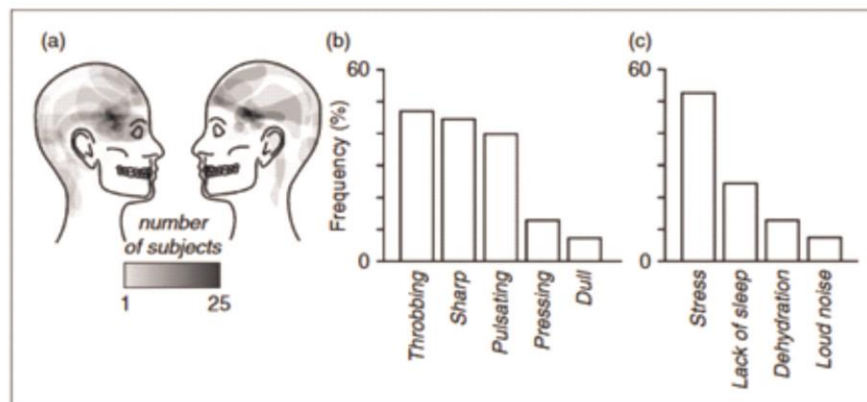


Figure 1. Pain distribution, quality and triggers in migraineurs ($n = 24$). (a) Overlap of individual migraine pain patterns: The white-grey-black scale bar corresponds to the pain overlap; (b) Frequency (percentage of subjects) of words chosen to describe the quality of migraine pain; (c) situations that most commonly trigger the onset of a migraine attack.

subjects most frequently described their migraine pain as “throbbing”, “sharp” and/or “pulsating” in nature and indicated that “stress”, “lack of sleep” and/or “dehydration” most often triggered their migraine attacks (Figures 1b and 1c). The mean estimated frequency of migraine attacks was 18.9 ± 2.3 per year, mean length of time since the onset of migraine attacks (years suffering) 14.6 ± 2.2 years, and mean pain intensity of migraines 3.7 ± 0.1 on a 6-point visual analogue scale. Although 15 of the 25 migraineurs were taking some form of daily medication (mostly the oral contraceptive pill), none of the migraine subjects was taking prophylactic medication prescribed for migraine. See Table 1 for migraine subject characteristics.

Grey matter volume changes (VBM)

Comparison of grey matter volumes in controls and migraineurs revealed significant regional grey matter volume changes in several regions (Figure 2, Table 2). Migraineurs displayed significant reductions in grey matter volume in the dorsal closed medulla in the region of the nucleus tractus solitarius (controls 0.27 ± 0.01 , migraineurs 0.22 ± 0.01 , $p < 0.001$), the region of the medullary raphe/spinal trigeminal nucleus (SpV) (mean \pm SEM grey matter probability \times volume: controls 0.16 ± 0.01 , migraineurs 0.11 ± 0.01 , $p < 0.001$), left and right dorsolateral pons (dlPons) (left: controls 0.27 ± 0.01 , migraineurs 0.23 ± 0.01 , $p = 0.001$; right: controls 0.286 ± 0.01 , migraineurs 0.23 ± 0.01 , $p < 0.001$) and in the region of the dorsomedial pons (dmPons) (controls 0.26 ± 0.01 , migraineurs 0.22 ± 0.01 , $p = 0.004$). In no brainstem region was grey matter volume greater in migraineurs compared with controls.

In migraine subjects, grey matter volumes in these clusters were not significantly correlated to migraine frequency (dorsal medulla: $r = -0.28$, $p = 0.19$; dorsal

medulla: $r = -0.14$, $p = 0.50$; raphe/SpV: $r = -0.31$, $p = 0.13$; left dlPons: $r = -0.45$, $p = 0.06$; right dlPons: $r = -0.38$, $p = 0.08$; dmPons: $r = -0.24$, $p = 0.27$), years suffering (dorsal medulla: $r = 0.18$, $p = 0.40$; raphe/SpV: $r = 0.18$, $p = 0.39$; left dlPons: $r = 0.17$, $p = 0.41$; right dlPons: $r = -0.38$, $p = 0.08$; dmPons: $r = 0.49$, $p = 0.02$), intensity of migraine pain (dorsal medulla: $r = 0.14$, $p = 0.45$; raphe/SpV: $r = -0.17$, $p = 0.44$; left dlPons: $r = -0.36$, $p = 0.08$; right dlPons: $r = -0.26$, $p = 0.22$; dmPons: $r = 0.09$, $p = 0.68$) or days to next migraine (dorsal medulla: $r = 0.21$, $p = 0.35$; raphe/SpV: $r = 0.40$, $p = 0.07$; left dlPons: $r = 0.19$, $p = 0.40$; right dlPons: $r = -0.06$, $p = 0.78$; dmPons: $r = 0.32$, $p = 0.15$). Comparison of those migraineurs taking daily medication with those that were not, revealed no significant differences in grey matter volumes in any of these regions (dorsal medulla: $p = 0.40$; raphe/SpV: $p = 0.19$; left dlPons: $p = 0.16$; right dlPons: $p = 0.51$; dmPons: $p = 0.45$). Comparison of those with and without aura also resulted in no significant differences (dorsal medulla: $p = 0.86$; raphe/SpV: $p = 0.39$; left dlPons: $p = 0.24$; right dlPons: $p = 0.34$; dmPons: $p = 0.93$). In addition, extraction of diffusivity values from each cluster revealed that only the medullary raphe displayed a different diffusion in migraineurs compared with controls (Figure 4a, Table 3). In the medullary raphe, mean, axial and radial diffusivity were significantly greater in migraineurs compared with controls.

Diffusion value changes (DTI)

In addition to changes in grey matter volume, DTI analysis at a more liberal statistical threshold revealed MD differences in two brainstem sites (Figure 3, Table 2). Compared with controls, migraineurs had greater MD in the region of the medullary raphe/SpV

Table 1. Migraine subject characteristics.

Subject	Age	Sex	Years suffering	Pain side	Aura	Frequency (per month)	Intensity (0-5)	Medication taken during migraine	Daily medication
1	31	F	25	R	Y	> 3	3-4	paracetamol	-
2	24	F	20	B	N	> 3	4	ibuprofen, paracetamol	OCP, budesonide /formoterol
3	26	F	12	R	N	2	3-4	ibuprofen	OCP
4	27	F	12	R	Y	1	4	ibuprofen	OCP
5	23	F	4	R	N	> 3	4	triptan	OCP, metformin hydrochloride
6	25	F	12	L	N	> 3	3	aspirin, rizatriptan	desvenlafaxine
7	21	F	1.5	L	N	> 3	3	ibuprofen, paracetamol, codeine	OCP
8	26	F	1	L	N	> 3	5	paracetamol	OCP
9	29	F	13	R	N	1	2.5	ibuprofen	zopiclone
10	26	F	5	R	N	1	2	Aspirin, codeine, ibuprofen	OCP
11	23	F	6	R	N	1	3-4	ibuprofen	OCP
12	23	F	10	B	N	0.5-1	4	ibuprofen, codeine	OCP
13	46	F	15-20	B	N	1	3	sumatriptan	-
14	41	F	40	B	N	2	4	sumatriptan	-
15	23	M	3-4	B	N	0.5-1	3.5	paracetamol, codeine	-
16	23	M	4-5	B	N	0.5-1	4	paracetamol	-
17	55	F	40	R	N	0.5-1	3-4	sumatriptan	telmisartan
18	26	M	20	R	N	0.5-1	4	metamizole	carbamazepine
19	49	F	30	B	N	0.5-1	5	rizatriptan, paracetamol	-
20	54	F	30	B	N	0.5-1	5	paracetamol, codeine eletriptan,	Candesartan
21	34	F	15	L	Y	2	3	paracetamol, ibuprofen	-
22	26	F	5	B	Y	1	3	paracetamol	OCP
23	25	F	7-8	L	N	> 3	3	rizatriptan benzoate	OCP
24	27	M	4	B	N	0.5-1	4	ibuprofen	serotonin reuptake inhibitor
25	28	F	25	R	Y	0.25	5	ibuprofen	methylphenidate

B = bilateral, L = left, OCP = oral contraceptive pill; R = right.

(mean \pm SEM [$\times 10^{-3}$] MD: controls 0.75 ± 0.02 , migraineurs 0.82 ± 0.02 , $p = 0.002$), left dIPons (controls 0.75 ± 0.01 , migraineurs 0.81 ± 0.01 , $p < 0.001$) and left midbrain periaqueductal gray matter (PAG: mean \pm SEM [$\times 10^{-3}$] MD: controls 0.90 ± 0.02 , migraineurs 0.96 ± 0.01 , $p = 0.005$). Within these three clusters, both axial and radial diffusion values were significantly greater in migraineurs compared with controls (raphe/SpV: axial: controls 1.03 ± 0.03 , migraineurs 1.14 ± 0.03 , $p = 0.002$; radial: controls 0.60 ± 0.02 , migraineurs 0.67 ± 0.02 , $p = 0.003$; dIPons: axial: controls 1.36 ± 0.02 , migraineurs 1.42 ± 0.02 , $p = 0.008$; radial: controls 0.45 ± 0.01 , migraineurs 0.52 ± 0.02 , $p = 0.007$; PAG: axial: controls 1.09 ± 0.02 , migraineurs 1.16 ± 0.02 , $p = 0.008$; radial: controls 0.81 ± 0.02 , migraineurs 0.87 ± 0.02 , $p = 0.005$). In no region was MD significantly less in migraineurs compared with controls.

In migraine subjects, MD values in these clusters were not significantly correlated to migraine frequency (raphe/SpV: $r = -0.03$, $p = 0.90$; dIPons: $r = 0.07$, $p = 0.72$; PAG: $r = 0.02$, $p = 0.91$), years suffering (raphe/SpV: $r = 0.28$, $p = 0.19$; dIPons: $r = 0.29$, $p = 0.16$; PAG: $r = 0.08$, $p = 0.71$), intensity of migraine pain (raphe/SpV: $r = 0.26$, $p = 0.22$; dIPons: $r = 0.32$, $p = 0.12$; PAG: $r = -0.17$, $p = 0.41$) or days to next migraine (raphe/SpV: $r = -0.29$, $p = 0.19$; dIPons: $r = 0.07$, $p = 0.75$; PAG: $r = 0.15$, $p = 0.51$). Comparison of those migraineurs taking daily medication with those that were not revealed no significant differences in MD in either of these regions (raphe/SpV: $p = 0.49$; dIPons: $p = 0.92$; PAG: $p = 0.47$). Comparison of those with and without aura also resulted in no significant differences (raphe/SpV: $p = 0.88$; dIPons: $p = 0.77$; PAG: $p = 0.50$). In addition, extraction of grey matter values from each cluster

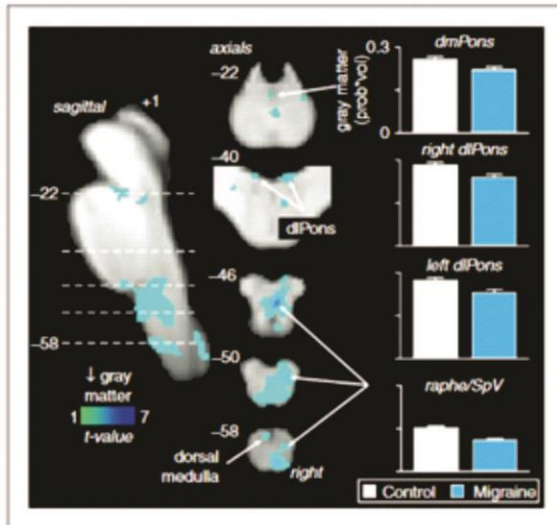


Figure 2. Regional grey matter volume changes in migraineurs ($n = 24$) compared with pain-free controls ($n = 57$) overlaid onto sagittal and axial brainstem template images. Significant grey matter volume decreases are represented by a t-statistic with a cool colour scale. Slice locations are indicated at the upper right of the sagittal and the upper left of the axial slices in Montreal Neurological Institute space. Plots of mean (\pm SEM) grey matter volumes derived from each region are shown to the right. Compared to controls, migraineurs have lower grey matter volumes in the right spinal trigeminal nucleus caudalis (SpV), medullary raphe, dorsal medulla, dorsolateral pons (dIPons) and dorsomedial pons.

revealed that grey matter was significantly reduced in migraineurs in the medullary raphe (controls 0.13 ± 0.01 , migraineurs 0.10 ± 0.01 , $p = 0.002$), but was not different between groups in the dIPons (controls 0.13 ± 0.01 , migraineurs 0.12 ± 0.01 , $p = 0.18$) or PAG (controls 0.18 ± 0.01 , migraineurs 0.17 ± 0.01 , $p = 0.44$) (Figure 4b, Table 3).

Discussion

The results of this study reveal that migraine is associated with changes in the volume and diffusion properties in a number of brainstem regions. Grey matter volume decreases occurred in the region that receives orofacial noxious afferents and in the dorsolateral and dorsomedial pons. In addition, both reduced grey matter volume and increased free water diffusivity occurred in areas of the descending pain modulatory system, that is, in the PAG, medullary raphe and dorsal medulla in the region of the subnucleus reticularis dorsalis. In migraine subjects, these grey matter volume and diffusivity changes were not influenced by daily medication use nor were they correlated to migraine frequency, duration or pain intensity.

Table 2. Montreal Neurological Institute (MNI) coordinates of significant grey matter volume ($p < 0.05$ false discovery rate corrected) and mean diffusivity ($p < 0.001$, uncorrected) differences between controls and migraineurs.

	MNI coordinates			cluster size	t-score
	x	y	z		
Grey matter volume: Controls > migraine					
Medullary raphe/spinal trigeminal nucleus	3	-36	-46	746	4.71
Dorsal closed medulla	1	-48	-63	48	3.57
Dorsolateral pons	4	-44	-40	66	4.60
right	11	-34	-25	33	4.39
left	-6	-44	-40	13	3.86
Dorsomedial pons	1	-26	-20	44	3.53
	0	-32	-22	10	3.02
Mean diffusivity: Migraine > controls					
Medullary raphe/SpV	2	-36	-47	15	3.00
Left dorsolateral pons	-4	-32	-18	7	3.25
Left midbrain periaqueductal gray	-6	-28	-3	5	2.78

Over the past decade a number of brain morphometric studies have explored grey matter changes associated with migraine (5,13,17–20). These studies report increased cortical volume/thickness in the primary somatosensory cortex, hippocampus and caudate nucleus and reduced volume in areas including the precentral gyrus, cingulate and insular cortices. None of these previous investigations focused their analysis specifically on the brainstem, and although one recent investigation did report a reduction in overall brainstem volume in migraineurs, the authors did not perform a voxel-by-voxel brainstem analysis (21). They did however find that migraine was associated with a significant overall brainstem volume reduction, consistent with the regional grey matter reductions reported in this investigation. Although investigation of the anatomy of higher brain centers is important, given the role of brainstem regions in transmitting noxious information from the cranial vessels and meninges, modulating noxious inputs and even its potential role as a migraine generator, the investigation of brainstem anatomy and function could highlight central changes critical for the generation of migraine pain.

It has been argued for some time that the headache phase of migraine results from activation of nociceptors in brain meninges and large cerebral arteries that are innervated by trigeminal afferents (22). In rodents, afferents innervating the dura mater and the middle meningeal artery terminate primarily in the caudalis and interpolaris divisions of the right spinal trigeminal nucleus as well as in the right upper cervical

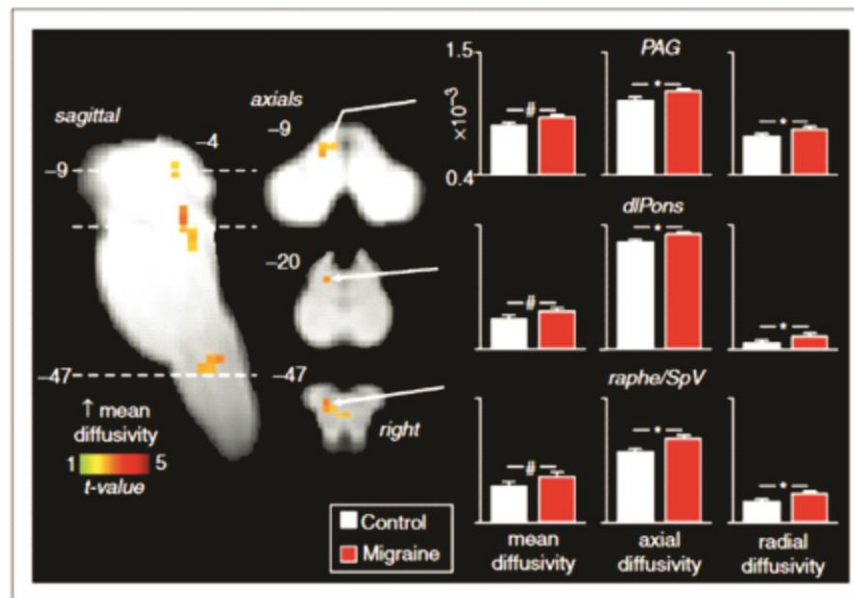


Figure 3. Regional mean diffusivity changes in migraineurs ($n = 24$) compared with pain-free controls ($n = 22$) overlaid onto sagittal and axial brainstem template images. Significant mean diffusivity (MD) increases are represented by a t -statistic with a hot colour scale. Slice locations are indicated at the upper right of the sagittal and the upper left of the axial slices in Montreal Neurological Institute space. Plots of mean (\pm SEM) MD, axial diffusivity and radial diffusivity derived from each region are shown to the right. Compared to controls, migraineurs show increased mean and axial diffusivity in the region of the medullary raphe/spinal trigeminal nucleus (SpV), dorsolateral pons (dlPons) and midbrain periaqueductal gray matter (PAG). # $p < 0.05$ voxel-by-voxel analysis; * $p < 0.05$ Bonferroni corrected 2-sample t -tests.

dorsal horn (23,24). Those afferents innervating the middle cerebral artery project to the trigeminal principal nucleus oralis and interpolaris subdivisions as well as the dorsal horn of the upper cervical spinal cord and the PAG (25). We found that migraine subjects had significantly reduced grey matter volumes in all divisions of SpV. We have recently reported decreased grey matter volumes in the right SpV in individuals with chronic orofacial neuropathic pain following endodontic treatment (14), although in contrast to migraineurs, these subjects also displayed reduced mean diffusivity in the same region.

The nature of the cellular changes underlying volumetric and diffusion changes is unclear. Whilst grey matter volume decrease may result from neuronal loss, it may also result from shrinkage or atrophy of neurons or glia, or synaptic loss (26). In addition, MD increases are a marker of more subtle changes in tissue microstructure, which may result from tissue shrinkage or gliosis (27). Whilst other forms of more constant neuropathic pain conditions are associated with neuronal degeneration in the region of primary afferent synapse, including significant reductions in inhibitory interneurons synapse (28–32) and increased sensitivity (33,34) it remains unknown if a similar phenomenon

occurs in migraineurs. Migraine is associated with cutaneous allodynia, which is likely driven by central sensitization within brainstem trigeminal neurons (35,36). Despite this increased sensitivity, it has been shown that during the interictal phase, migraineurs display reduced SpV sensitivity to trigeminal noxious stimulation compared with controls (37). Importantly, the same study showed that SpV activation during noxious stimuli increases to control levels in migraineurs in the 72-hour period prior to a migraine attack, suggesting the sensitivity of the trigeminal system alters over the migraine cycle. It is possible that there are also dynamic changes in regional grey matter volume within the brainstem that underlie this reported change in SpV sensitivity. We speculate that such dynamic changes could, for example, include changes in astrocyte activation and an associated release of gliotransmitters that sensitize trigeminal brainstem neurons, resulting in increased responsiveness to peripheral noxious inputs immediately before and during a migraine attack (38). Interestingly, none of the regional anatomical changes were correlated to migraine properties such as frequency, intensity or duration, which suggests that the changes are not cumulative over time and is consistent with the idea that they may be dynamic in nature and

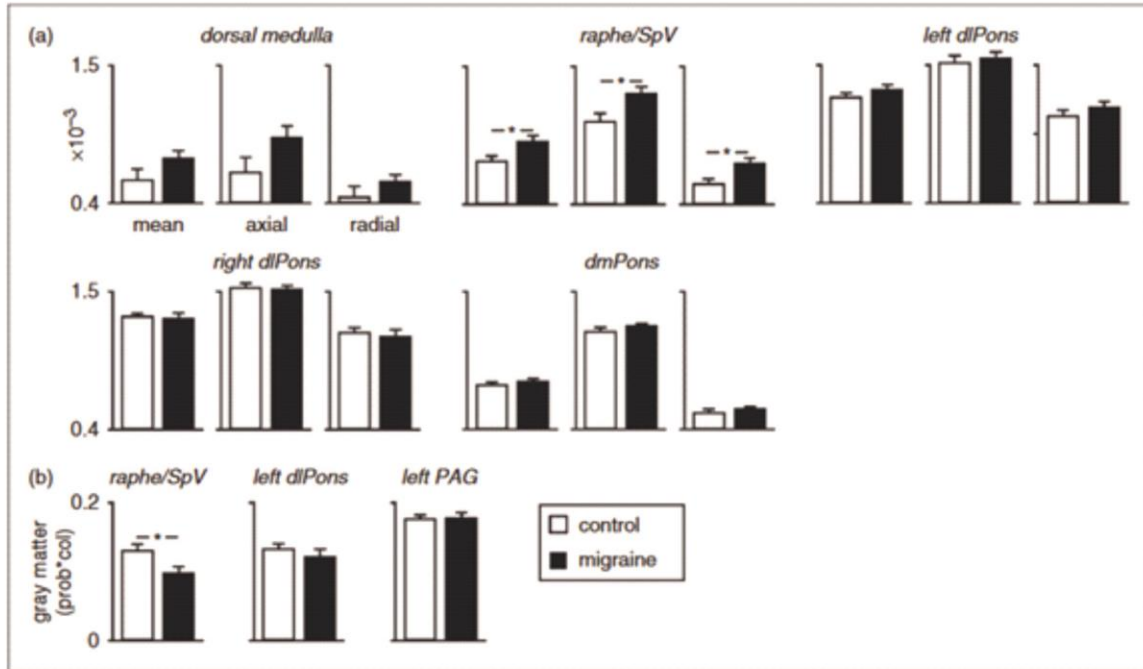


Figure 4. (a) Plots of mean (\pm SEM) MD, axial diffusivity and radial diffusivity derived from clusters displaying significantly lower grey matter volume in migraineurs compared with controls. Note that although all of these regions had significantly reduced grey matter volumes, only the medullary raphe also had significantly increased mean and axial diffusivity; (b) plots of mean (\pm SEM) grey matter volume derived from clusters displaying significantly increased mean diffusivity in migraineurs compared with controls. Only the medullary raphe displayed both grey matter volume and diffusivity changes in migraineurs. dlPons: dorsolateral pons, dmPons: dorsomedial pons; PAG: midbrain periaqueductal gray matter, SpV: spinal trigeminal nucleus. * $p < 0.05$ Bonferroni corrected two-sample t-tests.

Table 3. Diffusion and p values in clusters derived from the voxel based morphometry (VBM) grey matter volume analysis. The grey shading indicates clusters in which diffusivity values were significantly greater in migraineurs than in controls ($p < 0.05$, Bonferroni corrected). Note that only the medullary raphe/spinal trigeminal nucleus (SpV) displayed a significant increase in diffusivity compared with controls.

	Diffusivity values for clusters derived from VBM analysis				
	Dorsal medulla	Medullary raphe/SpV	Left dorsolateral pons	Right dorsolateral pons	Dorsomedial pons
Mean diffusivity ($\times 10^{-3}$)					
Controls	0.51 \pm 0.10	0.74 \pm 0.04	1.24 \pm 0.04	1.30 \pm 0.03	0.76 \pm 0.01
Migraineurs	0.70 \pm 0.07	0.90 \pm 0.05	1.30 \pm 0.04	1.29 \pm 0.04	0.78 \pm 0.01
Significance	$p = 0.07$	$p = 0.007$	$p = 0.19$	$p = 0.39$	$p = 0.09$
Axial diffusivity ($\times 10^{-3}$)					
Controls	0.64 \pm 0.12	1.06 \pm 0.06	1.53 \pm 0.04	1.55 \pm 0.03	1.19 \pm 0.02
Migraineurs	0.92 \pm 0.09	1.28 \pm 0.06	1.57 \pm 0.04	1.53 \pm 0.04	1.23 \pm 0.02
Significance	$p = 0.08$	$p = 0.007$	$p = 0.30$	$p = 0.36$	$p = 0.12$
Radial diffusivity ($\times 10^{-3}$)					
Controls	0.44 \pm 0.08	0.58 \pm 0.03	1.10 \pm 0.04	1.18 \pm 0.03	0.54 \pm 0.01
Migraineurs	0.57 \pm 0.06	0.726 \pm 0.04	1.17 \pm 0.04	1.15 \pm 0.03	0.56 \pm 0.01
Significance	$p = 0.10$	$p = 0.006$	$p = 0.13$	$p = 0.29$	$p = 0.10$

therefore unlikely to be correlated to such indices. Such dynamic changes would be consistent with astrocyte activation.

In addition to SpV, we found grey matter reduction and MD increases in the region of the medullary raphe, and MD increases with no grey matter change in the rostral dIPons and PAG. The PAG – medullary raphe – SpV/dorsal horn circuit forms part of a well-described endogenous analgesic brainstem circuitry that can inhibit incoming noxious information at the primary afferent synapse. The PAG region with altered diffusion was located in the region of the ventrolateral PAG column, an area that receives primarily deep noxious inputs and produces passive coping behaviors and opiate-mediated analgesia upon activation (39). Furthermore, experimental animal studies have shown that ventrolateral PAG stimulation inhibits SpV activity evoked by stimulation of the superior sagittal sinus (40), probably via the medullary raphe and in particular the nucleus raphe magnus (41,42). It is likely that altered PAG anatomy is associated with an altered ability of the individual to dampen incoming noxious trigeminal information, which would increase the propensity for migraine attacks.

We also found grey matter volume decreases in other brainstem regions thought to be responsible for endogenous analgesia, such as the dIPons and in the dorsal medulla in the region of the subnucleus reticularis dorsalis (43). We have recently shown that an individual's expression of conditioned pain modulation (CPM) analgesia, i.e., the ability for one noxious stimulus to inhibit another at a distant site, is associated with activity changes within the dIPons and the subnucleus reticularis dorsalis (43). Whilst reduced CPM responsiveness has been shown to occur in many chronic pain conditions (44), it appears that its role in migraine may be more subtle. Several reports suggested reduced CPM ability in migraine (45,46), others found no change (47,48) and one reported a gradual reduction in CPM responsiveness upon repeated noxious stimulation (49). These contradictory results suggest a more subtle role for endogenous pain mechanisms in migraine, and the apparent inconsistencies may reflect varying endogenous analgesic responsiveness across the migraine cycle. It might be the case that endogenous analgesic ability remains at control levels for the majority of an individual's migraine cycle but then reduces immediately prior to a migraine attack, increasing the likelihood of an attack. Consistent with this idea, it was recently reported that during a migraine attack, migraineurs displayed increased grey matter density in areas of the insula and putamen, changes that were not present during the interictal period (50), two regions that also display altered activity changes associated with CPM responsiveness (51).

In addition to anatomical changes in the SpV and brainstem, regions that can modulate trigeminal inputs, we also found decreased grey matter volume in the dorsomedial pons. This change was in the same region shown to be activated during migraine attacks (1,3,52). Furthermore, this region shows increased activation to noxious trigeminal stimulation during a migraine attack compared with that displayed during the interictal period (37). This pontine region encompasses the serotonergic paramedian raphe nucleus, which is consistent with the finding of increased serotonergic receptor availability within this region during migraine attacks (53). It has been shown that the pontine raphe region projects rostrally to the anterior forebrain and appears to be involved in emotional processing (54,55). Although this area may be involved in processing the emotional aspect of pain during migraine, its role is yet to be determined.

There are a number of methodological and subject related limitations to this study. It is known that analgesic and mood altering medications as well as the use of the contraceptive pill can change brain anatomy (56,57). Although only four of the 25 migraineurs were on daily analgesic or mood altering medications, 10 migraineurs were taking the oral contraceptive pill. Despite this, we are confident medication use did not play a significant role in our study, since we found no differences when comparing migraineurs that did and did not take any medication. In addition, since the spatial resolution of human brainstem imaging, particularly DTI, is relatively low, it is difficult to determine the precise location of each cluster with respect to small brainstem nuclei. We have however, ascribed the location of each significant cluster using brainstem atlases and placed the changes into context with respect to the existing human and experimental animal research. Future improvements in MRI spatial resolution will certainly aid in defining specific nuclei and tracts associated with migraine. Finally, we did use an uncorrected threshold for the initial overlay of diffusion differences between migraineurs and controls, which can result in false positives. However we used cluster correction to limit this potential issue and we are therefore confident that the changes reported in areas such as the PAG and medullary raphe are indeed appropriate (58).

Overall, our findings suggest that migraine is associated with anatomical changes within various brainstem structures involved in trigeminal noxious transmission and endogenous analgesia. Whilst our data clearly show that, even between attacks, migraineurs have altered brainstem structure, it remains unknown what effect these changes have on brainstem processing. Evidence of altered brainstem processing at different stages of the migraine cycle raises the possibility of dynamic changes in brainstem structure and

function throughout the migraine cycle, which may either trigger or alter the sensitivity of the brainstem so that an external trigger results in a migraine attack. Future investigations exploring brainstem resting activity, evoked activity and anatomy over the

migraine cycle may provide evidence supporting such a proposal. If dynamic changes in brainstem function and structure do occur, we may be in a position to modify these changes and potentially prevent the triggering of a migraine attack.

Key findings

- We found grey matter volume decreases and diffusivity increases in the brainstem of migraineurs.
- These anatomical changes occurred in parts of the trigeminal and endogenous analgesia brainstem systems.
- These changes may underlie increased sensitivity to noxious inputs or the initiation of migraine attacks.

Declaration of conflicting interests

The authors declared no potential conflicts of interest with respect to the research, authorship, and/or publication of this article.

Funding

The authors disclosed receipt of the following financial support for the research, authorship, and/or publication of this article: This work was supported by grants awarded by the National Health and Medical Research Council of Australia.

References

1. Bahra A, Matharu MS, Buchel C, et al. Brainstem activation specific to migraine headache. *Lancet* 2001; 357: 1016–1017.
2. Weiller C, May A, Limmroth V, et al. Brain stem activation in spontaneous human migraine attacks. *Nat Med* 1995; 1: 658–660.
3. Afridi SK, Giffin NJ, Kaube H, et al. A positron emission tomographic study in spontaneous migraine. *Arch Neurol* 2005; 62: 1270–1275.
4. Schwedt TJ, Chiang CC, Chong CD, et al. Functional MRI of migraine. *Lancet Neurol* 2015; 14: 81–91.
5. Kim JH, Suh SI, Seol HY, et al. Regional grey matter changes in patients with migraine: A voxel-based morphometry study. *Cephalalgia* 2008; 28: 598–604.
6. Porcaro C, Di Lorenzo G, Seri S, et al. Impaired brainstem and thalamic high-frequency oscillatory EEG activity in migraine between attacks. *Cephalalgia* 2016; doi: 10.1177/0333102416657146.
7. Goadsby PJ, Charbit AR, Andreou AP, et al. Neurobiology of migraine. *Neuroscience* 2009; 161: 327–341.
8. Akerman S, Holland PR and Goadsby PJ. Diencephalic and brainstem mechanisms in migraine. *Nat Rev Neurosci* 2011; 12: 570–584.
9. Goadsby PJ. The vascular theory of migraine – a great story wrecked by the facts. *Brain* 2009; 132: 6–7.
10. Goadsby PJ and Akerman S. The trigeminovascular system does not require a peripheral sensory input to be activated – migraine is a central disorder. Focus on ‘Effect of cortical spreading depression on basal and evoked traffic in the trigeminovascular sensory system’. *Cephalalgia* 2012; 32: 3–5.
11. Borsook D and Burstein R. The enigma of the dorsolateral pons as a migraine generator. *Cephalalgia* 2012; 32: 803–812.
12. Rocca MA, Ceccarelli A, Falini A, et al. Brain gray matter changes in migraine patients with T2-visible lesions: A 3-T MRI study. *Stroke* 2006; 37: 1765–1770.
13. Valfrè W, Rainero I, Bergui M, et al. Voxel-based morphometry reveals gray matter abnormalities in migraine. *Headache* 2008; 48: 109–117.
14. Wilcox SL, Gustin SM, Macey PM, et al. Anatomical changes at the level of the primary synapse in neuropathic pain: Evidence from the spinal trigeminal nucleus. *J Neurosci* 2015; 35: 2508–2515.
15. The International Classification of Headache Disorders 3rd edition (Beta version). *Cephalalgia* 2013; 33: 629–808.
16. Paxinos G and Huang X. *Atlas of the Human Brainstem*, 1st edn. San Diego, CA: Academic Press, 1995.
17. DaSilva AF, Granziera C, Snyder J, et al. Thickening in the somatosensory cortex of patients with migraine. *Neurology* 2007; 69: 1990–1995.
18. Maleki N, Becerra L, Brawn J, et al. Common hippocampal structural and functional changes in migraine. *Brain Struct Funct* 2013; 218: 903–912.
19. Maleki N, Becerra L, Brawn J, et al. Concurrent functional and structural cortical alterations in migraine. *Cephalalgia* 2012; 32: 607–620.
20. Schmidt-Wilcke T, Ganssbauer S, Neuner T, et al. Subtle grey matter changes between migraine patients and healthy controls. *Cephalalgia* 2008; 28: 1–4.
21. Bilgic B, Kocaman G, Arslan AB, et al. Volumetric differences suggest involvement of cerebellum and brainstem in chronic migraine. *Cephalalgia* 2016; 36: 301–308.
22. Olesen J, Burstein R, Ashina M, et al. Origin of pain in migraine: Evidence for peripheral sensitisation. *Lancet Neurol* 2009; 8: 679–690.
23. Liu Y, Broman J and Edvinsson L. Central projections of the sensory innervation of the rat middle meningeal artery. *Brain Res* 2008; 1208: 103–110.
24. Liu Y, Broman J and Edvinsson L. Central projections of sensory innervation of the rat superior sagittal sinus. *Neuroscience* 2004; 129: 431–437.
25. Arbab MA, Delgado T, Wiklund L, et al. Brain stem terminations of the trigeminal and upper spinal ganglia innervation of the cerebrovascular system: WGA-HRP transganglionic study. *J Cereb Blood Flow Metab* 1988; 8: 54–63.

26. May A and Gaser C. Magnetic resonance-based morphometry: A window into structural plasticity of the brain. *Curr Opin Neurol* 2006; 19: 407–411.
27. Sierra A, Laitinen T, Lehtimäki K, et al. Diffusion tensor MRI with tract-based spatial statistics and histology reveals undiscovered lesioned areas in kainate model of epilepsy in rat. *Brain Struct Funct* 2011; 216: 123–135.
28. Azkue JJ, Zimmermann M, Hsieh TF, et al. Peripheral nerve insult induces NMDA receptor-mediated, delayed degeneration in spinal neurons. *Eur J Neurosci* 1998; 10: 2204–2206.
29. de Novellis V, Siniscalco D, Galderisi U, et al. Blockade of glutamate mGlu5 receptors in a rat model of neuropathic pain prevents early over-expression of pro-apoptotic genes and morphological changes in dorsal horn lamina II. *Neuropharmacology* 2004; 46: 468–479.
30. Scholz J, Broom DC, Youn DH, et al. Blocking caspase activity prevents transsynaptic neuronal apoptosis and the loss of inhibition in lamina II of the dorsal horn after peripheral nerve injury. *J Neurosci* 2005; 25: 7317–7323.
31. Sugimoto T, Bennett GJ and Kajander KC. Transsynaptic degeneration in the superficial dorsal horn after sciatic nerve injury: Effects of a chronic constriction injury, transection, and strychnine. *Pain* 1990; 42: 205–213.
32. Whiteside GT and Munglani R. Cell death in the superficial dorsal horn in a model of neuropathic pain. *J Neurosci Res* 2001; 64: 168–173.
33. Woolf CJ and Mannion RJ. Neuropathic pain: Aetiology, symptoms, mechanisms, and management. *Lancet* 1999; 353: 1959–1964.
34. Cohen SP and Mao J. Neuropathic pain: Mechanisms and their clinical implications. *BMJ* 2014; 348: f7656.
35. Malick A and Burstein R. Peripheral and central sensitization during migraine. *Funct Neurol* 2000; 15: S28–S35.
36. Burstein R, Cutrer MF and Yarnitsky D. The development of cutaneous allodynia during a migraine attack: clinical evidence for the sequential recruitment of spinal and supraspinal nociceptive neurons in migraine. *Brain* 2000; 123: 1703–1709.
37. Stankewitz A, Aderjan D, Eippert F, et al. Trigeminal nociceptive transmission in migraineurs predicts migraine attacks. *J Neurosci* 2011; 31: 1937–1943.
38. Hughes SW, Lorincz ML, Parri HR, et al. Infralow (<0.1 Hz) oscillations in thalamic relay nuclei: basic mechanisms and significance to health and disease states. *Prog Brain Res* 2011; 193: 145–162.
39. Bandler R and Shipley MT. Columnar organization in the midbrain periaqueductal gray: Modules for emotional expression? *Trends Neurosci* 1994; 17: 379–389.
40. Knight YE and Goadsby PJ. The periaqueductal grey matter modulates trigeminovascular input: A role in migraine? *Neuroscience* 2001; 106: 793–800.
41. Basbaum AI and Fields HL. Endogenous pain control mechanisms: Review and hypothesis. *Ann Neurol* 1978; 4: 451–462.
42. Mason P. Deconstructing endogenous pain modulations. *J Neurophysiol* 2005; 94: 1659–1663.
43. Youssef AM, Macefield VG and Henderson LA. Pain inhibits pain; human brainstem mechanisms. *Neuroimage* 2016; 124: 54–62.
44. Yarnitsky D. Role of endogenous pain modulation in chronic pain mechanisms and treatment. *Pain* 2015; 156: S24–S31.
45. Sandrini G, Rossi P, Milanov I, et al. Abnormal modulatory influence of diffuse noxious inhibitory controls in migraine and chronic tension-type headache patients. *Cephalalgia* 2006; 26: 782–789.
46. de Tommaso M, Difruscolo O, Sardaro M, et al. Effects of remote cutaneous pain on trigeminal laser-evoked potentials in migraine patients. *J Headache Pain* 2007; 8: 167–174.
47. Perrotta A, Serrao M, Sandrini G, et al. Sensitisation of spinal cord pain processing in medication overuse headache involves supraspinal pain control. *Cephalalgia* 2010; 30: 272–284.
48. Teepker M, Kunz M, Peters M, et al. Endogenous pain inhibition during menstrual cycle in migraine. *Eur J Pain* 2014; 18: 989–998.
49. Nahman-Averbuch H, Granovsky Y, Coghill RC, et al. Waning of “conditioned pain modulation”: A novel expression of subtle pronociception in migraine. *Headache* 2013; 53: 1104–1115.
50. Coppola G, Di Renzo A, Tinelli E, et al. Evidence for brain morphometric changes during the migraine cycle: A magnetic resonance-based morphometry study. *Cephalalgia* 2015; 35: 783–791.
51. Youssef AM, Macefield VG and Henderson LA. Cortical influences on brainstem circuitry responsible for conditioned pain modulation in humans. *Hum Brain Mapp* 2016; 37: 2630–2644.
52. Denuelle M, Fabre N, Payoux P, et al. Hypothalamic activation in spontaneous migraine attacks. *Headache* 2007; 47: 1418–1426.
53. Demarquay G, Lothe A, Royet JP, et al. Brainstem changes in 5-HT_{1A} receptor availability during migraine attack. *Cephalalgia* 2011; 31: 84–94.
54. Vertes RP. A lectin horseradish peroxidase study of the origin of ascending fibers in the medial forebrain bundle of the rat. The upper brainstem. *Neuroscience* 1984; 11: 669–690.
55. Lee TM, Sun D, Wong NM, et al. A pontine region is a neural correlate of the human affective processing network. *EBioMedicine* 2015; 2: 1799–1805.
56. Younger JW, Chu LF, D’Arcy NT, et al. Prescription opioid analgesics rapidly change the human brain. *Pain* 2011; 152: 1803–1810.
57. Petersen N, Touroutoglou A, Andreano JM, et al. Oral contraceptive pill use is associated with localized decreases in cortical thickness. *Hum Brain Mapp* 2015; 36: 2644–2654.
58. Woo CW, Krishnan A and Wager TD. Cluster-extent based thresholding in fMRI analyses: Pitfalls and recommendations. *Neuroimage* 2014; 91: 412–419.

Appendix II.

Changes in brainstem pain modulation circuitry function over the migraine cycle

Title: Changes in brainstem pain modulation circuitry function over the migraine cycle.

Abbreviated title: Brainstem connectivity and migraine

Accepted for publication 2018: *Journal of Neuroscience*

Authors: Kasia K. Marciszewski¹, Noemi Meylakh¹, Flavia Di Pietro¹, Emily P. Mills¹, Vaughan G. Macefield², Paul M. Macey³ and Luke A. Henderson¹

¹Department of Anatomy and Histology, Sydney Medical School, University of Sydney, Sydney, NSW, Australia, 2006; ²School of Medicine, Western Sydney University, Sydney, Australia; ³UCLA School of Nursing and Brain Research Institute, University of California, Los Angeles, California 90095, United States.

Corresponding author: Luke A. Henderson, Department of Anatomy and Histology, F13, University of Sydney, Australia. lukeh@anatomy.usyd.edu.au (email); +612 9351 7063 (Tel) +612 9351 6556 (Fax)

Pages: 35; Figures: 5; Tables: 1

Words Abstract: 247; Introduction: 648; Discussion: 1750.

Conflict of interest: The authors declare no competing financial interests

Acknowledgements: This research was supported by the National Health and Medical Research Council of Australia, grant 1143547. We wish to thank the many volunteers in this study.

ABSTRACT

The neural mechanism responsible for migraine remains unclear. Whilst an external trigger has been proposed to initiate a migraine, it has also been proposed that changes in brainstem function are critical for migraine headache initiation and maintenance. Although the idea of altered brainstem function has some indirect support, no study has directly measured brainstem pain modulation circuitry function in migraineurs particularly immediately prior to a migraine. In male and female humans, we performed functional magnetic resonance imaging in 31 control and 31 migraineurs at various times in their migraine cycle. We measured brainstem function during noxious orofacial stimulation and assessed resting-state functional connectivity. Firstly, we found that in individual migraineurs, pain sensitivity increased over the interictal period, but then dramatically decreased immediately prior to a migraine. Secondly, despite overall similar pain intensity ratings between groups, in the period immediately prior to a migraine, compared to controls and other migraine phases, migraineurs displayed greater activation during noxious orofacial stimulation in the spinal trigeminal nucleus and reduced functional connectivity of this region with the rostral ventromedial medulla. Additionally, during the interictal phase, migraineurs displayed reduced activation of the midbrain periaqueductal gray matter and enhanced periaqueductal gray connectivity with the rostral ventromedial medulla. These data support the hypothesis that brainstem sensitivity fluctuates throughout the migraine cycle. However in contrast to the prevailing hypothesis, our data suggest that immediately prior to a migraine attack, endogenous analgesic mechanisms are enhanced and incoming noxious inputs are less likely to reach higher brain centres.

SIGNIFICANCE STATEMENT

It has been hypothesised that alterations in brainstem function are critical for the generation of migraine. In particular, modulation of orofacial pain pathways by brainstem circuits alter the propensity of external triggers or on-going spontaneous activity to evoke a migraine attack. We sought to obtain empirical evidence to support this theory. Contrary to our hypothesis, we found pain sensitivity decreased immediately prior to a migraine and this was coupled with increased sensitivity of the spinal trigeminal nucleus to noxious stimuli and resting connectivity within endogenous pain modulation circuitry alters across the migraine cycle. These changes may reflect enhanced and diminished neural tone states proposed to be critical for the generation of a migraine and underlie cyclic fluctuations in migraine brainstem sensitivity.

INTRODUCTION

Migraine is a common, distressing disorder characterised by headaches often accompanied by aura, nausea, and sensitivity to light and sound. While the exact neural mechanisms surrounding migraine head pain are still debated, human brain imaging investigations have shown that during a migraine attack activity increases in a number of cortical areas such as the cingulate cortex, insula, thalamus, and hypothalamus, as well as brainstem nuclei such as the spinal trigeminal nucleus (SpV), dorsal pons, and midbrain periaqueductal gray matter (PAG) (Bahra et al., 2001b; Borsook et al., 2016; Coppola et al., 2016; Denuelle et al., 2007; Tajti et al., 2012). These sites are particularly important in pain processing since the SpV is the site of orofacial nociceptor afferent termination and the PAG is involved in the modulation of noxious inputs and generation of autonomic and behavioural consequences of pain (Keay & Bandler, 2002; Sessle, 2000). Additionally, several studies have shown that even between attacks, migraineurs display neural changes such as decreased grey matter volume density, altered sensitivity to somatosensory stimuli, and changes in brainstem, thalamic and cortical oscillatory activity (C. D. Chong, Plasencia, Frakes, & Schwedt, 2017; K. K. Marciszewski, N. Meylakh, F. Di Pietro, V. G. Macefield, et al., 2018; V. A. Mathur et al., 2016; Noemi Meylakh et al., 2018; Porcaro et al., 2017a).

A recent review has proposed that these observed changes are not permanent, but dynamic in nature (May, 2017b). Building on the current focus of migraine research in identifying a structures in the brainstem pain-modulation system that may be associated with the initiation of a migraine attack (Akerman et al., 2011; Schulte & May, 2017), this review suggests that the initiation and maintenance of migraine attacks is unlikely to be caused by one area of the brainstem. It is far more likely that spontaneous fluctuations of complex networks involving the hypothalamus, brainstem pain-modulation circuitry, and possibly higher cortical areas, lead to the initiation and termination of headache attacks. While several independent functional studies have

identified activation of brainstem sites thought to be involved in endogenous pain-modulatory function, both during and between attacks (Stankewitz et al., 2011; Weiller, May, Limmroth, Juptner, Kaube, Schayck, Coenen, & Diener, 1995), few studies have tracked changes in brain sensitivity, activity, and volume throughout all stages of the migraine cycle. Importantly, few have explored the critical 24-hour period preceding a migraine, which is essential if we are to understand how migraines are initiated.

Using functional magnetic resonance imaging (fMRI), we recently reported increased resting infra-slow oscillatory activity (0.03-0.06Hz) and altered hypothalamic-brainstem functional connectivity in migraineurs *only* in the period immediately prior to a migraine attack, when individuals were not in pain (Noemi Meylakh et al., 2018). Importantly, these changes did not occur immediately after the migraine when individuals are recovering from an attack, or during the interictal phase. These data are consistent with the idea that the initiation of a migraine is associated with changes in brain function, in particular, changes within the brainstem. Indeed, it has been hypothesized that changes in sensitivity of brainstem regions to noxious orofacial inputs are critical for the initiation of a migraine. More specifically, in migraineurs, brainstem function oscillates between an (i) “enhanced” neural tone state during which the effectiveness of endogenous analgesic mechanisms is too great to allow incoming noxious inputs to evoke head pain, and a (ii) “diminished” state during which endogenous analgesic mechanisms are limited and incoming noxious inputs can evoke head pain (Burstein et al., 2015). Currently, there is little neural evidence to support the idea of altered brainstem endogenous modulation of SpV immediately prior to a migraine.

The aim of this investigation is to determine if functional connectivity within the brainstem endogenous pain modulating circuitry is altered throughout the migraine cycle. Furthermore, we aim to determine whether individuals with migraine show altered sensitivity and neural activity to noxious stimuli applied to the trigeminal nerve distribution in different stages of the migraine cycle. We hypothesise that migraineurs will show increased sensitivity and SpV activation to noxious

stimuli and reduced functional connectivity within the brainstem pain modulation circuitry immediately prior to a migraine attack.

METHODS

Subjects:

Thirty-one subjects with migraine (6 males, mean [\pm SEM] age: 29.6 \pm 1.7 years, range 19-55 years) and 60 pain-free controls (20 males; mean [\pm SEM] age: 26.2 \pm 0.9 years, range 19-56 years) were recruited from the general population using an advertisement. Migraine subjects were diagnosed according to the criteria set by the International Classification of Headache Disorders (ICHD) 3rd edition, sections 1.1 and 1.2. Seven migraineurs reported experiencing aura with their migraines, and the remaining 24 reported no aura. Of the 31 migraineurs, 28 were scanned during the interictal period (6 males, mean [\pm SEM] age: 29.6 \pm 1.8 years), that is, between 72 hours after and 24 hours prior to a migraine attack; 10 during the 24-hour period immediately prior to a migraine (3 males, age 29.1 \pm 3.4 years) and 10 within the 72-hour period following a migraine (1 male, age 31 \pm 3.1 years). For subjects scanned prior to an attack, there was no predicting factor that they were within 24 hours of a migraine. Six migraineurs were scanned during all 3 phases, and another 5 migraineurs were scanned during 2 of 3 phases.

All migraine subjects indicated the pain intensity (6-point visual analogue scale; 0 = no pain, 5 = most intense imaginable pain) and facial distribution (drawing) of pain they commonly experience during a migraine attack. Each subject described the qualities of their migraines and indicated any current treatments used to prevent or abort a migraine once started. Exclusion criteria for controls were the presence of any current pain or chronic pain condition, current use of analgesics, and any neurological disorder. Exclusion criteria for migraineurs were any pain condition other than migraine, and any other neurological disorder. Informed written consent was

obtained for all procedures according to the Declaration of Helsinki 7th revision and local Institutional Human Research Ethics Committees approved the study. Data from 25 of the 29 migraineurs were used in a previous investigation (K. K. Marciszewski, N. Meylakh, F. Di Pietro, V. G. Macefield, et al., 2018).

MRI acquisition:

In all subjects, prior to entering the MRI scanner, a 3x3cm MRI-compatible thermode (Medoc) was placed on the right side of the mouth covering the upper and lower lips for each subject. In migraineurs this was done on the side most commonly experiencing headaches (5 left-sided, 23 right-sided). Care was taken to secure the thermode in the same location in each individual subject and to ensure it did not cross the midline. A temperature that evoked moderate pain ratings was determined for each individual subject with a Thermal Sensory Analyser (TSA-II, Medoc), from a resting temperature of 32°C to temperatures at 0.5°C intervals between 44 and 49°C. Temperatures were randomly applied in 15 second intervals for 10 seconds during which each subject rated the pain intensity using a 10-point Computerised Visual Analogue Scale (CoVAS, Medoc; 0 = no pain, 10 = worst imaginable pain). The temperature at which individuals indicated a pain intensity rating of approximately 6 out of 10, was used for the remainder of the experiment.

All subjects then lay supine on the bed of a 3T MRI scanner (Philips, Achieva) with their head immobilised in a 32-channel head coil. With each subject relaxed and at rest, a high-resolution 3D T1-weighted anatomical image set covering the entire brain was collected (turbo field echo; field of view 250 x 250 mm, matrix size = 288 x 288, slice thickness = 0.87 mm, repetition time = 5600 ms, echo time = 2.5 ms, flip angle = 8°). A series of 180 gradient-echo echo planar resting-state fMRI volumes, using blood oxygen level-dependent (BOLD) contrast, was then collected. Each image volume contained 35 axial slices covering the entire brain (field of

view = 240 x 240 mm, matrix size = 80 x 78, slice thickness = 4 mm, repetition time = 2000 ms; echo time = 30 ms, flip angle = 90°). Following this resting state fMRI series, a series of 140 gradient-echo echo planar fMRI image volumes with BOLD contrast was collected with each image volume covering the entire brain (38 axial slices, repetition time = 2500 ms, raw voxel size 1.5 x 1.5 x 4.0 mm thick). Following a 30-volume baseline period, 8 noxious thermal stimuli were delivered (Figure 1A). Each noxious stimulus was delivered for 15 seconds (including ramp up and down periods of 2.5 seconds each), followed by a 6-volume baseline (32°C) period. During each period of noxious stimulation, the subject was asked to rate the pain intensity on-line using the CoVAS.

Pain rating analysis:

For each subject, the mean pain intensity ratings during each of the 8 noxious stimulus periods were calculated and plotted. Our aim was to explore changes in brain activation patterns over the migraine cycle compared with controls. Since we found that overall the control group rated the pain intensity higher than the migraineurs, we removed those controls with higher pain ratings in order to match pain intensities across all control and migraine groups (Figure 1B and 1C). In addition, for the pain activation protocol, we removed 7 migraineurs scanned during the interictal, 3 scanned immediately prior to migraine phase and 2 scanned immediately following migraine phase due to excessive head motion (>1mm volume-to-volume movement in the X, Y and Z planes and 0.05 radians in the pitch, roll and yaw directions. There was no significant difference in applied thermode temperature (°C) between the groups after removal of these subjects (Figure 1D).

The thermal stimulation analysis was conducted on a control group of 31 subjects (10 males, mean [\pm SEM] age: 26.5 \pm 1.2 years), interictal migraine group of 21 subjects (4 males, mean age: 29.8 \pm 2.1 years), immediately prior to migraine group of 7 subjects (2 males, mean

age: 30.4 ± 4.7 years) and immediately following migraine group of 8 subjects (1 male, mean age: 29.4 ± 1.9 years). There was no significant difference in age (t test; $p > 0.05$), gender composition (X^2 test, $p > 0.05$), pain rating (t test; $p > 0.05$), or stimulus temperature (t test; $p > 0.05$). To explore changes throughout the migraine cycle, we plotted the mean (\pm SEM) pain intensity ratings for the following periods: >30 days until next migraine ($n=12$), 30 to 10 days until next migraine ($n=4$), 9 to 2 days until next migraine ($n=5$), 1 day until next migraine ($n=7$), and 1 to 3 days following a migraine ($n=8$). In addition, in 5 subjects, thermal stimulation testing was performed during both the interictal and immediately prior to migraine phases and in another subject 4 sessions including one 2 days prior to a migraine were collected. For these subjects, their pain intensity ratings during each session were plotted individually. Finally, we used the same subjects to run the resting state connectivity analysis but only needed to remove 3 control subjects due to excessive head movement (28 controls, 28 interictal migraineurs, 10 immediately prior to a migraine, 10 immediately following migraine, no significant differences in age or gender).

MRI Image analysis:

Using SPM12 (K. J. Friston et al., 1994) and custom software, all fMRI images in the resting-state and the thermal stimuli protocol were motion corrected and subjects with excessive head movement removed as described above. Five migraineurs experienced migraines most commonly on the left side and the thermode was placed on the left side of the mouth, therefore their images were reflected in the X plane (“flipped”) so that fMRI signals could be assessed ipsilateral and contralateral to the most common side of migraine. The effect of movement on signal intensity was modelled and removed, and physiological (i.e. cardiovascular and respiratory) noise was modelled and removed using the DRIFTER toolbox (Särkkä et al., 2012). The fMRI images were linear detrended to remove global signal intensity changes and each subject’s fMRI image set was co-registered to their own T1-weighted anatomical image set so that the T1-

weighted and fMRI images were in the same locations in three-dimensional space. Using brainstem-specific isolation software (SUIT toolbox) (Diedrichsen, 2006b), a mask of the brainstem was created individually for each subject for both the T1 and fMRI image sets. Using these masks, the brainstem of the T1 and fMRI image sets were isolated and then spatially normalised to a brainstem-specific template in Montreal Neurological Institute (MNI) space and spatially smoothed using a 3mm full-width half maximum Gaussian filter.

Noxious thermal stimuli; experimental design and statistical analysis:

Significant changes in signal intensity during the 8 test stimuli were determined using a repeated box-car model convolved with a canonical haemodynamic response function and time dispersions. Firstly, we assessed regional signal intensity increases and decreases across all four subject groups, primarily to verify that orofacial noxious stimuli activate the region of the SpV (random effects conjunction ANOVA, $p < 0.05$, family-wise error corrected for multiple comparisons). Following this, significant differences in brainstem activation patterns were determined between (i) controls and interictal migraineurs, (ii) controls and migraineurs during the phase immediately prior to a migraine, and (iii) controls and migraineurs during the phase immediately following a migraine (two-group random effects analysis, $p < 0.001$ uncorrected for multiple comparisons, minimum cluster size 2 contiguous voxels, age and gender included as nuisance variables). Given we hypothesized that noxious thermal stimuli would be associated with activation in brainstem regions such as the SpV and PAG, we created regions of interests comprising 3mm-radius spheres in these brainstem sites based on the atlas by Paxinos and Huang (G. Paxinos & X.-F. Huang, 1995). Following the initial uncorrected threshold of $p < 0.001$, we applied small volume corrections using these regions of interest ($p < 0.05$) to reduce the likelihood of Type II errors.

Significant clusters were overlaid onto a standard brainstem template in MNI space. For each significant cluster, the percentage change in signal intensity was extracted by comparing

the signal intensity of the 30 baseline volumes with both the signal intensities during the 8 noxious thermal stimuli periods (“on” periods) and signal intensities during the intervening rest periods (“off” periods). These signal intensity changes were extracted for all four groups and significant differences between groups determined ($p < 0.05$, two-tailed, two-sample t test, Bonferroni corrected for multiple comparisons). Significant differences between controls and the group from which the cluster was derived during the original voxel-by-voxel analysis were not determined, to avoid “double-dipping”. In addition, to explore changes throughout the migraine cycle, we plotted the mean (\pm SEM) signal changes for the following periods: >30 days until next migraine ($n=12$), 30 to 10 days until next migraine ($n=4$), 9 to 2 days until next migraine ($n=5$), 1 day until next migraine ($n=7$), and 1 to 3 days following a migraine ($n=8$).

Functional connectivity: experimental design and statistical analysis:

We performed brainstem-only functional connectivity analyses using a seeding region encompassing the rostral ventromedial medulla (RVM) to determine resting connectivity strengths in the well-described PAG-RVM-SpV pain modulating pathway (Basbaum & Fields, 1984; Heinricher, Tavares, Leith, & Lumb, 2009; Ossipov, Dussor, & Porreca, 2010). The RVM seeding region comprised 6 contiguous voxels: 2 voxels each at 3 rostro-caudal levels from z co-ordinate -53 to -49 in MNI space (Figure 4). In each subject, signal intensity changes were extracted from the RVM seed and voxel-by-voxel analyses were performed to determine which brainstem areas displayed significant signal intensity covariations with this region. The connectivity maps were placed into second level, random-effects procedures to determine significant differences in RVM connectivity strength between controls and each of the migraine groups. Following an initial uncorrected threshold of $p < 0.001$, small volume corrections were applied on the midbrain PAG, dorsolateral pons, and SpV using 40mm^3 hyper-rectangles centred at the location of each region based on the Duvernoy’s Brainstem Atlas (Naidich et al., 2009) and the atlas by Paxinos and Huang (G. Paxinos & X.-F. Huang, 1995).

The resulting clusters of significant difference were used to extract connectivity strength values in each subject, and the mean (\pm SEM) values were plotted to provide a measure of connectivity direction. Additionally, connectivity strength values were extracted for all four groups and significant differences between groups determined ($p < 0.05$, two-tailed, two-sample t test, Bonferroni corrected for multiple comparisons). Significant differences between controls and the group from which the cluster was derived during the original voxel-by-voxel analysis were not determined, to avoid “double-dipping”. To explore changes throughout the migraine cycle, we plotted the mean (\pm SEM) connectivity strengths for the following periods: >30 days until next migraine ($n=16$), 30 to 10 days until next migraine ($n=4$), 9 to 2 days until next migraine ($n=8$), 1 day until next migraine ($n=10$), and 1 to 3 days following a migraine ($n=10$). Finally, we assessed whether there were any areas that displayed both altered activation during noxious thermal stimuli and altered functional connectivity, by determining the intersection of significant brainstem maps. For regions of overlap, linear relationships between percentage changes in signal intensity and resting RVM connectivity were determined (Pearson’s correlation, $p < 0.05$).

RESULTS

Migraine characteristics:

In the 31 migraineurs, 12 reported that their headaches were more common on the right side, while 5 reported more on the left and the remaining 14 reported that they were mostly bilateral. Migraine subjects most frequently described their migraine pain as “throbbing”, “sharp” and/or “pulsating” in nature and indicated that “stress”, “lack of sleep” and/or “dehydration” most often triggered their migraine attacks. The mean estimated frequency of migraine attacks was 22.2 ± 2.1 per year, mean length of time since the onset of migraine attacks (years suffering) 14.1 ± 1.8 years, and mean pain intensity of migraines 3.7 ± 0.2 on a 6-point visual analogue scale. Although 19 of the 31 migraineurs were taking some form of daily medication (mostly the oral contraceptive pill;

12 migraineurs), none of the migraine subjects was taking prophylactic medication prescribed for migraine.

Activation during noxious thermal stimuli:

The overall pain intensity ratings in all groups during the 8 brief noxious heat stimuli were similar in all four groups (mean \pm SEM VAS: *controls* 5.3 ± 0.4 ; *interictal* 4.7 ± 0.5 ; *immediately prior to migraine* 4.9 ± 0.7 ; *immediately following migraine* 4.9 ± 0.8 ; two-tailed *t* test, all $p>0.05$). There was also no significant difference in the applied thermode temperature used to evoke these pain levels between groups (mean temperature: *controls* 47.7 ± 0.1 °C; *interictal* 48 ± 0.2 °C; *immediately prior to migraine* 47.9 ± 0.3 °C; *immediately following migraine* 47.9 ± 0.4 °C; Figure 1B, C, D). Whilst pain intensity ratings remained constant over the three migraine periods, when intensity ratings were plotted relative to the next migraine, there was a gradual increase in pain intensity as the next migraine approached (Figure 1E). However, strikingly, these ratings did not continue to increase but instead decreased in the period immediately prior to a migraine. This change was clear at an individual level with dramatic decreases in perceived pain intensities in the period immediately before a migraine attack despite subjects receiving the same stimuli temperatures during each testing period (Figure 1F).

In all subjects, noxious thermal stimuli evoked increases in signal intensity in various brainstem regions, including the regions of the left and right SpV, left and right dorsolateral pons and in the medullary raphe (Figure 2). Comparison of signal intensity changes evoked by noxious thermal stimuli revealed regional differences over the migraine cycle. Whilst no significant difference occurred between controls and migraineurs during the phase immediately following a migraine, there were significant differences during the interictal and the phase immediately prior to a migraine. During the interictal phase of migraine, acute orofacial pain was associated with significantly reduced activation in the region of the left and right PAG compared with controls

(Figure 3A, Table 1). Extraction of signal intensity changes revealed that this decrease in activation was specific to the interictal phase and did not occur during the phases immediately prior to or following a migraine for both the right PAG (mean % change: *controls* 0.32 ± 0.08 ; *interictal* 0.04 ± 0.09 ; *immediately prior to migraine* 0.35 ± 0.11 ; *immediately following migraine* 0.30 ± 0.07) and left PAG (*controls* 0.26 ± 0.07 ; *interictal* -0.04 ± 0.11 ; *immediately prior to migraine* 0.22 ± 0.15 ; *immediately following migraine* 0.25 ± 0.06). Plots of signal intensity changes throughout the migraine cycle revealed that in migraineurs, signal intensity changes in both the left and right PAG remained stable at approximately zero throughout the interictal period and then increased dramatically to control levels in the period immediately prior to a migraine. Furthermore, there were no significant differences between signal intensity changes during the intervening “off” periods for both the right PAG (*controls* 0.07 ± 0.06 ; *interictal* -0.01 ± 0.06 ; *immediately prior to migraine* 0.06 ± 0.18 ; *immediately following migraine* -0.12 ± 0.11 , all $p>0.05$) and left PAG (*controls* 0.09 ± 0.06 ; *interictal* -0.07 ± 0.11 ; *immediately prior to migraine* -0.08 ± 0.14 ; *immediately following migraine* -0.09 ± 0.10 , all $p>0.05$).

In striking contrast, only during the phase immediately prior to a migraine was signal intensity significantly greater during noxious stimulation in migraineurs than in controls, with this increase encompassing the region of the right SpV (Figure 3B, Table 1). Extraction of signal intensity changes revealed a significant increase in signal intensity within the right SpV only during the phase that immediately preceded a migraine (*controls* 0.17 ± 0.05 ; *interictal* 0.11 ± 0.05 ; *immediately prior to migraine* 0.42 ± 0.12 ; *immediately following migraine* 0.15 ± 0.08). In addition, during the “off” periods there was no significant difference between controls and the interictal phase, although there were significantly greater signal intensity reductions during the phases immediately prior to and after a migraine (*controls* 0.13 ± 0.03 ; *interictal* -0.02 ± 0.07 ; *immediately prior to migraine* -0.17 ± 0.12 $p<0.05$; *immediately following migraine* -0.08 ± 0.05 , $p<0.05$). Plots of signal intensity changes throughout the migraine cycle revealed that in migraineurs, signal intensity changes in the SpV remained stable at approximately control levels throughout the

interictal period and then increased dramatically to well above control levels in the period immediately prior to a migraine.

Functional connectivity:

In addition to brainstem activation patterns during noxious thermal stimuli, we assessed resting functional connectivity of the endogenous pain modulation circuitry. That is, we assessed the connectivity of the well-described PAG-RVM-SpV circuitry by using an RVM seed. Remarkably, we found a very similar pattern of difference in migraineurs compared with controls to the above-mentioned activation patterns evoked by noxious stimuli, albeit in the opposite direction. That is, during the interictal phase, migraineurs displayed significantly greater connectivity strength between the left PAG and RVM (Figure 4A, Table 1). Again, extraction of connectivity strength values revealed that this difference in PAG-RVM connectivity occurred during the interictal phase only and was in the opposite direction to that of the controls and other migraine phases (mean connectivity strength: *controls* -0.11 ± 0.04 ; *interictal* 0.09 ± 0.03 ; *immediately prior to migraine* -0.09 ± 0.07 ; *immediately following migraine* -0.09 ± 0.03). Furthermore, the connectivity strength increase remained relatively stable over the interictal phase and then decreased dramatically in the period immediately prior to a migraine. As well as the PAG, connectivity strength was also significantly greater during the interictal phase in the region of the dorsolateral pons bilaterally (*controls* -0.10 ± 0.04 ; *interictal* 0.09 ± 0.03 ; *immediately prior to migraine* -0.03 ± 0.05 ; *immediately following migraine* -0.04 ± 0.05). Although the connectivity strength between this region and the RVM were less stable over the interictal phase.

In contrast, during the phase immediately prior to a migraine, RVM connectivity strength was significantly reduced in the region of the right SpV (Figure 4B, Table 1). Extraction of connectivity strength values confirmed the specificity of this change during the phase immediately prior to migraine only (*controls* 0.40 ± 0.03 ; *interictal* 0.38 ± 0.03 ; *immediately prior to migraine*

0.13±0.06; *immediately following migraine* 0.36±0.05). Furthermore, SpV-RVM connectivity strength remained stable during the interictal phase and then decreased dramatically during the 24 hour period immediately prior to a migraine.

Noxious stimuli activation and functional connectivity overlap:

The PAG and SpV displayed significant differences in activation during noxious stimuli and resting state functional connectivity. That is, the PAG displayed reduced activation and enhanced RVM connectivity during the interictal phase whereas the SpV displayed enhanced activation and reduced RVM connectivity during the phase immediately prior to a migraine (Figure 5). Plots of RVM connectivity strengths against PAG signal intensity changes revealed no significant linear relationship in any of the four subject groups (controls $r=0.01$, $p=0.94$, interictal $r=-0.07$, $p=0.77$, immediately prior to migraine $r=0.28$, $p=0.53$, immediately following a migraine $r=0.02$, $p=0.96$). In contrast, plots of RVM connectivity strengths against SpV signal revealed a significant positive relationship during the phase immediately prior to migraine only (controls $r=0.20$, $p=0.30$, interictal $r=0.03$, $p=0.90$, immediately prior to migraine $r=0.78$, $p=0.03$, immediately following a migraine $r=-0.12$, $p=0.78$).

DISCUSSION:

This study demonstrates that although sensitivity to applied noxious stimuli increases over the interictal period, in the 24 hour period prior to a migraine, this sensitivity decreases dramatically. This decrease in noxious input sensitivity is coupled with altered function in the brainstem pain modulation circuitry. In the period immediately prior to a migraine attack, migraineurs displayed greater SpV activation to noxious orofacial stimuli and reduced functional connectivity between the RVM and SpV, which may underlie a change in the modulation of

trigeminal noxious input to SpV by the RVM. These functional changes occurred despite the same applied stimuli and an overall similar perceived intensity level between controls and migraineurs during different phases of the migraine cycle. Furthermore, during the interictal phase, migraineurs displayed significantly reduced resting functional connectivity between the PAG and RVM. These data support the hypothesis that brainstem sensitivity fluctuates across the migraine cycle. However in combination with individual subject's pain intensity changes, these data suggest that in contrast to the idea that immediately prior to a migraine attack the brainstem displays diminished 'tone', our data suggests that during this period, endogenous analgesic mechanisms are enhanced and incoming noxious inputs are **less** likely to evoke head pain.

An important finding in this investigation is that at an individual level, pain sensitivity in migraineurs increases during the interictal period but then dramatically decreases in the 24 hour period prior to a migraine attack. This finding appears at odds with the idea that immediately prior to a migraine attack, brainstem endogenous analgesic pathways are in a state as to allow the easy passage of incoming noxious inputs to reach higher brain centres, although it is possible that sensitivity may increase during an actual migraine attack. In concert with the changes in pain sensitivity, we found that during the period immediately prior to a migraine, noxious orofacial stimuli evoked greater SpV activation despite similar pain intensity ratings between groups. It is important to note that this increase in SpV sensitivity occurred in the same location as the signal intensity increases evoked by orofacial noxious stimulation in all subjects and was not a separate part of the relatively long and complex SpV nucleus. Furthermore, we did not find a linear relationship between SpV signal intensity and pain perception. Whilst this may appear at odds with some expectations, BOLD signal intensity changes likely represent summed synaptic activity driven by total oxygen demand (Logothetis, 2003) and thus SpV signal intensity changes would represent a combination of afferent drive from the periphery and feedback from brainstem descending circuitry including that arising in regions such as the RVM and subnucleus reticularis dorsalis.

Although no other investigation has explored brainstem activation during orofacial noxious stimuli in the phase immediately prior to a migraine, Stankewitz and colleagues reported that orofacial noxious stimuli evoked greater SpV signal intensity increases the closer the migraineur was to their next migraine attack (Stankewitz et al., 2011). Although in this previous study, individuals were only examined as close as four days prior to their next migraine, our data reveals that SpV activation increases most dramatically in the 24-hour period prior to a migraine. Our finding that pain perception and SpV processing of noxious stimuli are dynamic raises the prospect that orofacial pain processing pathways may also change at the onset or during a migraine itself. Alternatively, since preclinical studies have reported convergence of dural-sensitive and facial cutaneous afferents in SpV (Burstein et al., 1998; Ellrich, Andersen, Messlinger, & Arendt-Nielsen, 1999) it is possible that a decrease in noxious cutaneous afferent drive onto second-order convergent SpV neurons results in an overall increase in dural afferent drive and a change in dural sensitivity. Whilst this is speculative, it is unlikely that the changes in SpV function reported here are involved in other functions besides the processing of orofacial noxious afferents.

The increase in SpV sensitivity immediately prior to a migraine was associated with a significant reduction in RVM-SpV connectivity. It is possible that during the phase immediately prior to migraine, RVM inputs to the SpV are reduced, resulting in an increase in SpV inhibition or reduction in SpV excitation and a reduction in the propensity for incoming noxious inputs to activate higher brain centres. Interestingly, we found that the greater the reduction in RVM-SpV connectivity the *smaller* the increase in SpV sensitivity to noxious inputs. There is considerable evidence that the RVM contains “ON” and “OFF” cells that can increase and decrease the excitability of neurons in the SpV/dorsal horn, respectively (H. Fields, 2004; H. L. Fields, Bry, Hentall, & Zorman, 1983; Hellman & Mason, 2012; Salas, Ramirez, Vanegas, & Vazquez, 2016). Indeed, it has been suggested that opposing RVM inhibitory and facilitatory effects are finely balanced at rest in pain-free individuals (H. L. Fields & Heinricher, 1985; Heinricher et al., 2009;

Ossipov et al., 2010), but that the system can switch between inhibitory and facilitating processes depending on the state of the individual (Fields, 2004). If the inhibitory effects of RVM on SpV during the interictal phase of migraine were increased as a migraine becomes imminent, one would expect that the greater the reduction in connectivity the greater the reduction in SpV sensitivity, a situation consistent with our findings.

Previous investigations have explored brainstem activation in migraineurs during the interictal phase and reported reduced dIPons activation during noxious thermal face and hand stimuli (Moulton et al., 2008). Whilst we did not find altered noxious stimulus evoked dIPons activity in this study during the interictal phase, we did find reduced activation in the PAG. Furthermore, this reduced activation was associated with an increase in resting connectivity between the RVM and both the PAG and dIPons. The PAG region that exhibited altered activation and resting functional connectivity was located in the region of the ventrolateral PAG column, an area that upon activation produces opiate-mediated analgesia, receives primarily noxious inputs from deep structures and is thought to mediate the behavioural responses to pain deemed inescapable, e.g. migraine (Keay & Bandler, 2002). Furthermore, preclinical studies have revealed that superior sagittal sinus stimulation – a key source of noxious trigeminal input in migraine – activates the ventrolateral PAG and that ventrolateral PAG stimulation can inhibit SpV activity evoked by superior sagittal sinus stimulation (Hoskin, Bulmer, Lasalandra, Jonkman, & Goadsby, 2001; Knight & Goadsby, 2001).

Our data suggests that PAG activity and connectivity sets the RVM-SpV into a state similar to non-migraine controls, since noxious orofacial activation evoked similar SpV signal intensity changes and pain intensity ratings in both controls and in migraineurs during the interictal phase. The precise roles of descending and ascending PAG inputs in altering the functional state of the PAG during the interictal phase of migraine are yet to be determined. We have recently shown increased PAG-hypothalamic connectivity only in the phase immediately prior to a migraine (Noemi Meylakh et al., 2018) and a recent case-study reported the hypothalamus displays

increased noxious stimuli sensitivity and increased functional coupling with the dorsomedial pons and SpV also during the phase immediately prior to an attack (Schulte & May, 2016). Indeed there is a hypothesis that activity changes within the hypothalamus initiate migraine attacks which is not inconsistent with the data presented here (Schulte, Allers, & May, 2017).

Previous human brain imaging studies have also reported altered resting PAG connectivity with higher brain regions implicated in pain modulation other than the hypothalamus, such as the amygdala, prefrontal and cingulate cortices (C. Mainero et al., 2011a). Furthermore, there is evidence that during the interictal phase, migraineurs displayed significantly reduced endogenous analgesic ability as assessed by diffuse noxious inhibitory control (Sandrini et al., 2006). Whilst these results suggest that during the interictal phase of migraine, pain sensitivity should be increased, we found no significant difference in pain intensity, and indeed we found that the temperature needed to evoke moderate pain were if anything greater in migraineurs than controls. Furthermore, our data suggests that endogenous pain modulating circuits are enhanced immediately prior to a migraine given that pain intensity sensitivities dramatically decreased during this period.

Whilst we are confident in the robustness of our results, there are some limitations which need noting. Firstly, it is possible that our interpretation of the signal intensity changes to noxious stimuli and RVM connectivity's are not related to alterations in endogenous pain modulatory circuitries. For example, it has been shown that RVM cells that process noxious information are also involved in micturition and micturition-related neurons have also been identified in the PAG and hypothalamus (Baez, Brink, & Mason, 2005; Numata et al., 2008). Given that in many migraineurs, increased urination occurs immediately prior to a migraine, it is possible that the changes reported here relate to symptoms other than the processing of incoming noxious inputs. Secondly, given the relatively low spatial resolution of fMRI scans, it is difficult to accurately localise each cluster to a specific brainstem nucleus or region. However, we used brainstem atlases to determine the location of each significant cluster, and our brainstem clusters overlap

with regions that have been shown to be involved in nociceptive transmission. Thirdly, the brainstem is prone to physiological noise and movement-related artefacts. To limit the influence of these factors, we applied a physiological noise correction to account for potential cardiac and respiratory noise and we modelled and removed effects of movement on signal intensity. Finally, with mounting evidence of migraine being a “cycling” brain disorder, scans in individual migraineurs over the course of a few weeks whilst measuring pain sensitivity and brain activity would provide evidence to support such a hypothesis.

In conclusion, it is becoming increasingly clear that the brainstem pain modulating circuitry is altered in migraineurs throughout the migraine cycle. Whilst there is a suggestion that pain sensitivity increases the closer one is to a migraine, our data shows that indeed pain sensitivity falls dramatically immediately prior to a migraine. Whilst data is consistent with the idea that brainstem circuits fluctuate from “enhanced” and “diminished” neural tone states, in the light of our data, the timing of these fluctuations needs to be re-examined (Burstein et al., 2015; May, 2017b). We speculate that during the interictal phase of migraine, the PAG influences the RVM-SpV circuit to produce a balance of ON and OFF cell function that is similar to that of controls and thereby results in similar SpV sensitivities to noxious inputs. In contrast, as a migraine approaches, the balance of ON and OFF influences on the SpV shifts to a state dominated by OFF cell inputs and, as a result, the SpV becomes less sensitive to incoming noxious inputs. Whether this brainstem state shifts again as a migraine attack develops is yet to be determined.

REFERENCES:

- Akerman S, Holland PR, Goadsby PJ (2011) Diencephalic and brainstem mechanisms in migraine. *Nat Rev Neurosci* 12:570-584.
- Baez MA, Brink TS, Mason P (2005) Roles for pain modulatory cells during micturition and continence. *J Neurosci* 25:384-394.
- Bahra A, Matharu MS, Buchel C, Frackowiak RS, Goadsby PJ (2001) Brainstem activation specific to migraine headache. *Lancet* 357:1016-1017.
- Basbaum AI, Fields HL (1984) Endogenous pain control systems: brainstem spinal pathways and endorphin circuitry. *Annu Rev Neurosci* 7:309-338.
- Borsook D, Veggeberg R, Erpelding N, Borra R, Linnman C, Burstein R, Becerra L (2016) The Insula: A "Hub of Activity" in Migraine. *Neuroscientist* 22:632-652.
- Burstein R, Nosedá R, Borsook D (2015) Migraine: multiple processes, complex pathophysiology. *J Neurosci* 35:6619-6629.
- Burstein R, Yamamura H, Malick A, Strassman AM (1998) Chemical stimulation of the intracranial dura induces enhanced responses to facial stimulation in brain stem trigeminal neurons. *J Neurophysiol* 79:964-982.
- Chong CD, Plasencia JD, Frakes DH, Schwedt TJ (2017) Structural alterations of the brainstem in migraine. *Neuroimage Clin* 13:223-227.
- Coppola G, Di Renzo A, Tinelli E, Di Lorenzo C, Di Lorenzo G, Parisi V, Serrao M, Schoenen J, Pierelli F (2016) Thalamo-cortical network activity during spontaneous migraine attacks. *Neurology* 87:2154-2160.
- Denuelle M, Fabre N, Payoux P, Chollet F, Geraud G (2007) Hypothalamic activation in spontaneous migraine attacks. *Headache* 47:1418-1426.
- Diedrichsen J (2006) A spatially unbiased atlas template of the human cerebellum. *Neuroimage* 33:127-138.

- Ellrich J, Andersen OK, Messlinger K, Arendt-Nielsen L (1999) Convergence of meningeal and facial afferents onto trigeminal brainstem neurons: an electrophysiological study in rat and man. *Pain* 82:229-237.
- Fields H (2004) State-dependent opioid control of pain. *Nat Rev Neurosci* 5:565-575.
- Fields HL, Heinricher MM (1985) Anatomy and physiology of a nociceptive modulatory system. *Philos Trans R Soc Lond B Biol Sci* 308:361-374.
- Fields HL, Bry J, Hentall I, Zorman G (1983) The activity of neurons in the rostral medulla of the rat during withdrawal from noxious heat. *J Neurosci* 3:2545-2552.
- Friston KJ, Holmes AP, Worsley KJ, Poline JP, Frith CD, Frackowiak RSJ (1994) Statistical parametric maps in functional imaging: A general linear approach. *Human brain mapping* 2:189-210.
- Heinricher MM, Tavares I, Leith JL, Lumb BM (2009) Descending control of nociception: Specificity, recruitment and plasticity. *Brain Res Rev* 60:214-225.
- Hellman KM, Mason P (2012) Opioids disrupt pro-nociceptive modulation mediated by raphe magnus. *J Neurosci* 32:13668-13678.
- Hoskin KL, Bulmer DC, Lasalandra M, Jonkman A, Goadsby PJ (2001) Fos expression in the midbrain periaqueductal grey after trigeminovascular stimulation. *J Anat* 198:29-35.
- Keay KA, Bandler R (2002) Distinct central representations of inescapable and escapable pain: observations and speculation. *Exp Physiol* 87:275-279.
- Knight YE, Goadsby PJ (2001) The periaqueductal grey matter modulates trigeminovascular input: a role in migraine? *Neuroscience* 106:793-800.
- Logothetis NK (2003) The underpinnings of the BOLD functional magnetic resonance imaging signal. *J Neurosci* 23:3963-3971.
- Mainero C, Boshyan J, Hadjikhani N (2011) Altered functional magnetic resonance imaging resting-state connectivity in periaqueductal gray networks in migraine. *Ann Neurol* 70:838-845.

- Marciszewski KK, Meylakh N, Di Pietro F, Macefield VG, Macey PM, Henderson LA (2018) Altered brainstem anatomy in migraine. *Cephalalgia* 38:476-486.
- Mathur VA, Moayed M, Keaser ML, Khan SA, Hubbard CS, Goyal M, Seminowicz DA (2016) High Frequency Migraine Is Associated with Lower Acute Pain Sensitivity and Abnormal Insula Activity Related to Migraine Pain Intensity, Attack Frequency, and Pain Catastrophizing. *Front Hum Neurosci* 10:489.
- May A (2017) Understanding migraine as a cycling brain syndrome: reviewing the evidence from functional imaging. *Neurol Sci* 38:125-130.
- Meylakh N, Marciszewski Kasia K, Di Pietro F, Macefield Vaughan G, Macey Paul M, Henderson Luke A (2018) Deep in the brain: Changes in subcortical function immediately preceding a migraine attack. *Human Brain Mapping* 0.
- Moulton EA, Burstein R, Tully S, Hargreaves R, Becerra L, Borsook D (2008) Interictal dysfunction of a brainstem descending modulatory center in migraine patients. *PLoS One* 3:e3799.
- Naidich TP, Duvernoy HM, Delman BN, Sorensen AG, Kollias SS, Haacke EM (2009) *Duvernoy's Atlas of the Human Brain Stem and Cerebellum*: Springer-Verlag Wien.
- Numata A, Iwata T, Iuchi H, Taniguchi N, Kita M, Wada N, Kato Y, Kakizaki H (2008) Micturition-suppressing region in the periaqueductal gray of the mesencephalon of the cat. *Am J Physiol Regul Integr Comp Physiol* 294:R1996-2000.
- Ossipov MH, Dussor GO, Porreca F (2010) Central modulation of pain. *J Clin Invest* 120:3779-3787.
- Paxinos G, Huang X-F (1995) *Atlas of the human brainstem*. Sydney: Academic Press.
- Porcaro C, Di Lorenzo G, Seri S, Pierelli F, Tecchio F, Coppola G (2017) Impaired brainstem and thalamic high-frequency oscillatory EEG activity in migraine between attacks. *Cephalalgia* 37:915-926.

- Salas R, Ramirez K, Vanegas H, Vazquez E (2016) Activity correlations between on-like and off-like cells of the rostral ventromedial medulla and simultaneously recorded wide-dynamic-range neurons of the spinal dorsal horn in rats. *Brain Res* 1652:103-110.
- Sandrini G, Rossi P, Milanov I, Serrao M, Cecchini AP, Nappi G (2006) Abnormal modulatory influence of diffuse noxious inhibitory controls in migraine and chronic tension-type headache patients. *Cephalalgia* 26:782-789.
- Särkkä S, Solin A, Nummenmaa A, Vehtari A, Auranen T, Vanni S, Lin F-H (2012) Dynamic retrospective filtering of physiological noise in BOLD fMRI: DRIFTER. *NeuroImage* 60:1517-1527.
- Schulte LH, May A (2016) The migraine generator revisited: continuous scanning of the migraine cycle over 30 days and three spontaneous attacks. *Brain* 139:1987-1993.
- Schulte LH, May A (2017) Of generators, networks and migraine attacks. *Curr Opin Neurol* 30:241-245.
- Schulte LH, Allers A, May A (2017) Hypothalamus as a mediator of chronic migraine: Evidence from high-resolution fMRI. *Neurology* 88:2011-2016.
- Sessle BJ (2000) Acute and chronic craniofacial pain: brainstem mechanisms of nociceptive transmission and neuroplasticity, and their clinical correlates. *Crit Rev Oral Biol Med* 11:57-91.
- Stankewitz A, Aderjan D, Eippert F, May A (2011) Trigeminal nociceptive transmission in migraineurs predicts migraine attacks. *J Neurosci* 31:1937-1943.
- Tajti J, Szok D, Pardutz A, Tuka B, Csati A, Kuris A, Toldi J, Vecsei L (2012) Where does a migraine attack originate? In the brainstem. *J Neural Transm (Vienna)* 119:557-568.
- Weiller C, May A, Limmroth V, Juptner M, Kaube H, Schayck RV, Coenen HH, Diener HC (1995) Brain stem activation in spontaneous human migraine attacks. *Nat Med* 1:658-660.

Table 1. Montreal Neurological Institute (MNI) coordinates, cluster size and t-score for regions in which activation during noxious stimuli or resting rostral ventromedial medulla connectivity were significantly different between controls and migraineurs.

Brain region	MNI Co-ordinate			cluster size	t-score
	x	y	z		
<i>Noxious stimuli activation</i>					
<i>controls>interictals:</i>					
left midbrain periaqueductal gray	-2	-36	-11	4	3.28
right midbrain periaqueductal gray	4	-38	-13	3	3.32
<i>immediately prior to migraine>controls:</i>					
right spinal trigeminal nucleus	8	-42	-48	3	3.67
ventral medial medulla	-2	-32	-49	4	3.31
<i>Resting rostral ventromedial medulla connectivity</i>					
<i>Interictals>controls:</i>					
left midbrain periaqueductal gray	-2	-36	-17	5	3.42
dorsolateral pons	4	-38	-25	9	3.41
<i>controls>immediately prior to migraine:</i>					
right spinal trigeminal nucleus	4	-42	-47	8	3.24

FIGURE LEGENDS

Figure 1: A: In each participant, a thermode was placed on the corner of the mouth and 8 noxious heat stimuli were delivered. Each participant rated the pain intensity during each noxious stimulus on a Computerised Visual Analogue Scale (CoVAS), where 0=no pain and 10=most pain imaginable. **B:** Plots of mean \pm SEM pain intensity ratings for each subject group. In each subject, pain intensity for each of the 8 noxious stimuli were averaged and these were then averaged across subjects for each group. The control group (n=60) was reduced to 31 subjects so that the average pain intensity was not significantly different between controls and each of the three migraine groups. **C:** Plots of mean \pm SEM pain intensity ratings for each of the 8 noxious stimuli for each subject group. **D:** Plots of mean \pm SEM stimulus temperatures for each subject group. **E:** Plots of pain intensity ratings for individual migraineurs with respect to their next migraine (black circles). In addition, mean \pm SEM pain intensity ratings for the following periods: >30 days until next migraine (n=12), 30 to 10 days until next migraine (n=4), 9 to 2 days until next migraine (n=5) and 1 day until next migraine (n=7) are also plotted (red filled squares). **F:** Plots of pain intensity ratings for 6 individual migraineurs with respect to their next migraine. Note that perceived pain intensity increases over the interictal period and then dramatically decreases immediately prior to their next migraine.

Figure 2: fMRI response to pain: Brainstem activation common to the four subject groups during 8 brief noxious stimuli overlaid onto a series of axial slices of a brainstem T1-weighted anatomical template. The location of each sagittal and axial slice in Montreal Neurological Institute space is indicated at the upper right of each image. Noxious stimuli applied to the right side of the mouth evoked signal intensity increases (hot colour scale) in the region of the spinal trigeminal nucleus (SpV) bilaterally, the region of the medullary raphe, and in the dorsolateral pons (dlPons).

Figure 3: fMRI response to pain by group: Significant differences in brainstem activation during noxious orofacial stimuli in migraineurs compared with controls. **A:** Significantly reduced activation (cool colour scale) in migraineurs during the interictal phase compared with controls overlaid onto a sagittal and axial slices of a T1-weighted brainstem template. The location of each slice in Montreal Neurological Institute space is indicated at the upper right of each image and indicated by the dashed horizontal lines. Plots of mean \pm SEM percentage signal intensity changes during noxious orofacial stimulation for the left and right midbrain periaqueductal gray (PAG) clusters during the stimulus periods (ON) and baseline periods (OFF) for each of the four subject groups are shown. In addition, to the right are plots of mean (\pm SEM) signal changes for the following periods: >30 days until next migraine (n=12), 30 to 10 days until next migraine (n=4), 9 to 2 days until next migraine (n=5), 1 day until next migraine (n=7), and 1 to 3 days following a migraine (n=8). Note the stability of the signal changes during the interictal period and the dramatic increases during the phase immediately prior to a migraine. **B:** Significantly greater activation (hot colour scale) in migraineurs during the phase immediately prior to a migraine compared with controls. Signal intensity changes during noxious stimuli in the spinal trigeminal nucleus (SpV) in all four subject groups during the on and off periods are shown. In addition, plots of signal changes over the migraine cycle are shown to the right and again note the stability during the interictal period and the dramatic change immediately prior to a migraine. * $p < 0.05$ derived from voxel-by-voxel analyses.

Figure 4: resting-state connectivity: Significant differences in rostral ventromedial medulla (RVM) resting connectivity in migraineurs compared with controls. **A:** Significantly greater connectivity (hot colour scale) in migraineurs during the interictal phase compared with controls overlaid onto a sagittal and axial slices of a T1-weighted brainstem template. The location of each slice in Montreal Neurological Institute space is indicated at the upper right of each image and indicated by the dashed horizontal lines. Plots of mean \pm SEM connectivity strengths (arbitrary

units) for the left midbrain periaqueductal gray (PAG) and dorsolateral pons (dlPons) clusters for each of the four subject groups are also shown. In addition, plots of connectivity changes over the migraine cycle are shown to the right and again note the stability during the interictal period and the dramatic change immediately prior to a migraine.

B: Significantly reduced connectivity strengths (cool colour scale) in migraineurs during the phase immediately prior to a migraine compared with controls. The plots to the right are connectivity strengths in the spinal trigeminal nucleus (SpV) in all four subject groups. * $p < 0.05$ derived from voxel-by-voxel analyses. The inset in the centre shows the RVM seed used for the analysis. In addition, plots of connectivity changes over the migraine cycle are shown to the right and again note the stability during the interictal period and the dramatic change immediately prior to a migraine.

Figure 5: Overlap between alterations in noxious stimulus evoked signal intensity changes and resting connectivity (red shading) overlaid onto axial slices of a T1-weighted brainstem template. The location of each slice in Montreal Neurological Institute space is indicated at the upper left of each image. To the right are plots of connectivity strengths (arbitrary units) against percentage signal intensity changes during noxious stimuli for the midbrain periaqueductal gray (PAG) and spinal trigeminal nucleus (SpV) in individual subjects for each of the four subject groups. The only significant linear relationship occurred in the SpV in the period immediately prior to a migraine. That is, the greater the connectivity to the rostral ventromedial medulla, the greater the noxious stimulus-evoked signal intensity.

Figure 1:

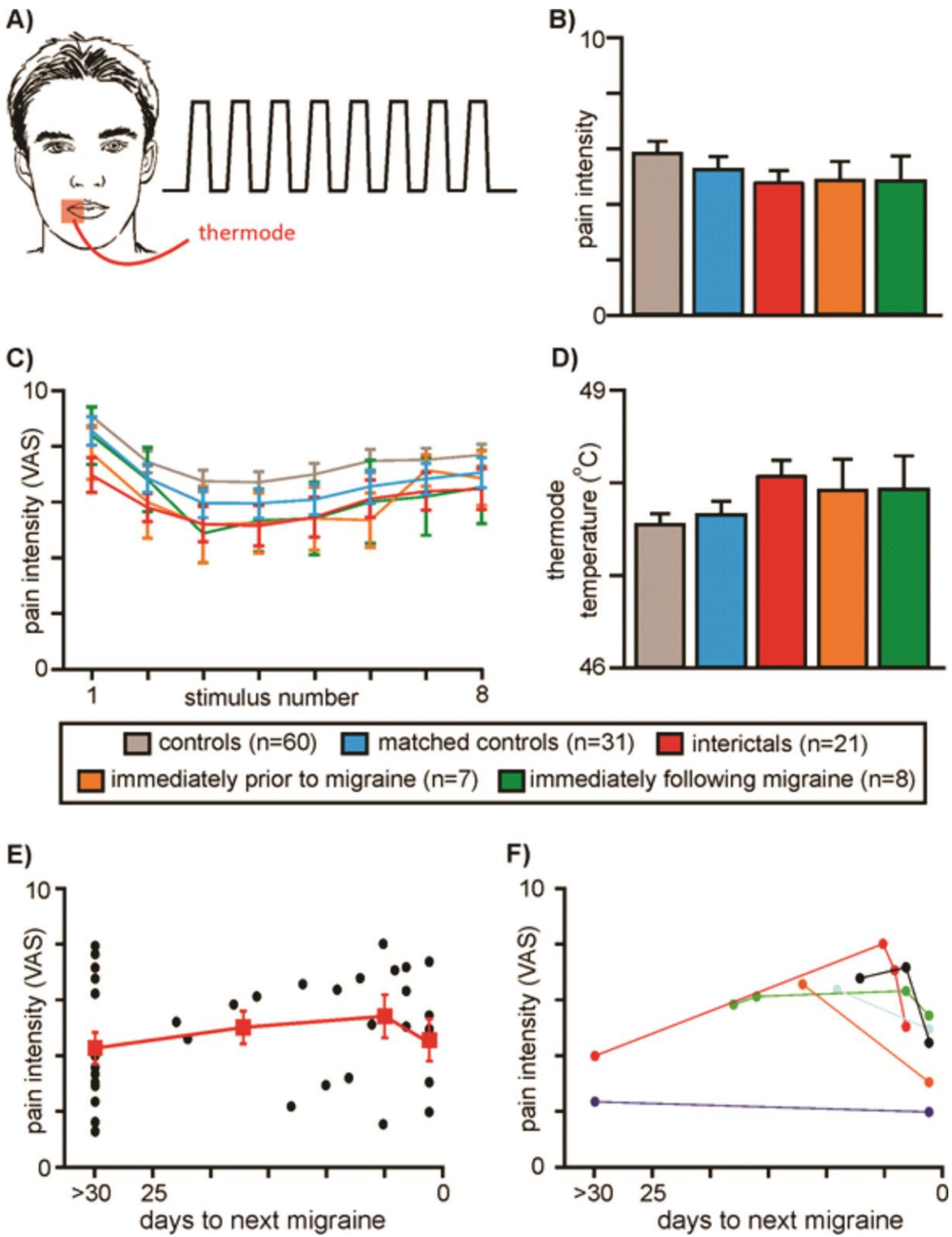


Figure 2:

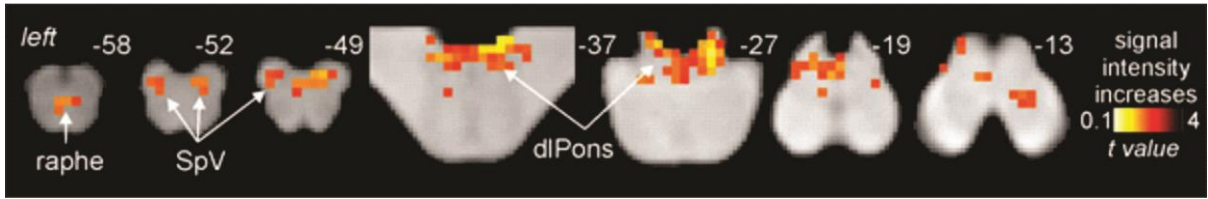


Figure 3:

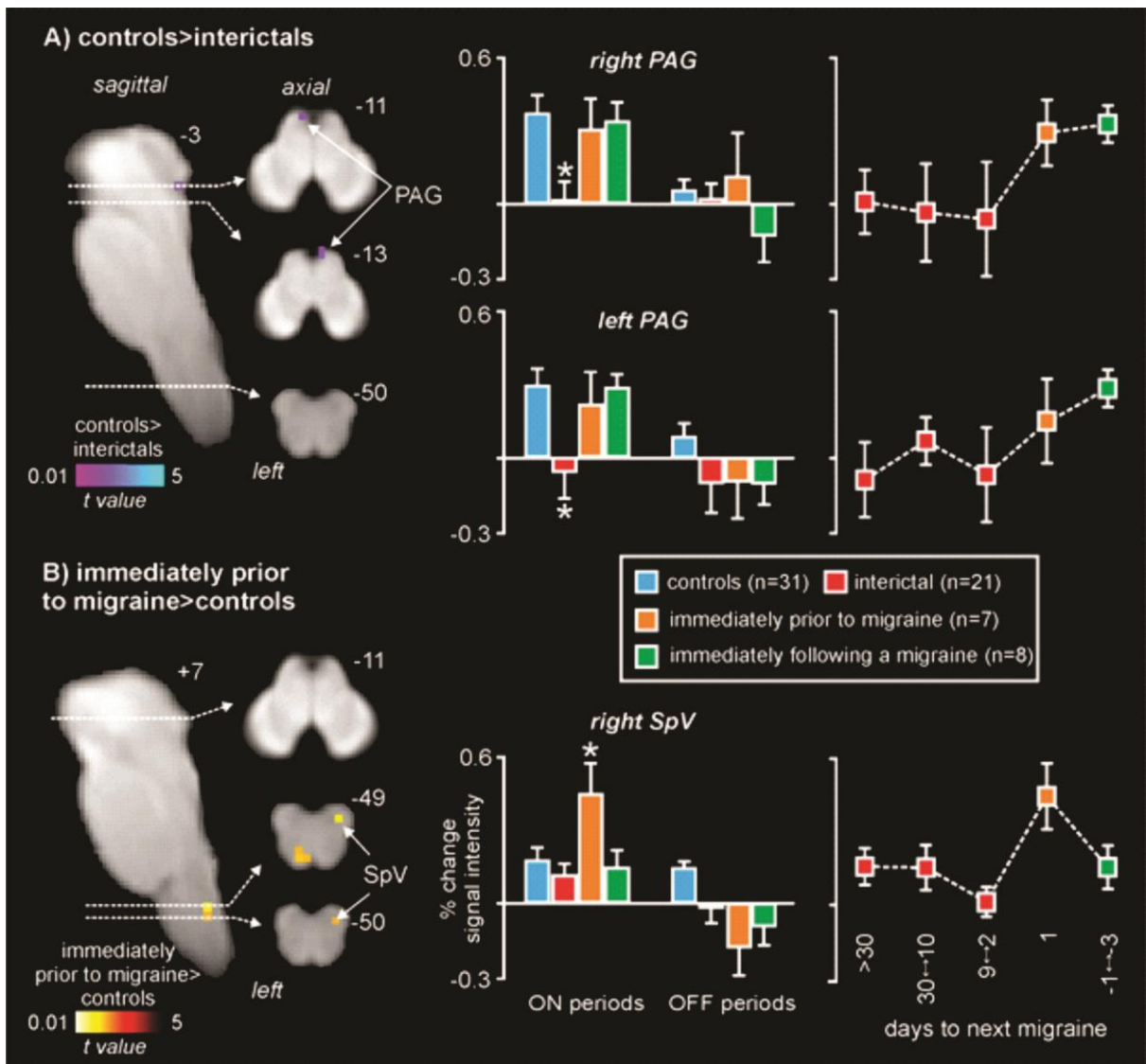


Figure 4:

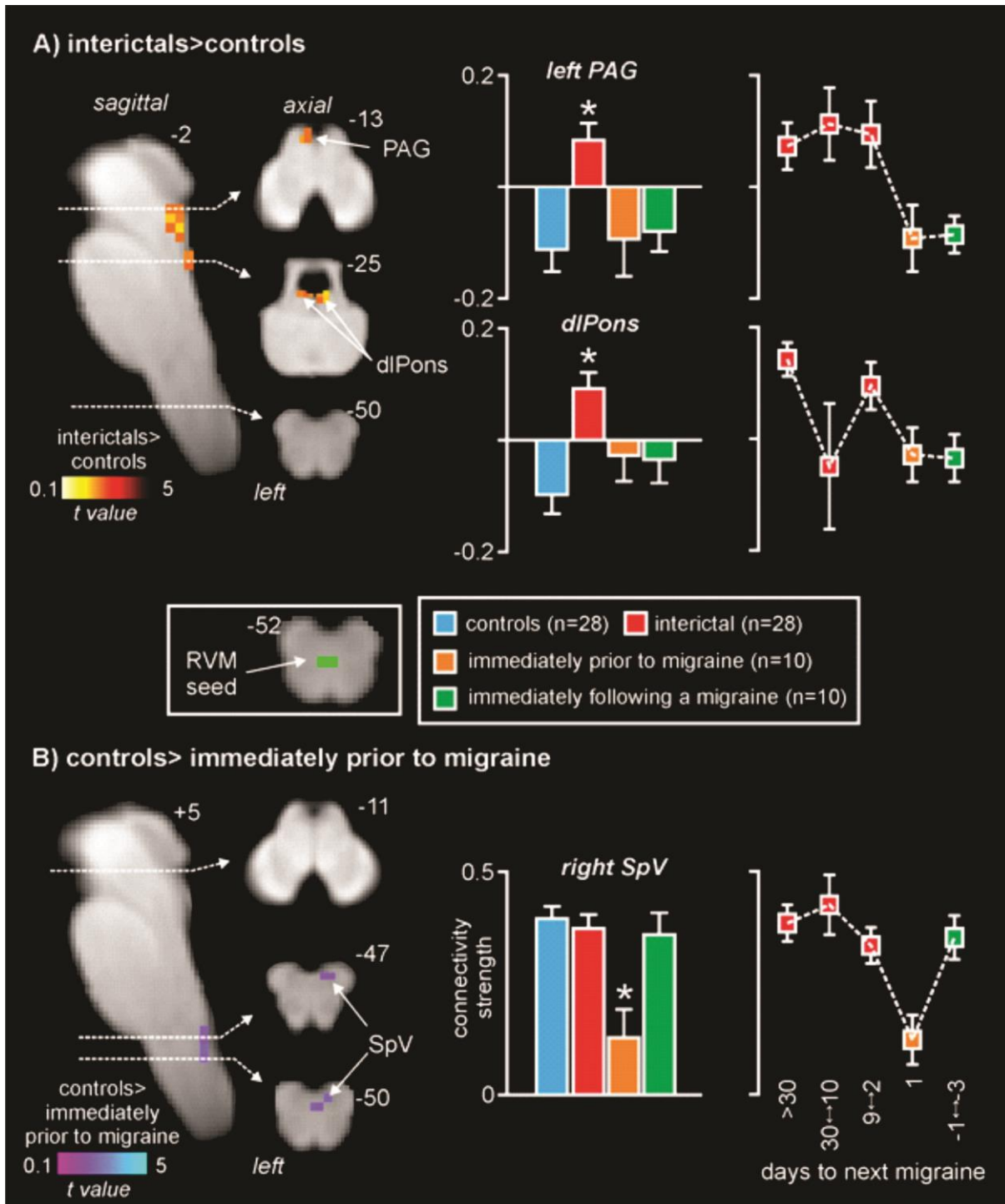
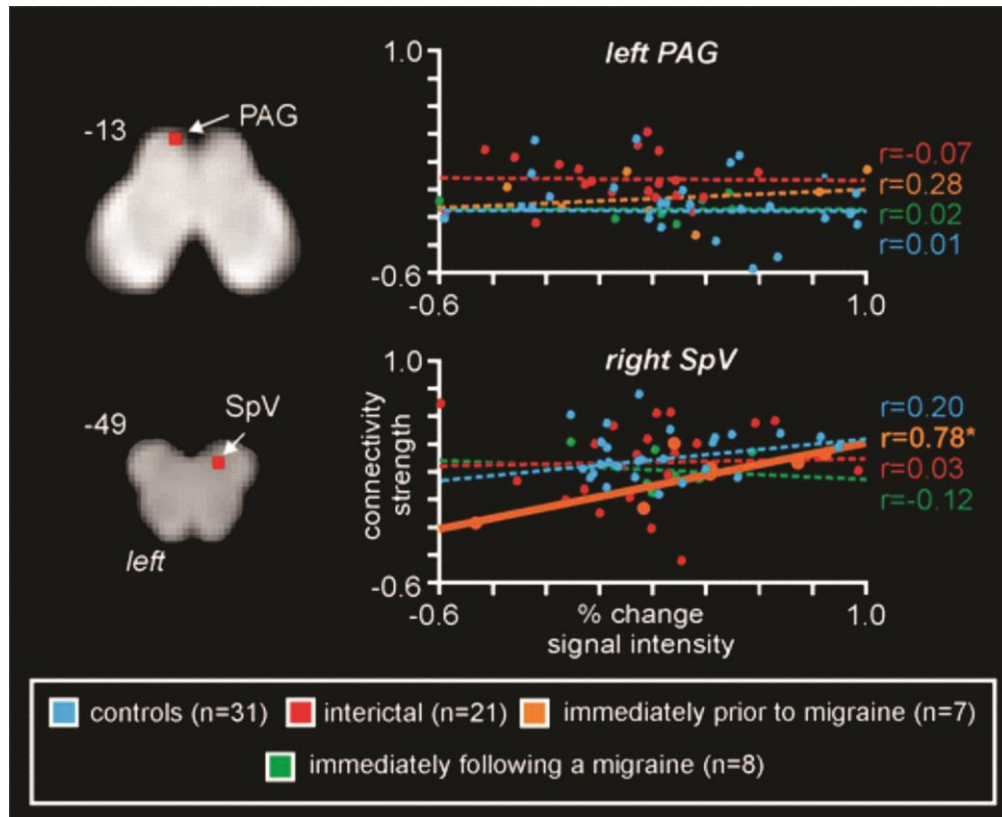


Figure 5:



Appendix III.

Fluctuating brainstem anatomy across the migraine cycle

Title: Fluctuating brainstem anatomy across the migraine cycle.

Abbreviated Title: Brainstem anatomy and migraine

Authors: Kasia K. Marciszewski¹, Noemi Meylakh¹, Flavia Di Pietro¹, Vaughan G. Macefield², Paul M. Macey³ and Luke A. Henderson¹

¹Department of Anatomy and Histology, Sydney Medical School, University of Sydney, Sydney, NSW, Australia, 2006; ²School of Medicine, Western Sydney University, Sydney, Australia;

³UCLA School of Nursing and Brain Research Institute, University of California, Los Angeles, California 90095, United States.

Corresponding author: Luke A. Henderson, Department of Anatomy and Histology, F13, University of Sydney, Australia. lukeh@anatomy.usyd.edu.au (email); +612 9351 7063 (Tel) +612 9351 6556 (Fax)

Submitted for publication 2018: *eNeuro*

Figures: 3; Tables: 1

Words: Abstract: 234; Introduction: 671; Discussion: 1507

Acknowledgements: We wish to thank the many volunteers in this study.

Conflict of interest: The authors declare no competing financial interests

Funding Source: National Health and Medical Research Council of Australia, grant 1143547.

ABSTRACT

The neural mechanisms responsible for the initiation and expression of migraines remain unknown. Though there is growing evidence of changes in brainstem anatomy and function between attacks, very little is known about brainstem function and structure in the period immediately prior to a migraine – which is critical if we are to understand how a migraine is generated. The aim of this investigation is to use brainstem-specific analyses of diffusion weighted images to determine if the brainstem pain processing regions display altered structure in individuals with migraine across the migraine cycle, and in particular immediately prior to a migraine. Diffusion tensor images (48 controls, 36 migraineurs) were used to assess brainstem anatomy in migraineurs compared with controls. We found that during the interictal phase, migraineurs displayed greater mean diffusivity in the region of the spinal trigeminal nucleus, dorsomedial/dorsolateral pons and midbrain periaqueductal gray matter. Remarkably, the mean diffusivity returned to controls levels during the 24-hour period immediately prior to a migraine, only to increase again within the three following days. These data show that regional brainstem anatomy changes over the migraine cycle, with specific anatomical changes occurring in the 24 hours prior to onset. These changes may contribute to the activation of the ascending trigeminal pathway by either an increase in basal traffic or by sensitising the trigeminal nuclei to external triggers, with activation ultimately resulting in perception of head pain during a migraine attack.

SIGNIFICANCE STATEMENT

It has been hypothesised that modulation of brainstem pain pathways may be critical for the initiation of migraine attacks. There is some evidence that altered brainstem function, possibly involving increased astrocyte activation, occurs immediately prior to a migraine attack. We sought to obtain evidence to support this theory. Using diffusion tensor imaging, we found that immediately prior to a migraine, mean diffusivity decreased in the spinal trigeminal nucleus, dorsomedial/dorsolateral pons and midbrain periaqueductal gray matter. Mean diffusivity then

increased again immediately following the migraine attack. Decreased mean diffusivity before a migraine is consistent with increased astrocyte activation, since astrocyte processes enlarge during activation. These changes may underlie changes in brainstem function that are essential for the generation of a migraine.

INTRODUCTION

Migraine is a common, debilitating disorder characterised by headaches and often accompanied by aura, nausea, and sensitivity to light and sound. Despite these well-characterised symptoms, the exact mechanisms underlying the initiation and maintenance of migraine head pain are still hotly debated. To date, human brain imaging investigations have revealed that during a migraine attack, activity increases in brain regions such as the cingulate cortex, insula, thalamus, hypothalamus and dorsal pons (S.K. Afridi et al., 2005; A. Bahra, M.S. Matharu, C. Buchel, R.S. Frackowiak, & P.J. Goadsby, 2001a; Denuelle, Fabre, Payoux, Chollet, & Geraud, 2004; Weiller, May, Limmroth, Juptner, Kaube, Schayck, Coenen, & Diener, 1995). In addition, a number of studies have identified anatomical, sensitivity and resting activity pattern changes between migraine attacks, i.e. in the interictal period (C. D. Chong et al., 2017; C.D. Chong & Schwedt, 2015; K.K. Marciszewski et al., 2018; V.A. Mathur et al., 2016; Porcaro et al., 2017b). These findings highlight the apparent brain dysfunction in migraineurs even when in a pain-free state.

A recent review has proposed that these observed changes in brain function are not stable, but dynamic in nature (May, 2017a). Some have suggested that functional brain changes actually trigger a migraine from basal firing (Goadsby & Akerman, 2012). Others have suggested that the brain fluctuates between a state where the effectiveness of endogenous analgesic mechanisms is too great to allow incoming noxious inputs to evoke head pain, and a state where incoming inputs can activate central pathways and evoke head pain (Akerman et al., 2011; Borsook & Burstein, 2012). Consistent with these hypotheses, it has recently reported that during the interictal phase, migraineurs display reduced grey matter density and increased free water movement within brainstem pain-modulating regions including the midbrain periaqueductal grey matter (PAG), dorsolateral pons (dlPons), medullary raphe and spinal trigeminal nucleus (SpV) (Marciszewski et al., 2018a). Furthermore, it was recently shown that immediately prior to a migraine resting infra-slow oscillatory activity increases in these same brainstem regions and

returns to controls levels shortly after the migraine and it was speculated that these oscillatory changes may result from transient increases in astrocyte activation and its associated gliotransmission (N. Meylakh et al., 2018). Given there is some evidence that astrocytes may play a role in aspects of migraine such as the propagation of cortical spreading depression (Nedergaard et al., 1995) and that a genetic form of migraine, Familial Hemiplegic Migraine, is associated with astrocyte dysfunction (Benarroch, 2005), it is not unreasonable to suggest that astrocytes may also play a critical role in migraine pathophysiology via actions within the brainstem.

It was recently reported that pain sensitivity to noxious stimuli in migraineurs is dramatically decreased in the 24 hour period prior to a migraine, and this decrease is associated with increased functional magnetic resonance imaging (fMRI) signal intensity within the SpV and reduced PAG-SpV connectivity (K. K. Marciszewski, N. Meylakh, F. Di Pietro, E. P. Mills, et al., 2018). This altered brainstem function may result from altered neural-glia interactions, though evidence of astrocyte activation in migraineurs, particularly in the period immediately prior to a migraine is lacking. This is likely due to the fact that it is not possible to predict when an individual will have a migraine and thus examining them in the 24-hour period before an attack is difficult. Although direct astrocyte measurement is not possible in living humans, local free water movement, as measured by diffusion tensor imaging, can be used as an indirect measurement of astrocyte activity. Due to the observation that when astrocytes are activated their processes expand, it is logical to assume that this event would be associated with a decrease in local free water movement.

As such, the aim of this investigation is to use diffusion tensor imaging (DTI) to determine if the brainstem displays microstructural alterations throughout the migraine cycle. More specifically we aim to explore changes in the 24-hour period prior to a migraine. We hypothesise that immediately prior to a migraine, mean diffusivity will decrease, consistent with an increase in astrocyte size, in areas of the brainstem that process and modulate pain such the PAG, dIPons,

medullary raphe and SpV. Furthermore, that decrease will be reversed during the period immediately following a migraine and return to interictal levels.

METHODS

Subjects

Thirty-six subjects with migraine (8 males, mean [\pm SEM] age: 30.6 \pm 1.7 years) and 48 age and gender matched pain-free controls (12 males, age: 32.1 \pm 1.7 years) were recruited for the study. All subjects were recruited from the general population using an advertisement. Migraine subjects were diagnosed according to the criteria laid out by the International Classification of Headache Disorders (ICHD), 3rd edition, sections 1.1 and 1.2 (ICHD-3 β , 2013) Seven migraineurs reported aura associated with their migraines and the remaining 29 reported no aura. Of the 36 migraineurs, 31 were scanned during the interictal period (7 males, age 30.0 \pm 1.9 years), that is, between 72 hours after and 24 hours prior to a migraine attack; 10 during the 24-hour period immediately prior to a migraine (4 males, age 27.2 \pm 3.0 years), and 13 within the 72-hour period following a migraine (4 males, age 31.7 \pm 2.9 years). For subjects scanned prior to an attack, there was no predicting factor that they were within 24 hours of a migraine. Ten migraineurs were scanned during the interictal period and period immediately prior to a migraine. In addition, six of these 10 subjects were also scanned during the period immediately after a migraine.

In addition, all migraine subjects indicated the pain intensity (6-point visual analogue scale; 0 = no pain, 5 = most intense imaginable pain) and facial distribution (drawing) of pain they commonly experience during a migraine attack. Each subject described the qualities of their migraines and indicated any current treatments used to prevent or abort a migraine once started. Exclusion criteria for controls were the presence of any current pain or chronic pain condition, current use of analgesics, and any neurological disorder. Exclusion criteria for migraineurs were any pain condition other than migraine, and any other neurological disorder. Informed written consent was obtained for all procedures according to the Declaration of Helsinki 7th revision and

local Institutional Human Research Ethics Committees approved the study.

MRI acquisition

Subjects lay supine on the bed of a 3T MRI scanner (Philips Achieva, Neuroscience Research Australia, Sydney) with their head immobilised in a fitting 32-channel head coil. With all subjects relaxed and at rest, in each subject a high-resolution T1-weighted anatomical image set covering the entire brain was collected (turbo field echo; field of view 250x250mm, matrix size=288x288, slice thickness=0.87mm, repetition time=5600ms, echo time=2.5ms, flip angle 8°). Following this, two high-resolution DTI image sets covering the entire brain were collected using a single-shot multisection spin-echo echo-planar pulse sequence (repetition time=8788ms; flip angle=90°, matrix size 112x112, field of view 224x224 mm, slice thickness=2.5mm, 55 axial slices). For each slice, diffusion gradients were applied along 32 independent orientations with $b=1000\text{s/mm}^2$ after the acquisition of five $b=0\text{ s/mm}^2$ (b_0) images. Two DTI acquisitions were averaged to improve signal-noise ratios.

Image analysis

DTI analysis

Using SPM12 software (K.J. Friston et al., 1994), the two DTI image sets from each subject were realigned based on the b_0 images, and the diffusion tensors calculated from the images using a linear model (Basser & Pierpaoli, 1996). Mean diffusivity (MD) whole-brain maps were then derived and co-registered to each individual subject's T1-weighted image. Using brainstem-specific isolation software (SUIT toolbox)(Diedrichsen, 2006a), a unique mask of the brainstem was manually created for each subject's MD maps. Using these masks, the brainstem was isolated, spatially normalised, re-sliced to the SUIT template in Montreal Neurological Institute (MNI) space, and spatially smoothed using a 3 mm full-width-at-half-maximum (FWHM) Gaussian filter.

Statistical analyses

Using a voxel-by-voxel analysis, significant differences in MD values were determined between (i) controls and migraineurs during the interictal period, (ii) controls and migraineurs during the period immediately *prior to* a migraine, and (iii) controls and migraineurs during the period immediately *following* a migraine ($p < 0.05$, false discovery rate corrected at a voxel level, minimum cluster size 5 contiguous voxels). Age and gender were included as nuisance variables. No voxels survived this stringent threshold and so we reduced the stringency ($p < 0.001$, uncorrected) and performed cluster correction (Bonferroni correction by the number of voxels in each cluster) to assess if more subtle diffusion changes occurred. A brainstem mask that excluded cerebrospinal fluid as well as the cerebellum was applied to each analysis.

Since we found significant MD increases during the interictal period that were eliminated immediately prior to a migraine, we extracted MD values from those significant clusters for all three migraine periods. Significant MD differences between controls and the period immediately prior to and following migraine were then determined for these clusters (two-tailed, two-sample t-test, $p < 0.05$). Significant MD differences between controls and the interictal period were not assessed since these were already established as significant with the voxel-based statistics, thus avoiding the issue of “double-dipping”. To explore changes throughout the migraine cycle, for the 10 migraineurs that were scanned during more than one period, we plotted MD values for each cluster. Significant MD differences between migraine periods were determined using paired t-tests (two-tailed $p < 0.05$). Additionally, for all migraineurs, MD values relative to the time until next migraine were plotted to determine if MD increased or decreased as a migraine event approached. Finally, for each cluster, significant relationships between MD and migraine characteristics were determined (Pearson's correlation, $p < 0.05$).

RESULTS

Migraine Characteristics

Using a self-report questionnaire, migraineurs reported the most common location of their migraines over the past 12 months. In 12 of the 36 migraineurs, headaches were more common on the right side, in six they were more common on the left, and in the remaining 18 they were most often bilateral. Migraine subjects most frequently described their migraine pain as “throbbing”, “pulsating”, and/or “sharp”, in nature. They indicated that “stress”, “lack of sleep”, and “dehydration” most often triggered migraine attacks. The mean (\pm SEM) estimated frequency of migraine attacks was 1.3 ± 0.1 per month, mean length of time since the onset of migraine attacks (years suffering) 16.2 ± 1.9 years, and mean pain intensity of migraines was 3.8 ± 0.1 on a 6-point visual analogue scale. Although 24 of the 36 migraineurs were taking some form of daily medication (mostly the oral contraceptive pill), none of the migraine subjects was taking prophylactic medication prescribed for migraine.

Mean Diffusivity

The DTI analysis revealed that compared to controls, migraineurs show regional differences in brainstem MD throughout the migraine cycle (Figure 1, Table 1). Consistent with our previous report, during the interictal period migraineurs showed increased MD compared with controls in regions encompassing the left SpV, left dIPons, right dorsomedial/dIPons and the PAG (Figure 1, Table 1). Strikingly, this MD increase during the interictal period was absent during the 24-hour period prior to a migraine, with no significant difference between controls and migraineurs in this period. The MD increase then returned to above control levels in the dm/dIPons and PAG in the 72-hour period immediately following a migraine. Extraction of MD values from the clusters displaying a significant increase during the interictal period confirmed this pattern of MD change, i.e., i) MD increase during the interictal period: (MD $\times 10^{-3}$ mean \pm SEM) left SpV *controls* 0.75 ± 0.02 , *migraineurs* 0.81 ± 0.01 ; left dIPons *controls* 0.78 ± 0.01 , *migraineurs* 0.84 ± 0.01 ; right dIPons *controls* 0.91 ± 0.01 , *migraineurs* 0.96 ± 0.02 ; left PAG *controls* 0.88 ± 0.01 , *migraineurs* 0.95 ± 0.01 ;

ii) no MD difference immediately prior to migraine: left SpV: *controls* 0.75 ± 0.02 , *migraineurs* 0.77 ± 0.01 , $p=0.37$; left dlPons: *controls* 0.78 ± 0.01 , *migraineurs* 0.80 ± 0.01 , $p=0.21$; right dlPons: *controls* 0.91 ± 0.01 , *migraineurs* 0.96 ± 0.03 , $p=0.06$; left PAG: *controls* 0.88 ± 0.01 , *migraineurs* 0.91 ± 0.02 , $p=0.22$; and iii) MD increase immediately following a migraine: left dlPons *controls* 0.78 ± 0.01 , *migraineurs* 0.84 ± 0.02 , right dlPons *controls* 0.91 ± 0.01 , *migraineurs* 0.99 ± 0.02 and left PAG *controls* 0.88 ± 0.01 , *migraineurs* 0.96 ± 0.02 , but not in the left SpV *controls* 0.75 ± 0.02 , *migraineurs* 0.79 ± 0.02 , $p=0.09$ (Figure 2A). In no brainstem region was MD significantly lower in migraineurs compared with controls.

Plots of MD values in the 10 migraineurs that were scanned during at least two of the three migraine periods revealed that the pattern of MD changes was consistent in individual subjects. That is, MD was lower immediately prior to a migraine compared with both the interictal and immediately following a migraine periods (Figure 2B). More specifically, of the 10 migraineurs, MD decreased immediately prior to a migraine compared to the interictal period in nine migraineurs within the left SpV, left dlPons and left PAG and in seven migraineurs within the right dlPons. Additionally, of the six migraineurs scanned during all three phases, five showed a MD decrease immediately prior to a migraine compared with both the interictal and immediately after a migraine within the left SpV, left dlPons and left PAG and in four migraineurs within the right dlPons. Furthermore, plots of MD values over the migraine cycle revealed that on average, MD gradually increased over the interictal period and then rapidly decreased in the 24-hour period immediately prior to a migraine (Figure 3). This MD decrease then increased towards interictal levels in the period immediately following a migraine.

In all migraine subject groups, MD values in these clusters were not significantly correlated to migraine frequency (left SpV: *interictal*: $r=0.01$, $p=0.94$; *immediately prior to migraine* $r=0.03$, $p=0.94$; *immediately following migraine* $r=0.24$, $p=0.40$; left dlPons: *interictals* $r=-0.07$, $p=0.71$; *immediately prior to migraine* $r=0.09$, $p=0.80$; *immediately following migraine* $r=0.40$, $p=0.15$; right dlPons: *interictals* $r=0.19$, $p=0.33$; *immediately prior to migraine* $r=0.16$, $p=0.65$; *immediately*

following migraine $r=0.35$, $p=0.22$; left PAG: *interictals* $r=-0.13$, $p=0.50$; *immediately prior to migraine* $r=0.45$, $p=0.20$; *immediately following migraine* $r=0.54$, $p=0.06$), years suffering (left SpV: *interictals* $r=0.10$, $p=0.61$; *immediately prior to migraine* $r=-0.62$, $p=0.06$; *immediately following migraine* $r=-0.40$, $p=0.15$; left dIPons: *interictals* $r=0.02$, $p=0.91$; *immediately prior to migraine* $r=-0.07$, $p=0.86$; *immediately following migraine* $r=-0.36$, $p=0.21$; right dIPons: *interictals* $r=-0.30$, $p=0.11$; *immediately prior to migraine* $r=-0.48$, $p=0.16$; *immediately following migraine* $r=-0.52$, $p=0.06$; left PAG: *interictals* $r=0.09$, $p=0.63$; *immediately prior to migraine* $r=-0.30$, $p=0.42$; *immediately following migraine* $r=-0.33$, $p=0.25$), or the intensity of migraine pain (left SpV: *interictals* $r=0.35$, $p=0.06$; *immediately prior to migraine* $r=0.09$, $p=0.81$; *immediately following migraine* $r=0.21$, $p=0.46$; left dIPons: *interictals* $r=-0.07$, $p=0.72$; *immediately prior to migraine* $r=-0.15$, $p=0.68$; *immediately following migraine*: $r=-0.36$, $p=0.20$; right dIPons: *interictals* $r=-0.04$, $p=0.81$; *immediately prior to migraine* $r=-0.14$, $p=0.68$; *immediately following migraine* $r=-0.18$, $p=0.55$; left PAG: *interictals* $r=0.13$, $p=0.49$; *immediately prior to migraine* $r=0.18$, $p=0.62$; *immediately following migraine* $r=0.04$, $p=0.90$).

DISCUSSION

This study demonstrates that migraine is associated with changes in regional anatomy that fluctuate over the migraine cycle in a number of brainstem regions. More specifically, during the long interictal period, migraineurs display increased free water movement compared with controls in areas that process orofacial pain, such as the SpV, dIPons and PAG. Remarkably, immediately prior to a migraine attack, this increase in diffusivity reduces to control levels before increasing again in the period immediately following migraine. It is clear from these data that in episodic migraineurs, regional brainstem microstructural changes occur throughout the migraine cycle, and that there are specific anatomical changes in the 24 hours prior to onset.

A number of migraine studies have used DTI to identify anatomical changes in large fibre bundles such as the corpus callosum, internal capsule and corona radiata, although these studies

did not explore changes in diffusion within grey matter or within the brainstem (Neeb et al., 2015; Zhang et al., 2017). Whilst a previous investigation used a region of interest approach to find that migraineurs show greater MD compared to controls within the red nucleus (Kara et al., 2013), no study has specifically explored the brainstem, particularly at different times over the migraine cycle. Consistent with a previous study, we found significant MD increases in SpV, dlPons and PAG (K.K. Marciszewski et al., 2018) and furthermore, we show that during the 24-hour period immediately prior to a migraine, these structural changes disappear so that migraineurs are no different from controls in the preictal period. However, these structural changes then return during the 72-hour period following the migraine event.

It has been argued by many that the headache period of migraine results from activation of trigeminal afferents in brain meninges and large cerebral arteries and these afferents terminate in the SpV and upper cervical dorsal horn (Y. Liu et al., 2004; Y. Liu, Broman, & Edvinsson, 2008; Olesen et al., 2009). Whilst the nature of the cellular changes underlying such diffusion changes is unclear, MD changes can be associated with oedema, vascular injury, inflammation, demyelination, cell count, and cellular morphology; as such our findings could therefore reflect several underlying biological changes (Alexander, Lee, Lazar, & Field, 2007; Hutchinson, Schwerin, Avram, Juliano, & Pierpaoli, 2017). The dynamic nature of the changes reported here suggest that they reflect processes that are not permanent or static in nature, but that can instead change relatively rapidly. Since MD changes can result from dynamic processes such as gliosis (Sierra et al., 2011), and there is evidence that migraine is associated with altered glial function (Benarroch, 2005; Nedergaard et al., 1995), it is possible that the MD decreases immediately prior to a migraine result from astrocyte activation and associated expansion of astrocytic processes. Indeed, a recent preclinical epilepsy investigation linked microstructural changes in astrocytic processes with altered measures of diffusivity (Salo, Miettinen, Laitinen, Grohn, & Sierra, 2017).

Consistent with the idea that migraine is associated with astrocyte activation, it was

recently shown that immediately prior to a migraine, resting infra-slow oscillatory activity (0.03-0.06Hz) increases in these same brainstem regions (N. Meylakh et al., 2018). Astrocytes can exhibit infra-slow calcium oscillations that can propagate among surrounding astrocytes and it has been proposed that in pathological situations, enhanced calcium-wave synchrony and amplitude may occur which can alter local neural function (Crunelli et al., 2002; Cunningham et al., 2006; Halassa et al., 2007; Lorincz et al., 2009; Parri & Crunelli, 2001). This raises the prospect that immediately prior to a migraine, astrocyte activation results in decreased mean diffusivity and increased infra-slow oscillatory activity resulting in altered sensitivity within brainstem regions that receive and process orofacial noxious information. Whether such a sensitivity change is adequate to evoke head pain from basal levels of neural traffic or simply to facilitate an incoming trigger to activate higher brain centres to produce head pain remains to be determined.

The hypothesis that the brainstem pain processing sites become more sensitive as a migraine approaches was supported by Stankewitz and colleagues, who reported that orofacial noxious stimuli evoked greater SpV signal intensity increases as a migraine attack approaches (Stankewitz et al., 2011). Although in this previous study individuals were only examined up to four days prior to their next migraine, a recent study showed that noxious stimuli evoked dramatic SpV activation increases, particularly in the 24-hour period prior to a migraine (K. K. Marciszewski, N. Meylakh, F. Di Pietro, E. P. Mills, et al., 2018). However, despite the increase in SpV activation, during acute orofacial stimuli, individuals' reported pain intensity ratings decreased as a migraine approached. This appears at odds with the idea that brainstem pain-processing circuits become more sensitive as a migraine approaches although there are a number of potential explanations: i) since these data reveal that both the anatomy and function of brainstem pain processing circuits are dynamic, it is possible that these pathways may change again at the onset or during a migraine itself, ii) since preclinical studies have shown convergence of dural-sensitive and facial cutaneous afferents in SpV (Burstein et al., 1998; Ellrich et al., 1999), a decrease in noxious

cutaneous afferent drive onto second-order convergent SpV neurons may result in an overall increase in dural afferent input sensitivity, iii) changes in descending brainstem modulatory inputs onto the SpV may evoke a heightening of dural afferent input sensitivity at the expense of inputs from other orofacial structures. Whilst these ideas are highly speculative, it is unlikely that the alterations in SpV anatomy and function are involved in other functions to the same degree as the processing of orofacial noxious afferents.

Whilst our data imply that the processes involved in migraine attack onset may be astrocytic in nature, whether astrocyte activity is specifically driving migraine initiation or simply a symptom of another process cannot currently be discerned. The gradual increase in MD in brainstem pain-related regions over the interictal period suggests that changes are occurring throughout the interictal period that then dramatically reverse immediately prior to a migraine to control levels. Whilst brainstem functional measures such as SpV signal intensity changes and infra-slow oscillations were at control levels during the interictal period and dramatically increased immediately prior to a migraine, MD was above control levels during the interictal period and reduced to control levels prior to migraine. This implies that brainstem anatomy is not simply changing prior to a migraine but is altered throughout the long interictal period. Several reports suggest reduced endogenous analgesic ability in migraine (de Tommaso et al., 2007; Sandrini et al., 2006) whilst others report no change (Perrotta et al., 2010; Teepker et al., 2014). This inconsistency may reflect subtle variations in endogenous analgesic responsiveness across the migraine cycle and it might be that endogenous analgesic ability gradually increases over the interictal period which is consistent with MD increases in pain-processing and modulating regions across the interictal period. Additionally, none of the regional microstructural changes we detected were correlated to migraine properties such as migraine frequency, intensity or duration, suggesting that the changes are not cumulative over time, and is consistent with the idea that they may be dynamic in nature. Whilst these results are in line with some migraine studies (Chen et al., 2016; Uggetti et al., 2017), others have reported significant linear relationships between

anatomical measures and migraine frequency (Kruit, Launer, Overbosch, van Buchem, & Ferrari, 2009; C. Mainero, J. Boshyan, & N. Hadjikhani, 2011b), intensity (Russo et al., 2012) and years suffering (C.D. Chong & Schwedt, 2015; J. Liu et al., 2012; Rocca et al., 2014; Schwedt et al., 2013); however, none of these studies explored the brainstem.

There are a number of methodological and subject-related limitations of this study. The spatial resolution of human DTI is relatively low and thus it is difficult to precisely localize each brainstem cluster with respect to small brainstem nuclei. However, the location of each cluster was defined using brainstem atlases and placed the changes into context with respect to the existing human and preclinical research. Secondly, we used an uncorrected threshold for the initial overlay of diffusion differences which can result in false positives. We limited this potential issue by applying cluster correction and we are therefore confident that the changes reported in areas such as the SpV are robust (Woo, Krishnan, & Wager, 2014). Thirdly, this is a cross-sectional study and mounting evidence of relatively rapid brainstem changes, scanning individual migraineurs over the course of several weeks while measuring indices of brain anatomy, activity, and sensitivity would provide more precise evidence supporting this hypothesis.

Overall, our findings suggest that migraine is associated with anatomical changes within brainstem structures involved in trigeminal noxious transmission and endogenous analgesia. More importantly, these anatomical changes alter over the migraine cycle specifically during the 24-hour period prior to a migraine attack. We speculate that these anatomical changes reflect astrocyte activation that alters local neural function by the release of gliotransmitters, which either trigger or alter the sensitivity of the brainstem so that an external trigger induces a migraine attack. Future investigations exploring brainstem resting activity, evoked activity and anatomy over the migraine cycle may provide evidence supporting such a proposal. If dynamic changes in brainstem function and structure do occur, we may be in a position to modify these changes and potentially prevent the triggering of a migraine attack.

REFERENCES

- Afridi S.K., Giffin N.J., Kaube H., Friston K.J., Ward N.S., Frackowiak R.S. & Goadsby P.J. (2005) A positron emission tomographic study in spontaneous migraine. *Arch Neurol* **62**, 1270-5.
- Akerman S., Holland P.R. & Goadsby P.J. (2011) Diencephalic and brainstem mechanisms in migraine. *Nat Rev Neurosci* **12**, 570-84.
- Alexander A.L., Lee J.E., Lazar M. & Field A.S. (2007) Diffusion tensor imaging of the brain. *Neurotherapeutics* **4**, 316-29.
- Bahra A., Matharu M.S., Buchel C., Frackowiak R.S. & Goadsby P.J. (2001) Brainstem activation specific to migraine headache. *The Lancet* **357**, 1016-7.
- Basser P.J. & Pierpaoli C. (1996) Microstructural and physiological features of tissues elucidated by quantitative-diffusion-tensor MRI. *J Magn Reson B* **111**, 209-19.
- Benarroch E.E. (2005) Neuron-astrocyte interactions: partnership for normal function and disease in the central nervous system. *Mayo Clin Proc* **80**, 1326-38.
- Borsook D. & Burstein R. (2012) The enigma of the dorsolateral pons as a migraine generator. *Cephalalgia* **32**, 803-12.
- Burstein R., Yamamura H., Malick A. & Strassman A.M. (1998) Chemical stimulation of the intracranial dura induces enhanced responses to facial stimulation in brain stem trigeminal neurons. *J Neurophysiol* **79**, 964-82.
- Chen Z., Chen X., Liu M., Liu S., Ma L. & Yu S. (2016) Nonspecific periaqueductal gray lesions on T2WI in episodic migraine. *J Headache Pain* **17**, 101.
- Chong C.D., Plasencia J.D., Frakes D.H. & Schwedt T.J. (2017) Structural alterations of the brainstem in migraine. *Neuroimage Clin* **13**, 223-7.
- Chong C.D. & Schwedt T.J. (2015) Migraine affects white-matter tract integrity: a diffusion-tensor imaging study. *Cephalalgia* **35**, 1162-71.

- Crunelli V., Blethyn K.L., Cope D.W., Hughes S.W., Parri H.R., Turner J.P., Toth T.I. & Williams S.R. (2002) Novel neuronal and astrocytic mechanisms in thalamocortical loop dynamics. *Philos Trans R Soc Lond B Biol Sci* **357**, 1675-93.
- Cunningham M.O., Pervouchine D.D., Racca C., Kopell N.J., Davies C.H., Jones R.S., Traub R.D. & Whittington M.A. (2006) Neuronal metabolism governs cortical network response state. *Proc Natl Acad Sci U S A* **103**, 5597-601.
- de Tommaso M., Difruscolo O., Sardaro M., Libro G., Pecoraro C., Serpino C., Lamberti P. & Livrea P. (2007) Effects of remote cutaneous pain on trigeminal laser-evoked potentials in migraine patients. *J Headache Pain* **8**, 167-74.
- Denuelle M., Fabre N., Payoux P., Chollet F. & Geraud G. (2004) Brainstem and hypothalamic activation in spontaneous migraine attacks. *Cephalalgia* **24**, 775-814.
- Diedrichsen J. (2006) A spatially unbiased atlas template of the human cerebellum. *NeuroImage* **33**, 127-38.
- Ellrich J., Andersen O.K., Messlinger K. & Arendt-Nielsen L. (1999) Convergence of meningeal and facial afferents onto trigeminal brainstem neurons: an electrophysiological study in rat and man. *Pain* **82**, 229-37.
- Friston K.J., Holmes A.P., Worsley K.J., Poline J.P., Frith C.D. & Frackowiak R.S. (1994) Statistical parametric maps in functional imaging: a general linear approach. *Hum Brain Mapp* **2**, 189-210.
- Goadsby P.J. & Akerman S. (2012) The trigeminovascular system does not require a peripheral sensory input to be activated--migraine is a central disorder. Focus on 'Effect of cortical spreading depression on basal and evoked traffic in the trigeminovascular sensory system'. *Cephalalgia* **32**, 3-5.
- Halassa M.M., Fellin T. & Haydon P.G. (2007) The tripartite synapse: roles for gliotransmission in health and disease. *Trends Mol Med* **13**, 54-63.

- Hutchinson E.B., Schwerin S.C., Avram A.V., Juliano S.L. & Pierpaoli C. (2017) Diffusion MRI and the detection of alterations following traumatic brain injury. *J Neurosci Res* **96**, 612-25.
- ICHD-3 β (2013) International Classification Committee of the International Headache Society: International Classification for Headache Disorders (ICHD)-3 β Manual. *Cephalalgia* **33**, 629-808.
- Kara B., Kiyat Atamer A., Onat L., Ulusoy L., Mutlu A. & Sirvanci M. (2013) DTI findings during spontaneous migraine attacks. *Clin Neuroradiol* **23**, 31-6.
- Kruit M.C., Launer L.J., Overbosch J., van Buchem M.A. & Ferrari M.D. (2009) Iron accumulation in deep brain nuclei in migraine: a population-based magnetic resonance imaging study. *Cephalalgia* **29**, 351-9.
- Liu J., Zhao L., Li G., Xiong S., Nan J., Li J., Yuan K., Von Deneen K.M., Liang F., Qin W. & Tian J. (2012) Hierarchical alteration of brain structural and functional networks in female migraine sufferers. *PLoS one* **7**, ePub.
- Liu Y., Broman J. & Edvinsson L. (2004) Central projections of sensory innervation of the rat superior sagittal sinus. *Neuroscience* **129**, 431-7.
- Liu Y., Broman J. & Edvinsson L. (2008) Central projections of the sensory innervation of the rat middle meningeal artery. *Brain Res* **1208**, 103-10.
- Lorincz M.L., Geall F., Bao Y., Crunelli V. & Hughes S.W. (2009) ATP-dependent infra-slow (<0.1 Hz) oscillations in thalamic networks. *PLoS One* **4**, e4447.
- Mainero C., Boshyan J. & Hadjikhani N. (2011) Altered functional MRI resting-state connectivity in periaqueductal gray networks in migraine. *Ann Neurol* **70**, 838-45.
- Marciszewski K.K., Meylakh N., Di Pietro F., Macefield V.G., Macey P.M. & Henderson L.A. (2018a) Altered brainstem anatomy in migraine. *Cephalalgia* **38**, 476-86.

- Marciszewski K.K., Meylakh N., Di Pietro F., Mills E.P., Macefield V.G., Macey P.M. & Henderson L.A. (2018b) Changes in brainstem pain modulation circuitry function over the migraine cycle. *J Neurosci*.
- Mathur V.A., Moayedi M., Keaser M.L., Khan S.A., Hubbard C.S., Goyal M. & Seminowicz D.A. (2016) High frequency migraine is associated with lower acute pain sensitivity and abnormal insula activity related to migraine pain intensity, attack frequency, and pain catastrophising. *Front Hum Neurosci* **10**, 489.
- May A. (2017) Understanding migraine as a cycling brain syndrome: reviewing the evidence from functional imaging. *Neurological Sciences* **38** **Supple 1**, 125-20.
- Meylakh N., Marciszewski K.K., Di Pietro F., Macefield V.G., Macey P.M. & Henderson L.A. (2018) Deep in the brain: Changes in subcortical function immediately preceding a migraine attack. *Hum Brain Mapp* **39**, 2651-63.
- Nedergaard M., Cooper A.J. & Goldman S.A. (1995) Gap junctions are required for the propagation of spreading depression. *J Neurobiol* **28**, 433-44.
- Neeb L., Bastian K., Villringer K., Gits H.C., Israel H., Reuter U. & Fiebach J.B. (2015) No microstructural white matter alterations in chronic and episodic migraineurs: a case-control diffusion tensor magnetic resonance imaging study. *Headache* **55**, 241-51.
- Olesen J., Burstein R., Ashina M. & Tfelt-Hansen P. (2009) Origin of pain in migraine: evidence for peripheral sensitisation. *Lancet Neurol* **8**, 679-90.
- Parri H.R. & Crunelli V. (2001) Pacemaker calcium oscillations in thalamic astrocytes in situ. *Neuroreport* **12**, 3897-900.
- Perrotta A., Serrao M., Sandrini G., Burstein R., Sances G., Rossi P., Bartolo M., Pierelli F. & Nappi G. (2010) Sensitisation of spinal cord pain processing in medication overuse headache involves supraspinal pain control. *Cephalalgia* **30**, 272-84.

- Porcaro C., di Lorenzo G., Seri S., Pierelli F., Tecchio F. & Coppola G. (2017) Impaired brainstem and thalamic high-frequency oscillatory EEG activity in migraine between attacks. *Cephalalgia* **37**, 915-26.
- Rocca M.A., Messina R., Colombo B., Falini A., Comi G. & Filippi M. (2014) Structural brain MRI abnormalities in pediatric patients with migraine. *J of Neurol* **261**, 350-7.
- Russo A., Tessitore A., Giordano A., Corbo D., Marcuccio L., De Stefano M., Salemi F., Conforti R., Esposito F. & Tedeschi G. (2012) Executive resting-state network connectivity in migraine without aura. *Cephalalgia* **32**, epub.
- Salo R.A., Miettinen T., Laitinen T., Grohn O. & Sierra A. (2017) Diffusion tensor MRI shows progressive changes in the hippocampus and dentate gyrus after status epilepticus in rat - histological validation with Fourier-based analysis. *NeuroImage* **152**, 221-36.
- Sandrini G., Rossi P., Milanov I., Serrao M., Cecchini A.P. & Nappi G. (2006) Abnormal modulatory influence of diffuse noxious inhibitory controls in migraine and chronic tension-type headache patients. *Cephalalgia* **26**, 782-9.
- Schwedt T.J., Schlaggar B.L., Mar S., Nolan T., Coalson R.S., Nardos B., Benzinger T. & Larson-Prior L.J. (2013) Atypical resting-state functional connectivity of affective pain regions in chronic migraine. *Headache* **53**, 737-51.
- Sierra A., Laitinen T., Lehtimäki K., Rieppo L., Pitkanen A. & Grohn O. (2011) Diffusion tensor MRI with tract-based spatial statistics and histology reveals undiscovered lesioned areas in kainate model of epilepsy in rat. *Brain Struct Funct* **216**, 123-35.
- Stankewitz A., Aderjan D., Eippert F. & May A. (2011) Trigeminal nociceptive transmission in migraineurs predicts migraine attacks. *J Neurosci* **31**, 1937-43.
- Teepker M., Kunz M., Peters M., Kundermann B., Schepelmann K. & Lautenbacher S. (2014) Endogenous pain inhibition during menstrual cycle in migraine. *Eur J Pain* **18**, 989-98.

Uggetti C., Squarza S., Longaretti F., Galli A., Di Fiore P., Reganati P.F., Campi A., Ardemagni A., Cariatì M. & Frediani F. (2017) Migraine with aura and white matter lesions: an MRI study. *Neurol Sci* **2017**, 11-3.

Weiller C., May A., Limmroth V., Juptner M., Kaube H., Schayck R.V., Coenen H.H. & Diener H.C. (1995) Brain stem activation in spontaneous human migraine attacks. *Nature Medicine* **1**, 658-60.

Woo C.W., Krishnan A. & Wager T.D. (2014) Cluster-extent based thresholding in fMRI analyses: pitfalls and recommendations. *Neuroimage* **91**, 412-9.

Zhang J., Wu Y.-L., Su J., Yao Q., Wang M., Li G.-F., Zhao R., Shi Y.-H., Zhao Y., Zhang Q., Lu H., Xu S., Qin Z., Cui G.-H., Li J., Liu J.-R. & Du X. (2017) Assessment of gray and white matter structural alterations in migraine without aura. *J Headache Pain* **18**, 74.

Table 1: Montreal Neurological Institute (MNI) coordinates, cluster size and t-score for regions of significant increases in mean diffusivity in migraineurs compared with controls.

Brain region	MNI			cluster size	t-score
	Co-ordinate				
	x	y	z		
interictals>controls					
left midbrain periaqueductal gray matter	-6	-28	-3	41	4.53
right dorsolateral pons	6	-36	-21	7	3.49
left dorsolateral pons	-4	-32	-15	8	3.93
left spinal trigeminal nucleus	-4	-40	-47	7	3.34
immediately following a migraine>controls					
left midbrain periaqueductal gray matter	-6	-28	-7	24	4.53
right dorsomedial/dorsolateral pons	2	-36	-25	22	4.06
left dorsolateral pons	-8	-38	-27	7	3.11

Figure Legends:

Figure 1: Regional mean diffusivity increases in migraineurs compared with controls overlaid onto axial brainstem template images. Significant mean diffusivity increases are represented by a t-value with a hot colour scale. Slice locations are indicated at the upper left of each axial slice in Montreal Neurological Institute space. Compared to controls, migraineurs have increased mean diffusivity during the interictal and immediately following migraine periods in the left spinal trigeminal nucleus (SpV), left and right dorsolateral pons (dlPons) and midbrain periaqueductal gray matter (PAG).

Figure 2: A: Plots of mean (\pm SEM) mean diffusivity changes in migraineurs compared with pain-free controls in the left spinal trigeminal nucleus (SpV), left and right dorsolateral pons (dlPons) and left midbrain periaqueductal gray matter (PAG). Compared to controls, migraineurs show increased mean diffusivity during the interictal and immediately following migraine periods but not during the period immediately prior to migraine. # $p < 0.05$ voxel-by-voxel analysis; * $p < 0.05$ 2-sample t-tests. **B:** Plots of mean diffusivity in 10 migraineurs that were scanned during at least two of the three migraine phases. Note the consistency of change in which mean diffusivity decreases during the period immediately prior to migraine. * $p < 0.05$ paired t-tests; # $p < 0.05$ derived from voxel-by-voxel analysis.

Figure 3: Plots of mean (\pm SEM) mean diffusivity changes in migraineurs over the migraine cycle in the left spinal trigeminal nucleus (SpV), left and right dorsolateral pons (dlPons) and left midbrain periaqueductal gray matter (PAG). Mean diffusivity values are averaged for those migraineurs scanned at least 30 days, 30-10 days, 9-2 days, and 1 day prior to their next migraine,

as well as 1-3 days following a migraine. Note how mean diffusivity gradually increases over the interictal period and falls dramatically immediately prior to a migraine before recovering.

Figure 1:

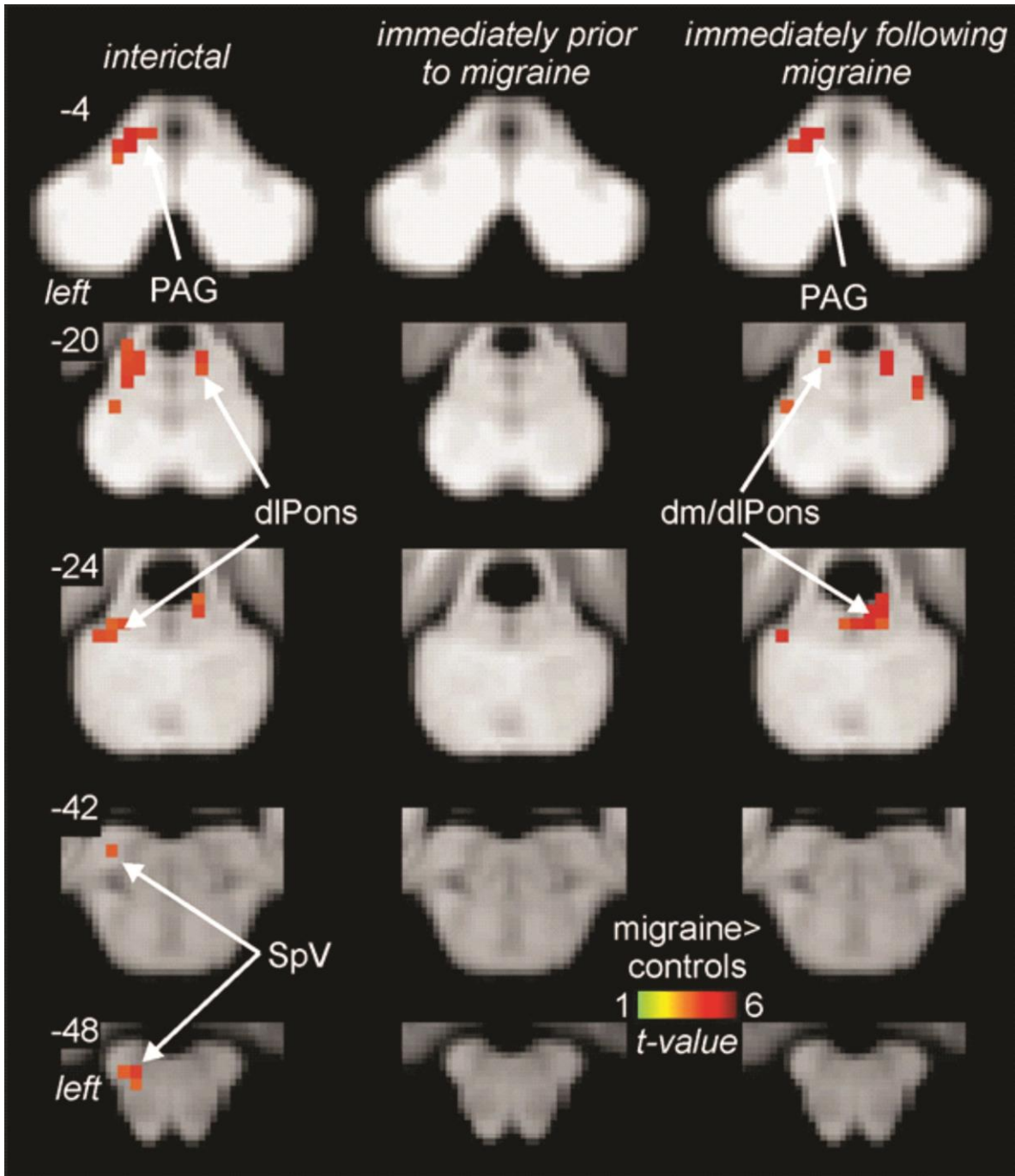


Figure 2:

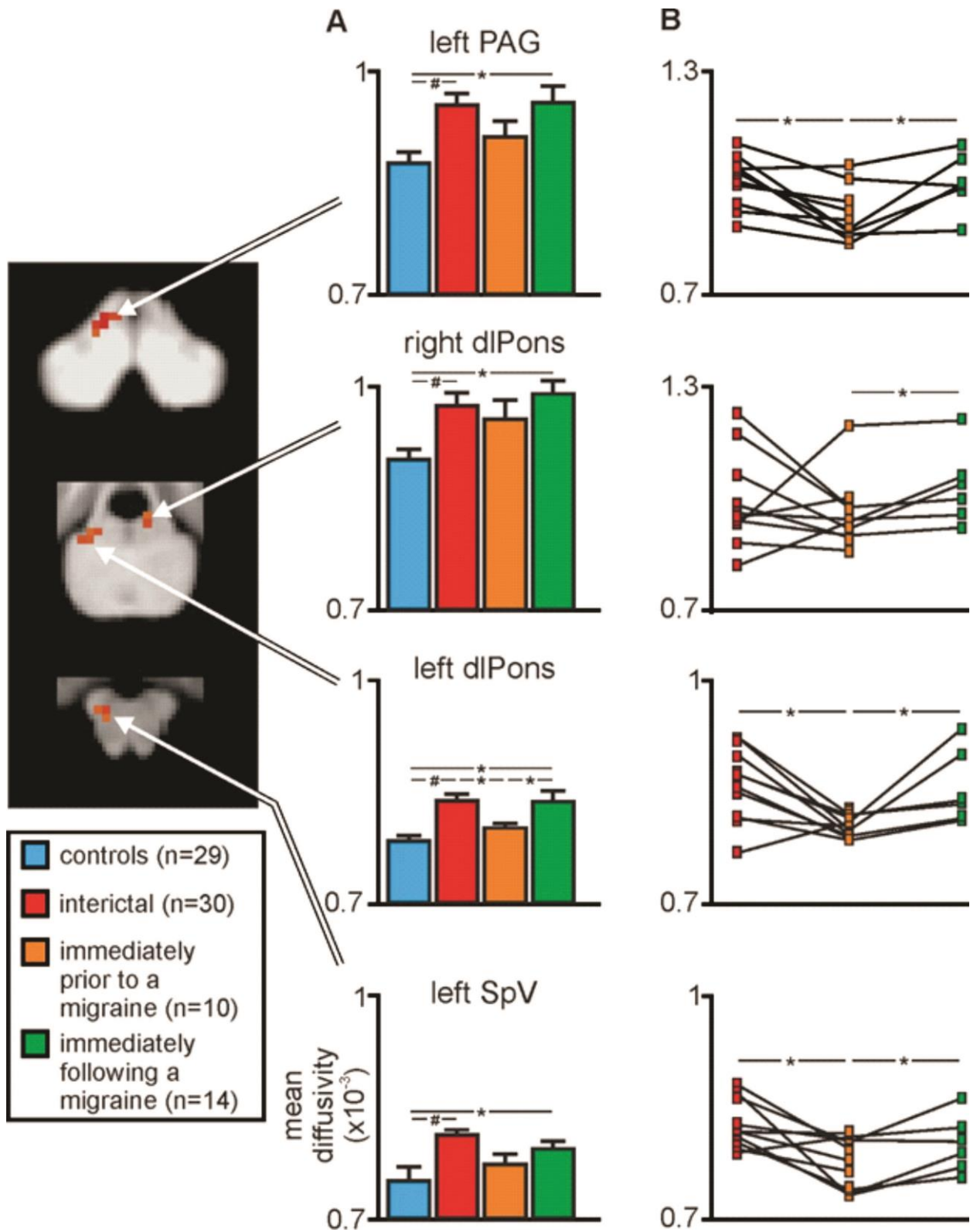
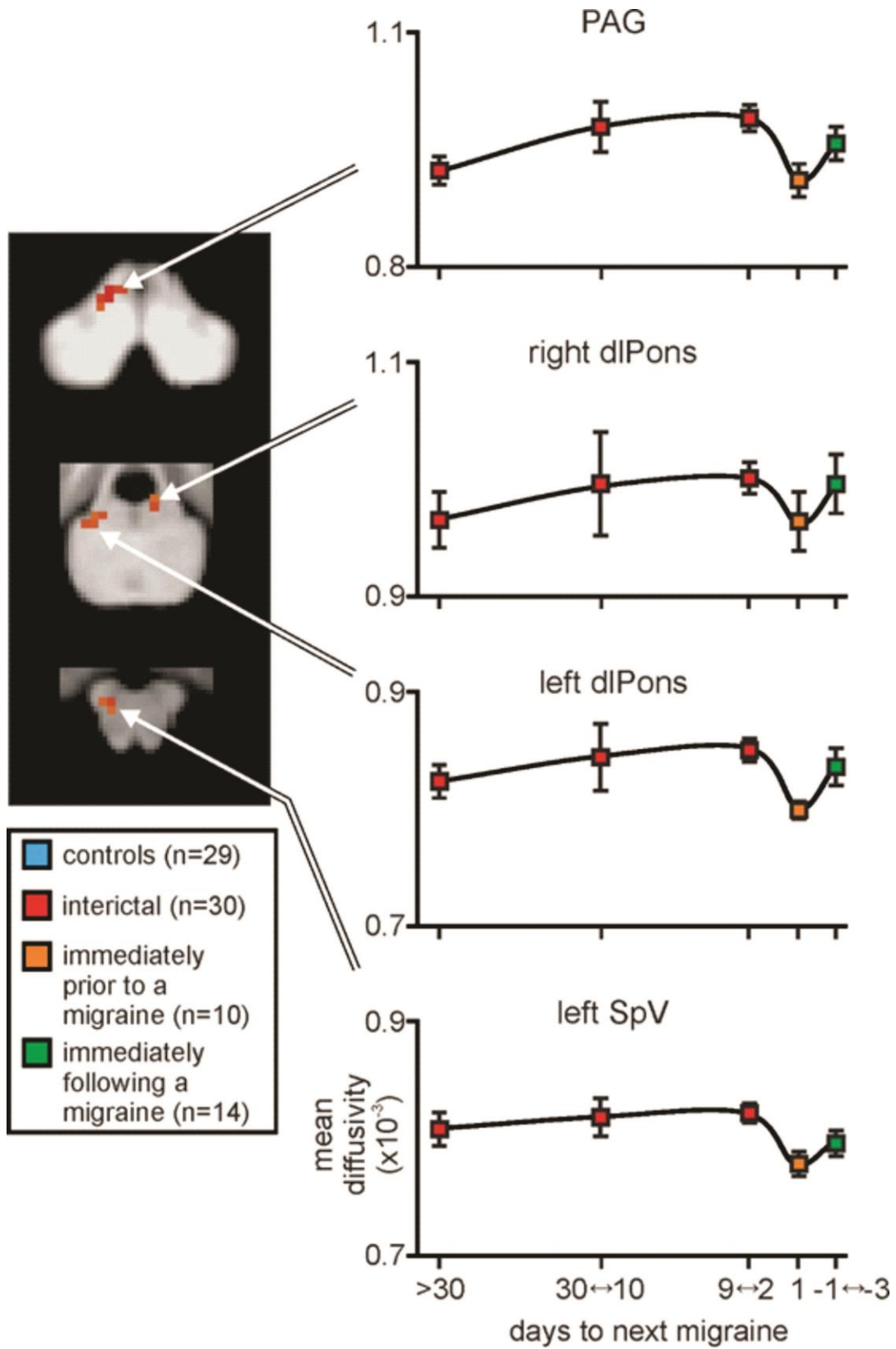


Figure 3:



Appendix IV.

Dorsal raphe nucleus and harm avoidance: A resting-state investigation

Dorsal raphe nucleus and harm avoidance: A resting-state investigation

N. Meylakh¹ · L. A. Henderson¹

Published online: 23 March 2016
© Springer Science+Business Media New York (outside the US) 2016

Abstract The temperament dimension of harm avoidance defines an individual's biological tendency to exhibit altering levels of anxious, inhibiting, and cautious behavior. High harm avoidance and anxiety are highly comorbid, likely due to activity in similar neural circuitries involving the dorsal raphe nucleus. Despite the many investigations that have explored personality factors and brain function, none have determined the influence of ongoing activity within dorsal raphe networks on harm avoidance. The aim of this study was to explore such a relationship. In 62 healthy subjects, a series of 180 functional magnetic resonance images covering the entire brain were collected, and each subject completed the 240-item TCI-R questionnaire. Independent component analyses were performed to define the dorsal raphe network and then to determine the regions significantly correlated with harm avoidance. The independent component analyses revealed three signal intensity fluctuation maps encompassing the dorsal raphe nucleus, showing interactions with regions of the amygdala, hippocampus, nucleus accumbens, and prefrontal, insular, and cingulate cortices. Within these systems, the resting signal intensity was significantly coupled to harm avoidance in the bilateral basal amygdala, bilateral ventral hippocampus, bilateral insula, bilateral nucleus accumbens, and medial prefrontal cortex. Note that we could not measure serotonergic output, but instead measured signal changes in the dorsal raphe that likely reflect synaptic activity. These data provide evidence that at rest, signal intensity fluctuations within the dorsal raphe networks are related to harm avoidance.

Given the strong relationship between harm avoidance and anxiety-like behaviors, it is possible that ongoing activity within this identified neural circuitry can contribute to an individual developing anxiety disorders.

Keywords Amygdala · Hippocampus · Anxiety · Functional magnetic resonance imaging

Robert Cloninger's biopsychosocial model conceptualizes personality as an interaction between inherited biological traits and changeable characteristics (Cloninger, Svrakic, & Przybeck, 1993). The model separates personality into seven dimensions: four temperaments, the "emotional core" of personality, and three character dimensions, evolving as an individual grows and interacts with society. It has been hypothesized that three of the temperament dimensions—harm avoidance, novelty seeking, and reward dependence—are associated with activity in specific neurotransmitter systems. Consequently, dysregulation of these particular systems can predispose an individual to experience abnormalities in their concomitant personality temperaments, and this can predispose the expression of a personality or affective disorder in a stressful environment (Loving, 1999).

Harm avoidance (HA) is defined as a "genetically determined bias toward being cautious, apprehensive and overly pessimistic" (Baeken, De Raedt, Ramsey, Van Schuerbeek, Hermes, Bossuyt, & Luypaert, 2009). Low HA has been associated with risk-taking, harmful behavior, impulsiveness, suicidal ideation, and aggression (Cloninger, 1986; Peirson, Heuchert, Thomala, Berk, Plein, & Cloninger, 1999), whilst high HA has been associated with behavioral inhibition, anxiety and neuroticism (Carver & Miller, 2006). HA is referred to as the anxiety-related personality dimension (Montag, Reuter, Jurkiewicz, Markett, & Panksepp, 2013), and therefore high HA levels are tightly associated with neurobiological pathologies such as

✉ L. A. Henderson
lukch@anatomy.usyd.edu.au

¹ Department of Anatomy and Histology, F13, University of Sydney, Sydney, NSW 2006, Australia

depression and anxiety (Arnold, Zai, & Richter, 2004; Commons, Connolley, & Valentino, 2003; Kenna, Roder-Hanna, Leggio, Zywiak, Clifford, Edwards, & Swift, 2012; Westlye, Bjornebeck, Grydeland, Fjell, & Walhovd, 2011).

It has been hypothesized that HA levels and anxiety are directly influenced by activity levels within the ascending serotonergic system, which predominantly originates within the dorsal raphe nucleus (DR; Waselus, Valentino, & Van Bockstaele, 2011). Recent neuroimaging studies support this hypothesis by suggesting that anxiety is regulated by serotonergic activity and that activity within the ascending serotonergic system plays a crucial role in the pathogenesis of anxiety disorders (Vertes & Linley, 2007; Westlye et al., 2011). Furthermore, high HA has been characterized by high levels of serotonin, which in turn underlies the biology of a highly anxious individual (Montag et al., 2013). Given the proposal that HA traits are biological and directly related to serotonergic activity, it is plausible that HA levels may have significant effects on the resting activity coupling between regions of the ascending serotonergic system. If activity coupling within the serotonergic system is indeed related to HA levels, individuals could be biased to react in a particular manner when placed into a challenging environment, which could predispose them to developing anxiety disorders. The DR could be a good region to provide insight into this system.

The aim of this study was to use resting-state functional magnetic resonance imaging (fMRI) to determine the relationships between the DR and HA. We hypothesized that the DR would be functionally connected to regions of the well-described ascending serotonergic system, including the hippocampus and amygdala (Vertes & Linley, 2007). Furthermore, we hypothesized that the strength of the functional coupling within some of these regions would be significantly correlated with an individual's HA. The results of this study will help us understand how ongoing activity within a particular neural system can influence personality trait expression; which will, in turn, lay the groundwork for exploring the activity of these circuits in individuals with personality and anxiety disorders.

Method

Sixty-two healthy subjects were recruited. The mean (\pm SEM) age of the subjects was 34.5 ± 2.2 years (range 20–65; 41 females, 21 males). Subjects were excluded from the investigation if they had any diagnosed neurological or psychological disorders, were taking any mood-altering medications, or had metal implants or other characteristics that would exclude them from magnetic resonance imaging (MRI) procedures. All procedures were approved by the Human Research Ethics Committees of the University of Sydney, and written consent was obtained from all subjects in accordance with the Declaration of Helsinki.

Psychological measures

All subjects completed the revised 240-item TCI-R (Cloninger et al., 1993), which assesses the seven dimensions of personality according to Cloninger's biopsychosocial model. Each subject was instructed to answer 240 questions on a 0 to 4 scale (0 *false*, 1 *mostly or probably false*, 2 *neither true nor false*, 3 *mostly or probably true*, 4 *true*). Each answer was then manually inserted into an installed TCI-R program that calculated the overall score for each subject for each dimension. For the purposes of this study, only HA scores were used for the analysis. The subjects completed the questionnaire within seven days of the MRI scanning session.

MRI acquisition and analysis

Brain imaging was performed using a 3-T MRI scanner (Philips, Achieva, 32-channel SENSE head coil). Subjects lay supine on the scanner bed with their heads secure in a tight-fitting head coil. With the subject relaxed and with eyes closed, a high-resolution 3-D T1-weighted anatomical image set was collected (turbo field echo; TE = 2.5 ms, TR = 5, 600 ms, flip angle = 8°, voxel size = 0.8 mm³). This was followed by a resting-state fMRI scan, during which a series of 180 gradient echo-planar fMRI image volumes, using blood-oxygen-level-dependent contrast, was collected. Each image volume contained 35 axial slices covering the entire brain (raw voxel = 3×3×4 mm thick, repetition time = 2,000 ms, echo time = 40 ms).

Using SPM8 (Friston, Holmes, Poline, Grasby, Williams, Frackowiak, & Turner, 1995), all of the fMRI images were realigned and bias-corrected to remove field inhomogeneities, and global signal drifts were removed using the detrending method described by Macey and colleagues (Macey, Macey, Kumar, & Harper, 2004). Movement parameters created from the realignment step were visualized, and we noted that no subject displayed movements of greater than 1 mm in any direction. As a result, all 62 subjects were used for further analysis. The fMRI image sets from each individual were then coregistered to each subject's own T1-weighted anatomical set, which was then spatially normalized to the Montreal Neurological Institute (MNI) template. These normalization parameters were then applied to the fMRI image sets so that both the T1-weighted anatomical and fMRI images sets were in the same location as the MNI template.

Given that we were interested first in defining an extensive neural circuitry that almost certainly receives inputs from multiple sites, and therefore contains multiple signal intensity input patterns, we used an ICA to search for consistent signal intensity change patterns across the subjects. ICA is a

technique that can extract independent sources of activity within a recorded mixture of sources and can detect underlying factors of a data set that are often lost in other analyses, such as seed-based techniques (Brown, Yamada, & Sejnowski, 2001; Frigyesi, Vecerla, Lindgren, & Hoglund, 2006). ICA is suited to neural systems analyses because it can detect ongoing activity fluctuations within widespread neural sites with great sensitivity. We performed an ICA with the Group ICA toolbox in SPM8 (Calhoun, Adali, Pearlson, & Pekar, 2001). Using the Infomax ICA algorithm, we estimated 40 independent component maps in which the signal intensities within multiple regions covaried. To explore those neural networks associated with the DR, we rank-ordered these components spatially with relation to the DR. That is, we created a volume of interest (VOI) restricted to the DR on a mean fMRI image set and then ranked in order those neural networks (components) that included signal intensity fluctuations within the DR. We created the DR VOI on the basis of Duvernoy's (1995) atlas, *The Human Brain Stem and Cerebellum*, and from an investigation of the cytoarchitecture of the human DR (Baker, Halliday, & Tork, 1990; see Fig. 1). Using this sorting method, we were able to define three separate signal intensity patterns that were associated with activity within three widespread neural circuits involving the DR.

Using a random-effects procedure, one-sample *t* tests were then performed on each of the three independent components to determine the brain regions in which signal intensity fluctuations were tightly coupled ($p < .05$, family-wise error corrected for multiple comparisons, minimum cluster extent ten voxels). The relationships between signal intensity fluctuations within the DR networks and HA were then determined by performing correlation analyses between HA and signal intensity fluctuations, with the effects of age and gender removed by including them as nuisance variables. Since we hypothesized that regions within the DR networks would be influenced by

HA, small-volume corrections were applied to each significantly correlated cluster ($p < .05$). In addition, for each significantly correlated cluster, parameter estimate values were extracted and plotted against individual HA values, and rho values were then calculated and significance determined ($p < .05$, Bonferroni corrected for multiple comparisons, $n = 6$). These parameter estimate values essentially quantify the functional connectivity strength between the brain regions in each network and how they vary with HA. A positive relationship suggests increased connectivity with increasing HA scores, and vice versa. Finally, for each cluster, significant differences in parameter estimate values between those individuals with high HA (HA score > 99) and low HA (HA score < 83) were determined (two-sample *t* test, $p < .05$, Bonferroni corrected for multiple comparisons, $n = 6$).

Results

Psychological measures

HA scores ranged from 52 to 120 with a mean (\pm SEM) of 91.3 ± 2.3 . This mean value lies within the range considered to be high average.

Dorsal raphe network

ICA revealed three components whose signals encompassed the DR (Fig. 2). Signal intensity fluctuations in Component 1 were restricted to the regions of the hypothalamus and insula. Signal intensity fluctuations within Component 2 also encompassed a large extent of the insula, but also included the caudate, putamen, and nucleus accumbens, as well as discrete regions of the anterior cingulate cortex (ACC), medial prefrontal cortex (mPFC), and dorsolateral prefrontal cortex (dlPFC). Finally, Component 3 included the vast majority of the amygdala, hippocampus, and temporal

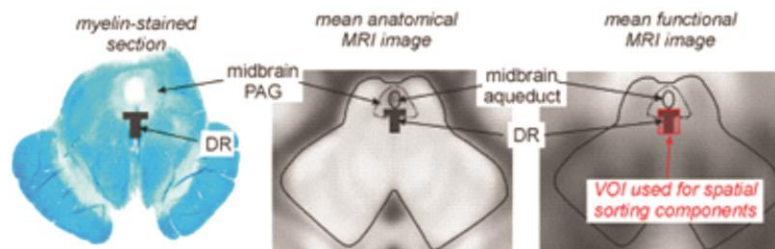


Fig. 1 Axial sections through the midbrain outlining the location of the dorsal raphe nucleus (DR) and the volume of interest (VOI) used to spatially sort the individual-component signal intensity changes. On the left is a myelin-stained image, in the middle a mean T1-weighted anatomical magnetic resonance imaging (MRI) image, and on the right

a mean functional MRI image averaged from all 62 subjects. The dotted line indicates the approximate boundaries of the midbrain periaqueductal gray (PAG). The red shading indicates the location of the VOI used for spatially sorting the signal components

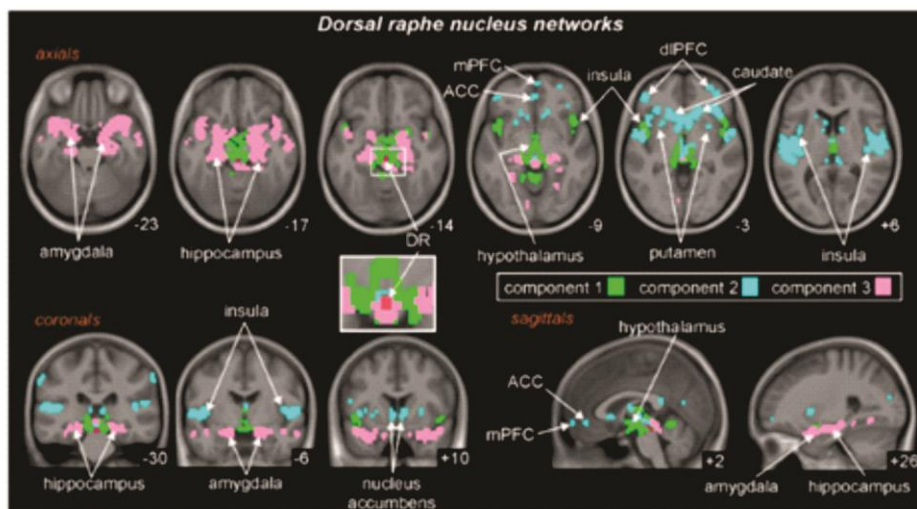


Fig. 2 Three separate signal intensity change pattern maps (Components 1, 2, and 3), each including the dorsal raphe nucleus (DR) overlaid onto a mean T1-weighted anatomical image set. Note that signal intensity within the DR covaried with the signal intensities within the amygdala, hippocampus, hypothalamus, anterior cingulate cortex (ACC), medial

prefrontal cortex (mPFC), dorsolateral prefrontal cortex (dlPFC), insula, and nucleus accumbens. Slice locations in Montreal Neurological Institute (MNI) space are indicated at the lower right of each image. The DR volume of interest used to spatially sort the signal component maps is shown in red

pole. Together these three components, which all included the region of the DR, encompassed the majority of the ascending serotonergic system.

Dorsal raphe network and harm avoidance

Assessing the influence of HA on resting-signal intensity fluctuations resulted in significant relationships in a number of discrete regions (Figs. 3 and 4, Table 1). These regions included bilateral insula, nucleus accumbens, ventral hippocampus, the basal nucleus of the amygdala, and mPFC. Interestingly, in some regions there appeared to be a lateralization effect with respect to the direction of these relationships. Signal intensity fluctuation magnitudes in the left amygdala were negatively correlated with HA ($r = -.46$, $p = .0002$), whereas signal fluctuations within the right amygdala were positively correlated with HA ($r = .37$, $p = .003$). Similarly, signal fluctuations within the left insula were negatively correlated with HA ($r = -.3$, $p = .016$), but within the right insula they were positively correlated ($r = .25$, $p = .046$). Conversely, the signal in the left ventral hippocampus displayed a positive relationship with HA ($r = .36$, $p = .004$), and the signal within the right ventral hippocampus a negative relationship ($r = -.41$, $p = .0009$). The mPFC also displayed both positive and negative correlations with HA (Component 2, $r = -.37$, $p = .003$; Component 3, $r = .32$, $p = .01$). Finally, both the right and left nucleus accumbens displayed negative relationships with HA (left, $r = -.37$, $p = .003$; right, $r = -.39$, $p = .002$), and the DR, a positive relationship ($r = .37$, $p = .003$).

In addition to being significantly correlated to HA, for each of these clusters, signal intensity magnitudes were significantly different between those individuals with high HA (score > 99) and those with low HA (score < 83) (mean [\pm SEM] parameter estimate values, low HA vs. high HA): left amygdala, 1.34 ± 0.18 vs. 0.53 ± 0.19 , $p = .002$; right amygdala, 0.45 ± 0.26 vs. 1.68 ± 0.36 , $p = .004$; left insula, -0.13 ± 0.15 vs. -0.52 ± 0.12 , $p = .027$; right insula, 0.41 ± 0.44 vs. 1.48 ± 0.31 , $p = .028$; left ventral hippocampus, 0.45 ± 0.2 vs. 0.97 ± 0.16 , $p = .025$; right ventral hippocampus, 1.37 ± 0.10 vs. 0.68 ± 0.14 , $p = .0001$; mPFC (Component 2), 0.01 ± 0.18 vs. -0.46 ± 0.13 , $p = .021$; mPFC (Component 3), 0.80 ± 0.19 vs. 0.23 ± 0.13 , $p = .01$; right nucleus accumbens, 1.04 ± 0.21 vs. 0.42 ± 0.15 , $p = .01$; left nucleus accumbens, 0.84 ± 0.12 vs. 0.30 ± 0.14 , $p = .003$; and DR, 1.52 ± 0.21 vs. 1.02 ± 0.22 , $p = .04$.

Discussion

In accordance with the aim of this study, these data reveal that at rest, signal intensity fluctuations within discrete parts of DR networks are influenced by an individual's HA, which raises the possibility that ongoing activity within these regions may be involved in the expression of a particular behavioral response in relevant situations. In this investigation, we showed that DR signal intensity fluctuations covaried with the amygdala, hippocampus, insula, and nucleus accumbens, as well as the cingulate and prefrontal cortices, which is consistent with our first hypothesis. In addition, to address our second

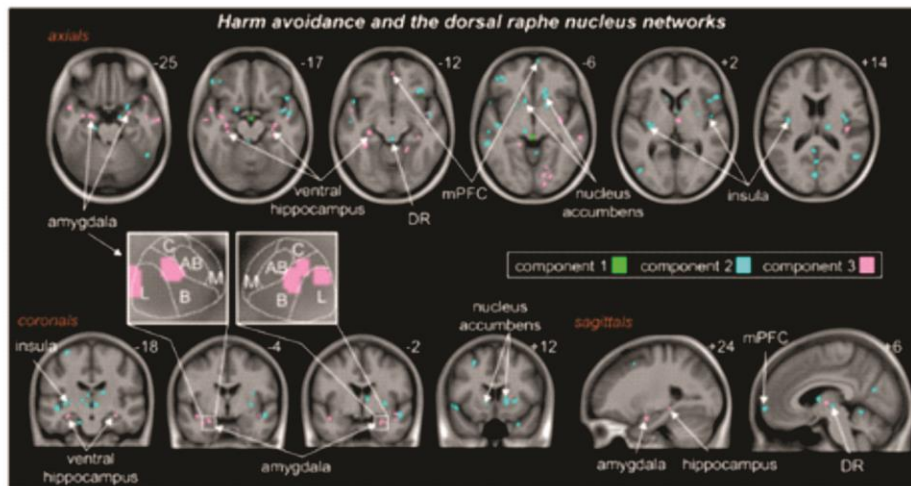


Fig. 3 Resting-signal intensity fluctuations of the previously defined networks significantly correlated to harm avoidance (HA) were overlaid on a mean T1-weighted anatomical image set. Note that resting-signal connectivity was correlated with HA in a number of regions in the region of the dorsal raphe nucleus (DR), the left and right amygdala in the region of the basal and basolateral nuclei, left and right ventral hippocampus, left and right

nucleus accumbens, left and right insula, and medial prefrontal cortex (mPFC). This reflects areas that correlate with HA. The slice locations in Montreal Neurological Institute (MNI) space are indicated at the upper right of each image. Amygdala nuclei: AB, accessory basal nucleus; B, basal nucleus; C, central nucleus; L, lateral nucleus; M, medial nucleus

hypothesis, we found that the strength of these signal intensity fluctuations was significantly correlated with HA in a number of regions, including the bilateral basal amygdala, ventral

hippocampus, insula, and nucleus accumbens, as well as the medial prefrontal cortex. These results are interesting when considering potential roles of the serotonergic system in the

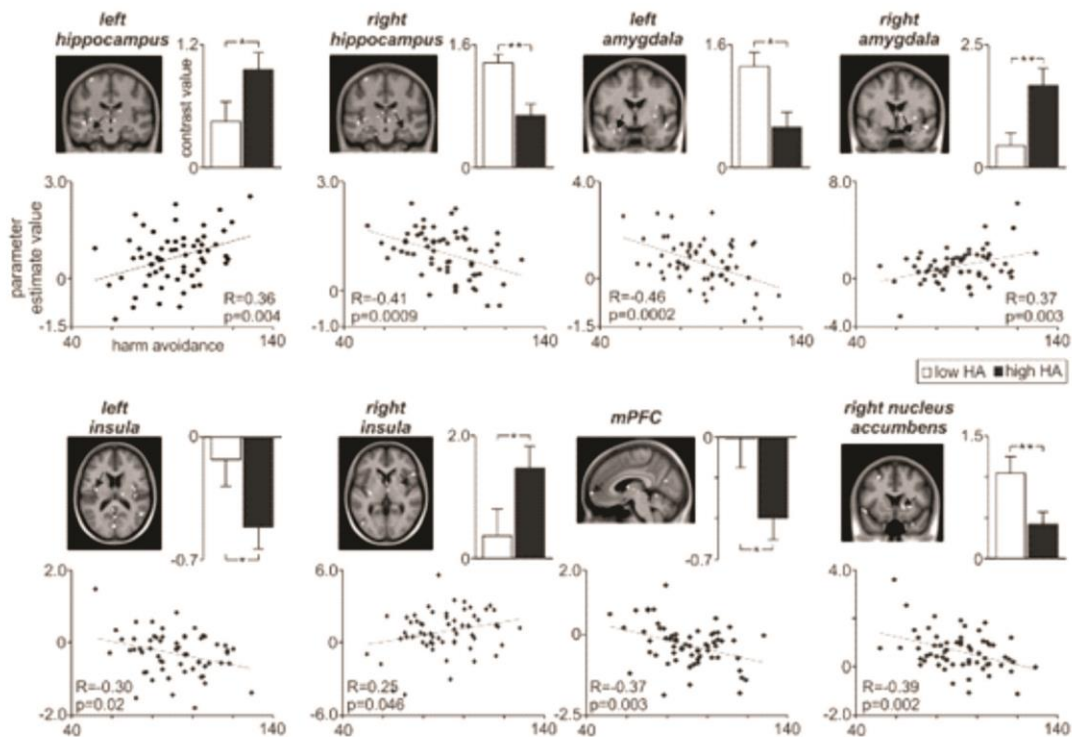


Fig. 4 Plots of harm avoidance (HA) against parameter estimate values (i.e., resting-signal connectivity strength) in significantly correlated regions. In addition to displaying significant linear relationships, in each

region the magnitudes of resting connectivity strength were significantly different in those individuals with low HA (white bars) versus those with high HA (black bars). * $p < .05$, ** $p < .01$. mPFC: medial prefrontal cortex

Table 1 Brain regions in which signal intensity was significantly correlated to harm avoidance

	MNI Coordinates			Cluster Size	<i>t</i> Value
	<i>X</i>	<i>Y</i>	<i>Z</i>		
Right amygdala	26	0	-24	7	2.57
	30	-2	-24	6	2.42
Left amygdala	-24	-4	-22	10	2.54
Left hippocampus	-28	-26	-14	23	3.62
	-30	-18	-16	22	3.36
	-24	-4	-22	10	2.54
	-32	-6	-24	8	2.86
Right hippocampus	32	-16	-16	26	3.87
Left insula	-34	-12	14	11	3.32
Right insula	42	-12	-4	21	3.75
Left nucleus accumbens	-10	16	0	12	2.38
Right nucleus accumbens	16	20	-6	17	2.70
Medial prefrontal cortex	2	54	-8	17	3.16
	8	62	-4	6	3.08
Dorsal raphe nucleus	4	-18	-2	16	3.43

expression of HA behaviors, because the networks identified are based not only on activity within and between the DR, but are also consistent with the well-known ascending serotonergic system (Vertes & Linley, 2007).

Our ICA revealed 40 neural networks, three of which were selected for their higher overlap with the DR. ICA is a technique that decomposes a signal into independent parts, and as a consequence, it is significantly more powerful and sensitive than standard fMRI image analysis techniques (McKeown & Sejnowski, 1998). The identification of differing signal intensity patterns within the DR networks with largely different parts of the brain highlights the importance of performing an ICA as opposed to a standard functional connectivity analysis. The latter is unable to resolve separate signal sources, and therefore much of the signal would be hidden (Frigyesi et al., 2006). Furthermore, this signal decomposition procedure allowed us to reduce the effects of extraneous parameters such as heart rate or head movement, by removing those component maps known to be sensitive to heart rate (such as those encompassing the brain ventricles), or movement (such as those comprising the edge of the brain). Following removal of these component maps, within the DR networks identified we found that HA was significantly correlated with resting activity in the basal amygdala and ventral hippocampus. This is in accordance with the Deakin and Graeff hypothesis, suggesting that serotonergic neurons in the DR project to the basolateral amygdala and ventral hippocampus in the process of mediating conflict and anxiety (Paul & Lowry, 2013). Indeed, it is well-known that the amygdala plays a critical role in emotional regulation and anxiety, and that amygdala

dysregulation predisposes an individual to developing anxiety disorders, which are associated with significantly increased HA (Hariri & Whalen, 2011; Pessoa, 2011; Starcevic, Uhlhuth, Fallon, & Pathak, 1996). The amygdala has been proposed to play a key role in anxiety, due to its participation in the processing of warnings and sensitivity to punishment, its regulation of stress-related memory through induced plasticity, and its control of the fear-anxiety hierarchy (Gray & McNaughton, 2000; McNaughton & Corr, 2004; Roozendaal, McEwen, & Chattarji, 2009). Furthermore, serotonin-mediated amygdala activity has been implicated as being a potential pathway through which selective serotonin reuptake inhibitors (SSRIs) can achieve their anxiolytic effect (Bigos, Pollock, Aizenstein, Fisher, Bies, & Hariri, 2008). A limitation of this study is that we could not measure serotonergic output; rather, we inferred it from signal intensity changes within the DR. Of course, this limits the inferences we can make with regard to the integration of our results with the role of serotonin in behavioral responses.

In this study, we found that the signal intensity fluctuations significantly correlated to HA were located primarily within the basal subdivision of the amygdala, which projects heavily to the nucleus accumbens and to prefrontal and hippocampal cortices (Roozendaal, McReynolds, Van der Zee, Lee, McGaugh, & McIntyre, 2009). A significant correlation between HA and bilateral basal amygdala activity is consistent with previous investigations that have shown that amygdala responses during emotional conflict are significantly altered in individuals with generalized anxiety disorder, a condition also characterized by increased levels of HA (Etkin, Prater, Hoefft, Menon, & Schatzberg, 2010; Starcevic et al., 1996). In addition to altered responsiveness, human positron emission tomography (PET) has revealed that HA is associated with increased resting activity in the right amygdala (Silk, 1998). This is further supported by a PET study showing that the processing of aversive emotions in the amygdala is directly connected to the availability of the serotonin receptor 5-HT_{1A} in the DR (Selvaraj, Mouchlianitis, Faulkner, Turkheimer, Cowen, Roiser, & Howes, 2015). The direct link between serotonin release and amygdala activity was further demonstrated by Fisher and colleagues (Fisher, Meltzer, Ziolk, Price, Moses-Kolko, Berga, & Hariri, 2006), who reported a significant relationship between reduced serotonin release and increased amygdala activity. These data suggest that stressful events can lead to sustained functional and anatomical changes within the basal amygdala, which may contribute to the development of anxiety disorders.

In addition to the amygdala, the hippocampus also displayed significant signal covariation correlated with HA. This HA relationship was restricted to the ventral hippocampal region, which is consistent with Deakin and Graeff's hypothesis that DR serotonergic neurons enable anxiety-like behavior through distribution to the ventral hippocampus (Paul

& Lowry, 2013). A view is emerging that the hippocampus is a functional heterogeneous structure along its longitudinal axis, with the dorsal hippocampus involved in learning and spatial memory, and the ventral aspect in regulating anxiety-like and emotional/motivational behaviors (Bannerman, Rawlins, McHugh, Deacon, Yee, Bast, & Feldon, 2004; Fanselow & Dong, 2010; Strange, Witter, Lein, & Moser, 2014). This differentiation is supported by the finding that serotonergic fibers provide denser input to the ventral hippocampus (Kheirbek & Hen, 2011; Tanaka, Samuels, & Hen, 2012) and findings of strong connections between the ventral hippocampus and other brain regions known to be involved in emotional behavior regulation, such as the nucleus accumbens, prefrontal cortex, and amygdala (Bannerman et al., 2004; Sahay & Hen, 2007). The hippocampus plays an important role in anxiety; hippocampal lesions result in behavioral disinhibition and reduced anxiety (Bannerman et al., 2004). Additionally, increased hippocampal volume has been associated with increased behavioral inhibition and increased anxiety, whereas smaller volumes have been associated with impulsiveness (Cherbuin, Windsor, Anstey, Maller, Meslin, & Sachdev, 2008). Both the amygdala and the ventral hippocampus have been found to contribute to the processing of anxiogenic stimuli, and considering that anxiety disorders are on average accompanied by high HA (Tuominen, Salo, Hirvonen, Nagren, Laine, Melartin, & Hietala, 2012), these studies support our findings of correlations with HA in these two regions.

We also found significant resting-activity correlations with HA in the insular cortex and the nucleus accumbens. The insula has been heavily implicated in emotion processing and anxiety, and has been proposed to be part of a network that predisposes individuals with anxiety-related temperamental traits, such as high HA, to express elevated symptoms under stress (Stein, Simmons, Feinstein, & Paulus, 2007). Despite a lack of evidence for the role of the insula in emotional networks, apart from its role during cognitive/emotional task paradigms, PET studies have shown that HA is associated with altered baseline activity in the insula (Silk, 1998). Similarly, although the nucleus accumbens is frequently associated with evoked behaviors such as reward and is most often associated with dopaminergic activity, it does receive direct inputs from both the basal amygdala and the ventral hippocampus (Roozandaal et al., 2009; Sahay & Hen, 2007). The nucleus accumbens has also been implicated in the fear system, with serotonergic projections from the DR innervating the nucleus accumbens and amygdala, amongst other areas of the forebrain, guiding individuals away from danger cues (Deakin & Graeff, 1991). Indeed, nucleus accumbens activity has been associated with modulation of instrumental action involving response inhibition, with the goal of avoiding aversion and increasing chances of reward (Levita, Hoskin, & Champi, 2012). Given this background, it is possible that the coupling between HA and activity within the nucleus

accumbens is associated with an individual avoiding aversion when placed into a relevant situation.

Interestingly, the bilateral directions of the relationships between signal intensity fluctuations within the left and right amygdala, ventral hippocampus, and insula were the opposite of each other; that is, on one side they were positive, and on the other negative. Higher-order lateralization is a well-described phenomenon, and lateralized function has been described for many higher-order brain regions. Indeed, it was recently shown that the right amygdala displayed stronger HA-dependent resting functional connectivity with the insula, dlPFC, and orbitofrontal PFC compared to the left amygdala, whereas the left amygdala displayed greater connectivity than the right with the nucleus accumbens/subgenual cingulate cortex (Baeken, Marinazzo, Van Schuerbeek, Wu, De Mey, Bossuyt, & De Raedt, 2014). Furthermore, during a risk-taking decision-making task, it has been shown that right insula activation was significantly stronger when individuals selected a risky as compared with a safe response (Paulus, Rogalsky, Simmons, Feinstein, & Stein, 2003). Our study also supports lateralized brain function with respect to HA and suggests that ongoing activity within the amygdala, hippocampus, and insula displays lateralized differences that may be critical when an individual is choosing an appropriate behavioral response.

Surprisingly, we did not find significant signal correlations between resting activity within the cingulate cortex and HA. This lack of a relationship at rest does not eliminate the possibility that evoked activity in the cingulate cortex is related to HA. Indeed, the ACC has been found to be involved in the control of active avoidance in response to a stimulus (McNaughton & Corr, 2004), suggesting that signal correlations within the cingulate cortex and HA would occur under a cognitive/task paradigm. Since resting signal intensity fluctuations were assessed in this study, the responsiveness of the cingulate to appropriate tasks could not be determined. Furthermore, although self-report questionnaires are efficient to administer and guarantee that all subjects receive the same questions under the same conditions, it is widely known that they can be biased, unreliable, and influenced by an individual's subjective mental state at the time (Chien & Dunner, 1996).

One of the most effective anxiolytic compounds, SSRIs, acts on the serotonergic system, and it has been proposed that an individual's response to SSRIs can be predicted by his or her temperamental tendencies (Phan, Lee, & Coccaro, 2011). However, the direction of the relationship between serotonin release and HA remains unresolved, with empirical research presenting very contradictory findings. For example, some evidence suggests that serotonin facilitates anticipatory worry but at the same time restrains spontaneous panic (Deakin & Graeff, 1991). Complicating the situation is the finding that serotonin release is tightly regulated by autoreceptors that control it via negative-feedback inhibition. Indeed, increasing

autoreceptor function is anxiolytic, which is presumably associated with reduced serotonergic function and, as our data suggest, reduced HA (McDevitt & Neumaier, 2011). Overall, it appears that our current understanding of serotonin release, and the mechanism of action of SSRIs, is still in its infancy, and further investigations will be needed to determine the precise relationship between serotonin and HA.

Conclusions

Our results define a neural network that activity at rest is modulated by HA in healthy individuals. Given the strong relationship between HA and anxiety-like behaviors, it is possible that the magnitude of the resting signal intensity fluctuations in these DR networks renders an individual vulnerable to developing anxiety disorders. Increasing the understanding of HA as a biological predisposition underlain by a DR network could lead to interesting insights into the role of the serotonergic system, especially since we found that the DR networks overlapped with regions of the ascending serotonergic system. Furthermore, establishing these networks suggests that when an individual's HA level has reached a certain threshold due to stress, the individual may be very susceptible to developing psychological symptoms.

Author note N.M. collected and analyzed all of the data, wrote the first draft of the manuscript, altered it following feedback, and approved the final manuscript. L.A.H. designed the study, collected the data, directed the analysis and manuscript writing, and approved the final manuscript. The authors have no conflicts of interest. This research was supported by the National Health and Medical Research Council of Australia, Grant No. 1032072.

References

- Arnold, P. D., Zai, G., & Richter, M. A. (2004). Genetics of anxiety disorders. *Current Psychiatry Reports*, 6, 243–254.
- Baeken, C., De Raedt, R., Ramsey, N., Van Schuerbeek, P., Hermes, D., Bossuyt, A., & Luypaert, R. (2009). Amygdala responses to positively and negatively valenced baby faces in healthy female volunteers: Influences of individual differences in harm avoidance. *Brain Research*, 1296, 94–103. doi:10.1016/j.brainres.2009.08.010
- Baeken, C., Marinazzo, D., Van Schuerbeek, P., Wu, G. R., De Mey, J., Luypaert, R., & De Raedt, R. (2014). Left and right amygdala—Mediofrontal cortical functional connectivity is differentially modulated by harm avoidance. *PLoS ONE*, 9, e95740. doi:10.1371/journal.pone.0095740
- Baker, K. G., Halliday, G. M., & Tork, I. (1990). Cytoarchitecture of the human dorsal raphe nucleus. *Journal of Comparative Neurology*, 301, 147–161.
- Bannerman, D. M., Rawlins, J. N., McHugh, S. B., Deacon, R. M., Yee, B. K., Bast, T., & Feldon, J. (2004). Regional dissociations within the hippocampus—Memory and anxiety. *Neuroscience & Biobehavioral Reviews*, 28, 273–283. doi:10.1016/j.neubiorev.2004.03.004
- Bigos, K. L., Pollock, B. G., Aizenstein, H. J., Fisher, P. M., Bies, R. R., & Hariri, A. R. (2008). Acute 5-HT reuptake blockade potentiates human amygdala reactivity. *Neuropsychopharmacology*, 33, 3221–3225.
- Brown, G. D. A., Yamada, S., & Sejnowski, T. J. (2001). Independent component analysis at the neural cocktail party. *Trends in Neurosciences*, 24, 54–63.
- Calhoun, V. D., Adali, T., Pearlson, G. D., & Pekar, J. J. (2001). A method for making group inferences from functional MRI data using independent component analysis. *Human Brain Mapping*, 14, 140–151.
- Carver, C. S., & Miller, C. J. (2006). Relations of serotonin function to personality: Current views and a key methodological issue. *Psychiatry Research*, 144, 1–15. doi:10.1016/j.psychres.2006.03.013
- Cherbuin, N., Windsor, T. D., Anstey, K. J., Maller, J. J., Meslin, C., & Sachdev, P. S. (2008). Hippocampal volume is positively associated with behavioural inhibition (BIS) in a large community-based sample of mid-life adults: The PATH through life study. *Social Cognitive and Affective Neuroscience*, 3, 262–269.
- Chien, A. J., & Dunner, D. L. (1996). The Tridimensional Personality Questionnaire in depression: State versus trait issues. *Journal of Psychiatric Research*, 30, 21–27.
- Cloninger, C. R. (1986). A unified biosocial theory of personality and its role in the development of anxiety states. *Psychiatric Developments*, 4, 167–226.
- Cloninger, C., Svrakic, D. M., & Przybeck, T. R. (1993). A psychobiological model of temperament and character. *Archives of General Psychiatry*, 50, 975–990.
- Commons, K. G., Connolly, K. R., & Valentino, R. J. (2003). A neurochemically distinct dorsal raphe-limbic circuit with a potential role in affective disorders. *Neuropsychopharmacology*, 28, 206–215.
- Deakin, J. F., & Graeff, F. G. (1991). 5-HT and mechanisms of defence. *Journal of Psychopharmacology*, 5, 305–315.
- Duvernoy, H. M. (1995). *The human brain stem and cerebellum: Surface, structure, vascularization, and three-dimensional sectional anatomy with MRI*. New York: Springer.
- Etkin, A., Prater, K. E., Hoeff, F., Menon, V., & Schatzberg, A. F. (2010). Failure of anterior cingulate activation and connectivity with the amygdala during implicit regulation of emotional processing in generalized anxiety disorder. *American Journal of Psychiatry*, 167, 545–554.
- Fanselow, M. S., & Dong, H. W. (2010). Are the dorsal and ventral hippocampus functionally distinct structures? *Neuron*, 65, 7–19.
- Fisher, P. M., Meltzer, C. C., Ziolk, S. K., Price, J. C., Moses-Kolko, E. L., Berga, S. L., & Hariri, A. R. (2006). Capacity for 5-HT1A-mediated autoregulation predicts amygdala reactivity. *Nature Neuroscience*, 9, 1362–1363.
- Frigyesi, A., Veerla, S., Lindgren, D., & Höglund, M. (2006). Independent component analysis reveals new and biologically significant structures in micro array data. *BMC Bioinformatics*, 7, 290. doi:10.1186/1471-2105-7-290
- Friston, K. J., Holmes, A. P., Poline, J. B., Grasby, P. J., Williams, S. C., Frackowiak, R. S., & Turner, R. (1995). Analysis of fMRI time-series revisited. *NeuroImage*, 2, 45–53.
- Gray, J. A., & McNaughton, N. J. (2000). *The neuropsychology of anxiety*. Oxford: Oxford Medical.
- Hariri, A. R., & Whalen, P. J. (2011). The amygdala: Inside and out. *F1000 Reports: Biology*, 3, 2.
- Kenna, G. A., Roder-Hanna, N., Leggio, L., Zywiak, W. H., Clifford, J., Edwards, S., & Swift, R. M. (2012). Association of the 5-HTT gene-linked promoter region (5-HTTLPR) polymorphism with psychiatric disorders: Review of psychopathology and pharmacotherapy. *Journal of Pharmacogenomics and Personalized Medicine*, 5, 19–35. doi:10.2147/PGPM.S23462

- Kheirbek, M. A., & Hen, R. (2011). Dorsal vs. ventral hippocampal neurogenesis: Implications for cognition and mood. *Neuropsychopharmacology*, *36*, 373–374.
- Levita, L., Hoskin, R., & Champi, S. (2012). Avoidance of harm and anxiety: A role for the nucleus accumbens. *NeuroImage*, *62*, 189–198. doi:10.1016/j.neuroimage.2012.04.059
- Lovinger, D. M. (1999). The role of serotonin in alcohol's effects on the brain. *Current Separations*, *18*, 23–28.
- Macey, P. M., Macey, K. E., Kumar, R., & Harper, R. M. (2004). A method for removal of global effects from fMRI time series. *NeuroImage*, *22*, 360–366.
- McDevitt, R. A., & Neumaier, J. F. (2011). Regulation of dorsal raphe nucleus function by serotonin autoreceptors: A behavioral perspective. *Journal of Chemical Neuroanatomy*, *41*, 234–246.
- McKeown, M. J., & Sejnowski, T. J. (1998). Independent component analysis of fMRI data: Examining the assumptions. *Human Brain Mapping*, *6*, 368–372.
- McNaughton, N., & Corr, P. J. (2004). A two-dimensional neuropsychology of defense: Fear/anxiety and defensive distance. *Neuroscience & Biobehavioral Reviews*, *28*, 285–305. doi:10.1016/j.neubiorev.2004.03.005
- Montag, C., Reuter, M., Jurkiewicz, M., Markett, S., & Panksepp, J. (2013). Imaging the structure of the human anxious brain: A review of findings from neuroscientific personality psychology. *Reviews in the Neurosciences*, *24*, 167–190.
- Paul, E. D., & Lowry, C. A. (2013). Functional topography of serotonergic systems supports the Deakin/Graeff hypothesis of anxiety and affective disorders. *Journal of Psychopharmacology*, *27*, 1090–1106. doi:10.1177/0269881113490328
- Paulus, M. P., Rogalsky, C., Simmons, A., Feinstein, J. S., & Stein, M. B. (2003). Increased activation in the right insula during risk-taking decision making is related to harm avoidance and neuroticism. *NeuroImage*, *19*, 1439–1448.
- Peirson, A. R., Heuchert, J. W., Thomala, L., Berk, M., Plein, H., & Cloninger, C. R. (1999). Relationship between serotonin and the temperament and character inventory. *Psychiatry Research*, *89*, 29–37.
- Pessoa, L. (2011). Emotion and cognition and the amygdala: From “what is it?” to “what’s to be done?”. *Neuropsychologia*, *49*, 681–694. doi:10.1016/j.neuropsychologia.2011.02.030
- Phan, K. L., Lee, R., & Coccaro, E. F. (2011). Personality predictors of antiaggressive response to fluoxetine: Inverse association with neuroticism and harm avoidance. *International Clinical Psychopharmacology*, *26*, 278–283.
- Roosendaal, B., McEwen, B. S., & Chattarji, S. (2009). Stress, memory and the amygdala. *Nature Reviews Neuroscience*, *10*, 423–433.
- Roosendaal, B., McReynolds, J. R., Van der Zee, E. A., Lee, S., McGaugh, J. L., & McIntyre, C. K. (2009). Glucocorticoid effects on memory consolidation depend on functional interactions between the medial prefrontal cortex and basolateral amygdala. *Journal of Neuroscience*, *29*, 14299–14308. doi:10.1523/JNEUROSCI.3626-09.2009
- Sahay, A., & Hen, R. (2007). Adult hippocampal neurogenesis in depression. *Nature Neuroscience*, *10*, 1110–1115.
- Selvaraj, S., Mouchlianitis, E., Faulkner, P., Turkheimer, F., Cowen, P. J., Roiser, J. P., & Howes, O. (2015). Presynaptic serotonergic regulation of emotional processing: A multimodal brain imaging study. *Biological Psychiatry*, *78*, 563–571. doi:10.1016/j.biopsych.2014.04.011
- Silk, K. R. (1998). *Biology of personality disorders*. Washington: American Psychiatric Press.
- Starcevic, V., Uhlenhuth, E. H., Fallon, S., & Pathak, D. (1996). Personality dimensions in panic disorder and generalized anxiety disorder. *Journal of Affective Disorders*, *37*, 75–79.
- Stein, M. B., Simmons, A. N., Feinstein, J. S., & Paulus, M. P. (2007). Increased amygdala and insula activation during emotion processing in anxiety-prone subjects. *American Journal of Psychiatry*, *164*, 318–327.
- Strange, B. A., Witter, M. P., Lein, E. S., & Moser, E. I. (2014). Functional organization of the hippocampal longitudinal axis. *Nature Reviews Neuroscience*, *15*, 655–669.
- Tanaka, K. F., Samuels, B. A., & Hen, R. (2012). Serotonin receptor expression along the dorsal–ventral axis of mouse hippocampus. *Philosophical Transactions of the Royal Society*, *367*, 2395–2401. doi:10.1098/rstb.2012.0038
- Tuominen, L., Salo, J., Hirvonen, J., Nagren, K., Laine, P., Melartin, T., & Hietala, J. (2012). Temperament trait harm avoidance associates with mu-opioid receptor availability in frontal cortex: A PET study using [(11)C]carfentanil. *NeuroImage*, *61*, 670–676.
- Vertes, R. P., & Linley, S. B. (2007). Comparison of projections of the dorsal and median raphe nuclei, with some functional considerations. *International Congress Series*, *1304*, 98–120.
- Waselus, M., Valentino, R. J., & Van Bockstaele, E. J. (2011). Collateralized dorsal raphe nucleus projections: A mechanism for the integration of diverse functions during stress. *Journal of Chemical Neuroanatomy*, *41*, 266–280.
- Westlye, L. T., Bjomebekk, A., Grydeland, H., Fjell, A. M., & Walhovd, K. B. (2011). Linking an anxiety-related personality trait to brain white matter microstructure: Diffusion tensor imaging and harm avoidance. *Archives of General Psychiatry*, *68*, 369–377. doi:10.1001/archgenpsychiatry.2011.24